

ARCHITECTURE AND DYNAMICS OF HORMONE-DRIVEN GENE REGULATORY NETWORKS IN PLANT IMMUNITY

Niels Aerts



Architecture and dynamics of hormone-driven gene regulatory networks in plant immunity

Niels Aerts

Architecture and dynamics of hormone-driven gene regulatory networks in plant immunity

PhD thesis

Niels Aerts, January 2024

Utrecht University | Plant-Microbe Interactions

The work described in this thesis was supported by NWO Tuinbouw & Uitgangsmaterialen Talent Programme Grant no. ALWGS.2016.005.

Copyright © 2024, Niels Aerts

ISBN: 978-94-6483-578-6

Cover: Joey Roberts, Ridderprint, www.ridderprint.nl.

Layout: Joey Roberts, Ridderprint, www.ridderprint.nl.

Printing: Ridderprint, www.ridderprint.nl.

Architecture and dynamics of hormone-driven gene regulatory networks in plant immunity

Opbouw en dynamiek van hormoongestuurde genregulatienetwerken in het immuunsysteem van planten

(met een samenvatting in het Nederlands)

Proefschrift

ter verkrijging van de graad van doctor aan de
Universiteit Utrecht
op gezag van de
rector magnificus, prof. dr. H.R.B.M. Kummeling,
ingevolge het besluit van het college voor promoties
in het openbaar te verdedigen op

maandag 8 januari 2024 des ochtends te 10.15 uur

door

Niels Aerts

geboren op 13 september 1991
te Utrecht

Promotoren:

Prof. dr. S.C.M. van Wees

Prof. dr. ir. C.M.J. Pieterse

Beoordelingscommissie:

Prof. dr. A.F.J.M. van den Ackerveken

Prof. dr. ir. G.C. Angenent

Prof. K.J. Denby

Dr. K. Kajala

Prof. dr. R. Sasidharan

Dit proefschrift werd (mede) mogelijk gemaakt met financiële steun van de Nederlandse Organisatie voor Wetenschappelijk Onderzoek (NWO) Tuinbouw & Uitgangsmaterialen Talent Programme Grant no. ALWGS.2016.005.

CONTENTS

Chapter 1

General introduction: Multiple levels of crosstalk in hormone networks regulating plant defense **7**

Chapter 2

Architecture and dynamics of the abscisic acid gene regulatory network **33**

Chapter 3

Dynamic modulation of the jasmonic acid gene regulatory network by abscisic acid **77**

Chapter 4

Nuclear NPR1 modulates salicylic acid/jasmonic acid crosstalk via transcriptional control of WRKY transcription factors **115**

Chapter 5

Transcriptional regulation of plant innate immunity **153**

Chapter 6

General discussion **171**

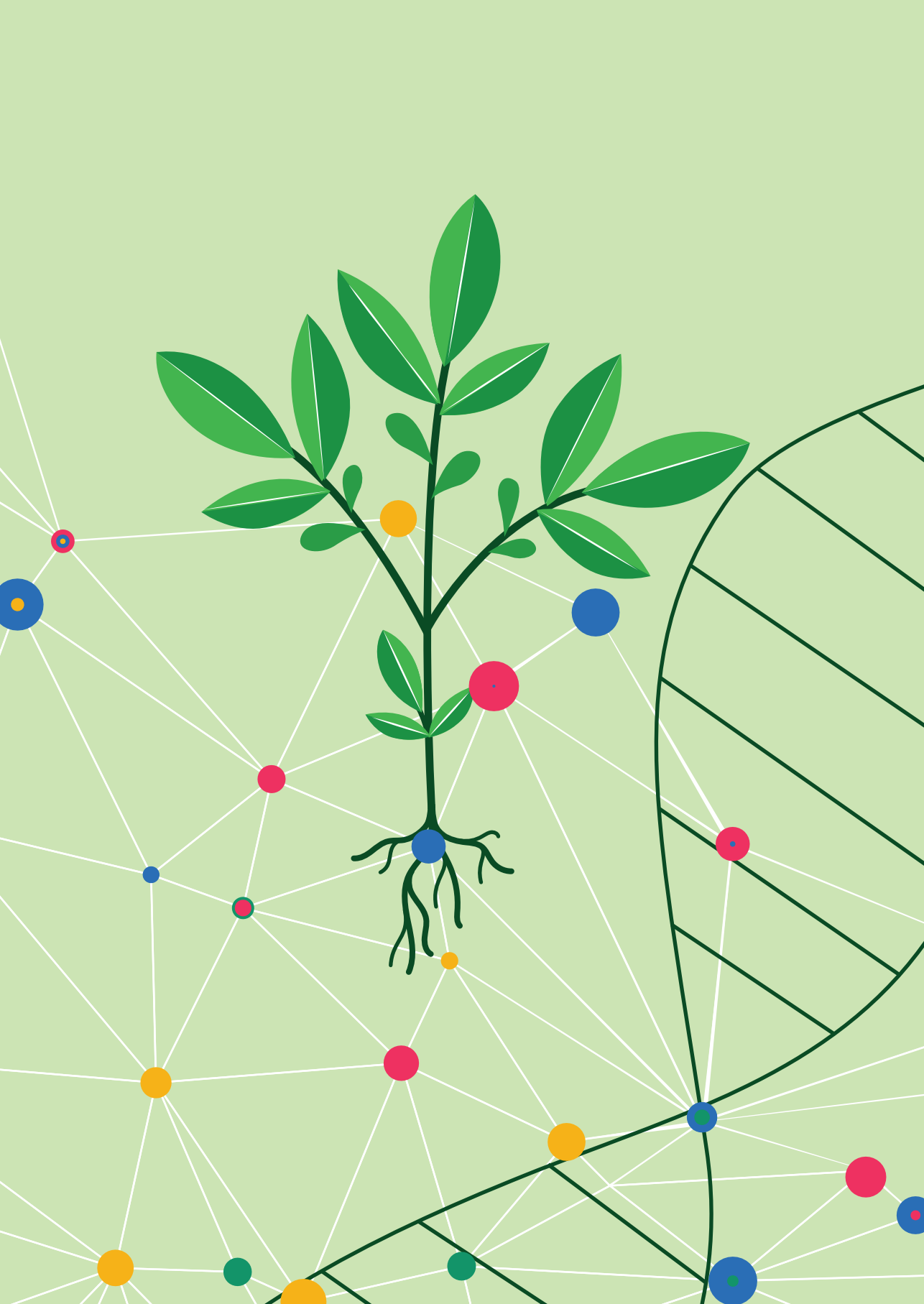
References **187**

Samenvatting **214**

Dankwoord **218**

Curriculum vitae **221**

List of publications **222**





CHAPTER 1

General introduction:

Multiple levels of crosstalk in hormone networks regulating plant defense

Niels Aerts, Marciel Pereira Mendes, Saskia C.M. Van Wees

Plant-Microbe Interactions, Department of Biology, Utrecht University, P.O. Box 800.56, 3508 TB Utrecht, The Netherlands



Adapted from:

Aerts, N., Mendes, M.P. and Van Wees, S.C.M. (2021) Multiple levels of crosstalk in hormone networks regulating plant defense. *The Plant Journal*, **105**, 489-504.

ABSTRACT

Plant hormones are essential for regulating the interactions between plants and their complex biotic and abiotic environments. Each hormone initiates a specific molecular pathway, and these different hormone pathways are integrated in a complex network of synergistic, antagonistic, and additive interactions. This inter-pathway communication is called hormone crosstalk. By influencing the immune network topology, hormone crosstalk is essential for tailoring plant responses to diverse microbes and insects in diverse environmental and internal contexts. Crosstalk provides robustness to the immune system but also drives specificity of induced defense responses against the plethora of biotic interactors. Recent advances in dry-lab and wet-lab techniques have greatly enhanced our understanding of the broad-scale effects of hormone crosstalk on immune network functioning and have revealed underlying principles of crosstalk mechanisms. Molecular studies have demonstrated that hormone crosstalk is modulated at multiple levels of regulation, such as by affecting protein stability, gene transcription and hormone homeostasis. These new insights into hormone crosstalk regulation of plant defense are reviewed here, with a focus on crosstalk acting on the jasmonic acid pathway in *Arabidopsis thaliana*, pinpointing the transcription factors MYC2 and ORA59 as major targets for modulation by other hormones.

INTRODUCTION

Plants in nature and agriculture are constantly interacting with their biotic and abiotic environment. To ensure their survival in different and often hostile conditions they have evolved a sophisticated and flexible environmental signaling network that is steered by plant hormones. This elaborate hormone-controlled network finetunes the plants' responses according to highly dynamic and heterogeneous circumstances. Immune signaling is part of this overarching network and can be activated and tweaked by the intricate molecular communication between the plant and the microbe or insect that it encounters. The intertwining of the immune network with other stress and internal networks allows for adjustments in plant defense responses according to the abiotic conditions, plant developmental stage and time of day (Atkinson and Urwin, 2012, Lu *et al.*, 2017, Nobori and Tsuda, 2019; Figure 1).

Plant hormones are central regulators of plant immunity. Depending on the type of attacker, different hormones accumulate in the plant, whereby each hormone regulates its own core pathway in the immune network (Figure 1). The two most studied defense pathways are those regulated by jasmonic acid (JA) and salicylic acid (SA), which form the backbone of the hormone-regulated part of the immune system (Wasternack and Song, 2017, Zhang and Li, 2019). The JA pathway can be subdivided into two branches (Pieterse *et al.*, 2012). The ERF branch of the JA pathway is co-regulated by ethylene (ET) and is activated by infection with pathogens with a necrotrophic lifestyle. The MYC branch of the JA pathway is co-regulated by abscisic acid (ABA) and generally provides protection against chewing insects. The SA pathway is considered to be mostly directed against pathogens with a biotrophic lifestyle. So, the infection or infestation strategy of the attacker determines which hormones accumulate and which pathways the plant activates to express the appropriate defense responses to the attacker at hand. Moreover, hormone homeostasis is greatly influenced by the status of the plant, being internal, for example age, or being external, for example experiencing other stresses (Berens *et al.*, 2019, Nobori and Tsuda, 2019). Overall, the final hormone balance and responsiveness is a cumulative result of the activation of plant immunity and the plant's internal and external context (Figure 1).

The plant immune system is built on two layers, and hormone signaling is essential for both layers. In the first layer, plants recognize small, conserved microbe- or insect-derived molecules, called M/PAMPs or HAMPs (for Microbe/Pathogen-Associated Molecular Patterns or Herbivore-Associated Molecular Patterns). If there is damage caused by an attacker, plant-derived small molecules called Damage Associated Molecular Patterns (DAMPs) are released, and these can also be recognized. Recognized P/M/H/DAMPs trigger immune signaling, resulting in pattern-triggered immunity (PTI), which wards off most of the non-adapted microbes and insects (Dangl *et al.*, 2013, Erb

and Reymond, 2019). However, successful microbes and insects, which can be pathogenic, beneficial or neutral to the plant, can secrete variable effectors into the host plant to suppress PTI signaling. This is known as effector-triggered susceptibility (ETS) and commonly is established by repression of effective defense hormone pathways (Han and Kahmann, 2019). Resistant plants recognize these effectors or their action, setting off a second layer of immunity called effector-triggered immunity (ETI). In the case of plant interactions with biotrophic pathogens ETI often results in a hypersensitive response (HR), which arrests the invading pathogen (Cui *et al.*, 2015). During PTI, ETS and ETI, plant hormones trigger extensive transcriptional reprogramming and thereby tightly regulate defense responses (Berens *et al.*, 2017). This ultimately leads to elimination of harmful microbes and insects, and accommodation of beneficial microbes and insects, which can occur simultaneously in the plant.

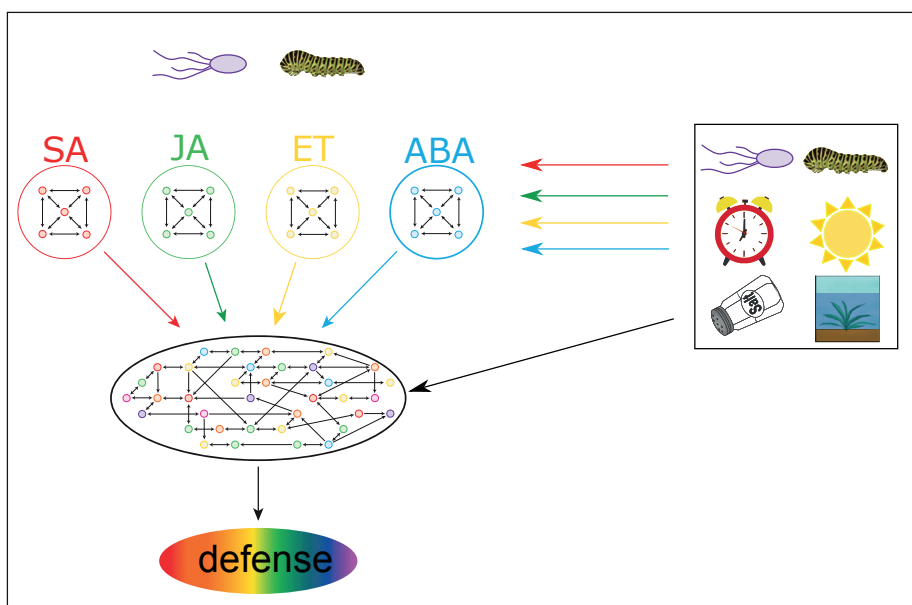


Figure 1: Schematic overview of integration of hormone networks involved in plant defense.

Microbes and insects elicit the accumulation of specific blends of hormones. The main hormones involved in the regulation of plant defense responses are salicylic acid (SA), jasmonic acid (JA), ethylene (ET), and abscisic acid (ABA). Each hormone regulates its own pathway, but also influences other hormone pathways in a complex mix of synergistic, antagonistic, and additive interactions, a phenomenon known as hormone crosstalk. Moreover, accumulation of these hormones and the responsiveness to them can be further modulated by light quality, time of day, abiotic stresses such as drought, flooding and salt stress, and by prior or simultaneous interactions with other microbes or insects. Integration of the different hormone networks shapes the defense response, leading to elimination or accommodation of the microbe or insect in diverse external and internal contexts.

It is important for plant health and long-term survival that defense responses are finetuned to turn on effective defenses but switch off ineffective defenses. Moreover, defense responses need to be balanced with general housekeeping and responses to other stresses (Vos *et al.*, 2013, Vos *et al.*, 2015, Berens *et al.*, 2017, Van Butselaar and Van den Ackerveken, 2020). To this end, different hormone networks interact in a complex interplay of synergistic, antagonistic and additive interactions, a phenomenon known as hormone crosstalk (Figure 1). Hormone crosstalk is an important component of the architecture of the immune signaling network. Besides finetuning and balancing of responses, antagonistic interactions can also serve to provide robustness to the response. For example, two sectors can positively regulate the same immune response, but negatively regulate each other. That means that if one sector is compromised (for example by manipulation by a pathogen) the other sector is derepressed and can take over the function of the first sector. The classical example of crosstalk in defense regulation is that between the SA and JA pathways. Antagonism between these two pathways is the most studied and prevalent form, although large-scale additive and synergistic interactions have been described as well (Hickman *et al.*, 2019). Additionally, the ERF branch and MYC branch of the JA pathway have been reported to repress each other (Pieterse *et al.*, 2012, Gimenez-Ibanez and Solano, 2013, Wasternack and Hause, 2013).

A molecular and systems-level understanding of hormone crosstalk will improve our predictions of effects that disruption or overactivation of parts of the network have on the overall plant response. Implementation of this knowledge can help breeders to engineer crops with a strengthened immune response without undesired traits like enhanced susceptibility to other attackers or decreased plant growth and yield. Here, we review recent advances in our understanding of hormone crosstalk within the immune network. Different levels of regulation, from network and genome scale to single gene and protein scale, are described. We focus on crosstalk in the JA pathway in *Arabidopsis thaliana* (hereafter *Arabidopsis*), as a showcase for the multiple regulation levels of pathway interference in hormone defense signaling.

Crosstalk at the network level

Studying crosstalk at the network level enables the investigation of crosstalk without defining beforehand all the individual components. This coarse-grain overview can reveal the overall architecture of the hormone-regulated plant immune system. Furthermore, it can provide hypotheses about crosstalk at more fine-grain levels, which can be validated experimentally.

A network approach encompasses gathering information on a genome-wide scale. As RNA-seq is the most widely available genome-wide technique, information on the transcriptome is most commonly used for network-scale analyses until now. However,

newly emerging technologies also allow gathering information on other regulation levels such as the proteome and transcriptome (Lee and Bailey-Serres, 2019, Zander *et al.*, 2020). In addition to these molecular data, relatively simple phenotypical readouts can be used for network analyses. The different types of data are usually gathered from leaves of plants that are elicited by a stimulus such as hormone application or pathogen infection. Comparisons can be made between effects that one stimulus has on various mutants that are impaired in hormone signaling sectors. Alternatively, effects of different hormone treatments on one plant genotype (wild type) can be compared.

Network modeling using hormone mutants

A good example of network-level research is a series of papers that describe how different hormone sectors interact to regulate PTI and ETI (Tsuda *et al.*, 2009, Kim *et al.*, 2014, Hillmer *et al.*, 2017, Mine *et al.*, 2017). The researchers used single and higher-order mutants of key regulators of the SA, JA and ET pathways to understand how each sector contributes to PTI and ETI. A mutant of PAD4 was added because although PAD4 is known to be induced by SA and SA-eliciting pathogens, itself can regulate both SA-dependent and -independent responses (Jirage *et al.*, 1999, Glazebrook *et al.*, 2003). Using bacterial growth as a readout, they found that each of the four sectors alone positively contributes to both PTI and ETI (see also Figure 1). However, interactions between the sectors differ between the PTI and ETI response (Tsuda *et al.*, 2009). The PTI response involves both synergistic and antagonistic interactions (Tsuda *et al.*, 2009, Kim *et al.*, 2014) and gene expression in this response is almost always influenced by one or multiple interactions between sectors (Hillmer *et al.*, 2017). Robustness during PTI is mostly provided by the JA and ET sectors. This was demonstrated by the finding that in a mutated JA or ET background knocking out another sector had much more impact on MAMP-induced immunity levels against two *Pseudomonas syringae* strains than in the wild-type background (Kim *et al.*, 2014). In contrast, during ETI all of the sectors act antagonistically and can (partially) take over the response if one of the sectors is inactive. This crosstalk mechanism ensures that the ETI response is robust against manipulation or dysfunction of one of the involved network sectors caused by an attacker or another stimulus (Tsuda *et al.*, 2009).

An example of how network robustness can be achieved was elegantly demonstrated in a follow-up paper by Mine *et al.* (2017). They provided evidence for a robust regulation of SA biosynthesis by interactions between transcriptional regulators of the JA, SA and PAD4 sectors. These regulators form a so-called incoherent type 4 feed-forward loop, in which two components positively regulate one target, but one of these two components also negatively regulates the other component (Mangan and Alon, 2003). In this case, both PAD4 and the JA master regulator MYC2 (Kazan and Manners, 2013) positively regulate *EDS5* (Mine *et al.*, 2017), a gene essential for SA biosynthesis (Rekhter *et al.*, 2019),

but MYC2 represses *PAD4* (Mine *et al.*, 2017). These interactions provide robustness to the system, which was demonstrated by the following. In wild-type plants *PAD4* positively contributed to basal and flg22-induced *EDS5* expression, whereas the JA sector had no effect on *EDS5* expression and in fact contributed negatively to SA accumulation (Mine *et al.*, 2017). However, when *PAD4* was compromised, which in nature could result from activity of a pathogen effector or high temperature, MYC2 was able to activate *EDS5* and hence, the JA pathway could positively influence SA biosynthesis. This was demonstrated using the *dde2 pad4* mutant (impaired in JA signaling and the *PAD4* sector), which, compared to the *pad4* single mutant, contained lower levels of flg22-induced *EDS5* expression and free SA (Mine *et al.*, 2017). So, in the case of SA biosynthesis the JA sector can functionally replace the *PAD4* sector when the latter is compromised. Moreover, a direct interaction between the MYC2 and *PAD4* proteins has been shown to affect free SA accumulation (Cui *et al.*, 2018), as described in the section ‘Crosstalk at the hormone homeostasis level’. Vice versa, the SA sector stimulates JA biosynthesis during ETI (Liu *et al.*, 2016), which is described in the section ‘Crosstalk by modulation of protein stability’.

Network modeling using time series of hormone treatments of wild-type plants

A complementary approach to the above-described systems biology network studies using mutants as conducted by the Tsuda and Katagiri groups is using hormone applications to wild-type plants. A high-throughput time series set-up can provide extra power to the analysis, as this unveils regulatory connections between different components that shape the dynamic architecture of the network. Such an approach facilitates our understanding of the temporal information flow through the different sectors of the individual hormone regulatory networks, including the interactions with sectors of other hormone networks. This approach was taken for JA (Hickman *et al.*, 2017, Zander *et al.*, 2020), the JA-mimic phytotoxin (of *P. syringae*) coronatine (Attaran *et al.*, 2014), SA (Hickman *et al.*, 2019), ET (Chang *et al.*, 2013) and ABA (Song *et al.*, 2016), which followed up on seminal time series papers studying responses to pathogen infection (Windram *et al.*, 2012, Lewis *et al.*, 2015).

Hickman *et al.* (2017) built a gene regulatory network (GRN) model of the JA response based on a transcriptome study of a time series of 14 time points within 16 h after a one-time treatment of mature *Arabidopsis* with aqueous methyl jasmonate (MeJA, which is converted to JA in the plant). The majority of the differentially expressed genes was detected as such within 2 h after treatment. Correlation analysis of expression at different time points showed that there were six distinct phases of upregulation and four distinct phases of downregulation. Each phase was enriched for different processes and contained specific TFs that were predicted to regulate genes in subsequent phases, based on enrichment of TF binding motifs in genes differentially expressed during these phases.

Intersections of the JA network with other hormone networks were also observed. For example, genes related to the SA pathway were downregulated in early phases (1-2 h) and genes related to the growth hormone auxin were downregulated in later phases (3-4 h).

Zander *et al.* (2020) integrated various data types to elucidate the JA response in etiolated seedlings that had perceived continuous treatment with gaseous MeJA for up to 24 h. They focused on the role of MYC2 (Boter *et al.*, 2004, Lorenzo *et al.*, 2004, Dombrecht *et al.*, 2007) and MYC3 (Fernández-Calvo *et al.*, 2011) as master regulators of the JA response by conducting ChIP-seq of these TFs, and ChIP-seq or DAP-seq (basically *in vitro* ChIP-seq) of five of their targets. In addition, six other known JA-related TFs were included in their ChIP-seq/DAP-seq experiments. They also generated proteome and phosphoproteome data, and integrated this with the other data types to infer a regulatory network. This network contained known and new components of the JA regulatory network and pointed to known and novel nodes of crosstalk of the JA pathway with other hormone pathways. An important role for MYC2 and MYC3 in modulation of other hormone pathways was demonstrated by the finding that 37-59% of genes that were annotated as being part of other hormone signaling pathways were bound by MYC2 and MYC3, and that the transcription of these genes responded to the MeJA treatment. Furthermore, the JA-induced transcriptional repressor STZ was predicted to suppress genes from several other hormone pathways, including the SA, GA and brassinosteroid (BR) pathways (Hickman *et al.*, 2019, Zander *et al.*, 2020).

In a follow-up paper of the Hickman *et al.* (2017) paper on individual MeJA treatment, another part of the same experiment was reported, for which plants received a single SA treatment or a combination treatment of MeJA with SA (Hickman *et al.*, 2019). The single SA treatment had a greater impact on the transcriptome than the single MeJA treatment, affecting the expression of more genes and having more prolonged effects. Validation of the built SA GRN model confirmed that specific TFs regulate specific paths in the network that are biologically relevant for defense against biotrophic pathogens. Comparison of the individual SA and MeJA treatments showed that there is a high level of interplay between the SA and JA networks (see also Figure 1). Of the MeJA-responsive genes 69% was also modulated by the individual SA treatment, and of the SA-responsive genes (which was a greater set) 26% was modulated by MeJA. Contrary to the paradigm of SA/JA antagonism, only half of the overlapping genes were regulated in an opposite manner (upregulated by SA and downregulated by MeJA or vice versa), while the other half of the genes were regulated in a similar direction by the two hormones. Noteworthy, hormone biosynthesis and pathways regulators like *LOX2*, *MYC2*, *EDS1* and *PAD4* were generally upregulated by the respective hormone treatment but downregulated by the other hormone treatment (Figure 2A, see also section 'Crosstalk at the hormone homeostasis level'). Moreover, many of the SA- and MeJA-co-upregulated genes were canonical SA and JA pathway genes, like *GRX480*, *ANAC019*, *ANAC055*, some *JAZs*, and

RAP2.6. Many of these genes are also associated with ET and ABA signaling, hinting to their responsiveness to a broad range of hormone-inducing environmental stimuli. The combined SA and MeJA treatment showed that 68% of the MeJA-responsive genes changed their expression when SA was added to the treatment, while this was the case for only 12% of SA-responsive genes. While antagonistic and synergistic effects of the dual treatment were observed, the vast majority of the effects were just additive. Short-term effects by MeJA were overridden by SA effects over time, resulting in a dominance of the SA profile over the MeJA profile (Hickman *et al.*, 2019).

Chang *et al.* (2013) combined ChIP-seq of the ET master regulator TF EIN3 with RNA-seq at 5 time points within 24 h following continuous ET treatment. ET was found to influence many other hormone pathways besides the JA pathway (Lorenzo *et al.*, 2003, Anderson *et al.*, 2004), as the GA, auxin, BR, ABA, SA and cytokinin pathways were also affected by ET treatment.

A study by Song *et al.* (2016) investigated the ABA network based on RNA-seq time series and ChIP-seq experiments with 21 ABA-responsive TFs in the presence of ABA. A complex network of regulation by multiple master regulators, including extensive feedback regulation, was revealed. A thousand genes involved in other hormone pathways were bound by at least one of the investigated ABA-responsive TFs. However, the genes that were bound by a large number of TFs and/or by TFs that showed increased binding after ABA treatment usually belonged to the ABA pathway itself.

CROSSTALK AT THE PROTEIN LEVEL

Proteins can modulate the functioning of other proteins in their own pathway or in other hormone pathways through various mechanisms, such as co-activation, repression, competitive binding to multiple targets, and chemical modification (e.g. phosphorylation, ubiquitination, sumoylation, nitrosylation or sulfonylation). Several molecular players in crosstalk have been demonstrated to modulate proteins that act in other hormone pathways. These include hormone receptors and their interactors. In addition, TFs have been implicated as crosstalk mediators at the protein level, with leading roles for the bHLH TF MYC2 and the ERF TF ORA59 as important targets for crosstalk in the JA pathway (Figure 2).

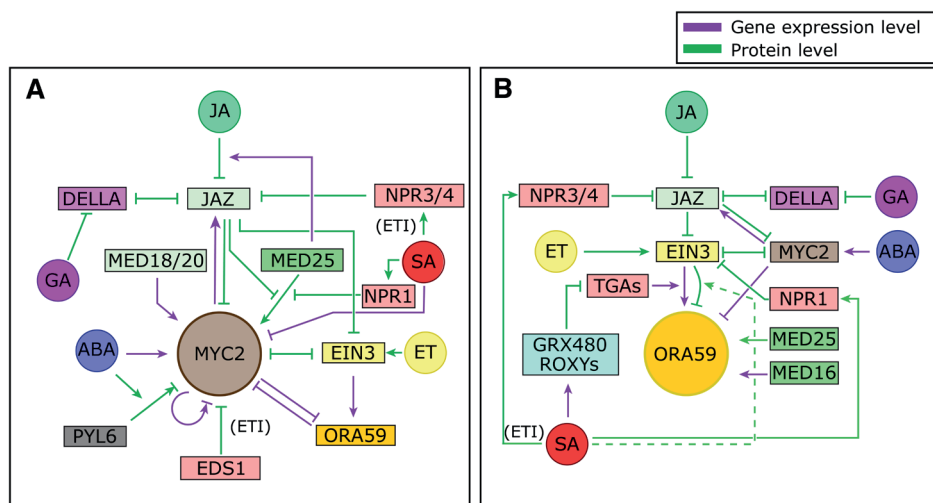


Figure 2: Schematic overview of hormone crosstalk acting on two key transcription factors, MYC2 and ORA59, of the two branches of the jasmonic acid pathway.

(A) Crosstalk acting on the MYC branch master regulator MYC2. In the context of defense, MYC2 mostly regulates anti-insect responses. MYC2 is repressed by interacting JAZ repressors and itself can induce transcription of these JAZs. Jasmonic acid (JA) induces the breakdown of JAZs thus leading to activation of MYC2. MED25 promotes MYC2 transcriptional activity, but JAZs and SA-activated NPR1 prevent binding of MED25 to MYC2. MED25 also promotes JAZ breakdown by recruiting COI1, and alters JAZ splicing and thereby JAZ sensitivity to JA. MED18 and MED20 promote transcription of MYC2. EIN3 is activated by JA-mediated breakdown of JAZ proteins and ethylene (ET)-mediated stabilization. It binds to and represses MYC2 and vice versa. EIN3 also transcriptionally activates ORA59 and ORA59 can repress MYC2 transcription and vice versa (either directly or indirectly, see also panel B). MYC2 can enhance its own transcription in the short term but represses it in the long term. During AvrRps4-induced ETI, EDS1 can repress MYC2. Furthermore, SA can promote degradation of JAZs via NPR3 and NPR4 during ETI. Generally, SA is an inhibitor of MYC2 transcription. Abscisic acid (ABA) directly activates transcription of MYC2 and enhances binding of the ABA receptor PYL6 to MYC2, modulating transcriptional activity of MYC2, which differentially acts on the JAZ6 and JAZ8 promoters (leading to repression versus activation). DELLA proteins bind JAZs and thereby JAZs and DELLAs prevent each other from binding to their respective target TFs. Gibberellin (GA) induces breakdown of DELLAs and thus indirectly represses MYC2.

(B) Crosstalk acting on the ERF branch master regulator ORA59. ORA59 mostly regulates defense against necrotrophic pathogens. ORA59 is indirectly regulated by both JA and ET through their action on EIN3: JA releases EIN3 from its repression by JAZs, and ET stabilizes EIN3. When released from repression and degradation, EIN3 activates transcription of ORA59. TGA TFs are also needed for this activation. GRX480 and other ROXYs are induced by SA and repress the transcriptional activity of these TGAs, leading to reduced transcription of ORA59. EIN3 also mediates degradation of ORA59. Because this only leads to reduced ORA59 functioning under high SA levels and not under high ET levels we propose that SA specifically modulates EIN3 activity such that it leads to ORA59 degradation (dotted line). SA activates NPR1's activity as a co-transcriptional regulator. NPR1 can interact with EIN3, leading to repression of EIN3 transcriptional activity. We propose that it is unlikely that NPR1 modulates EIN3-mediated ORA59 activation during SA/JA crosstalk (Section 'Crosstalk by modulation of protein stability'). EIN3 is further repressed by MYC2 through direct binding and this also occurs the other way around. MYC2 is repressed by interaction of JAZ repressors and itself activates transcription of these JAZs. It is also transcriptionally activated by ABA. ORA59 expression is inhibited by MYC2, both directly and possibly indirectly via inhibition of EIN3 by MYC2. DELLAs bind to JAZs and thereby they inhibit each other from binding to target TFs in their respective pathways. GA leads to breakdown of DELLAs, thus indirectly repressing ORA59. MED25 interacts with ORA59 and

promotes its transcriptional activity, and MED16 promotes *ORA59* transcription. Modulation of JAZ breakdown and JAZ RNA splicing by MED25 is not shown here (see panel A). During ETI, SA can promote degradation of JAZs via NPR3 and NPR4. Note that in most cases where EIN3 is mentioned, EIL1 likely has the same function. However, in most research only EIN3 was extensively characterized.

Mechanisms acting on the gene expression level are colored purple and mechanisms acting on the protein level are colored green. Arrows and bar-headed lines indicate positive and negative effects, respectively. Mechanisms acting downstream of MYC2 and *ORA59* or at the hormone homeostasis level are not shown.

Crosstalk by protein-protein interactions

Protein-protein interactions are of major importance for hormone crosstalk. Recently, an extensive network of protein-protein interactions between members of all hormone pathways in Arabidopsis was revealed using yeast two-hybrid with 1,226 genes with probable or genetically demonstrated functions in plant hormone signaling (Altmann *et al.*, 2020). Not only was there high connectivity within each single hormone pathway, but also many inter-pathway contact points were uncovered. Validation of a subset of these inter-pathway contact points suggested that many of these interactions indeed likely represented crosstalk mechanisms. This was demonstrated by the finding that a mutant of one interaction partner influenced the plant phenotype that correlated with the hormone-associated function of the other interaction partner. It should be noted that such validation does not explicitly show that the convergence of two pathways depends on the detected protein interaction. Alternatively, it could be regulated by another factor that acts downstream in the pathway of the mutated gene.

Hormone receptors were especially often found to interact with proteins that were not involved in the canonical hormone pathway of the receptor (Altmann *et al.*, 2020). This suggests that signaling by hormone receptors through non-canonical pathways has a more prominent role in integrated hormone signaling than previously anticipated. One such example was previously shown for the ABA receptor PYL6, which interacts with the JA master regulator MYC2 (Aleman *et al.*, 2016; Figure 2A). In the presence of ABA, the binding of PYL6 to MYC2 is enhanced, which alters the transcriptional specificity of MYC2 from promoting *JAZ6* expression to *JAZ8* expression. The genome-wide implications of this mechanism have yet to be determined. Another example of an interaction between hormone receptors and key components of non-canonical hormone pathways is that of the SA receptors NPR3 and NPR4 with JAZ repressors. This is discussed in the section 'Crosstalk by modulation of protein stability'.

MYC branch/ERF branch antagonistic crosstalk in the JA defense pathway is likely also (partly) regulated by protein-protein interactions. MYC2 can suppress the ERF branch by directly binding to the TF EIN3, which causes reduced binding of EIN3 to the promoter of a target gene (Song *et al.*, 2014, Zhang *et al.*, 2014; Figure 2). This effect was only shown for the promoter of *HLS1*, a gene involved in the formation of the apical hook in etiolated seedlings (Song *et al.*, 2014, Zhang *et al.*, 2014). It is thus unclear if this mechanism also

underlies MYC2-mediated antagonism on JA-responsive defense genes in the ERF branch. Vice versa, binding of EIN3 and EIL1 to MYC2 represses the transcriptional activity of MYC2 (Figure 2). This could likely explain the enhanced level of MYC2-regulated *VSP2* expression in the *ein3 eil1* mutant and the reduced growth of a caterpillar that was feeding on this mutant (Song *et al.*, 2014). The reciprocal inhibition between MYC2 and ERF branch signaling components is not only regulated at the level of protein-protein interactions but also at the level of transcriptional regulation. This was demonstrated by the direct positive effect of MYC2 on expression of the F-box protein-coding gene *EBF1*, whose protein product targets EIN3 for degradation (Zhang *et al.*, 2014), thus further suppressing ET signaling through a combined effect of MYC2 on ET signaling via transcription, protein stability and protein-protein interaction.

Crosstalk by modulation of protein stability

Modulation of stability of activators and especially repressors is an important regulation mechanism in many different pathways. The most famous example from hormone defense signaling is that of JAZ proteins, which form a co-receptor complex with the E3 ubiquitin ligase F-box protein COI1 for JA-Ile, the active form of JA (Fonseca *et al.*, 2009, Sheard *et al.*, 2010). JAZ proteins inhibit transcription within the MYC and ERF branch through direct binding to key TFs, recruitment of co-repressors, and inhibition of the interaction of the Mediator subunit MED25 with MYCs (see section 'Crosstalk by the Mediator complex'). Upon perception of JA-Ile, JAZs are degraded by the 26S proteasome, which releases the previously bound TFs, and initiates the JA response (Chini *et al.*, 2007, Thines *et al.*, 2007; Figure 2). The key function of JAZ proteins is substantiated by experiments that identified JAZs as targets for interference of immune signaling by pathogen and insect effectors. For example, HARP1, an effector of the chewing Cotton bollworm (*Helicoverpa armigera*) was recently shown to bind to multiple JAZs in Arabidopsis, cotton (its preferred host) and tobacco (Chen *et al.*, 2019). This led to an increase in stability of JAZs, likely because it prevented JA-Ile induced binding of JAZs with COI1. Via this mechanism, HARP1 reduced wound-induced defense signaling and increased plant susceptibility to the insect (Chen *et al.*, 2019). HopX1, an effector from the hemi-biotrophic bacterial pathogen *Pseudomonas syringae* pv. *tabaci* 11528, was also found to interact with JAZs but in contrast this led to a decrease (rather than an increase) in their stability, in a COI1-independent manner. The resulting activation of the JA pathway in turn leads to repression of the SA pathway and thus increased susceptibility to this pathogen (Gimenez-Ibanez *et al.*, 2014). Similarly, the effector HopZ1a from *P. syringae* pv. *syringae* A2 causes degradation of JAZs and consequent activation of the JA pathway and repression of SA signaling. However, in contrast to the effect of HopX1, the JAZ degradation by HopZ1a depends on COI1, and likely involves acetylation of JAZs (Jiang *et al.*, 2013). The most studied example of an

effector that causes degradation of JAZs, the JA-Ile mimic coronatine, is discussed in the section 'Crosstalk at the hormone homeostasis level'.

Degradation of JAZ proteins is essential for synergistic effects between the JA pathway and the ET, ABA, SA and BR pathways, as we will outline in this paragraph. Synergism between the JA and ET pathways drives activation of the ERF branch of defense. JAZ proteins can physically interact with and repress the ET response TFs EIN3 and EIL1 by recruitment of the chromatin modifier HDA6 as a co-repressor (Zhu *et al.*, 2011). In the presence of JA, the JAZs are degraded and thereby the interaction between HDA6 and EIN3/EIL1 is reduced and thus EIN3/EIL1 transcriptional activity enhanced. In combination with ET's activity to stimulate EIN3/EIL1 protein accumulation, the de-repression of EIN3/EIL1 by JA enhances transcription of *ERF1* and *ORA59* (Zhu *et al.*, 2011; Figure 2), which are key TFs in the ERF branch of the JA pathway (Pré *et al.*, 2008, Pieterse *et al.*, 2012). ABA/JA synergistic crosstalk is also partly regulated through stability of a JAZ protein. This is mediated by the RING E3 ligase KEG, which is promoted for self-ubiquitination and subsequent degradation by ABA. KEG normally decreases the COI1-mediated degradation of JAZ12, but this is prevented under high ABA conditions due to degradation of KEG, leading to reduced JAZ12 levels (Pauwels *et al.*, 2015). This was associated with an enhanced expression level of the MYC branch marker gene *VSP2* under basal conditions in a *keg* knockdown line (Pauwels *et al.*, 2015). No evidence was found for a role of JAZ (de)stabilization in antagonistic SA/JA crosstalk on JA-responsive gene expression when plants were exogenously treated with SA and/or MeJA (Van der Does *et al.*, 2013, Liu *et al.*, 2016). However, a role for SA-mediated JAZ degradation was reported in synergistic SA/JA crosstalk occurring during ETI triggered by *P. syringae* pv. *maculicola* (*Psm*) ES4326 carrying the effector AvrRpt2 (Liu *et al.*, 2016). JAZ proteins were shown to bind to the SA response regulators NPR3 and NPR4, and this binding was enhanced by SA. Being substrate adaptors for Cullin 3 (Cul3) ubiquitin E3 ligases, NPR3 and NPR4 target the JAZs for degradation (Liu *et al.*, 2016; Figure 2). This results in increased JA signaling, which is necessary for a full HR response. It is unclear why SA-mediated breakdown of JAZ proteins would occur only during ETI triggered by *Psm* ES4326 AvrRpt2 but not after exogenous SA application. In rice, BR/JA crosstalk is regulated through modulation of OsJAZ4 stability (He *et al.*, 2020). This is mediated by OsGSK2, a kinase that itself is negatively regulated by BR in Arabidopsis through dephosphorylation and degradation (Peng *et al.*, 2008, Kim *et al.*, 2009, He *et al.*, 2020). OsGSK2 was shown to interact with and phosphorylate OsJAZ4, which subsequently leads to disruption of the OsJAZ4-OsNINJA and OsJAZ4-OsJAZ11 interaction and to degradation of OsJAZ4 in an OsCOI1-dependent manner (He *et al.*, 2020). In accordance, high BR levels lead to reduced OsGSK2 levels and activity, which in turn leads to higher OsJAZ4 levels and thus decreased JA signaling, resulting in enhanced susceptibility to the Rice black-streaked dwarf virus (He *et al.*, 2017).

SA/JA antagonistic crosstalk is partly regulated through modulation of stability of the ERF branch master regulator TF ORA59, a master regulator in the ERF branch of the JA pathway (Pré *et al.*, 2008). SA treatment leads to breakdown of ORA59 (Van der Does *et al.*, 2013, He *et al.*, 2017), but not in an *ein3 eil1* mutant (He *et al.*, 2017). Furthermore, SA increases EIN3 protein abundance and co-transfection of *EIN3* and *ORA59* in *Nicotiana benthamiana* leads to degradation of ORA59, unless a proteasome inhibitor is added (He *et al.*, 2017). Also, EIN3 interacts with ORA59 (He *et al.*, 2017). Hence, the SA-mediated degradation of ORA59 depends on the interaction of ORA59 with EIN3 and likely also its homolog EIL1 (Figure 2B). However, the underlying molecular mechanism by which SA can induce EIN3-mediated breakdown of ORA59 is not completely clear. It is unlikely that the SA-increased protein abundance of EIN3 can explain SA-mediated ORA59 degradation, since ET also increases EIN3 protein abundance (Dolgikh *et al.*, 2019), but has a positive effect on ORA59 functioning in the ERF branch of defense (Pré *et al.*, 2008). We propose that SA modulates the activity of EIN3 such that it specifically causes degradation of ORA59 (Figure 2B, dotted line). Recently, it was found that the SA master transcriptional regulator NPR1 can bind to EIN3 and repress its transcriptional activity in regulation of apical hook formation (Huang *et al.*, 2020; Figure 2B). Hypothetically, an NPR1-EIN3 interaction may also be required for EIN3-mediated breakdown of ORA59 during SA/JA crosstalk. In contrast, under high ET conditions, which would increase EIN3 levels, the SA/JA crosstalk was shown to be independent of NPR1 (Leon-Reyes *et al.*, 2009), making this hypothesis very unlikely. This suggests that another protein that functions in the SA pathway must be the missing link for SA/JA crosstalk via EIN3-mediated ORA59 degradation.

Crosstalk by competitive binding of proteins to multiple other proteins

A regulatory protein can be held inactive if binding to its downstream target protein is prevented due to its bound status to another protein. An example of such a crosstalk mechanism that is based on competitive binding to multiple proteins is provided by the interaction between JAZs and DELLAs, which are repressors of the JA response and the GA response, respectively (Hou *et al.*, 2010). When they are bound to each other, JAZs compete for binding of DELLAs to growth-promoting PIF TFs, and DELLAs compete for binding of JAZs to the JA master regulator MYC2 (Hou *et al.*, 2010, Hou *et al.*, 2013; Figure 2). When plants are attacked by an insect the JA levels rise, causing degradation of JAZs, and thus release of MYC2, so that JA-responsive transcription is initiated. At the same time, more DELLAs can bind to PIFs, and elongation growth is inhibited. Other JA-pathway-regulating TFs that physically associate with JAZs, such as EIN3 and EIL1, are likely also indirectly affected by DELLAs, which may impact transcription of *ORA59* (Hou *et al.*, 2013; Figure 2). In contrast, if GA levels are high, such as under far-red light

conditions (Franklin, 2008), DELLAs are degraded, thereby releasing PIFs and thus leading to elongation growth, while the JAZs can now bind more MYC2, leading to repression of JA-mediated defense responses (Hou *et al.*, 2013; Figure 2). This crosstalk mechanism between JA and GA signaling is traditionally viewed as important for regulation of the defense-growth trade-off (Hou *et al.*, 2013). However, recently, conflicting results on the role of the JAZ-DELLA interaction in the JA-mediated growth effects were reported, and other interaction points of the JA pathway with growth signaling have been pinpointed (Chakraborty *et al.*, 2019, Liu *et al.*, 2019, Major *et al.*, 2020, Ortigosa *et al.*, 2020).

Crosstalk by redox regulation and ROXY glutaredoxins

Redox status is an important determinant of protein functioning and as such plays a role in plant defense hormone signaling, among which hormone crosstalk. The defense hormone SA itself induces cycles of oxidation and reduction in the cell, leading to an increase in the amount of the antioxidant glutathione and changing the ratio between the oxidized and reduced state of glutathione (Spoel and Loake, 2011). The changes in redox potential and the change in glutathione state as a result of SA elevation has consequences for oxidation or reduction of cellular proteins, and thereby modulates their function. The increase in glutathione levels was found to coincide with the time frame in which SA could suppress JA signaling. That is, SA treatment prior to MeJA treatment led to a reduction of MeJA-induced *PDF1.2* expression only if MeJA was applied in the time frame when glutathione levels were increased by SA. Additionally, chemical inhibition of glutathione biosynthesis severely diminished the ability of SA to suppress MeJA-induced *PDF1.2* expression (Koornneef *et al.*, 2008). This suggests that the SA-induced shift in redox potential is involved in SA/JA antagonistic crosstalk.

Glutaredoxins are small oxidoreductases that are involved in reduction of oxidative modifications using glutathione (Ströher and Millar, 2012). Four of the CC-type glutaredoxins, which are also known as ROXYs and include GRX480, are induced by SA and can suppress induction of *ORA59* by EIN3, making them potential candidates for SA-mediated crosstalk on the ERF branch (Zander *et al.*, 2012; Figure 2B). Several lines of evidence indicate that under high ET levels group II TGA TFs regulate *ORA59* induction, but that the TGAs recruit ROXYs under high SA levels (Ndamukong *et al.*, 2007, Zander *et al.*, 2010, Zander *et al.*, 2012, Zander *et al.*, 2014). It was believed that this would lead to redox modification of the TGAs, which would cause a decrease of their transcriptional activity. However, the ROXYs were recently shown to recruit the co-repressor TPL through the same motif that was shown to be essential for repression of *ORA59* transcription (Uhrig *et al.*, 2017). This suggests that the effect of GRX480 and other ROXYs on SA/ERF branch crosstalk via suppression of TGA-mediated transcription of *ORA59* is caused by recruitment of a transcriptional co-repressor rather than by redox modification.

CROSTALK AT THE GENE EXPRESSION LEVEL

Regulation of gene expression is a major mechanism of hormone crosstalk. In fact, most of the regulation at the protein level that is discussed above eventually leads to altered transcription of downstream target genes. In this section we discuss that crosstalk can act across multiple regulatory scales of gene expression, from binding of a TF to the promoter of a gene to translation of mRNA to protein.

Crosstalk by binding of TFs to promoters

Most TFs have affinity for binding to a specific DNA motif (Franco-Zorrilla *et al.*, 2014, Weirauch *et al.*, 2014, O'Malley *et al.*, 2016). TF-DNA binding in the promoter region of a gene largely determines activation or repression of transcription. A gene may be subjected to crosstalk if, for example, TFs from different hormone pathways compete for binding to the same DNA motif in the promoter of a gene. Also, binding of different TFs to different DNA motifs or cooperative binding of different TFs to the promoter of a gene may modulate the expression of that gene by multiple hormones. The increasing amount of available ChIP-seq and DAP-seq data (of currently >500 Arabidopsis TFs) greatly facilitates the identification of DNA motifs and their trans-acting TFs (O'Malley *et al.*, 2016, Zander *et al.*, 2020). Besides DNA sequence, many other factors determine where a TF binds to DNA, as demonstrated by the fact that TFs from the same family often bind to very similar motifs, but regulate divergent genes (O'Malley *et al.*, 2016). This can for example be determined by the chromatin structure, which can be more compact or relaxed, depending on acetylation/methylation/ubiquitination of the histones. This local chromatin status of genomic DNA influences the exposure of *cis*-regulatory DNA elements for proteins and consequently transcription. Additional important factors that determine transcriptional activity are the 3D structure of the DNA (Muiño *et al.*, 2014, Mathelier *et al.*, 2016), methylation of the DNA (O'Malley *et al.*, 2016), and spacing between adjacent DNA motifs (Krawczyk *et al.*, 2002, O'Malley *et al.*, 2016). Although to our knowledge these types of information have not been implicated in hormone crosstalk research yet, they provide an enormous potential to uncover cross-regulatory mechanisms based on differential TF-DNA binding.

Investigations with overexpression and/or knockout lines implied a role for several SA-activated WRKY TFs in SA/JA crosstalk (reviewed by Caarls *et al.* (2015)). The role of the WRKY-bound W-box motif in SA/JA crosstalk was investigated using RNA-seq data derived from time course experiments with MeJA, SA and MeJA+SA combination treatments (See also section 'Network modeling using time series of hormone treatments of wild-type plants'). The W-box was, as expected, significantly enriched in SA-upregulated genes as well as in MeJA-downregulated genes (Hickman *et al.*, 2017, Hickman *et al.*, 2019).

However, there was no enrichment of the W-box in MeJA-upregulated genes that were antagonized by SA in the combination treatment (Hickman *et al.*, 2019). This is in contrast with a previously reported microarray-based study of a single, relatively late time point (28 h), in which the W-box was enriched in a small number of ERF branch response genes that were upregulated by MeJA, but antagonized by the combination with SA (Van der Does *et al.*, 2013). This difference may be explained by the fact that compared to the above-mentioned RNA-seq study the ERF branch was activated to a higher extent by the MeJA treatment in the latter experiment. Thus, WRKY TFs may regulate SA/JA crosstalk through binding to a subset of promoters of MeJA-inducible genes in the ERF branch to repress their expression under certain conditions, but likely do not play such a role in the entire JA pathway, which is in line with the finding that in contrast to the ERF branch response genes, the MYC branch response genes that were antagonized by SA were not enriched in the W-box (Van der Does *et al.*, 2013).

Two other motifs, the GCC-box and the G-box, which are mostly known for their role in JA and ET signaling, may also be important in SA-mediated crosstalk. These motifs are bound by ERF TFs, among which ORA59, and bHLH TFs, among which MYC2, respectively. Both motifs are enriched in MeJA-induced genes that are suppressed by SA (Van der Does *et al.*, 2013, Hickman *et al.*, 2019). Moreover, a synthetic promoter only containing four repeats of the GCC-box was demonstrated to be inducible by a single MeJA treatment but repressed by a combination treatment of MeJA and SA (Van der Does *et al.*, 2013). A study by Caarls *et al.* (2017) investigated if this was caused by repressive SA-induced ERFs or EAR-domain containing ERFs that may compete with JA-induced ERF activators for binding to target genes in the ERF branch. Gene expression analyses of 16 *erf* mutants learned that the tested ERFs are not required for SA/JA crosstalk. To the best of our knowledge there are also no potential JA-pathway-repressing bHLH TFs from the SA pathway known. It is worth noting that there is a clade of bHLH TFs that repress the JA pathway, consisting of JAM1, JAM2 and JAM3, but they are described as JA-responsive rather than SA-responsive (Sasaki-Sekimoto *et al.*, 2013). Together, these results suggest that it is unlikely that the JA pathway is antagonized through large-scale binding of SA-responsive TFs directly to the promoters of JA-activated genes. Instead SA may antagonize the JA pathway by inhibiting the transcriptional activity of certain key activator TFs of the JA pathway such as ORA59 and MYC2. In agreement with this hypothesis, SA treatment is known to cause reduced transcription of the *ORA59* gene and degradation of the ORA59 protein (see sections 'Crosstalk by modulation of protein stability' and 'Crosstalk by redox regulation and ROXY glutaredoxins', and Figure 2B).

There is ample evidence for extensive regulation of ORA59 and MYC2 by several proteins that are involved in hormone crosstalk (previous and subsequent sections, Figure 2), but the exact underlying mechanisms have not always been elucidated. For example, Verhage *et al.* (2011) showed that basal and caterpillar-induced *ORA59* mRNA levels were

higher in a *myc2* mutant and caterpillar-induced *MYC2* levels were higher in an *ORA59* RNAi-line. This suggests that *MYC2* and *ORA59* directly or indirectly repress each other's transcription (Figure 2), in addition to the reciprocal inhibitory effects of binding between *MYC2* and EIN3, the upstream regulator of *ORA59* (Figure 2 and section 'Crosstalk by protein-protein interactions'). Later, it was shown that repression of *ORA59* by *MYC2* was mediated by direct binding of *MYC2* to a G-box in the *ORA59* promoter (Zhai *et al.*, 2013), but to the best of our knowledge the mechanism underlying the repressive effect of *ORA59* on transcription of *MYC2* has not been elucidated yet. Another example is the finding that *MYC2* is transcriptionally upregulated by both JA and ABA and can itself regulate genes in both JA and ABA signaling (Abe *et al.*, 1997, Abe *et al.*, 2003, Hickman *et al.*, 2017; Figure 2). As such, *MYC2* is both an integrator and regulator of JA and ABA signaling. Possibly, the enhanced *MYC2* expression by ABA treatment is related to ABA-enhanced JA biosynthesis (see section 'Crosstalk at the hormone homeostasis level'), which not only activates *MYC2* transcriptional activity but also enhances transcription of *MYC2* through auto-regulation (Wang *et al.*, 2019; Figure 2).

Crosstalk by the Mediator complex

The multiprotein Mediator complex forms the molecular bridge that relays signals from DNA-binding TFs to the transcription machinery (Zhai and Li, 2019). It plays an important role in hormone signaling pathways, including in hormone crosstalk. MED25 is the most studied Mediator subunit in defense hormone signaling. It interacts with the TFs *MYC2*, *MYC3*, *MYC4*, *ORA59* and *ERF1*, as well as with the JA receptor component *COI1*. In doing so, MED25 is involved in the transcriptional activity of these TFs in both the *MYC* and *ERF* branch (Çevik *et al.*, 2012, Chen *et al.*, 2012, An *et al.*, 2017). Additionally, MED25 promotes JAZ breakdown by recruiting *COI1* to target promoters (An *et al.*, 2017). Vice versa, JAZ proteins inhibit the MED25-MYC interaction (Zhang *et al.*, 2015; Figure 2A)

MED25 promotes transcription in the JA pathway via various mechanisms such as recruitment of RNA polymerase II, histone acyltransferase *HAC1* and JA-related enhancers to promoters that are targeted by for example *MYC2* and *ORA59* (Çevik *et al.*, 2012, Chen *et al.*, 2012, An *et al.*, 2017, Wang *et al.*, 2019, You *et al.*, 2019; Figure 2). Moreover, MED25 has a role in alternative splicing of JAZ proteins, which determines their sensitivity to JA (Wu *et al.*, 2020; Figure 2A). This multifaceted role makes MED25 an obvious candidate player in crosstalk regulation. Indeed, *med25* mutant studies and interaction studies of MED25 with *MYC2* and *ABI5* (key regulators of JA and ABA signaling, respectively) suggest that it plays a positive role in JA signaling but has a negative role in ABA signaling (Chen *et al.*, 2012).

Other Mediator subunits have also been implicated in defense hormone crosstalk. This was mostly based on mutant studies. MED14, MED15 and MED16 were found to be involved in suppression of *MYC* branch marker genes by SA and ET (Wang *et al.*, 2015,

Wang *et al.*, 2016). This suggests that these three Mediator subunits are required for SA/JA and ERF branch/MYC branch crosstalk. In another study, MED18 and MED20 were found to be involved in activation of transcription of *MYC2* and the MYC branch marker gene *VSP1* by *Fusarium oxysporum*, and in repression of SA pathway marker genes (Fallath *et al.*, 2017; Figure 2A). It is important to note that in all experiments the Mediator subunits were not only found to suppress a certain pathway, but also to activate another pathway that is known to antagonize the suppressed pathway. Therefore, it is possible that the repression by Mediator subunits is not a direct effect on that pathway, but rather an indirect effect resulting from activation of a repressor derived from the antagonizing pathway. For example, MED16 was found to suppress MYC branch marker gene expression, but also to activate *ORA59* expression (Wang *et al.*, 2015; Figure 2B). *ORA59* represses *MYC2* expression (see section 'Crosstalk by binding of TFs to promoters' and Figure 2A), which may explain how MED16 causes suppression of MYC branch response genes.

Crosstalk affecting mRNA maturation and translation to protein

Above we described the different steps in initiation of transcription. The subsequent steps in gene expression are also potential points of crosstalk. For example, crosstalk may act through modulation of alternative splicing, stability of mRNA, retention of mRNA in the nucleus or translation efficiency of mRNA into protein in the cytosol. In ET and JA signaling extensive regulation of these regulatory steps is suggested by the findings that only a subset of genes that are bound by key TFs show alterations in mRNA levels (Chang *et al.*, 2013, Zander *et al.*, 2020) and that transcript and protein abundance do not match up after MeJA treatment (Zander *et al.*, 2020).

Some JAZ proteins undergo alternative splicing, potentially making them insensitive to JA-Ile-induced breakdown mediated by COI1 (Chung *et al.*, 2010). So far, no evidence for selective favoring of undegradable JAZ isoforms during SA/JA crosstalk has been found (Van der Does *et al.*, 2013). The *myc2* mutant was shown to affect phosphorylation of proteins that act in the spliceosome (Zander *et al.*, 2020). In agreement with this, the isoforms of 151 transcripts were switched after MeJA treatment (Zander *et al.*, 2020). Only two of these genes were related to JA, while the rest was related to other processes, including ABA signaling. This suggests that *MYC2* can influence other signaling pathways by modulation of transcript splicing. However, the importance of this observed alternative splicing by JA and the role of *MYC2* in this mechanism needs further investigation.

Besides stability of proteins, also stability of mRNA molecules themselves may potentially serve as a way for hormones to influence each other's pathway activities. A role for RNA-binding proteins and small RNAs (Narsai *et al.*, 2007) in determining mRNA stability during plant immune responses and root nodule symbiosis has been indicated (Staiger *et al.*, 2013, Zanetti *et al.*, 2020). For proper responsiveness to the hormone ET, the

mRNA of the F-box protein-coding gene *EBF2* is targeted to decay in P-bodies (Merchante *et al.*, 2015). However, to the best of our knowledge the role of mRNA stability in hormone crosstalk has not been explored yet.

Mature mRNAs can be temporarily disengaged from the translation process by retaining them in the nucleus. There is recent evidence for a role of nuclear retention of selective mRNAs in the control of gene expression activity during adaptation to hypoxia, an abiotic stress. After reaeration the mRNAs are quickly released to the cytosol to be translated into protein (Lee and Bailey-Serres, 2019). However, there is no evidence yet that regulation of plant immunity or hormone crosstalk acts on temporary retention of mRNAs in the nucleus in order to divert all the plant's molecular attention to the most critical response.

The final step in gene expression is that from translation of mRNA into protein. Translation efficiency is influenced by different features of the mRNA (Merchante *et al.*, 2017). The literature on translational regulation of plant immunity, although scarce, points to translational control of specific mRNAs via upstream, short open reading frames (uORFs) during defense activation by the pathogen elicitors AvrRpm1 and elf18 in Arabidopsis (Pajeroska-Mukhtar *et al.*, 2012, Meteignier *et al.*, 2017, Xu *et al.*, 2017). The elicitor treatments transiently alleviate the repressive effect of the uORFs on expression of the main ORF, heat shock factor gene *TBF1*, so that ribosomes can engage in its translation, leading to activation of the immune system. Furthermore, it has been shown that in establishment of root nodule symbiosis small RNAs are crucial, because they determine stability and translatability of mRNAs (Zanetti *et al.*, 2020). If and how control at the translation level can affect crosstalk between different hormone pathways in defense is not known yet.

CROSSTALK AT THE HORMONE HOMEOSTASIS LEVEL

The previous sections focused on crosstalk by hormones via their interference with responsiveness to other hormones, namely downstream of these other hormones. Here, we describe effects that hormones have on the levels of other hormones. For example, ABA is known to enhance the biosynthesis of JA (Adie *et al.*, 2007, Fan *et al.*, 2009, Wang *et al.*, 2018). This is correlated with the ABA-induced expression of *PLIP2* and *PLIP3*, which encode lipases that catalyze the release of polyunsaturated fatty acids (PUFAs) (Wang *et al.*, 2018), which can be further metabolized to form JA (Wasternack and Hause, 2013). In accordance, overexpression lines of *PLIP2* and *PLIP3* show enhanced JA signaling (Wang *et al.*, 2018). The ERF TF gene *ORA47* is upregulated via *MYC2* by JA treatment (Zander *et al.*, 2020) and directly targets promoters of JA and ABA biosynthesis genes, which leads

to enhanced JA levels, and upon wounding also to enhanced ABA levels (Pauwels *et al.*, 2008, Chen *et al.*, 2016, Hickman *et al.*, 2017, Zander *et al.*, 2020). Hence, the canonical JA pathway regulator MYC2 acts at multiple levels as an integrator of JA and ABA signaling: MYC2 is itself positively regulated by JA and ABA at the protein and gene expression level (see sections 'Crosstalk by protein-protein interactions' and 'Crosstalk by binding of TFs to promoters') and subsequently, MYC2 regulates JA and ABA levels. Apart from activating JA biosynthesis genes, MYC2 also activates transcription of JAZ repressors, whose protein products in the long term attenuate the JA response via repression of MYC2 and other JA master regulators (Chini *et al.*, 2007). This form of short-term self-activation and long-term self-inhibition of MYC2 is reinforced by MED25. This mediator subunit promotes looping of a MYC2 enhancer, which is also bound by MYC2 itself, to the MYC2 promoter. For unknown reasons this leads to self-activation of the MYC2 promoter during short-term JA responses but inhibition of the MYC2 promoter during long-term JA responses (Wang *et al.*, 2019). Besides JA, other hormones also activate or repress transcription of different JAZ genes, which potentially modulates JA responsiveness, resulting in synergism, antagonism, or reestablishment of the basal situation when both pathways are elicited in the same cell (Hickman *et al.*, 2019).

SA and JA can also influence each other's levels. RNA-seq analyses of MeJA treatment pointed to repression of JA and SA biosynthesis genes by the respective reciprocal treatments with SA and MeJA (Hickman *et al.*, 2017, Hickman *et al.*, 2019). Several underlying mechanisms for this antagonism in transcriptional activity and the resultant decrease in hormone levels have been elucidated. For example, SA inhibits activity of the catalase CAT2, which leads to reduced activity of the acyl-CoA oxidases ACX2 and ACX3, which are enzymes involved in JA biosynthesis. This effect of SA leads to lower JA levels and reduced defense against *Botrytis cinerea* (Yuan *et al.*, 2017). Additionally, WRKY51, which is transcriptionally activated by SA, inhibits JA biosynthesis by repressing transcription of the JA biosynthesis gene AOS (Yan *et al.*, 2018). This repression is mediated by a complex containing WRKY51, JAV1 and JAZ8. However, during wounding JAV1 is degraded, leading to de-repression of AOS and increased JA biosynthesis (Yan *et al.*, 2018). Vice versa, JA also has the potential to reduce free SA levels. This is exploited by biotrophic pathogens to reduce effective plant defense responses. For example, *Pseudomonas syringae* pv. *tomato* (Pst) DC3000 produces the JA-Ile mimic coronatine (COR), which, via MYC2, MYC3 and MYC4, activates transcription of three NAC transcription factors, ANAC019, ANAC055 and ANAC072 (Zheng *et al.*, 2012, Gimenez-Ibanez *et al.*, 2017). These NAC TFs repress expression of the SA biosynthesis gene *ICS1* and activate expression of the SA methyltransferase gene *BSMT1* (Zheng *et al.*, 2012). This leads to lower levels of free SA and reduced defense against *Pst* DC3000. The bacterial effectors HopX1 and HopZ1a (see section 'Crosstalk by modulation of protein stability') are likely to have the same effect on free SA levels as COR has. This was investigated for HopZ1a, which reduces

the transcription level of *ICS1* (Jiang *et al.*, 2013). Another study found that the negative effect of MYC2 on SA accumulation is antagonized by EDS1 during ETI that is triggered by the pathogen effector AvrRps4 (Cui *et al.*, 2018; Figure 2A). This antagonism by EDS1 involves the competitive binding of EDS1 to PAD4, which otherwise binds to MYC2. This results in reduced binding of MYC2 to the *ANAC019* promoter and less *BSMT1* expression, thus enhancing SA levels (Cui *et al.*, 2018, Bhandari *et al.*, 2019).

Research on the effect of crosstalk on hormone levels has been restricted mostly to measurements of the (proven) active compound, like JA or JA-Ile. However, the concentrations of hormone derivatives, resulting from effects on biosynthesis or catabolism, will also change and these may also modulate plant responses. For example, a mutation in the JA biosynthesis gene *OPR3* that completely blocked the canonical JA biosynthesis pathway and led to accumulation of the JA precursors OPDA and dn-ODPDA enabled research on the role of these compounds in the absence of JA (Chini *et al.*, 2018). It was demonstrated that these JA precursors promote thermotolerance through a mechanism independent of COI1 in Arabidopsis as well as in a bryophyte and a charophyte alga (Monte *et al.*, 2020). Whether hormone derivatives are targeted by other hormones and whether the derivatives themselves could affect other hormone pathways remains to be investigated.

PERSPECTIVES

This review reports on several molecular components in hormone crosstalk that regulate plant defense responses. In most cases their regulation at the transcriptional or protein level has been demonstrated, but the exact mechanisms underlying their role in hormone crosstalk have often not been fully elucidated yet. The integration of data derived from different technologies aiming to address different regulation levels have the potential to unveil these crosstalk mechanisms in different internal and external contexts of the plant.

The network-level understanding of defense hormone crosstalk as a whole is still rudimentary. Until now, most research has been restricted to the use of hormone mutants, single hormone applications, or TF-DNA binding studies under control conditions. These systems approaches gave us a little glimpse of regulatory nodes in hormone signaling networks and their possible role in hormone crosstalk. However, addition of multiple hormones and the integration of multiple data types regarding different levels of regulation are crucial to unveil new crosstalk mechanisms. Such multi-omics research is now possible thanks to modern wet-lab technologies as well as advanced data analysis and modeling tools (Zander *et al.*, 2020). A network-level understanding of crosstalk is also necessary to ultimately grasp the impact of hormone signal integration under different conditions for the plant. Therefore, we need to learn not only the 'how', but also

the 'when' and 'where' of hormone crosstalk. In addition to interactions with microbes and insects, other environmental conditions of the plant and the internal context in the plant determine its hormone balance and hormone responsiveness (Figure 1). Indeed, the extent of crosstalk between hormone pathways during immune responses has been shown to be influenced by additional stresses, location of the stimulus, and plant age. Likely, different crosstalk mechanisms, such as described above and below in this review, are engaged in different situations and are regulated in a spatiotemporal manner.

The order in which sequential stresses occur and the nature of the stresses determine whether hormone crosstalk is effective. For example, for primed expression of JA-mediated defenses in systemic tissue that expresses *MYC2* after local herbivory by caterpillars of *Pieris rapae*, the ABA pathway needs to be activated by a secondary infestation (Vos *et al.*, 2013b). In contrast, ABA can inhibit the JA pathway in tissue that is primed for dehydration stress: a first experience of dehydration stress leads to induction of the JA pathway, but this does not occur during a second dehydration stress (Ding *et al.*, 2013), which is likely due to a lack of *MYC2* activation during the second stress if ABA levels had already increased previously (Liu *et al.*, 2016, Avramova, 2019). An RNA-seq experiment studying responsiveness to the sequential stresses drought, herbivory and necrotrophic pathogen infection showed that the transcriptome profiles during the sequential stresses rapidly change to largely resemble those of the last stress (Coolen *et al.*, 2016). This shows that many crosstalk mechanisms can be overridden by a second, dominating stress. Nevertheless, it was also found that the first stress leaves a relatively small expression signature, which is enriched for hormone signaling genes, suggesting a lasting effect of induced hormone signaling by the first stress.

A spatial separation between SA and JA signaling has been demonstrated when a local HR is activated during ETI as a result of infection with the avirulent pathogen *Pst* DC3000 carrying *AvrRpt2*. The zone around the HR-induced cell death is surrounded by a small layer where the SA marker gene *PR1* is highly expressed, followed by a region where the JA marker gene *VSP1* is highly expressed. This demands differential prioritization of SA versus JA antagonism mechanisms. In the SA-zone SA-mediated defenses against *Pst* DC3000 *AvrRpt2* can be activated, while in the JA-zone runaway cell death and secondary infections by necrotrophic pathogens are limited, which could otherwise take advantage of the dead tissue generated by the HR response (Betsuyaku *et al.*, 2018).

Leaf age is another factor that can influence hormone crosstalk. Biotic and abiotic stress responses are differently balanced in older leaves compared to younger leaves (Berens *et al.*, 2019). Abiotic stress suppresses immune responses in older leaves through ABA. This antagonistic effect on immunity is blocked in young leaves, which is dependent on NPR1 as well as on the SA biosynthesis component PBS3, but independent of ICS1. This suggests an SA-independent function of NPR1 and PBS3 in regulating leaf-age dependent crosstalk (Berens *et al.*, 2019).

Above examples illustrate that knowing the ‘when’ and ‘where’ of hormone pathway integration in immune networks is important to predict the outcome of immune signaling. To advance our knowledge, future research should focus on the different levels of hormone network regulation under different internal and external conditions. For such biological experimental systems, it would be even more meaningful to use single-cell methods instead of bulk analyses. This will provide a better spatiotemporal resolution, which is particularly powerful when studying plant-microbe interactions, where relevant molecular events are often restricted to localized cell populations (of specific cell types), ranging from being infected themselves, to residing in the same leaf or in distant tissue and not (yet) being infected. Together, this molecular and systems level knowledge is crucial to design crops with a strengthened immune response without undesired side-effects like enhanced sensitivity to other stresses or decreased plant growth and yield.

OUTLINE OF THE THESIS

Plant hormones control plant immunity and other essential plant processes via elaborate, interconnected GRNs. In the past decades, scientists have gained substantial knowledge on the architecture of hormone-driven GRNs regulating plant defense, and have found numerous examples of crosstalk between these GRNs. However, several major questions remain within this scientific field. For example, while SA/JA crosstalk has received considerable scientific attention, mechanisms that govern ABA/JA crosstalk have not been so well studied. Also, the dynamics of immune-related GRNs and crosstalk between these GRNs have not been well studied, except for our earlier studies on the JA and SA GRNs (Hickman *et al.*, 2017, Hickman *et al.*, 2019). Finally, while many mechanisms involved in SA/JA crosstalk have been found, some details hereof are still unclear, and additional mechanisms may still be undiscovered.

In this thesis, we investigate the architecture and dynamics of hormone-driven GRNs in plant immunity. More specifically, we focus on the modulation of the JA GRN by the ABA GRN and specific components of the SA GRN. In earlier work we already investigated the (single) JA and SA GRNs (Hickman *et al.*, 2017, Hickman *et al.*, 2019), therefore in **Chapter 2** of this thesis we describe our analysis of the architecture and dynamics of the ABA GRN. We analyzed a high-density time series experiment of ABA-treated Arabidopsis rosettes. We show that the ABA GRN consists of several dozens of co-expressed gene modules with partly unique and partly overlapping functions. We then integrated our data with publicly available DAP-seq data and data of ABA-treated Arabidopsis seedlings inhibited in translation to predict important TFs regulating the ABA GRN, and infer a model of the ABA GRN, consisting of three regulatory hierarchical levels. The predicted TFs came

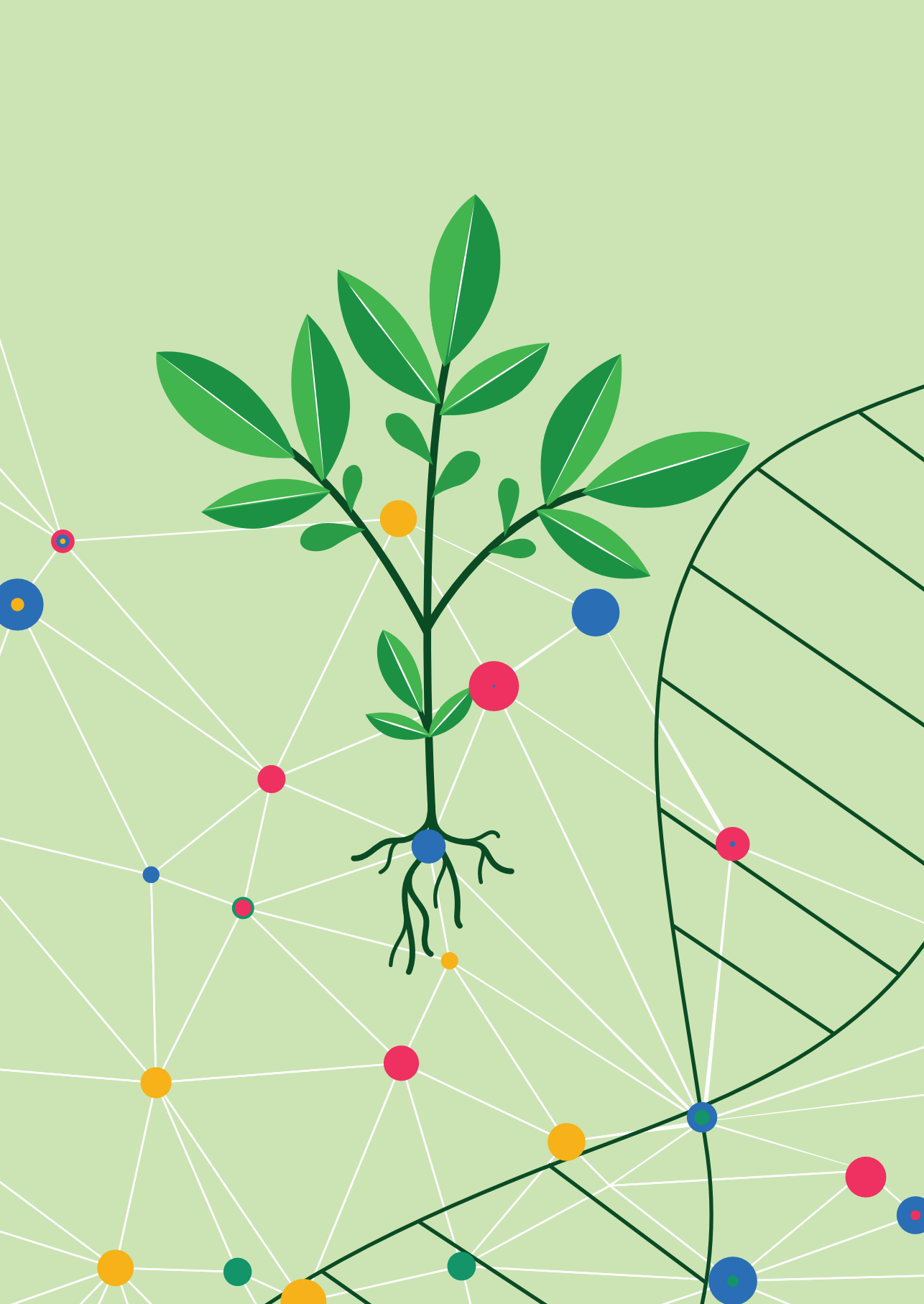
from a diverse set of TF families, with the bZIP family being the most prominent. Finally, we validated the biological importance of newly predicted TFs in the ABA GRN, and this showed that the trihelix TF GT3a is an ABA-activated regulator of drought tolerance.

In **Chapter 3** we describe our analysis of how the ABA GRN modulates the JA GRN. For this, we analyzed the ABA time series data, as well as time series data of MeJA-treated Arabidopsis rosettes (described by Hickman *et al.* (2017)) and of ABA + MeJA-treated Arabidopsis rosettes, all derived from the same experiment. We show that ABA modulates expression of around 2/3rd of all MeJA-responsive genes. We also show that the ABA and JA GRNs have substantial similarities, and that their combined effect on gene expression is often not additive. We also show that ABA has a large effect on the expression of JA metabolism genes, thus likely affecting JA levels. We also investigated mechanisms controlling ABA/JA crosstalk, which resulted in the prediction of ABA-regulated TFs that affect transcription of MeJA-induced genes, and the discovery that ABA represses the ERF branch of the JA GRN partially by affecting ORA59 protein accumulation independent of its transcription, and by targeting ERF1 at an unknown level. Together, this shows that ABA targets the JA GRN at multiple levels of regulation.

In **Chapter 4** we dive deeper into mechanisms that govern SA/JA crosstalk. We show that NPR1 has a nuclear role in regulating SA/JA crosstalk. We found that when SA activates NPR1, partly by causing its nuclear localization, the transcription of several WRKY TFs is increased. Some of these WRKY TFs repress *PDF1.2* expression, partly by reducing accumulation of ORA59 protein independent of its transcription. Together, this shows that SA affects the JA network via diverse mechanisms, involving nuclear-localized NPR1 and several WRKY TFs with various modes of action.

Chapters 2-4 mostly focus on transcriptional regulation of hormone networks regulating plant immunity. In these chapters we analyzed steady-state mRNA levels (measured via RNA-seq) and TF-target predictions based on *in vitro* experiments. However, many factors determine where and when a TF binds on the DNA and what the fate of the resulting transcribed mRNA is. To better understand (hormone-driven) GRNs in the future it is important that these factors are also investigated in detail. Therefore, in **Chapter 5** we review the state-of-the-art concerning the transcriptional regulation of plant immunity, including many regulatory mechanisms that generally get overlooked. We end this chapter with a look into the future.

Finally, in **Chapter 6** I further discuss the findings of this thesis and put them in a broader perspective. Also, I describe my vision on how research on hormone-driven GRNs in plant immunity should progress in the future.





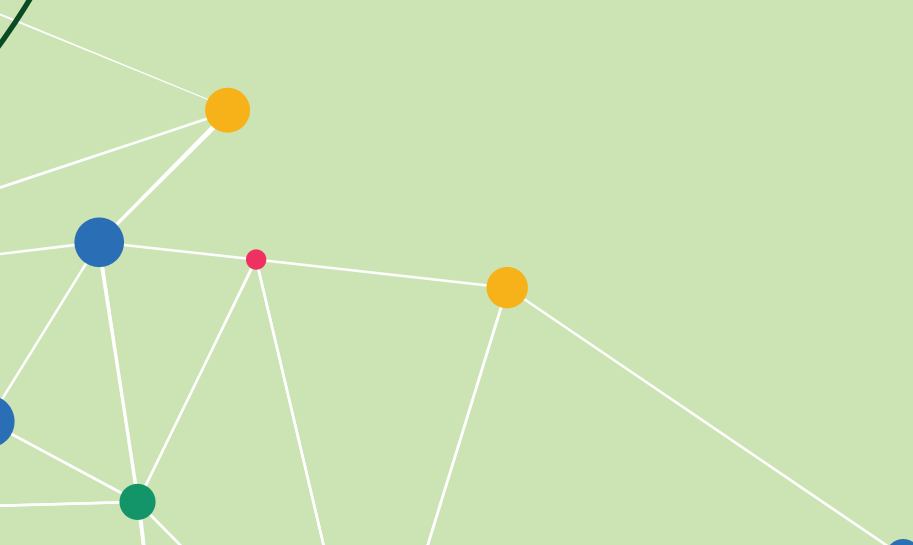
CHAPTER 2

Architecture and dynamics of the abscisic acid gene regulatory network

Niels Aerts¹, Richard Hickman¹, Anja J.H. Van Dijken¹, Michael Kaufmann¹, Basten L. Snoek², Corné M.J. Pieterse¹, Saskia C.M. Van Wees¹

¹Plant-Microbe Interactions, Department of Biology, Utrecht University, P.O. Box 800.56, 3508 TB Utrecht, The Netherlands

²Theoretical Biology and Bioinformatics, Department of Biology, Utrecht University, P.O. Box 800.56, 3508 TB Utrecht, The Netherlands



ABSTRACT

Abscisic acid (ABA) is a plant hormone that regulates essential plant processes in development and responsiveness to abiotic and biotic stresses. ABA perception triggers a post-translational signaling cascade that elicits the ABA gene regulatory network (GRN), encompassing hundreds of transcription factors (TFs) and thousands of transcribed genes. To further our knowledge of the architecture and dynamics of the ABA GRN, we performed an RNA-seq time series experiment consisting of 14 time points in the 16 h following a one-time ABA treatment of 5-week-old *Arabidopsis* rosettes. During this time course, ABA rapidly changed transcription levels of 7151 genes, which were partitioned into 44 coexpressed modules that carry out diverse biological functions. We then integrated our time-series data with publicly available TF binding site data, motif data, and RNA-seq data of plants treated with ABA and the translation inhibitor cycloheximide, and predicted (i) which TFs regulate the different coexpression clusters, (ii) which TFs contribute the most to target gene amplitude, (iii) timing of engagement of different TFs in the ABA GRN, and (iv) hierarchical position of TFs and their targets in the multi-tiered ABA GRN. The ABA GRN was found to be highly interconnected and regulated at different amplitudes and timing by a wide variety of TFs, of which the bZIP family was the most prominent. We biologically validated the importance of TFs with a newly predicted role in the ABA GRN and found that the trihelix TF GT3a is likely an ABA-induced positive regulator of drought tolerance.

INTRODUCTION

During its lifetime, a plant constantly modulates its physiology to optimize development and adaption to its environment. To regulate these processes on a molecular level, plants possess elaborate gene regulatory networks (GRNs). Large parts of these networks are regulated by plant hormones. One of the best studied plant hormones is abscisic acid (ABA). This hormone is involved in different phases of plant development and controls responses against many different stresses (reviewed by Chen *et al.*, 2020). In seeds, ABA promotes desiccation tolerance, de-greening, and accumulation of reserve products; ABA also prevents premature germination. In seedlings, ABA can induce post-germination growth arrest, a process in which growth of a newly germinated embryo is temporarily arrested when exposed to unfavorable conditions, such as drought and high salinity (Lopez-Molina *et al.*, 2001, Chen *et al.*, 2020). In the adult stage, ABA protects the plant against dehydration and (associated) osmotic stress by, among other things, increasing transcription of wax synthesis genes and promoting closure of stomata (Chen *et al.*, 2020). It is also involved in plant immunity, by interacting with jasmonic acid (JA) and salicylic acid (SA) signaling to promote resistance against chewing insects but repress resistance against various pathogens (Pieterse *et al.*, 2012). Furthermore, ABA co-regulates the transport of nutrients from source to sink, promotes senescence and recycling of nutrients for future generations, and influences reproduction by coordinating fruit growth and ripening (Chen *et al.*, 2020).

In the last two decades, molecular studies, mostly using *Arabidopsis thaliana* (hereafter named Arabidopsis), elucidated how ABA is perceived and how this leads to alterations in transcriptional activity. ABA binds to receptors of the PYR/PYL/RCAR family (Fujii *et al.*, 2009, Ma *et al.*, 2009, Park *et al.*, 2009, Santiago *et al.*, 2009). This stimulates their interaction with PP2C and likely also PP2A and TOPP phosphatases, thereby inactivating the phosphatases (Yang *et al.*, 2017). Under low ABA levels, active PP2Cs, PP2As and TOPPs inactivate SnRK2 kinases by dephosphorylation (Fujii *et al.*, 2009, Umezawa *et al.*, 2009, Vlad *et al.*, 2009, Waadt *et al.*, 2015, Hou *et al.*, 2016). When high ABA levels trigger the inactivation of the phosphatases, SnRK2 kinases are no longer repressed so that they can then be activated through autophosphorylation, phosphorylation by other kinases and, in the case of SnRK2.6, persulfidation of cysteine residues by ABA-induced H₂S (Hou *et al.*, 2016, Yang *et al.*, 2017, Chen *et al.*, 2020). Activated SnRK2 kinases can then phosphorylate and thereby activate different transcription factors (TFs) that act as master regulators in the ABA network by subsequently inducing different downstream subnetworks (Umezawa *et al.*, 2010, Song *et al.*, 2016). The networks are regulated both transcriptionally and post-translationally. For example, key components of the network, including ABA receptors, PP2Cs and TFs, can be regulated through ABA-dependent ubiquitination (Yang *et al.*, 2017). The ABA transcriptional gene regulatory network is highly interconnected,

with many genes being regulated by multiple TFs, and TFs facilitating binding of other TFs to neighboring binding sites. The network is built up hierarchically, with some TFs acting higher up in the network and regulating TFs and other genes lower in the network (Song *et al.*, 2016). In summary, the ABA network is activated through post-translational events that induce an elaborate transcriptional cascade, and is further modulated through post-translational regulation.

Many key TFs of the ABA network have been identified. Most belong to the basic leucine zipper (bZIP) family of TFs. For example, the bZIP TFs AREB1, AREB2, ABF1 and ABF3 are activated by ABA treatment, causing them to bind to hundreds of genes with a so-called ABA responsive element (ABRE) in their promoter (Choi *et al.*, 2000, Uno *et al.*, 2000, Yoshida *et al.*, 2010, Yoshida *et al.*, 2015, Sun *et al.*, 2022). Many of these target genes are related to ABA signaling and many are conserved between Brassicaceae species (Sun *et al.*, 2022). Also, the *areb1 areb2 abf1* triple mutant was reported to be more susceptible to drought stress and less sensitive to ABA with respect to primary root growth, thus showing the importance of these TFs in ABA-related abiotic stress responses (Yoshida *et al.*, 2010, Yoshida *et al.*, 2015). AREB3 was also characterized as an ABRE-binding TF, but its role in ABA signaling has not been shown as convincingly as the other AREBs/ABFs (Uno *et al.*, 2000, Bensmihen *et al.*, 2005, Qian *et al.*, 2019). The bZIP TF ABI5 is another well-described master regulator of ABA-related responses, acting downstream of SnRK2 kinases in both seeds and vegetative tissue (Finkelstein and Lynch, 2000, Skubacz *et al.*, 2016). This TF is extensively regulated, both at the transcriptional and post-translational level, and in turn it regulates many responses, which besides ABA signaling also involve crosstalk with other hormone pathways (Skubacz *et al.*, 2016). More recent research has implicated other bZIP TFs in the ABA pathway, such as GBF3, which improves plant tolerance to drought, high salinity and osmotic stress (Ramegowda *et al.*, 2017), although a further characterization of this TF is still needed to better understand the underlying mechanisms. In addition, several members of other TF families such as NF-YB, NF-YC, NAC, MYB, HD-ZIP, C2H2, bHLH, ERF, HSF, WRKY and CAMTA have been associated with ABA-inducible responses (Wu *et al.*, 2009, Rushton *et al.*, 2012, Pandey *et al.*, 2013, Song *et al.*, 2016).

Despite many advances in our understanding of the ABA network, there is still a lot unknown about its overall architecture and dynamics. The most extensive effort to elucidate the ABA GRN was published by Song *et al.* (2016). The authors performed an RNA-seq time series experiment with ABA-treated *Arabidopsis* seedlings and selected 21 TFs for ChIP-seq with and without ABA treatment based on the criteria that they were transcriptionally responsive to ABA in this time series, had high overall expression levels and came from a wide range of TF families. They then used this ChIP-seq and RNA-seq data to reconstruct an ABA-dependent hierarchical GRN. This work provided a considerable improvement in our knowledge of the ABA network in seedlings, but also

had some limitations. For example, their work could limitedly reveal the dynamics of the network because the seedlings were kept continuously in a medium with ABA, and the time series had a relatively low time resolution, namely 4, 8, 12, 24, 36, and 60 h after the start of the treatment. Also, by focusing on TFs that were themselves differentially expressed at the mRNA level, TFs in the ABA signaling network that are regulated by post-translational mechanisms only, were omitted. Finally, it is unclear whether the ABA pathway in seedlings and mature plants is similar.

To further investigate the ABA network, we performed a high-resolution RNA-seq time series experiment, consisting of 14 time points of one-time treated mature Arabidopsis leaves. We integrated our dataset with publicly available microarray data of an ABA treatment in the presence of a translation inhibitor, and with TF-DNA binding data. This generated a three-level hierarchical ABA network, starting with TFs that are predicted to be post-translationally activated or repressed, and ending with clusters of coexpressed genes, which are regulated by the first or second level of TFs. This network contains TFs with a known function in ABA signaling, as well as TFs with a previously unidentified function. We validated a selection of these unknown TFs and found that the Trihelix TF GT3a is a novel ABA-induced regulator of drought tolerance in Arabidopsis.

RESULTS

A high-density time course of ABA-induced transcriptional programming

We profiled the temporal transcriptome changes of Arabidopsis leaves induced by ABA. To this end, the full rosette of a 5-week-old plant was dipped into an ABA (50 μM) or mock solution. The 6th true leaf of the rosette was harvested at 14 time points, consisting of 0.25, 0.5, 1, 1.5, 2, 3, 4, 5, 6, 7, 8, 10, 12 and 16 h after treatment (Table S1). The RNA of three replicates (ABA) or four replicates (mock) per treatment/time point combination was sequenced. The mock time series consisted of more replicates because it had been sequenced in our previous studies analyzing methyl jasmonate (MeJA, a form of JA that is rapidly converted to free JA in the plant) and SA treatments (Hickman *et al.*, 2017, Hickman *et al.*, 2019), which were part of a larger experiment that also contained the ABA treatment (analyzed in the current study). From the Hickman *et al.* studies (2017; 2019) we deduced that three replicates were likely enough for microarray analyses of the remaining hormone samples, thus saving overall costs.

We first inspected the normalized count data (Table S2) by plotting a principal component analysis (PCA). This showed that time after treatment and time-specific treatment effects were the main factors that separated the samples along the first and second principal components, respectively (Figure S1). This demonstrates that circadian

regulation is important for gene expression and suggests that the effect of treatment on gene expression was different at different time points, meaning that we chose an appropriate range of time points to study the transcriptional dynamics of the ABA network. In general, samples from the same time and treatment clustered together, demonstrating that biological variation was limited. Nevertheless, not all time points were separated, especially in the mock treatment and at later stages of the ABA treatment, likely because there the differences between the dense time points were relatively small. For the later-sequenced ABA time series a different library preparation and sequencing method was used than for the mock time series. To verify that these differences in sample processing did not introduce large differences in the data we also sequenced 12 untreated control samples, of which eight were taken along in the processing of the mock time series in the Hickman *et al.* studies and four in the ABA time series analyzed here. These control samples clustered together in the PCA plot regardless of their processing method (Figure S1, see also Methods), indicating that cross-comparisons between the two time series can be safely made.

Clustering analysis identified modules of coexpressed genes associated with specific biological processes

Analysis of differentially expressed genes (DEGs) upon ABA treatment compared to mock treatment over time was done using the same generalized linear model (GLM)-based method as described earlier in our JA network paper (Hickman *et al.*, 2017). A total of 7151 genes were indicated as differentially expressed (Table S3). Of these, 3487 genes were on average upregulated, and 3664 genes were on average downregulated. DEGs were clustered based on their expression profile over time to identify gene sets that potentially have a similar function and are regulated through similar mechanisms. Clustering of coexpressed genes was done on the \log_2 -fold change of ABA/mock treatment using SplineCluster (Heard *et al.*, 2006). This resulted in 17 clusters of predominantly upregulated genes and 27 clusters of predominantly downregulated genes (Figure 1A; Figure S2; Table S4). Most of the upregulated clusters displayed a single peak in expression, after which expression levels declined again. The peak timing varied across the clusters, with one cluster already reaching its peak at 15 min (c11), most clusters peaking between 2-3 h (including c2, c10 and c16 from Figure 1B), and some peaking only after 4 h (e.g., c5 and c6). After the peak, expression generally declined to basal levels (e.g., c3, c4, c10 and c16), or slightly above basal levels (e.g., c1-3). In some cases, the initial drop in expression was followed by a slight, steady increase in expression (c9 and c12). A similar trend of peaks at different times could be observed for the downregulated clusters, many of which had a pattern that resembled a mirrored version of some of the upregulated clusters (e.g., c18, c22-24, c26, c34 and c39-c44; Figure 1 and Figure S2). Clusters with more complex

patterns showing multiple peaks were more prevalent in the downregulated clusters (e.g., c20, c21, c29, c30, c33, c35; Figure 1 and Figure S2), but it should be noted that these clusters typically had a lower expression amplitude and/or represented fewer genes.

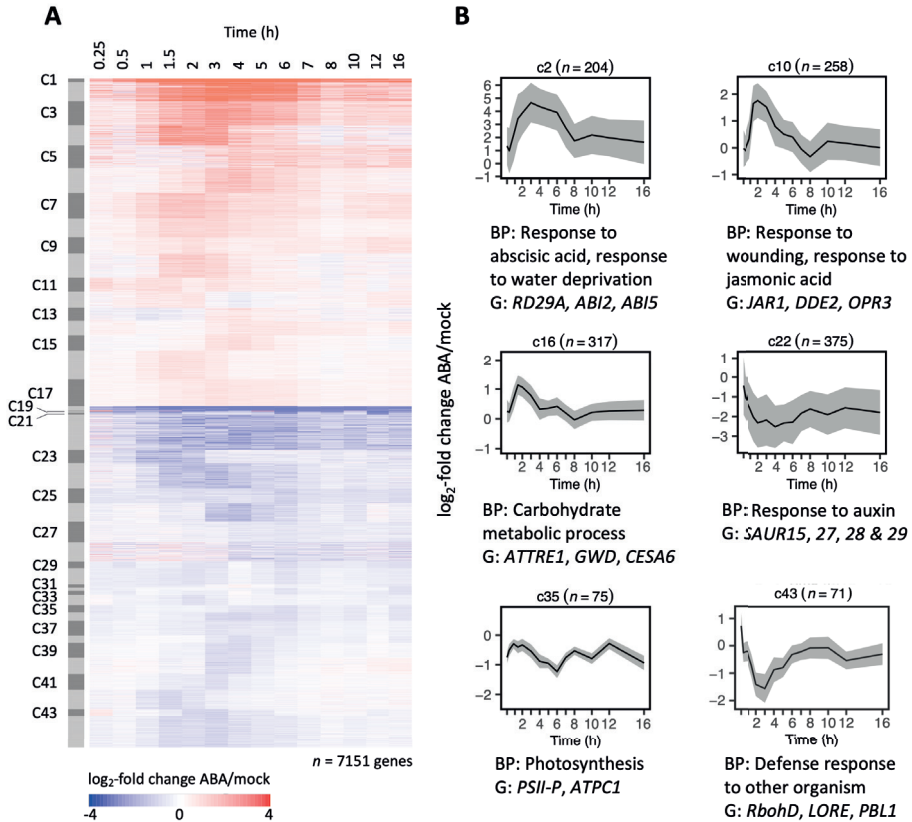


Figure 1: Clustering of coexpressed genes after ABA treatment.

(A) The 7151 DEGs over the time course of 16 h after ABA treatment were clustered according to their expression pattern (\log_2 of ABA/mock) using SplineCluster, resulting in 44 distinct clusters (c1-c44). Each row of the heatmap represents an individual gene and indicates the \log_2 of read counts of ABA/mock treatment.

(B) Representative clusters with distinct functional enrichment. Shown is the mean \log_2 -fold change of ABA/mock over all measured time points (in h) of all genes in a cluster (black line), with grey error bars indicating the standard deviation. Cluster number (c) and cluster size (n , number of genes) are denoted above each plot. Selected enriched biological process GO terms (BP) and representative genes (G) are indicated below each panel. Full results depicting all 44 clusters are available in Figures S2 and full GO term enrichment analysis can be found in Figure 2 and Table S5.

Gene ontology (GO) term enrichment analysis was conducted to identify the biological processes that are regulated by the genes in the different clusters. Multiple clusters of upregulated genes were enriched in GO terms associated with well-known ABA responses, such as 'response to ABA', 'response to water deprivation' and 'response to salt stress' (Figure 1B; Figure 2; Table S5). Clusters of downregulated genes were generally enriched in GO terms related to primary plant functions, such as 'RNA processing', 'ribosome biogenesis', 'translation', 'amide biosynthesis process' and 'photosynthesis' (Figure 1B; Figure 2). This may indicate that the plant attenuates certain general processes to focus on ABA-upregulated responses. Several GO terms were specifically enriched in only one of the clusters, such as 'carbohydrate metabolic process' and 'vacuolar transport' in upregulated clusters c16 and c17, respectively, and 'response to auxin' in the big downregulated cluster c22 (Figure 1B; Figure 2). Some clusters were enriched in GO terms that do not represent core ABA functions. Clusters c2, c4 and c10 for example were enriched in GO terms related to the JA pathway, such as 'response to wounding', 'response to JA' and 'defense response to insect' (Figure 1B; Figure 2). Indeed, these clusters contain known JA-related genes such as *VSP1*, *VSP2* (c2), *JAZ10* and *JOX4* (c4), and *JAZ1* and *AOS* (c10). This suggests that these ABA-activated gene modules are possibly either involved in the interplay between the ABA and JA pathways or engaged downstream of the integration point between these pathways. Indeed, ABA is known to co-activate the anti-herbivory MYC branch of the JA pathway (Pieterse *et al.*, 2012, Aerts *et al.*, 2021). On the other hand, the downregulated cluster c43 was enriched in the GO term 'defense response to other organism', containing genes like *RBOHD*, *SD1-29/LORE* and *PBL1* (Figure 1B; Figure 2; Table S5). These genes are known to act in immune responses to microbe-associated molecular patterns (MAMPs) and pathogen effectors (Kadota *et al.*, 2015, Qi *et al.*, 2017, Luo *et al.*, 2020). Cluster c43 thus likely mediates the suppressive action of ABA on defense against biotrophic pathogens (Pieterse *et al.*, 2012, Aerts *et al.*, 2021). Interestingly, multiple clusters with seemingly erratic patterns, such as c33, c35 and c36, were enriched for specific GO terms (Figure 2), suggesting that the fluctuations in expression of these ABA-responsive genes can be biologically meaningful.

In summary, the analysis of our data pinpointed many clusters of genes with distinct expression patterns, enriched for both general and specific processes. This shows that our data cover the resolution (14 time points) and dynamics to pick up coherent gene modules that regulate diverse processes within the ABA network.

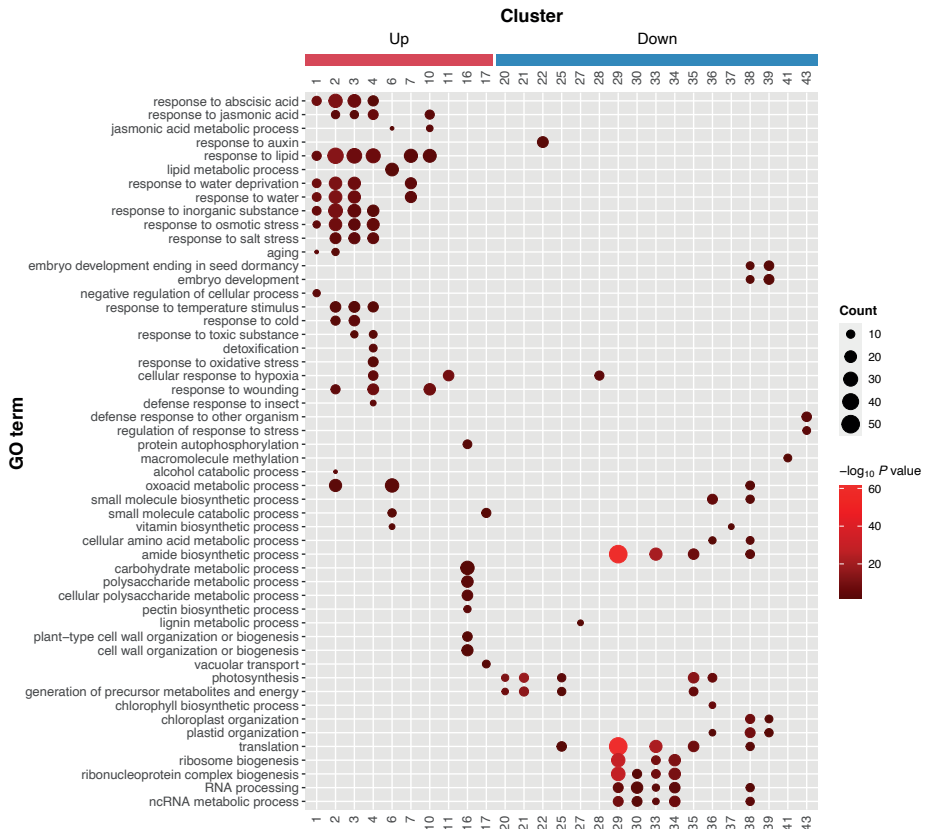


Figure 2: GO term enrichment of different ABA clusters.

GO term enrichment was performed on each of 44 clusters of coexpressed genes after ABA treatment using clusterProfiler. Redundant GO terms were removed and only the clusters containing significant GO terms were included (see Methods). Dot size represents the number of genes in a cluster with the GO term and color represents the $-\log_{10}$ of the P value based on the hypergeometric distribution.

Prediction of TFs regulating different gene clusters

TFs are key regulators of transcriptional reprogramming in GRNs. Their coordinated action results in distinct expression patterns of their target genes, enabling tight regulation of specific processes by coexpressed gene modules. To identify TFs that control different modules in the ABA GRN we analyzed enrichment of DNA sequences in the promoter region of genes in the different ABA clusters to which TFs can potentially bind. For this analysis we integrated our cluster data with publicly available datasets on TF-DNA interactions. One is the DAP-seq dataset of O'Malley *et al.* (2016), in which TF binding sites (TFBSs) were experimentally determined by *in-vitro* binding assays of 349 TFs to isolated

genomic DNA. The other two datasets we used contain 438 TF-DNA sequence motifs derived from (TF) protein-(DNA) binding microarrays (PBMs; Franco-Zorrilla *et al.*, 2014, Weirauch *et al.*, 2014). These two types of data provide similar, yet distinct and additional information. TFs usually bind to a specific DNA motif, so the enrichment of motifs in a cluster gives an indication about which TFs can regulate the cluster. However, for several reasons motif information is not always accurate in predicting which TF binds where. Firstly, some TFs can bind a variety of DNA sequences. Secondly, multiple TFs from the same TF family usually bind similar motifs. Thirdly, the presence of a motif does not always mean that a TF binds there, as this can depend on e.g. the context of the motif, which includes nearby DNA sequences. Therefore, the enrichment analysis of DAP-seq-derived TFBSs likely gives a more accurate prediction on which exact TFs regulate which clusters. This is complemented by motif information derived from the PBM studies with other TFs.

Our integrated analyses showed that many different TFBSs and motifs were enriched in the different clusters of ABA-coregulated genes (Figure 3A; Figure S3). In general, enrichment of TFBSs and motifs was higher and more diverse in upregulated clusters than in downregulated clusters (Figure 3A; Figure S3). This suggests that upregulation is regulated by more TFs than downregulation, possibly allowing tighter or more specific regulation.

The most represented family of enriched TFs in both analyses were the bZIP TFs. All the upregulated clusters except clusters c5, c14 and c15 were enriched in bZIP TFBSs and/or motifs, whereas in the downregulated clusters only clusters c28 and c42 were enriched in bZIP TFBSs and none in bZIP motifs (Figure 3A and 3B; Figure S3). The bZIP TF family consists of different groups (Dröge-Laser *et al.*, 2018). Most bind to a motif that includes the ACGT core sequence, such as the G-box (CACGTG; Jakoby *et al.*, 2002). Group A contains ABA responsive element binding factors (ABFs), the best-known bZIP TFs that regulate ABA signaling. ABFs bind to a G-box-related motif known as the ABA responsive element (ABRE), with the consensus sequence ACGTG/TC (Dröge-Laser *et al.*, 2018). Indeed, TFBSs from this group were highly enriched in clusters of upregulated genes (c1-4, c6-8, c10-12, and c16-17; Figure 3B) and the enriched motifs within the bZIP family were almost exclusively variants of the G-box, including the ABRE (Figure S3). TFBSs from multiple other bZIP groups were also enriched (Figure 3B). One of these is group D, which consists of TGA TFs, which bind to variants of the TGA motif with the consensus sequence TGACG. Interestingly, while TFBSs of some TGA TFs were enriched in multiple upregulated clusters (c1-4, c7, c9, c12 and c13) and one downregulated cluster (c42) (Figure 3B), motifs of this group were not enriched in any of the clusters, even though the TGAs were represented on the PBMs (Figure S3; Table S6). TGA TFs have generally not been associated with ABA signaling (Dröge-Laser *et al.*, 2018). However, our TFBS analysis suggests that some TGA TFs may have a role in ABA signaling, possibly by binding to TGA motifs in a specific genomic context that cannot be found using motif analysis. This also demonstrates the added value of analyzing TFBSs besides motifs.

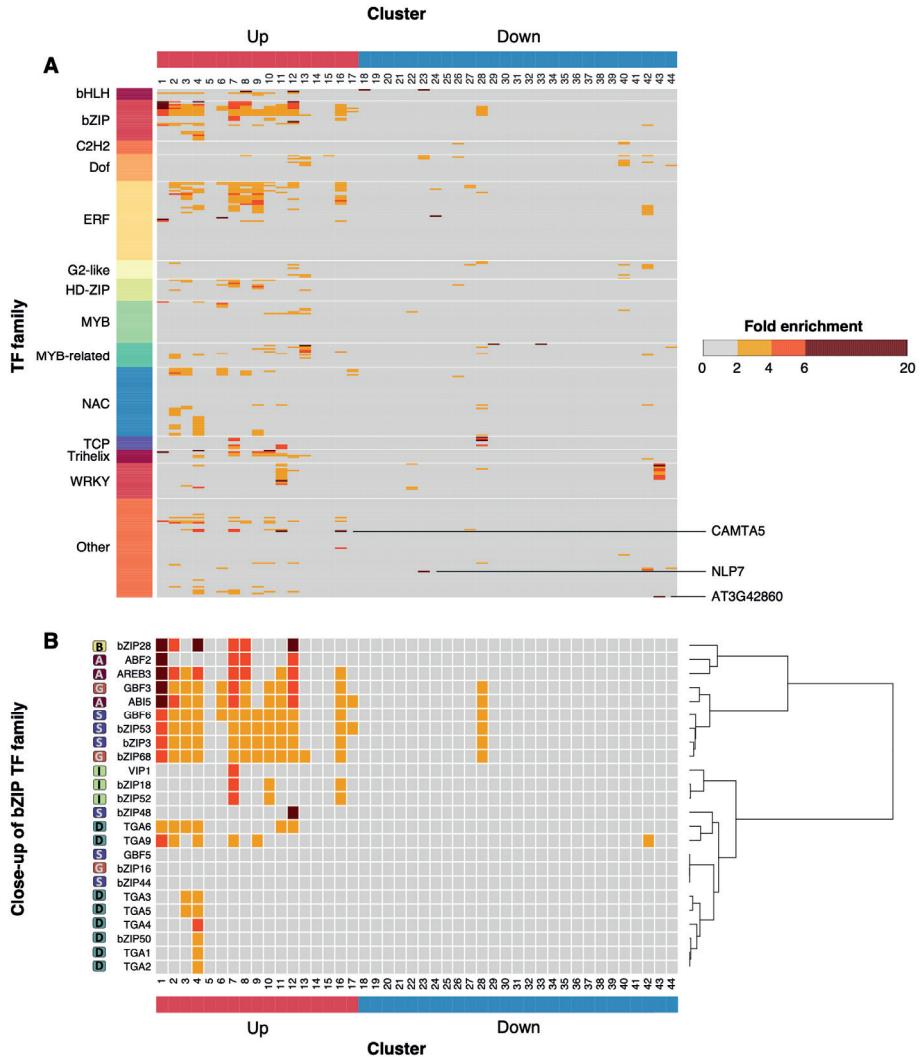


Figure 3: Enrichment of TF-DNA binding sites in clusters of coexpressed genes after ABA treatment.

(A) Fold enrichment of TFBSs in clusters of coexpressed genes after ABA treatment. TFBSs were inferred from the filtered DAP-seq dataset (Methods). Color within heatmap represents fold enrichment, which was calculated by dividing the number of genes with at least one occurrence of the TFBS by the expected number. Colored bar above the heatmap indicates if genes in the cluster are on average upregulated or downregulated after ABA treatment. Only the highly significant TFBSs are depicted (Methods). TFs within each family were ordered in the figure based on presence/absence of binding sites in the clusters using the `hclust` function with the `ward.D` method, except in the 'other' category.

(B) Close-up of enrichment of binding sites of bZIP TFs. Letter in front of each TF indicates to which group of bZIP TFs it belongs, according to Dröge-Laser *et al.* (2018). Colors of heatmap and bar below are the same as in (A). Ordering of TFs in the figure was done similarly as in (A), and the corresponding dendrogram is shown on the right. The clusters are aligned in both panels.

TFBSs from other TF families were also enriched in different clusters. In general, there was a higher diversity and number of enriched TFBSs than motifs, which supports the added value of TFBS enrichment analysis compared to motifs (Figure 3A; Figure S3). One of the most noticeable families with many enriched TFBSs was the ERF family (Figure 3A): of the 47 ERF TFBSs in the dataset, 22 were enriched in upregulated clusters and 11 in downregulated clusters (among which 9 in both up- and downregulated clusters). Of the 22 enriched ERF TFBSs in the upregulated clusters, 16 belong to the group of dehydration responsive element binding (DREB) ERF TFs (Table S7). These TFs have been reported to regulate responses to various stresses including drought and high salinity, but the functioning of the majority of DREBs is considered as ABA-independent (Lata and Prasad, 2011). Nevertheless, transcription of 10 out of the 16 DREBs with enriched TFBSs in upregulated clusters was altered by the ABA treatment (see also Table S7; Table S3). These results could point to a role for ABA in regulation of DREB target genes directly via a (post-)transcriptional effect on DREBs. Motifs of DREB TFs, as for example the transcriptionally induced DEAR2, CBF1 and CBF3, were also enriched, albeit to a much lesser extent than TFBSs (Figure S3; Table S6). This again underlines the added value of analyzing TFBSs rather than just motifs.

Other families with enriched TFBSs included MYB-related, NAC and WRKY TFs (Figure 3A) and motifs of these TFs were also enriched (Figure S3). Several NAC and WRKY TFs are indeed known to function in ABA signaling (Nakashima *et al.*, 2012, Rushton *et al.*, 2012), but MYB-related TFs have generally not been associated with ABA signaling (Dubos *et al.*, 2010). In addition, TFBSs of some C2H2, Dof, G2-like, HD-ZIP, MYB, Trihelix, and CAMTA TFs were enriched (Figure 3A) even though none had enriched motifs, or at least not in the same clusters (Figure S3).

The bHLH TF family was an exception to the observation that TFBSs of a TF family were generally more often enriched than motifs. In this family, TFBSs of only a few members were enriched (Figure 3A), but the motifs from almost all members were enriched in at least one of the upregulated clusters (Figure S3). This may be caused by the fact that there are fewer bHLH TFs included in the DAP-seq dataset. Moreover, the enriched motifs bound by bHLH family TFs are very similar to the G-box-related sequences bound by bZIP TFs (Figure S3; Table S6), and may therefore mostly represent functional binding sites for bZIP TFs rather than for bHLH TFs. Nevertheless, the enrichment of some bHLH TFBSs may point to a contribution of at least some bHLH TFs to ABA signaling (Figure 3A).

Taken together, upregulated clusters are generally targeted by more TFs than downregulated clusters. The enrichment analyses suggest that bZIP TFs are the main regulators of the transcriptionally coexpressed genes upon ABA treatment, but TFs from other families additionally provide regulation. Also, the specificity of this regulation is likely determined by more than just a DNA motif.

Regression-based analysis reveals key TFs in ABA responsiveness

Motif or TFBS enrichment analyses in clusters can identify key regulator TFs, but provide no information about the quantitative effects of a TF on transcription of target genes. To overcome this, we employed a regression-based method to associate TFBSs with amplitude of target mRNAs. The principle of this regression analysis is as follows. First, we defined the response variable as the maximum \log_2 -fold expression difference per gene (either up- or downregulated) during our time series between ABA and mock treatment (i.e., the amplitude of the response). We used the TFs from the filtered DAP-seq data (Methods) as potential regressors, considering only presence/absence of the binding site. We then performed bidirectional stepwise regression to come to a model containing the TFs that are most significantly associated to transcriptional amplitude. The regression coefficient of each TF in this model represents the mean \log_2 -fold difference in amplitude after ABA treatment between genes containing the TFBS for that TF and genes without the TFBS. The P value for each TF depicts the significance of the TF in the regression model. The final model contained a variety of TFs from different TF families, which were associated with relatively strong up- or downregulation of target genes (Figure 4). The list included known regulators of ABA-associated responses, such as ANAC055 (Takasaki *et al.*, 2015), CAMTA1 (Pandey *et al.*, 2013) and the less-well described AREB3/DPBF3 (Uno *et al.*, 2000, Bensmihen *et al.*, 2005, Qian *et al.*, 2019; see also Introduction), but also TFs that have not yet been characterized as part of the ABA network, such as bZIP68 and GT3a. Interestingly, bZIP68 had the highest P value of all TFs in the model, meaning that it was very significantly linked to target gene expression, and GT3a had the second highest regression coefficient, meaning it was linked to a large difference in target gene amplitude after ABA treatment. This makes them good candidates for inclusion in the ABA network. A relatively low number of TFBSs were associated with downregulation of genes in the model (Figure 4). The TF with the largest and most significant negative regression coefficient was bHLH122, a known positive regulator of resistance to drought, osmotic stresses and NaCl, and a negative regulator of ABA catabolism (Liu *et al.*, 2014). Although it was originally reported as unresponsive to ABA, we found that its transcription was significantly enhanced upon ABA treatment (Table S3), suggesting it may act within the ABA GRN, mostly as a repressor of transcription.

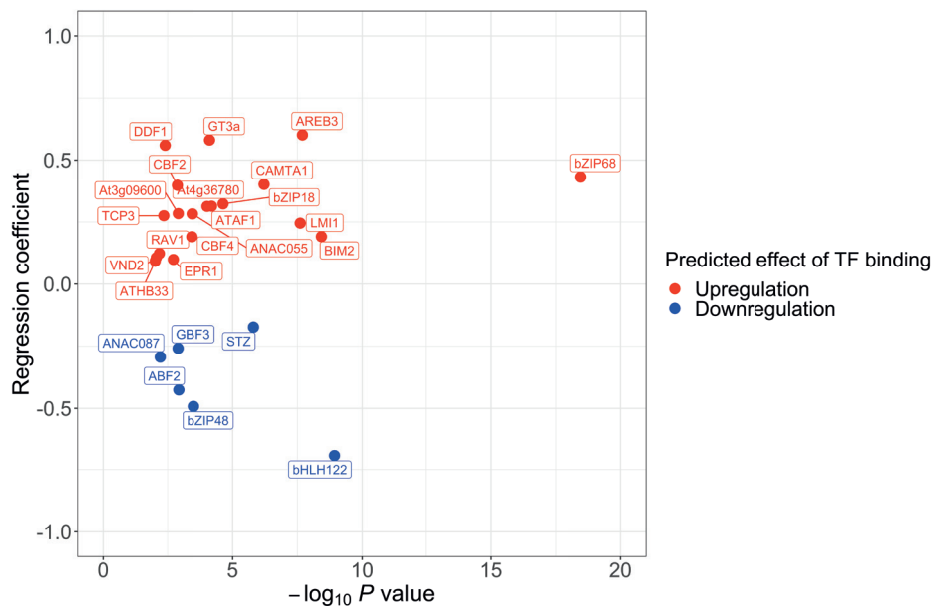


Figure 4: Linear regression model of the contribution of TFBSs to target gene amplitude after ABA treatment. Bidirectional stepwise linear regression was used to associate presence/absence of TFBSs with amplitude of target mRNAs, measured as the \log_2 -fold change of ABA/mock. TFBSs were taken from the filtered DAP-seq dataset (see Methods). Individual TFs are plotted according to their regression coefficient (the mean \log_2 -fold difference in amplitude after ABA compared to mock treatment between genes containing the TFBS for that TF and genes without the TFBS) and the \log_{10} of their P value (the significance of this association). TFs are colored according to their predicted contribution to ABA-induced transcription (positive in red, negative in blue).

Predicting time-dependent roles for TFs in the ABA GRN

GRNs often consist of multiple steps of regulation. TFs are activated at different times after stimulation of a cell and can activate each other in a signaling cascade. To determine which TFs are important at which time after activation of the ABA network we used Dynamic Regulatory Events Miner 2.0 (DREM 2.0; Schulz *et al.*, 2012). This algorithm builds a temporal GRN model by combining time series RNA-seq data with static TF-TFBS data. DREM2.0 divides genes in temporal groups based on the premise that the genes in a group may have a similar expression pattern until a certain time point (e.g., they are upregulated) but follow different patterns at a later time point (e.g., one subgroup gets more upregulated whereas another subgroup remains at the same level or is more downregulated). The algorithm then looks for enrichment of TFBSs in each subgroup of genes after this split (referred to here as a path: a section stretching from one split to the next, or to the end of the time series), hypothesizing that the differential behavior of the subgroup is caused by TFs for which TFBSs are enriched.

We performed this analysis using the \log_2 -fold change of ABA/mock expression data combined with the filtered DAP-seq data (Methods). The resulting GRN consisted of a large number of unique trajectories (a sequence of paths) with multiple splits and many TFs assigned to the various paths, suggesting a high level of complexity of the ABA GRN (Figure 5). Strikingly, genes that were upregulated at the earliest time point (15 min) were enriched for dozens of different binding sites, whereas strongly downregulated genes at that time point were only enriched for the binding site of bHLH122 (Figure 5), which is the TF that we also identified in our regression analysis due to its association with strong downregulation of genes (Figure 4). The fact that in general, over the whole time course, more enriched TFBSs were apparent in upregulated versus downregulated paths is consistent with our previous analyses. This suggests that activating TFs are more prevalent in the ABA network than repressing TFs. The trajectory of the highest upregulated genes (consisting of paths P1, P4 and P6 in Figure S4) was enriched for binding sites of TFs such as BIM2, AREB3, ABI5 and bZIP68, of which AREB3 and ABI5 were associated with the split at 30 min leading to the highest amplitude of induction (Figure 5; Table S8). These TFs were also strongly enriched in upregulated clusters of the SplineCluster analysis (Figure 3) and most also occur in the regression analysis (Figure 4), which reinforces their predicted importance in the ABA GRN.

One of the interesting observations was that some TFBSs were enriched in both upregulated and downregulated paths. For example, GT3a TFBSs were enriched from the earliest time point on in a trajectory peaking at around the 3 h time point, but also in a path that split from that trajectory and strongly declined in expression towards basal levels from 3 h onwards, which was reached at about 8 h (Figure 5; paths P1 and P4 (up) and P20 (down) in Figure S4; Table S8). This suggests that the GT3a binding site is associated with downregulation after the 3 h time point, even though the early time points in the DREM analysis and the regression analysis (Figure 4) suggested that it was associated with upregulated genes. Possibly, GT3a acts as both an upregulator and downregulator of expression of different genes depending on, e.g., the presence of certain co-factors at later time points. An alternative explanation may come from the fact that the *GT3a* gene itself is rapidly upregulated at early time points, but its expression level sharply declines after its peak at 1 h after ABA treatment, returning to basal levels at about 7 h (Figure S5). This may consequently lead to initial upregulation of target genes by GT3a, followed by a drop in their expression after 3 h due to reduced levels of GT3a protein. The fact that our analysis can pick up such complex behavior of the GRN demonstrates the advantage of doing a single pulse treatment at the start of the time series over a continuous treatment. It enables not only to see how the network is initially activated, but also how it is shut off, which is biologically relevant as well, thus revealing a more complete picture of the complex temporal transcriptional regulation of the network.

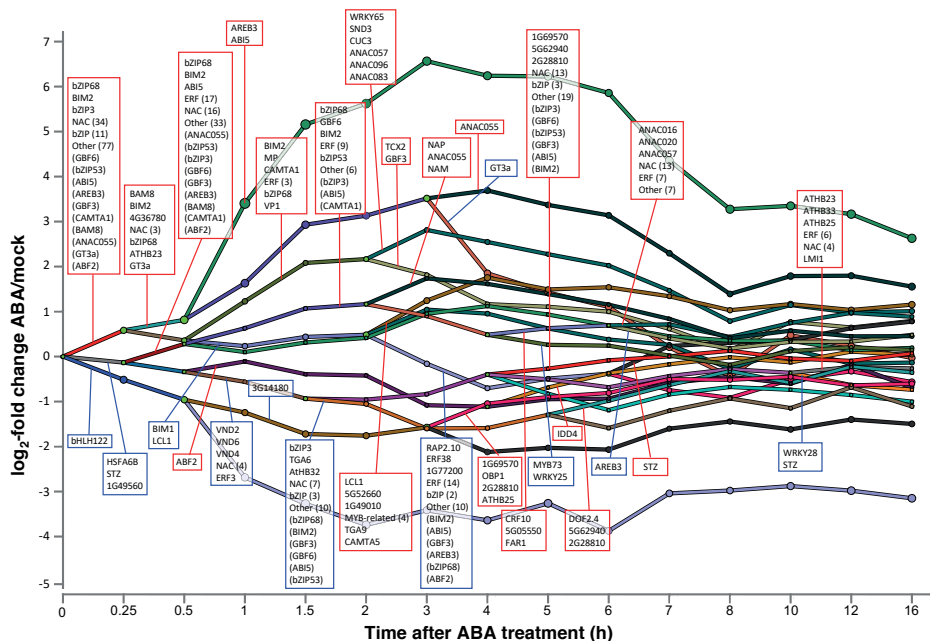


Figure 5: Temporal role of TFs in the ABA GRN.

Dynamic Regulatory Event Miner 2.0 (DREM 2.0) analysis was performed using the log₂-fold change of ABA/mock expression data (DEGs only) and the TFBS data from the filtered DAP-seq data (Methods). Lines represent clusters of genes with a similar expression pattern. Expression is indicated as the log₂-fold change between ABA and mock treatment over the entire time series (in h). The most significantly associated TFs for each path are denoted if their 'Score split' was < 0.001. In the case of multiple significant TFs, the three most significant ones are denoted, and the rest are summarized by family (number of TFs indicated between parentheses). If more than three families are present, the less prevalent families are summarized as 'Other' (number of TFs indicated between parentheses). Enriched TFs that are described throughout the Results section but are not in the top three most enriched TFs are indicated at the bottom of the box between parentheses for reference. A red line indicates an association with upregulation of expression and a blue line indicates an association with downregulation of expression. The full list of enriched TFs per path can be found in Table S8 (supported by the corresponding path numbers in Figure S4).

Predicting the earliest regulators (first level) of the ABA response

The DREM model predicted that more than a hundred TFs regulate the ABA response within 15 min. However, this may be an overestimation of the number of TFs that act at the first level of the ABA GRN, since plant GRNs are typically activated by only a relatively small number of master regulators that activate other TFs lower in the hierarchy (Song *et al.*, 2016). In the ABA GRN, a number of these master regulators that act at the first level have been identified and were found to be activated mostly by phosphorylation (Sah *et al.*, 2016, Yang *et al.*, 2017). Here, we aimed to discover additional master regulator TFs that act immediately, at the first level of the ABA GRN. Hereto, we integrated our microarray time series dataset with the aforementioned filtered DAP-seq dataset and a

previously published microarray dataset in which translation was inhibited. In the latter dataset, which was generated by Lumba *et al.* (2014), Arabidopsis mutant seedlings defective in ABA biosynthesis (*aba2*) were treated with a combination of ABA and the translation inhibitor cycloheximide (CHX). Since translation is blocked by CHX, the DEGs in the ABA+CHX treatment are regulated by TFs that are themselves modulated through post-translational changes mediated by ABA rather than changes in transcription and/or translation. Therefore, these regulating TFs seemingly act as a first level of TFs in the ABA GRN.

To identify putative first regulators of the ABA GRN we investigated enrichment of TFBSs in the promoters of DEGs in the Lumba *et al.* (2014) dataset that also were DEGs in our dataset. Of the 282 genes in the Lumba *et al.* (2014) dataset, 229 were also differentially expressed in our time series dataset. TFs for which enriched TFBSs in these 229 genes were detected were considered putative first level TFs of the ABA GRN. These TFs do not need to be differentially transcribed themselves in our dataset, because they are predicted to regulate their target genes independent of translation, as suggested by the CHX-insensitive expression behavior of genes that contain a TFBS for them. We predicted 21 TFs as first regulators in the ABA GRN, each regulating between 6 and 116 of the 229 DEGs (Figure 6). All except DDF2 were also part of the regulators assigned to the first upregulated path in the DREM model (Table S8, path P1 in Figure S4), which is in line with them being regulators at the first level. Among them are well-known TFs that are activated post-translationally and can start the ABA transcriptional cascade, such as AREB1/ABF2 (Choi *et al.*, 2000, Uno *et al.*, 2000) and ABI5 (Skubacz *et al.*, 2016). We also found again the TFs bZIP68 and GT3a that have not been characterized as part of the ABA network yet, but were also picked up with our regression and DREM analyses. In these analyses, they were both predicted to (generally) upregulate their target genes and to be active at several stages in the ABA response, including at the initial time point (Figure 5). In summary, we picked up known first level TFs, predicted novel TFs with a potential role in the initiation of ABA signaling, which confirmed the correct positioning of some TFs in the DREM model, and condensed the information on first level TFs derived from the DREM model.

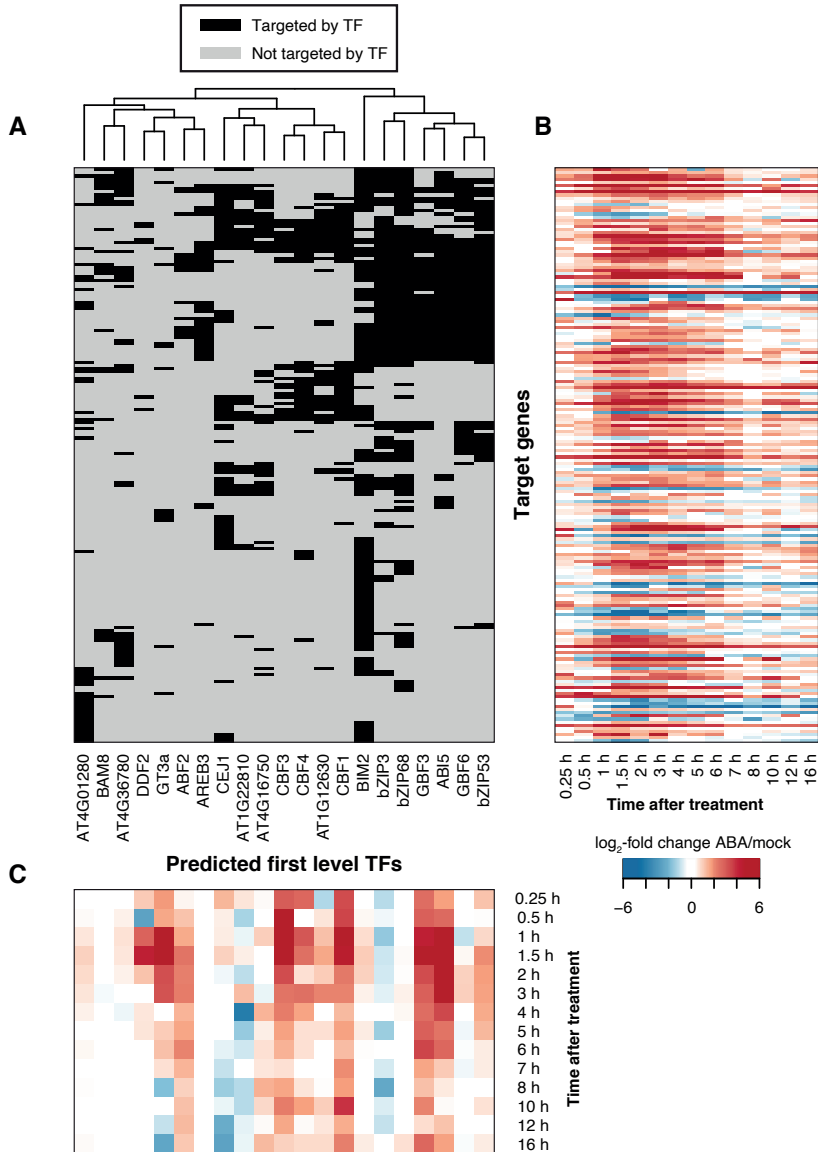


Figure 6: Predicted earliest regulators (first level) of the ABA response.

(A) Heatmap showing TFBSs for TFs from filtered DAP-seq data (Methods) in the promoters of DEGs in our dataset that were also differentially expressed after ABA + CHX treatment according to Lumba *et al.* (2014) and have an enriched TFBS for at least one of the TFs. TFs and target genes were ordered using the `heatmap.2` function from the `gplots` package (v3.0.1.1) in R.

(B) Expression of target genes depicted as \log_2 -fold change between ABA and mock treatment throughout the 14 time points after ABA treatment. Each row represents one gene, and the rows correspond to the rows in panel (A).

(C) Expression of the genes encoding the TFs predicted as first level TFs in this analysis depicted as \log_2 -fold change between ABA and mock treatment throughout the 14 time points after ABA treatment. Each column represents one gene, and the columns correspond to the columns in panel (A).

To better understand the relationship between the different TFs at the first level we assessed their similarity in binding to their predicted 229 target genes. This revealed that the majority of genes are targeted by multiple TFs. Moreover, there is a group of seven (bZIP and bHLH) TFs (BIM2, bZIP3, bZIP68, GBF3, ABI5, GBF6 and bZIP53) with a particularly large overlap in their targets, and a second group of seven ERFs with overlapping targets (Figure 6A). Such an overlap may contribute to robustness of (part of) the network and/or ensure that target genes can be activated under different conditions by these different TFs. Less than half of the genes encoding the predicted TFs at the first level were highly responsive to ABA (Figure 6C), which is consistent with the hypothesis that they can initiate the transcriptional cascade after being post-translationally activated. Generally, the target genes of the predicted first level TFs were upregulated (Figure 6B), suggesting that these TFs are mainly involved in transcriptional activation. Nevertheless, downregulation of genes by the same TFs was also predicted to occur (Figure 6B). There was no apparent relationship between TFBSs and the expression pattern of the target genes and the TF-encoding genes (Figure 6A, B, C), suggesting that additional features that were not included in our analysis are at play e.g., regulation by other TFs at later stages.

Predicting a core hierarchical ABA GRN

After initiation of a GRN, several TFs at the second level usually relay the signal from the first level TFs to target genes at the third level. Some of these third level target genes may also be regulated directly by first level TFs. To get a more complete overview of such a hierarchical architecture of the ABA GRN we expanded our analysis of the first level TFs to create a three-level hierarchical ABA GRN (Figure 7; Table S9). The first level consisted of TFs that we previously predicted to regulate the first transcription step in the ABA GRN. Next, we used the filtered DAP-seq data to select all the targets of these TFs that were differentially expressed in our ABA time series dataset. We filtered this DEG list for TF-encoding genes, and when the TFBSs for these TFs were enriched in at least one of the clusters from our expression-profile-based clustering analysis we designated these TFs as the second level of the GRN, and the clusters as the final level. We assigned an edge between TFs in the GRN if any of the TFs in the GRN regulated any of the other TFs according to the filtered DAP-seq data. Additionally, we added edges from TFs at the first and second levels to a cluster if the binding sites for these TFs were enriched in this cluster. The reconstructed hierarchical GRN was highly interconnected (Figure 7), similar to what was observed for TFs at the first level and their targets (Figure 6). This again suggests that the ABA GRN is either very precisely regulated by specific combinations of TFs, or that there is much redundancy within the network. Considering that only 349 of about 2000 TFs in the Arabidopsis genome are present in the DAP-seq dataset that was used to construct our current GRN, the number of regulating TFs in the ABA GRN is even

larger in reality. Several TFs seem to act as hubs in the network, which can be quantified by measures such as a TF's betweenness centrality (Figure 7; Table S9). This is based on the amount of information that passes through a node (here: a TF) in a network, reflected by how often a TF is part of the shortest regulatory path between two genes. Different TFs such as BIM2, ANAC083 and WRKY28 seem to be important hubs in the network.

It is worth noting that the network is not so strictly layered as how we arranged it, which is also why we refer to the layers as 'levels'. For example, many TF-encoding genes at the first level were predicted to be regulated by other TFs that act at the first level or by themselves (autoregulation; Figure 7, upper double row), which correlated with a higher degree of differential expression compared to the TF-encoding genes that were not regulated by TFs from the first level. These first-level TF genes that are both post-translationally and transcriptionally regulated could thus have a greater effect on the ABA GRN.

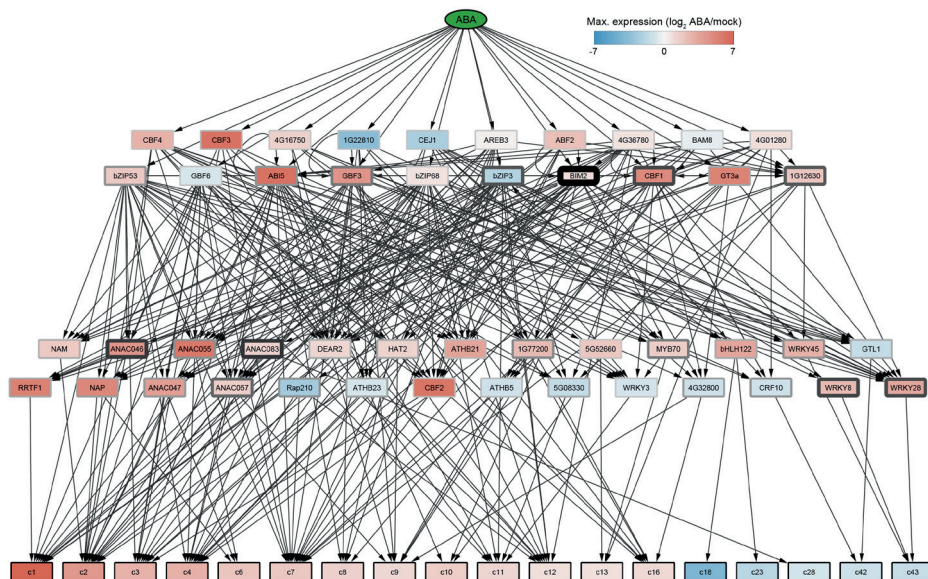
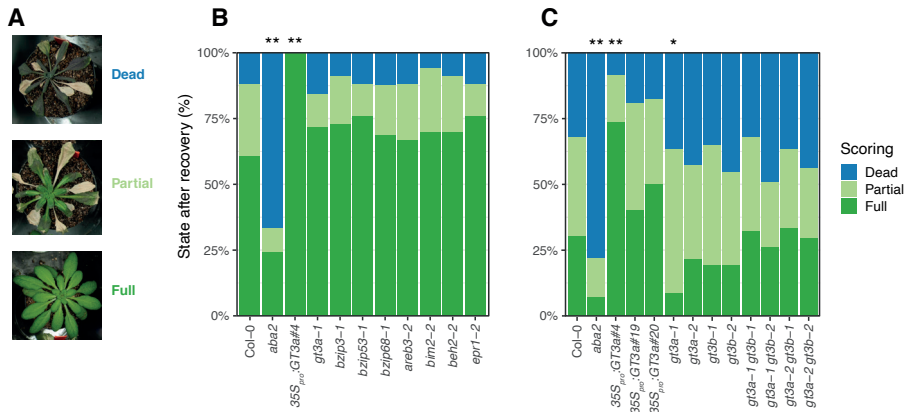


Figure 7: Three-level hierarchical ABA GRN.

The first level consists of the TFs that we predicted to constitute the initial response regulators, because they are post-translationally regulated by ABA and their TFBSs show enrichment in the DEGs of our ABA time series. The second level consists of differentially expressed TF-encoding genes that are transcriptional targets of the first level and for which TFBSs are enriched in at least one of the clusters of DEGs after ABA treatment. The third level is represented by the clusters that are targeted by the TFs at the first and/or second levels. 'ABA' is used as the root of the network. The edges go from ABA to the TFs at the first level and from TFs at the first and second levels to target genes at the first, second and third levels. Edge thickness and color (gray to black) correlates with betweenness centrality, which was calculated using all the genes in the clusters with TFBSs for the TFs in the GRN. Color represents the maximum \log_2 -fold difference between ABA and mock treatment of a gene or a cluster (average of all genes) in our ABA RNA-seq time series.

Biological validation of GT3a as a novel regulator of drought tolerance

We next set out to validate the biological importance of different novel candidate TFs in the ABA GRN. These TFs were selected based on the analyses described above, showing e.g. highly enriched TFBSs in clusters, significant association with target gene amplitude, and/or presence in the DREM and/or hierarchical GRN models. Mutants of the candidate TFs were tested for drought tolerance. For one of our favorite candidates, the TF GT3a, we also designed overexpression lines, because high levels of redundancy with the homologous TF GT3b were expected. We included the ABA-deficient mutant line *aba2* as a positive control. For the drought assay, plants were grown for 25 days, after which water was withheld for 12 days. Then, water was supplied for 7 days, and recovery was scored in three categories: fully recovered, partially recovered, and dead (Figure 8A). About 60% of Col-0 plants recovered fully and about 25% recovered partially (Figure 8B). In contrast, only one third of the *aba2* mutants recovered to some extent, demonstrating that the assay was able to pick up differences in recovery ability between different lines. None of the tested mutants showed a significantly different recovery compared to Col-0 in this experiment (Figure 8B). However, all plants of the $35S_{pro}:GT3a$ line (#4) recovered fully, suggesting that GT3a is important for tolerance to drought stress and/or recovery after drought (Figure 8B). We repeated the assay with three $35S_{pro}:GT3a$ overexpression lines that express various levels of *GT3a* (Figure S6), two mutant alleles of *gt3a* and its closest homologue *gt3b*, and the double *gt3a gt3b* mutants (all four combinations of the *gt3a* and *gt3b* mutant alleles). Figure 8C shows that the $35S_{pro}:GT3a$ line #4 again recovered significantly better than Col-0, but this was not the case for the other two overexpression lines, which had lower *GT3a* overexpression levels (Figure S6), although a trend for higher recovery was visible. In this experiment, the *gt3a-1* single mutant recovered significantly worse than Col-0, although surprisingly none of the double mutants carrying this allele had a significantly worse recovery, nor did the other double mutants. Together, this suggests that GT3a is likely involved in drought tolerance in a possibly redundant way, but not redundantly with GT3b.



DISCUSSION

A time-resolved analysis of the ABA GRN

We profiled gene expression changes induced by ABA treatment in Arabidopsis in a high-density time-course experiment, and integrated this with publicly available DAP-seq data and RNA-seq data to get a detailed overview of the architecture and dynamics of the ABA GRN. This provided four types of network information: (i) coexpression of genes in functionally diverse modules, which are steered by predicted TFs; (ii) contribution of TFs to amplitude of gene expression levels; (iii) time-resolved engagement of TFs regulating certain target genes; (iv) hierarchical position of TFs at different levels of the ABA GRN.

Our pulse treatment revealed 'on' and 'off' network dynamics

Our time series data showed a rich diversity in expression dynamics (Figure 1; Figure 5; Figure S2), forming a good basis for most of our network analyses. For our pulse

treatment with ABA, we dipped the rosette in an ABA (or mock) solution for 3 s after which the plants continued to grow under regular conditions. This revealed various time- and amplitude-related variations in gene transcription, representing the 'on' status (activation/repression) and the 'off' status (return to basal level). This pulse treatment therefore allowed, for example, for more precise clustering of genes. We showed that many clusters were enriched for specific functions (Figure 2), suggesting that the precise clustering was biologically relevant. Moreover, we could relate the role of TFs to the timing in expression of their target genes. For example, in the DREM analysis, TFs were implicated in different paths, both in 'on' and 'off' directions, and starting at different times after the ABA treatment (Figure 5). The large-scale off-switching of transcription to return to basal levels was not observed in another RNA-seq time series study where *Arabidopsis* seedlings were kept constantly in an ABA solution (Song *et al.*, 2016). Our approach thus demonstrates the value of a pulse treatment for elucidating different modes of a GRN.

Activating TFs are more prevalent in the ABA GRN than repressing TFs

Even though the total number of up- and downregulated genes after ABA treatment was similar, our analyses showed that the number of TFs associated with upregulation was larger than that with downregulation. This was apparent in all our network analyses: more motifs and TFBSs were enriched in upregulated than downregulated coexpressed gene clusters (Figure 3), TFs associated with upregulation of target genes were overrepresented in our regression model (Figure 4), more TFs were associated with DREM paths going up (increased expression of target genes) than going down (reduced expression of target genes; Figure 5), the differentially expressed target genes of the earliest acting (first level) TFs in our ABA network were more often upregulated than downregulated (Figure 6), and our ABA hierarchical GRN contained 13 of the 17 upregulated clusters, but only 5 of the 27 downregulated clusters (Figure 7). This seems to suggest that downregulation requires fewer TFs than upregulation, but alternative explanations, which are related to the (DAP-seq and motif) methods that we used, are also possible. For example, silencers that are located further away from the promoter may play a relatively large role in repression, many TFs that control downregulation could be absent in the used motif and DAP-seq datasets, or specific combinations of TFs may be required for repression.

Immediate early TFs regulating a hierarchical ABA GRN

We inferred the temporal role of TFs in the ABA GRN using DREM2.0 and found that at the earliest time point more than 100 TFs were predicted to be involved in upregulation of genes (Figure 5). Similarly, dozens of TFs were predicted to regulate DEGs in a comparable

study after 1 h of ABA treatment of seedlings, based on integration of RNA-seq data with ChIP-seq and the same DAP-seq data (Song *et al.*, 2016). We expected this to be an overestimation of the number of TFs that act at the first level of the ABA GRN, because networks of other hormones like that of SA, JA and ethylene are regulated by only a handful of master regulator TFs (Howe *et al.*, 2018, Binder, 2020, Aerts *et al.*, 2021, Peng *et al.*, 2021). ABA signaling is known to be initiated by post-translationally modified TFs and we thus designed a method to predict which TFs might initiate the ABA GRN independent of their own transcription. For this, we combined our RNA-seq data with a publicly available dataset of ABA + CHX-treated *aba2* plants (Lumba *et al.*, 2014). This significantly reduced the number of candidate first-level regulators of the ABA GRN to only 21 TFs (Figure 6). Consequently, while the DREM2.0 analysis suggested the importance of, for example, many NAC TFs in the regulation of the earliest responding genes, they were now placed at the second level of the hierarchical network. The use of a CHX-based dataset combined with TFBS data to determine the earliest, post-translationally activated TFs is to our knowledge novel and likely provides a better prediction of first-level regulation of a GRN than the DREM2.0 method. The identified TFs acting the earliest in the ABA hierarchical GRN included TFs that are known to be activated post-translationally and functioning as master regulators of the ABA response, such as ABI5 and AREB1/ABF2 (Choi *et al.*, 2000, Uno *et al.*, 2000, Skubacz *et al.*, 2016). Future studies may focus on the importance of the yet unknown first-level TFs. Interestingly, bZIP68, one of these TFs, was found to be regulated by redox status, where oxidation of a cysteine residue causes bZIP68 to shuttle from the nucleus to the cytosol, relieving its repressive effect on stress-tolerance-related genes, including genes related to ABA signaling (Li *et al.*, 2019). It is tempting to speculate that ABA may have the same effect, since it also causes an increase in ROS in, e.g., guard cells (Postiglione and Muday, 2020) and was found to induce oxidation of the bZIP68 protein, albeit to a lesser extent than direct H₂O₂ treatment (Li *et al.*, 2019).

We next extended the analysis of the first level to second and third levels in a hierarchical GRN, where the first level of TFs initiates the GRN, the second level transmits the signal, and the third level directly regulates the responding genes (Figure 7). Extensive cross-regulation was found both within and between levels, indicating high complexity of the ABA GRN. It is apparent that several clusters are missing at the third level, suggesting that the model is incomplete, which may be related to certain limitations of the used DAP-seq data (discussed in “The use of DAP-seq data for GRN inference”).

Key TFs in the ABA GRN

Many of the analyses that we conducted were aimed at finding key transcriptional regulators in the ABA GRN. In agreement with the existing literature (Banerjee and Roychoudhury, 2017), the most prominent TFs with a predicted function in the ABA GRN

were members of the bZIP family of TFs, such as ABI5, AREB3, AREB1/ABF2, bZIP68, bZIP3, GBF3, GBF6 and bZIP53. However, all analyses also identified TFs from many other families. For example, ERF TFs were prevalent at the first level of the hierarchical GRN, NAC TFs were prevalent throughout the DREM model, the trihelix TF GT3a was amongst the most significant TFs in several analyses, and the WRKY TF WKRY28 and the bHLH TF BIM2 were hubs in the hierarchical ABA GRN analysis. This shows that the ABA response involves a diverse set of TFs that together fine-tune downstream responses.

We took two approaches to assess how biologically accurate our network predictions were. First, we verified whether characterized TFs with a known role in ABA signaling were present in our different analyses. Indeed, several of these TFs were identified, such as AREB1/ABF2 (Choi *et al.*, 2000, Uno *et al.*, 2000), ABI5 (Skubacz *et al.*, 2016) and ANAC055 (Takasaki *et al.*, 2015). Moreover, TFs that have not been so well characterized as important ABA regulators but have been linked to ABA-related processes, such as GBF3 (Ramegowda *et al.*, 2017) and WRKY28 (Babitha *et al.*, 2013), were unveiled as players in the ABA GRN. Second, we validated the role of TFs that have not yet been linked to ABA signaling. For this, we used mostly single mutant lines of TFs and overexpression lines of our favorite candidate, GT3a. In a drought recovery assay, we found that GT3a is likely a positive regulator of drought tolerance. This was based on higher drought recovery of an overexpression line with high *GT3a* mRNA levels, and a trend in the same direction of two overexpression lines with lower expression (Figure 8). The *gt3a-1* mutant showed increased susceptibility to drought in one of two experiments, but none of the double mutants with *gt3b-1* or *gt3b-2* did, suggesting that this phenotype of *gt3a-1* may not be biologically meaningful. In general, none of the tested single mutants of TFs showed a drought-related phenotype. This could be due to high levels of redundancy between different TFs in the network. This hypothesis is supported by multiple lines of evidence. First, there is much overlap in TFs that regulate targets in the different network models, both in our own study and in a previous study in seedlings (Song *et al.*, 2016). Second, previous studies showed that phenotypes of single mutants of certain ABA-related TFs were absent or only weak, and instead higher-order mutants or overexpression lines were required to get a distinct phenotype (Wu *et al.*, 2009, Yoshida *et al.*, 2010, Yoshida *et al.*, 2015, Qian *et al.*, 2019). In line with this, even though there is some evidence for involvement of AREB3 in ABA-regulated control of stomatal movement, the (single) *areb3-1* mutant is not impaired in stomatal movement (Qian *et al.*, 2019), and our study shows that the *areb3-2* mutant is also not affected in drought tolerance (Figure 8B).

The use of DAP-seq data for GRN inference

DAP-seq data reveal TFBSs in (target) genes. We integrated publicly available DAP-seq data with our high-density time series RNA-seq data for diverse analyses regarding the role

of TFs in the ABA GRN: cluster enrichment analysis (Figure 3), regression-based analysis (Figure 4), DREM2.0 network analysis (Figure 5), and hierarchical GRN analysis (Figure 6 and Figure 7). One possible weakness of these analyses is that they all rely on a DAP-seq dataset. DAP-seq can be regarded as an *in vitro* version of the better-known method ChIP-seq, and has many of the same drawbacks, such as the fact that a binding event does not necessarily mean that the TF regulates the associated target gene (Heyndrickx *et al.*, 2014) and that TFs sometimes regulate genes by binding enhancers or silencers that are far away from their target gene, making it impossible to predict the target (Weber *et al.*, 2016). Also, the TF-DNA binding events that require interactions with co-factors or other TFs are not considered. Such interactions may alter the DNA binding specificity of a TF and can thus be essential for the ability to bind certain binding sites (Jolma *et al.*, 2015, Li *et al.*, 2023), which recently has been addressed by a novel DAP-seq method that enables studying TF heterodimers (Li *et al.*, 2023). Finally, another potential drawback of DAP-seq is that chromatin context is absent. However, this may be at our advantage because the TFs in the DAP-seq experiment were not hindered by e.g. heterochromatin to bind to all of their potential target DNA, as would be the case for (*in vivo*) ChIP-seq. Another major advantage of DAP-seq is its relatively high throughput: in the dataset we used, 349 TFs were tested (O'Malley *et al.*, 2016). However, this is still only about one fifth of all TFs in *Arabidopsis*, and more TF binding data are needed in the future to fully elucidate GRNs using methods such as those described here.

A possible high-throughput alternative to using genomic TFBSs derived from DAP-seq data is using motifs, derived from, e.g., PBMs or indirectly derived from DAP-seq data by analyzing motifs under DAP-seq peaks and searching matches to those motifs in the genome (Franco-Zorrilla *et al.*, 2014, Weirauch *et al.*, 2014, De Clercq *et al.*, 2021). We integrated PBM-derived motifs with cluster data (Figure S3), but found a much less diverse set of enriched TFs compared to our analysis based on TFBSs derived from DAP-seq data. This is likely because motifs can be very similar for different TFs and do not consider the entire genomic context, which is important for TF binding (e.g., Gordán *et al.*, 2013, Mathelier *et al.*, 2016). Thus, the motif-based analysis included more false positive targets, making this information relatively unreliable (see also De Clercq *et al.*, 2021). Therefore, we proceeded to use only DAP-seq data in subsequent analyses, as it represents a good middle ground between ChIP-seq and motifs, balancing specificity with high throughput.

Outlook

Our study provided a comprehensive look of the architecture and dynamics of the ABA GRN in mature plants and the position of several key TFs in the network was predicted. In the future, our information-rich data can be combined with new publicly available datasets and analyzed using the latest of the ever-evolving network inference tools

to get even more accurate network predictions. Also, it can be combined with other perturbation time series data to elucidate the overall stress network of Arabidopsis. We are planning some of these approaches ourselves, but also highly encourage other scientists to make the most of our unique dataset.

METHODS

Plant materials

The Arabidopsis wild type for all experiments was the Columbia (Col-0) accession. All mutants were in the Col-0 background. The T-DNA insertion lines were genotyped, and homozygous mutant plants were selected for production of seeds, which were used for all experiments. An overview of all genotyped lines and the primers used for detection of the expected mutations is depicted in Table S10. The *aba2-1* mutant that was used was described by González-Guzmán *et al.* (2002).

For the generation of $35S_{pro}::GT3a$ overexpression lines the following steps were taken. The coding sequence (CDS) of *GT3a* (AT5G01380) was cloned into the binary expression vector pFAST-R02 as follows. First, cDNA was made using RevertAid H Minus Reverse Transcriptase (Thermo Fisher Scientific, Waltham MA, USA) from total RNA isolated from 10-day-old Arabidopsis Col-0 seedlings. Next, the *GT3a* CDS, including the stop codon (1033 bp in total), was PCR-amplified with primers containing Gateway-compatible overhangs (Table S11) using Phusion High-Fidelity DNA Polymerase (Thermo Fisher Scientific). The PCR product was purified after gel electrophoresis using the Illustra GFX PCR DNA and Gel Band Purification Kit (Merck, Darmstadt, Germany). This DNA fragment was cloned into the pDONR221 vector by Gateway BP reaction (Thermo Fisher Scientific), resulting in pDONR221_GT3a-CDSstop. The coding sequence was Sanger sequenced to verify that no mutations were introduced during the PCR amplification. A Gateway LR reaction was used to generate the final pFAST-R02_GT3a-CDSstop construct, which was subsequently transformed into *Agrobacterium tumefaciens* EHA105 via electroporation and thereafter transfected to Arabidopsis accession Col-0 using the floral dip method (Harrison *et al.*, 2006). Twenty-nine individual transgenic lines (i.e., originating from a separate seed after floral dip) were selected and analysed by qPCR for expression levels of *GT3a*. Based on segregation on herbicide resistance in the subsequent generation (3:1 resistant:sensitive segregation on Basta) and *GT3a* expression level (high, average, low) three representative transgenic lines were selected for bioassays and thereto further propagated and selected to form a homozygous seed batch (Table S11; Figure S6).

Plant growth conditions for time series experiment

For the RNA-seq ABA time series experiment seeds were stratified in 0.1% agar at 4°C for 48 h, and then sown on river sand in closed trays with transparent lids to ensure 100% humidity, under the light regime described below. After two weeks the germinated seedlings were transferred to 60-ml pots that contained a river sand:soil mixture (5:12) that had been autoclaved twice for 1 h. The pots containing single plants were placed in open trays at 21°C and 70% humidity under a 10-h day (75 $\mu\text{mol}/\text{m}^2/\text{s}^1$) and 14-h night cycle. Watering was done three times per week. Once a week, instead of water, the plants received a modified half-strength Hoagland solution that contained 10 μM sequestrene (Fe-EDDHA, Royal Brinkman, 's-Gravenzande, the Netherlands).

Drought stress assay: growth conditions, watering regime and scoring

Seeds were stratified in 0.1% agar at 4°C for 48 h, and sown immediately on sterilized sand:soil mixture (5:12) in 60-ml pots (soil was prepared the same as for the time series). Each pot was weighed to ensure an equal amount of wetted soil in each pot (less than 1 g difference was allowed). The first two weeks the plants were grown under 100% humidity by closing the trays with transparent lids, after which the lids were removed. Plants were cultivated in a growth chamber set at 21°C and 70% humidity under a 10-h day (200 $\mu\text{mol}/\text{m}^2/\text{s}^1$) and 14-h night cycle, receiving the same watering/Hoagland regime as described for the time series, until the plants were three weeks old. Then, each pot was placed on a 60-mm petri dish, which functioned as a saucer, so that water could be supplied to the plants individually. The pots were weighed, and water was supplied until a weight of 87 g was reached, which was the same weight as during sowing. This was repeated two and four days later, where the fourth day marked the start of the drought period, during which water was withheld. At the fifth day of the drought period, all pots were weighed again and watered, so that each pot weighed the same and the plants thus received a similar drought stress intensity. The weight was set at about 70 g, which was around 2 g more than the heaviest pot in the experiment at that time. When about 50% of the Col-0 plants seemed unable to recover (purple coloring, curling (especially at the center) and apparent loss of turgor of the leaves), which was at about 12-13 days after the start of the drought period, the pots were rewatered to the same weight as before the drought period (87 g). Watering was resumed normally for one week, after which plant survival was scored into three categories as follows. Plants having a completely green rosette were scored as 'fully recovered', plants with only some new green leaves were scored as 'partially recovered' and plants that had no new green leaves were scored as 'dead'.

RNA-seq time series experimental setup

The RNA-seq experiment of the ABA time series was part of a larger experiment including other defense-related hormone treatments, such as MeJA, of which the results were published by Hickman *et al.* (2017). Rosettes of 5-week-old Arabidopsis Col-0 plants were dipped into an ABA (50 μ M; Duchefa Biochemie, Haarlem, the Netherlands) or mock solution for 3 s. The solutions were tap-water based and also contained 0.015% (v/v) Silwet L77 (Van Meeuwen Chemicals BV, Weesp, the Netherlands; nowadays this compound is known as CoatOSil 77 (Momentive, New York, NY, USA)) and 0.1% (v/v) ethanol because this was the stock solvent for ABA. The sixth true leaf (counted from the oldest) was harvested from each rosette, representing one replicate, at 15 min, 30 min, and 1, 1.5, 2, 3, 4, 5, 6, 7, 8, 10, 12 and 16 h after treatment (Table S1). For the mock series four replicates were sequenced and for the ABA series three. The mock time series had more replicates because it was sequenced together with a MeJA, SA, and SA + MeJA time series in two previous studies (Hickman *et al.*, 2017, Hickman *et al.*, 2019), and these data showed that three replicates were likely sufficient for the intended analyses of the other hormone treatments, thus lowering overall costs.

RNA extraction and sequencing

Total RNA was extracted using the RNeasy Plant Mini Kit (Qiagen, Venlo, the Netherlands), according to the manufacturer's instructions. The optional on-column DNase treatment step was included. RNA for the mock time series was extracted and sequenced as part of a previous study on the JA and SA networks (Hickman *et al.*, 2017, Hickman *et al.*, 2019), whereas RNA for the ABA time series was extracted later from leaf material that had been stored at -80°C. RNA quality was assessed on the 2100 Bioanalyzer (Agilent, Santa Clara, CA, USA) using the RNA 6000 Nano Labchip Kit (Agilent) and in case of insufficient quality (RIN < 8.0) additional samples harvested from the same experiment were used for a new RNA isolation. The mock time series libraries were prepared using the TruSeq mRNA Sample Prep Kit (Illumina, San Diego, CA, USA) and they were sequenced on the HiSeq 2000 platform (Illumina) with read lengths of 50 bases (see also Hickman *et al.*, 2017; Hickman *et al.*, 2019). For the ABA time series, the TruSeq mRNA Stranded Sample Prep Kit (Illumina) was used for library preparation and the sequencing was done on the NextSeq 500 platform (Illumina) with read lengths of 75 bases. To verify that both sequencing methods were sufficiently concordant, the RNA-seq data of eight untreated samples that had been processed along with the mock samples in the study of Hickman *et al.* (2017) were compared to four untreated samples (replicates of the same experiment) that were processed along with the ABA samples in the current study.

RNA-seq data processing

All reads of the mock and ABA treatments, which originated from two different library preparations and sequencing methods (see above), were counted as unstranded reads. The reads were aligned to the Arabidopsis genome (TAIR v10) using TOPHAT v2.0.4 (Trapnell *et al.*, 2009) with the settings 'transcriptome-mismatches 3', 'N 3', 'bowtie1', 'no-novel-juncs', 'genome-read-mismatches 3', 'p 6', 'read-mismatches 3', 'G', 'min-intron-length 40', 'max-intron-length 2000'. Next, reads were assigned to annotated gene models of TAIR v10 using HTSeq-count v0.6.1 (Anders *et al.*, 2015) with default settings except '-s no'. Normalization was done using the medium count ratio, following the principle applied in the DESeq2 R package (Anders and Huber, 2010). We verified that the two different library prep and sequencing methods of the mock and ABA time series did not lead to biases in the data by plotting all samples, including the untreated control samples (t0), in a PCA plot. The PCA was done on the \log_2 of the read counts using the `prcomp` function from the `stats` package in R (version 4.1.2) with default settings. Irrespective of the library prep and sequencing method, all control samples clustered together (Figure S1). The mock and ABA samples were distributed separately from the control samples along the first two principal components. This demonstrates that the different library preps and sequencing methods did not influence the comparative analysis of the ABA and mock treatments.

Differential expression analysis

Differential expression analysis was done according to the same strategy outlined in Hickman *et al.* (2017). Briefly, normalized counts over time were modeled using a GLM with a log link function and a negative binomial distribution. A full model that incorporated treatment and time was compared to a reduced model with only time as an independent variable using an ANOVA with a χ^2 test. The resulting *P* values were adjusted using the Bonferroni correction. Genes with an adjusted *P* value < 0.05 were considered for further analysis, using a slightly different version of the GLM that modeled counts as dependent only on time and the time*treatment interaction parameter, where this interaction parameter for each time point represents the treatment effect at that time point. From the significant genes according to the initial ANOVA and χ^2 test, those that in the second GLM version had at least at one time point a *P* value for the time*treatment parameter < 0.01, an absolute fold change > 2 at that time point, and on average at least 10 counts in one of the treatments at that time point were considered differentially expressed. Because GLMs do not always work when there are too many 0 counts, the same analysis was also run after all genes in all samples were assigned a pseudocount of 1. DEGs according to this pseudocount-based analysis were added to those of the first analysis (without pseudocount) only if it had been impossible to run the GLM on these genes in the first

analysis (but not if the genes were first calculated to be non-DEGs and after addition of a pseudocount they were DEGs).

Clustering analysis

Clustering was done on the \log_2 -fold change of all DEGs between ABA and mock treatment using SplineCluster (Heard *et al.*, 2006), with a prior precision value set to 10^{-5} . An additional reallocation function (Heard, 2011) that redistributes cluster outliers into more appropriate clusters was also performed.

GO term enrichment analysis

GO term enrichment analysis was done using the `enrichGO` function in `clusterProfiler` v4.2.1 (Yu *et al.*, 2012, Wu *et al.*, 2021a) with the following parameter changes. The `OrgDb` used was `org.At.tair.db` with 2021-09-01 as the GO source date, `'ont'` was set to `'BP'`, the `pAdjustMethod` was set to `'BH'`, and the `qvalueCutoff` and `pvalueCutoff` were set to 0.01. Finally, `minGSSize` was set to 10 to not include extremely rare GO terms, and the `maxGSSize` was set to 1093 (5% of the total number of annotated genes in the dataset) to exclude generic GO terms. The enrichment analysis was executed for each cluster separately. Potentially redundant GO terms were identified by investigating the overlap of genes belonging to different GO terms in each cluster. If there were three or more unique genes, the GO term was listed as enriched. If a GO term had no more than two unique genes compared to another GO term, the GO term with the highest *P* value was marked as potentially redundant. If the potentially redundant GO term was marked as such in all the clusters where it was enriched, it was considered as fully redundant, and thus not considered for visualization in Figure 2. Otherwise, the enrichment of the potentially redundant GO term was considered discriminative, and its enrichment was visualized in all clusters where it was enriched.

Promoter motif and TFBS enrichment analysis

Enrichment analysis of experimentally derived TFBSs to the genome was done based on a published DAP-seq dataset, which contains *in vitro* binding data of TFs to isolated genomic *Arabidopsis* DNA (O'Malley *et al.*, 2016). DAP-seq peaks were downloaded from Plant Cistrome DB (O'Malley *et al.*, 2016), omitting ampDAP data. To increase the chance that a DAP-seq peak was meaningful for gene regulation, the dataset was filtered based on a method that we adapted from Narsai *et al.* (2017). Whereas they took the top 25% strongest peaks per TF dataset for analysis, we calculated the 25th percentile *q* value of the total dataset and applied it to each individual TF-target dataset as a cutoff. This method

ensured that each TF-target dataset was reduced based on the same significance cutoff, rather than on the same proportion. Subsequently, a possible target gene was assigned to each peak based on two criteria, using ChIPpeakAnno (Zhu *et al.*, 2010). First, the peak had to fall within 3000 bp upstream or 5000 bp downstream of the transcription start site (TSS). Second, only the closest gene was chosen as the possible target gene. TFs in the final dataset were only retained if they were sufficiently expressed in our dataset (not necessarily differentially expressed), meaning that they had at least 97 reads in all samples combined (i.e., 1 read per sample on average) and had 1 or more reads in at least 15 samples. Fold enrichment of the binding sites for a TF was determined for each TF/cluster combination by dividing the number of genes assigned as a target of the TF in a cluster by the expected number. The expected number was calculated based on the total number of genes in the genome, the number of genes in the genome assigned as a target of the TF, and the number of genes in the cluster. The *P* value for the enrichment was calculated based on the hypergeometric distribution. For visualization of the enriched TFBS analysis (Figure 3) the fold enrichment was set to 1 if the corresponding *P* value of the enrichment was higher than 0.001, to ensure that only highly significant TFBSs (fold enrichments >2 and *P* value <0.001) were depicted.

For the motif enrichment analysis, TF-DNA sequence motifs that were derived from two PBM-based studies were retrieved in the form of position weight matrices (Franco-Zorrilla *et al.*, 2014, Weirauch *et al.*, 2014). Promoter sequences, which in this analysis were defined as the 500 bp upstream of TSSs, were download from TAIR v10. Occurrence of each motif in the promoter sequences of each gene in the genome was determined using FIMO (Grant *et al.*, 2011) with a *P* value cutoff of 10^{-4} . Fold enrichment of a motif was determined for each motif/cluster combination, similarly to the TFBS analysis, by dividing the number of genes with at least one motif in a cluster by the expected number. The *P* value for the enrichment was calculated based on the hypergeometric distribution. Motifs were visualized using WebLogo version 3.5.0 (Crooks *et al.*, 2004). Similar to the visualization of TFBS enrichment, the motif enrichment (visualized in Figure S3) was set to 1 if the corresponding *P* value of the enrichment was higher than 0.001, to ensure that only highly significant motifs (fold enrichments >2 and *P* value <0.001) were depicted.

Prediction of potential regulatory TFs by stepwise regression

A stepwise regression approach was taken to identify TFBSs associated with up/downregulation of target genes after ABA treatment. The maximum or minimum (depending on which was the largest) \log_2 -fold difference of ABA/mock out of the 14 time points was determined per gene for all genes in the genome and used as dependent variable. TFs from the filtered DAP-seq data (see “Promoter motif and TFBS enrichment analyses”) were used as potential regressors, based on presence/absence of their binding

sites in each gene. Bidirectional stepwise regression was used to come to a final model with only the most significant TFs. This was done using the stepAIC function from the MASS package (v7.3-55) in R (version 4.1.2).

DREM analysis

DREM analysis (Schulz *et al.*, 2012) was done with DREM v.2.0.3 on the \log_2 -fold change of DEGs after ABA treatment compared to mock treatment using default settings. No (further) normalization was done on the data. The filtered DAP-seq dataset described above ("Promoter motif and TFBS enrichment analysis") was used as the TF-gene interaction file. TFs were considered significant for a path if 'Score Split' of that path in the path table was < 0.001 . The 'Score Split' of a TF in a path is the probability of seeing a greater number of genes with a binding site for the TF in that path based on the hypergeometric distribution, given the number of genes with and without the binding site in the path before the split and the number of genes in the path itself. Note that because the split is calculated using the TFBS data the 'Score Split' is not a true P value.

Prediction of the earliest regulatory TFs (first level) of the ABA response

DEGs from *aba2* mutant plants, which were treated with ABA and the translation inhibitor CHX, were downloaded from Lumba *et al.* (2014). Subsequently, the DEGs that were common with the DEGs in our ABA time series were selected, forming a list of 'first DEGs'. Next, enrichment of TFBSs from the filtered DAP-seq dataset (see "Promoter motif and TFBS enrichment analyses"; O'Malley *et al.*, 2016) was determined in this set of first DEGs. This was done by comparing the observed number of first DEGs with a certain TFBS to the number expected by chance. The P value for this enrichment was determined based on the hypergeometric distribution. From this, TFs with significantly enriched binding sites (>2 -fold enrichment, $P < 0.01$) were selected as putative first regulators (first level of the ABA network) that are post-translationally activated by ABA.

Hierarchical network analysis

For the hierarchical network analysis, the first level of candidates was determined according to the analysis outlined above ("Prediction of the earliest regulatory TFs (first level) of the ABA response"). The second and third levels were determined as follows. As a start, TFs with enriched DAP-seq binding sites in the genes forming the expression-profile-based clusters (see "Clustering analysis") were considered as candidate TFs for the second level. Candidate TFs were then definitively assigned to the second level if their encoding genes were differentially expressed after ABA treatment and if they were

targets of TFs from the first level according to the filtered DAP-seq data (see “Promoter motif and TFBS enrichment analyses”). The third level consisted of the clusters themselves, but only those clusters that had enriched binding sites for TFs from the first or second level of the network were incorporated in the final network. TFs at the first level were removed if they did not regulate any genes encoding TFs at the second level and if their binding sites were not enriched in any of the clusters. Edges were assigned between TFs in the network if one TF regulated the transcription of another TF according to the filtered DAP-seq data and our expression data. Additionally, edges were added from TFs at the first level and second level to a cluster if the binding sites of these TFs were enriched in the promoters of genes in the cluster. The network was visualized using Cytoscape v3.7.2. The betweenness centrality of each node in the network was calculated using the Network Analyzer tool in Cytoscape. For this analysis, the clusters at the third level were replaced with the actual genes at that level, and edges were drawn from a TF to a gene if the TF regulated that gene according to the filtered DAP-seq data.

ACKNOWLEDGEMENTS

We are grateful for the contribution of Marcel van Verk for initial support with project design, data processing and basic analyses, and for the contributions of Jannes van der Meijden and Eva Willems in establishing a drought and recovery assay in our lab. This work was supported by the Netherlands Organization for Scientific Research (ALWGS.2016.005 to NA and VIDI 11281 to SCMWW) and the European Research 979 Council (Grant 269072 to CMJP).

SUPPLEMENTARY MATERIAL

Supplementary figures

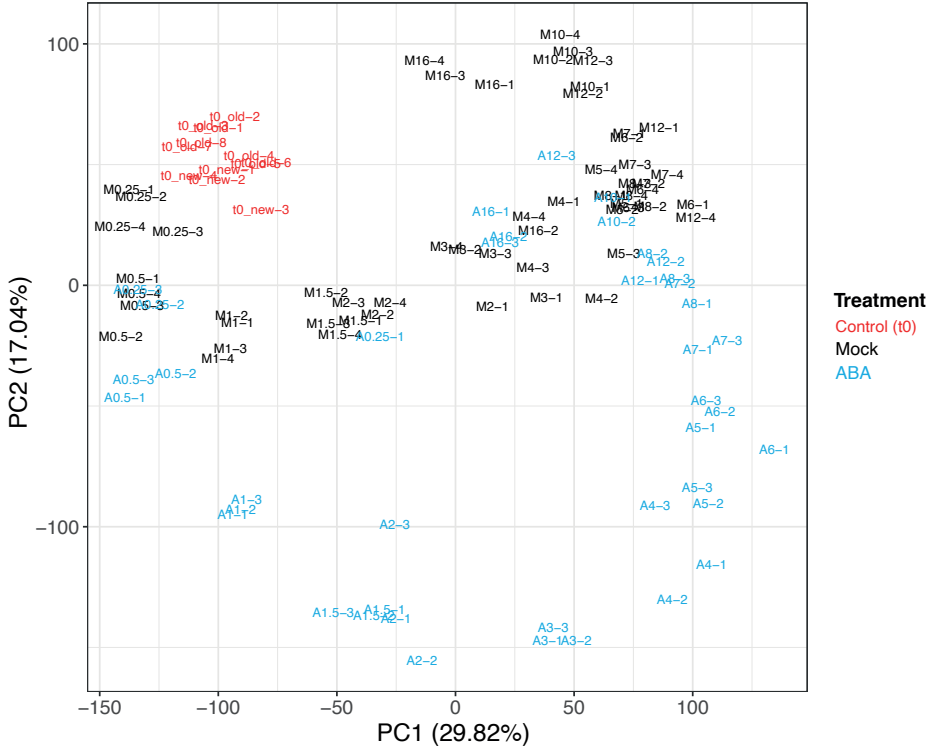


Figure S1: PCA of all samples from the ABA RNA-seq time series.

PCA was performed based on the \log_2 of the normalized read counts of all genes that were considered expressed (see Methods). Sample names reflect their treatment (M for mock and A for ABA), time (h) after treatment and replicate number (after the dash). “t0” represents control samples taken just before treatment; “old” or “new” reflects time of sequencing, where “old” samples were sequenced together with the mock time series using an unstranded library prep, and “new” samples were sequenced together with the ABA samples using a stranded library prep. Samples are colored according to their treatment. PC: principal component.

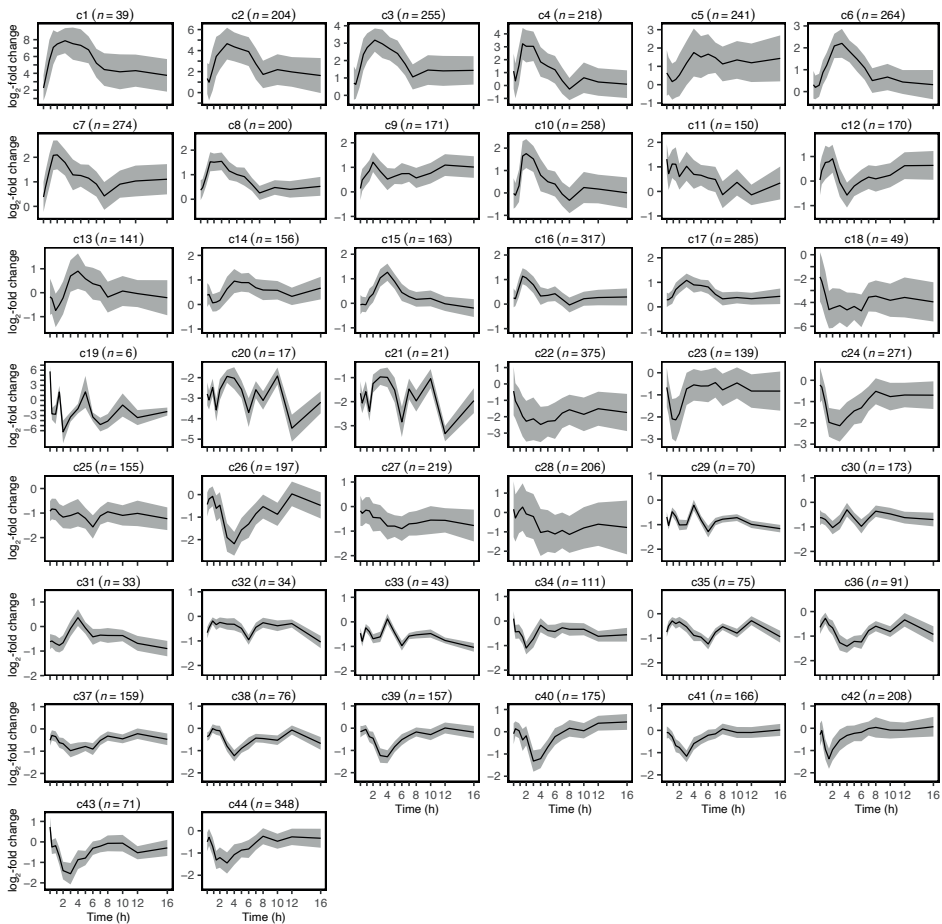


Figure S2: Expression profiles of clusters of coexpressed genes after ABA treatment.

The set of 7151 DEGs over the time course of 16 h after ABA treatment was clustered according to their expression pattern (\log_2 of ABA/mock) using SplineCluster, resulting in 44 distinct clusters (c1-c44). The black line represents the mean \log_2 -fold change (ABA/mock) of all genes in a cluster and the grey ribbon represents the standard deviation. The number of genes (n) in each cluster is indicated above each corresponding plot.

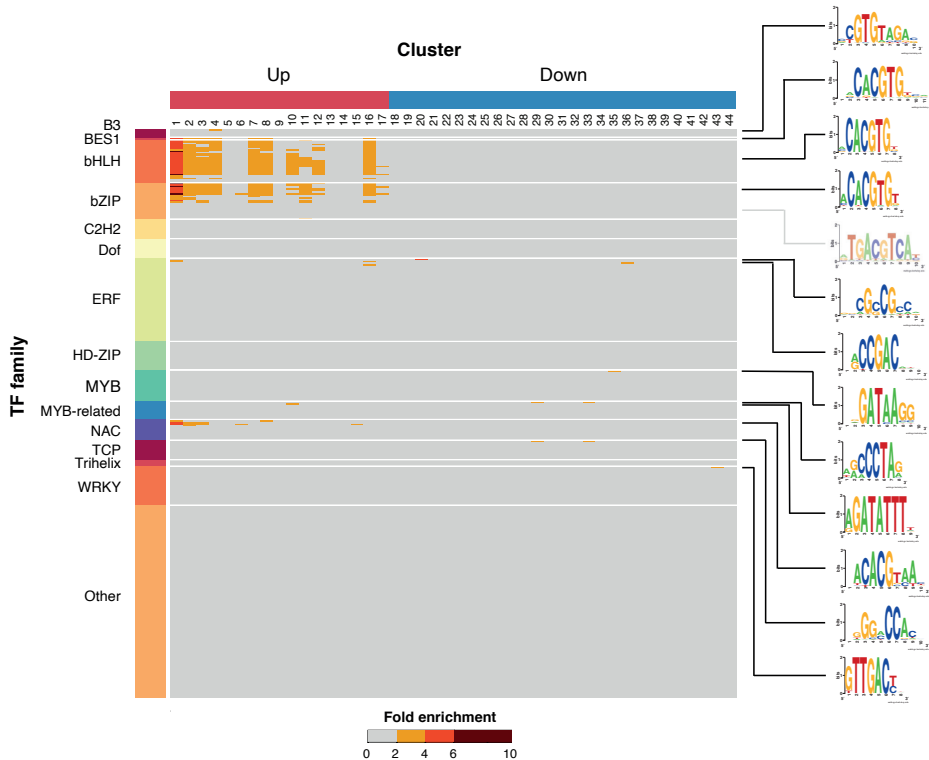


Figure S3: Fold enrichment of TF-DNA binding motifs in clusters of coexpressed genes after ABA treatment.

Occurrences of TF-DNA binding motifs from PBM data (Franco-Zorrilla *et al.*, 2014, Weirauch *et al.*, 2014) was determined in the 500 bp upstream of the TSS of all genes in the genome using FIMO (Grant *et al.*, 2011). Fold enrichment of each motif in each cluster compared to the whole genome was determined. Color in the heatmap represents fold enrichment. Color above the heatmap indicates if genes in the cluster are on average upregulated or downregulated. Only the highly significant motifs are depicted (see Methods). Motifs within each family were ordered in the figure based on presence/absence of binding sites in the clusters using the hclust function with the ward.D method. Representative motif logos of enriched motifs are shown on the right. In cases where multiple types of motifs are enriched in one family, a representative motif of each type is shown separately. In the case of the bZIP family, the not-enriched TGA motif is shown semi-transparently besides the much-enriched G-box-like motif (the upper motif) to demonstrate that although motifs of many bZIP family members are enriched, these are specifically not TGA motifs. The full set of motifs is shown in Table S6.

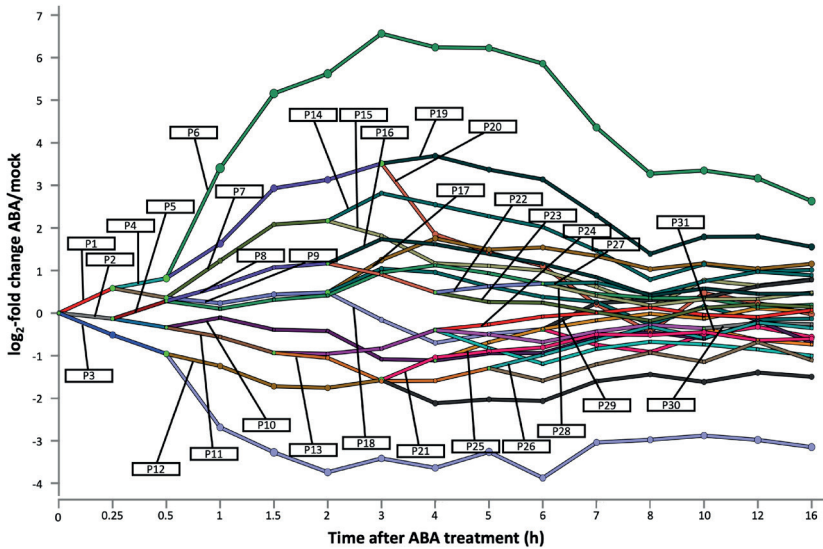


Figure S4: Numbered DREM paths from DREM analysis.

Figure acts as a supplement of Figure 5 and full explanation of the figure can be found there. This figure displays a number (P1-31) for each path with significantly enriched TFs in the DREM analysis (Figure 5), and this number is used in Table S8, where all significantly enriched TFs in the numbered paths can be found.

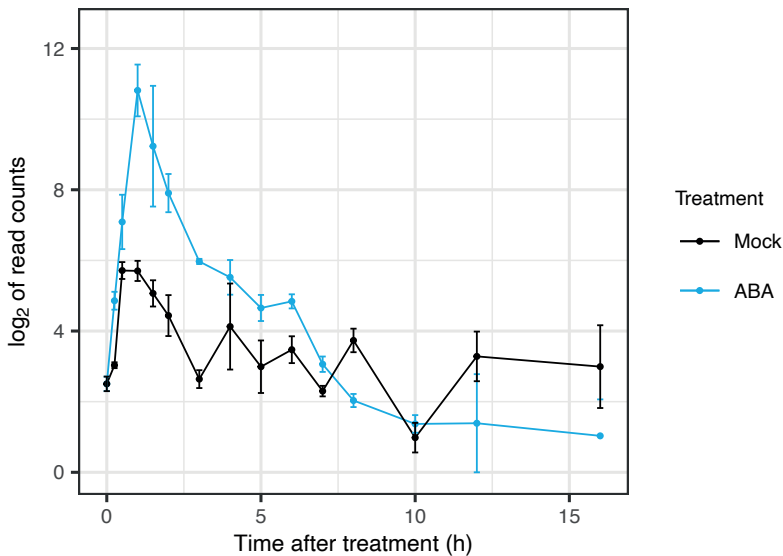


Figure S5: Expression profile of *GT3a* in a 16-h time course after ABA or mock treatment.

Mean and SE of the log₂ of the read counts is plotted for each time point (in h). Colors indicate treatments.

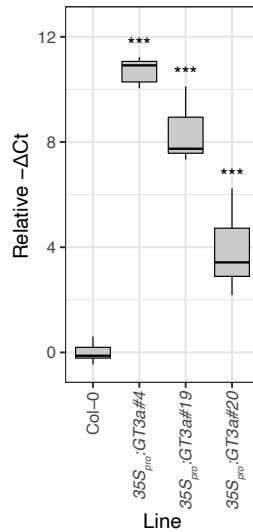


Figure S6: Relative expression levels of 35S_{pro}:GT3a overexpression lines.

Expression was measured by qPCR in one mature leaf of a four-week-old plant under basal conditions. The expression levels were calculated per sample as the difference in the Ct value (ΔCt) between *GT3a* and the reference gene AT1G13320. This ΔCt value was multiplied by -1 and normalized with the mean $-\Delta Ct$ value of Col-0 to determine the $-\Delta Ct$ relative to Col-0. Significant differences were calculated using one-way ANOVA followed by a Dunnett's test ($*P > 0.05$, $**P > 0.01$, $*P > 0.001$; $n=5$).

SUPPLEMENTARY TABLES

Supplementary tables S1-S9

Supplementary tables S1-S9, including full legends, are available upon request. Below, short legends for each of these supplementary tables are listed.

- Table S1:** Time series experimental set-up and mRNA sequencing details.
- Table S2:** Normalized read counts of all genes and biological replicates over a 16-h period after ABA or mock treatment.
- Table S3:** Z scores and fold change of DEGs after ABA treatment.
- Table S4:** Cluster membership of all DEGs after ABA treatment.
- Table S5:** GO term enrichment analysis in clusters of coexpressed genes after ABA treatment.
- Table S6:** Enrichment of motifs in clusters of DEGs after ABA treatment.
- Table S7:** Enrichment of TFBSs from DAP-seq data in clusters of DEGs after ABA treatment.
- Table S8:** Enrichments of TFBSs in DREM paths.
- Table S9:** Node and edge table of hierarchical ABA network.

Supplementary tables S10 and S11

Table S10: Overview of mutant lines used in this study.

'Mutant' is the name of the mutant line used in this study. Allele numbering was done based on previous studies, where the first described mutant is allele 1, the second allele 2 etc. In the zygosity column '+' means homozygous wild type, '+-' means heterozygous and '-' means homozygous mutant.

Gene	Locus	T-DNA line	Mutant	Zygosity	Genotyping primer fw	Genotyping primer rv	Reference for mutant
GT3a	AT5G01380	GK-591B09	<i>gt3a-1</i>	--	AAGGTTTATTTTCTCCACCAGG [†] TTTACGCGTTTATTGGTGAGC [†]	TTTACGCGTTTATTGGTGAGC [†] AAGCCTATTAAGCAAAGCATCG [†]	None
		SALK_134703C	<i>gt3a-2</i>	--	TTACCCGTTTGCCTCATAAAC	GAAGTCGTGGCTGCTAAGATG	None
GT3b	AT2G38250	SALK_133090C	<i>gt3b-1</i>	--	TGAATGAAAAAGCAGATTAACAG	GTGACGAGTTCTCCACTTG	None
		SALK_038142C	<i>gt3b-2</i>	--	TAAGAAACGCATACGCCATTC	CCGAAAAGAACATTGCAAAG	None
BIM2	AT1G69010	SALK_074689C	<i>bim2-1</i>	++ [‡]	ATGCTTTGTGCGAATATCTGT	CAGATTCTTCTCAACGCTTG	Yin et al., 2005
BIM2	AT1G69010	GK-351G11	<i>bim2-2</i>	--	ATCTGGAGAAAAGAGAAGGCG	TTCAGATTTTGGCCAGTGGATC	None
EPR1	AT1G18330	SAIL_195_F11	<i>epr1-1</i>	+ [§]	AAGCTACCAGCGTCAATGATG	TGCGTTACAATATGAAAAATGTGC	Khanna et al., 2006
		SALK_047716C	<i>epr1-2</i>	--	AGCAAGTGGAAAGTCAGAGACG	CAAGCTTGGCTATTGCAGAAC	Rawat et al., 2009 (there: <i>rve7-1</i>)
BEH2	AT4G36780	SALK_098067C	<i>beh2-2</i>	--	ACCCCTGTTTCCACAAGAATC	TGCGTTACAATATGAAAAATGTGC	None, Lachowiec et al., 2018 [†]
AREB3	AT3G56850	SALK_061079C	<i>areb3-1</i>	--	TCTTCTTTGATGGGTGTTTG	CAAGCTTGGCTATTGCAGAAC	Hoth et al., 2010 ^{††}
		SALK_204251C	<i>areb3-2</i>	--	TCTTGTGTCTCTGTATGCAG	AGCAGGCTTACACTCATGAGC	None
bZIP3	AT5G15830	SAIL_261_F01	<i>bzip3-1</i>	--	GCCACCCTTGGTTGTTAAAC	TTTGTCAITGATGCCCTCTCC	Sangi et al., 2018
bZIP53	AT3G62420	SALK_069883C	<i>bzip53-1</i>	--	TAAGGAGAGACTAAGCCCATC	TCGGATCATTATCGGATTCAG	Weltmeijer et al., 2006
bZIP68	AT1G32150	GK-627H10	<i>bzip68-1</i>	--	GTAACAGCCACTCAGCAGCTC	TTGCTAATTGCTATCATCGGAG	Li et al., 2019

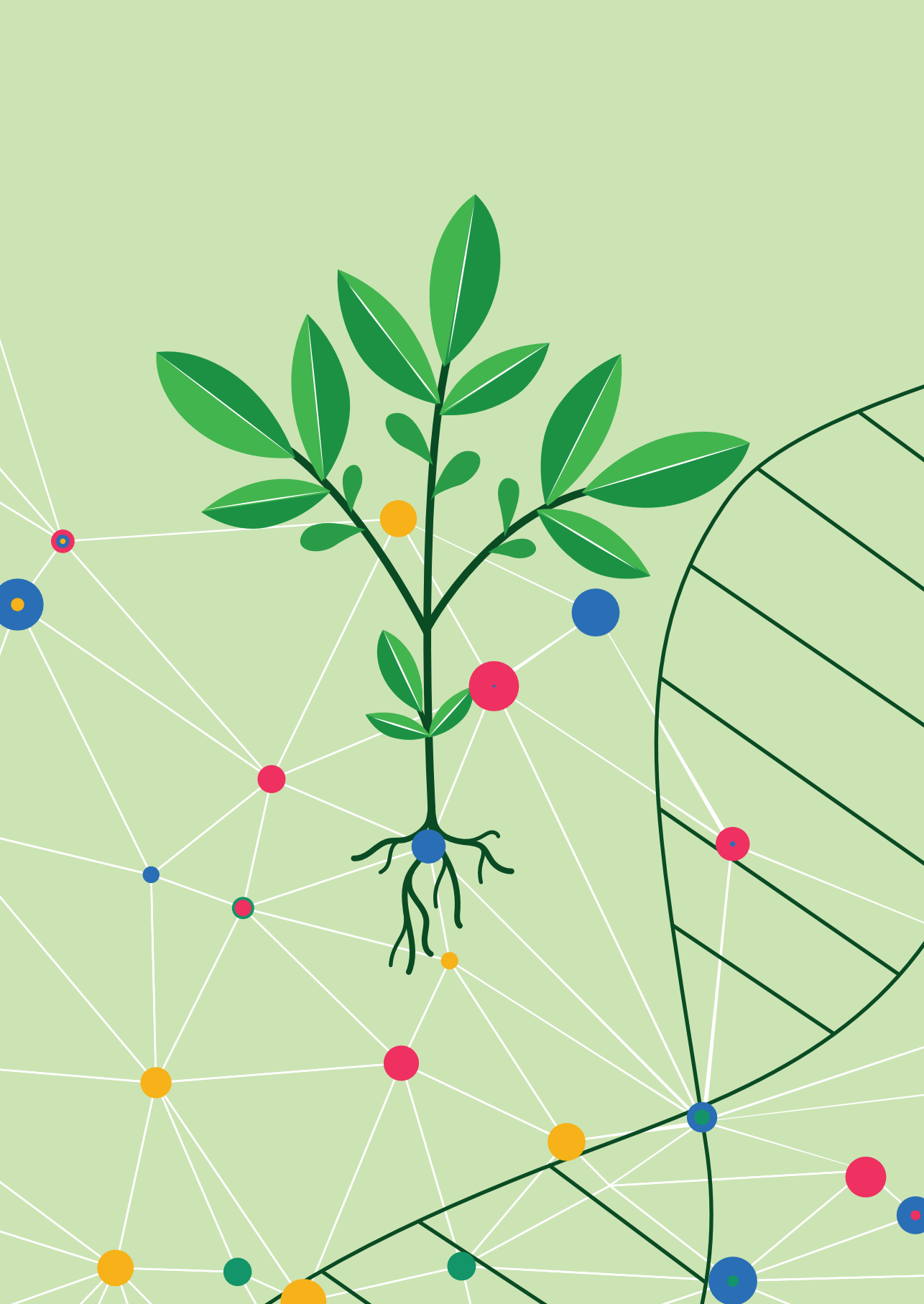
[†]For the GK-591B09 line two sets of primers were needed for genotyping. ^{††}Yin et al. (2005) used a different primer set for verification and did manage to obtain homozygous mutant lines. [§]Khanna et al. (2006) did not report any problems with obtaining homozygous lines, but did not disclose the primer pair used for genotyping. [¶]We initially overlooked the existence of the mutant line described in this work, so we analyzed another mutant allele and designated that *beh2-2*. ^{**}This line is not a true knockout line according to Hoth et al. (2010).

Table S11: Supplementary information on generation of *GT3a* overexpression lines.

(A) Primers used for amplification of the *GT3a* CDS with Gateway-compatible overhangs. The sequence overlapping the *GT3a* sequence is denoted in upper case letters and the Gateway-specific sequence is denoted in lower case letters. The *TA* sequence denoted in italic uppercase letters in the forward primer was added to allow cloning of an N-terminal tag in a possible future project.

(B) Line number, line name and relative overexpression (OX) levels of three different *GT3a* overexpression lines used for bioassays. The first number denotes a T1 plant with a unique insert and the second number denotes a unique T2 offspring plant, which was later verified to be homozygous for the insert. Relative *GT3a* expression levels were determined in 4-week-old plants under basal conditions and are shown in Figure S6.

A: Primers used		
Primer name	Primer sequence	
GT3a_attB1_F	ggggacaagttgtacaaaaagcaggctTAATGGACCGACGTAACCT	
GT3a_attB2_R-stop	ggggaccacttgtacaagaagctgggtaTTAGAAACCTTGATTATGATGATCA	
B: Lines used in this study		
Line number	Line name	Relative OX level
#4-3	<i>35S_{pro}:GT3a#4</i>	High
#19-5	<i>35S_{pro}:GT3a#19</i>	Middle
#20-1	<i>35S_{pro}:GT3a#20</i>	Low





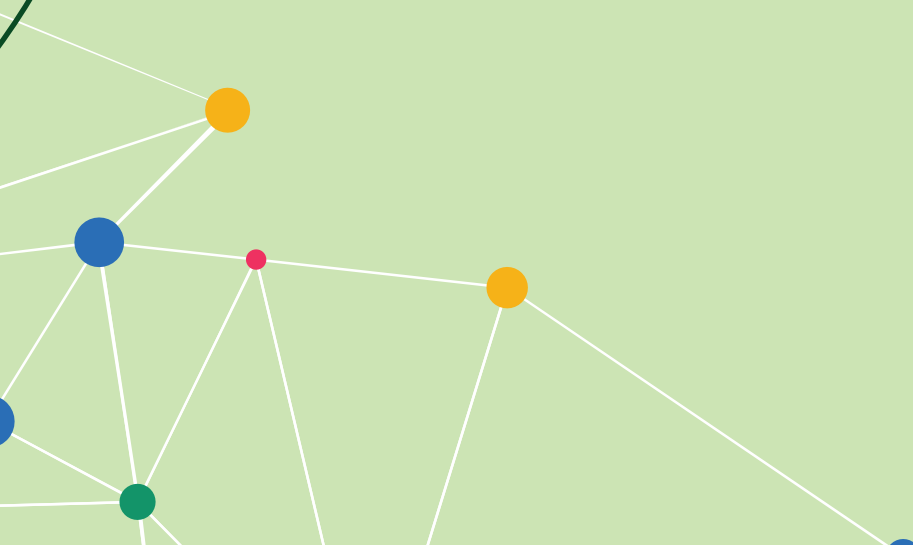
CHAPTER 3

Dynamic modulation of the jasmonic acid gene regulatory network by abscisic acid

Niels Aerts¹, Basten L. Snoek², Tessa W. Visscher¹, Corné M.J. Pieterse¹ and Saskia C.M. Van Wees¹

¹Plant-Microbe Interactions, Department of Biology, Utrecht University, P.O. Box 800.56, 3508 TB Utrecht, The Netherlands

²Theoretical Biology and Bioinformatics, Department of Biology, Utrecht University, P.O. Box 800.56, 3508 TB Utrecht, The Netherlands



ABSTRACT

The plant hormone jasmonic acid (JA) is a crucial regulator of defense against pathogens and pests. Crosstalk with other hormones shapes the final outcome of the JA-mediated response. Abscisic acid (ABA) acts as a coregulator of the JA response as it potentiates the JA-regulated anti-insect defense sector in the JA-dependent immune network, while it attenuates the JA-regulated defense sector directed against necrotrophic pathogens. To investigate how ABA modulates the JA gene regulatory network (GRN), we generated RNA-seq time series data consisting of 14 time points after treatment of *Arabidopsis thaliana* rosettes with methyl jasmonate (MeJA), ABA, or the combination of the two hormones. We found that MeJA and ABA regulate, and partly co-regulate, expression of thousands of genes. Of the MeJA-responsive genes, 2/3rd changed their expression level in a combined treatment with ABA, suggesting extensive modulation of the JA network by ABA. Notably, ABA accelerated the induction of MeJA-responsive JA biosynthesis and catabolism genes, indicating that ABA can affect the JA response at the level of JA production and turn over. We predicted 20 different transcription factors as ABA-regulated modulators of the JA network. Also, using a *Botrytis cinerea* infection assay with mutants of JA master regulators we found that ORA59 and ERF1 are themselves targeted by ABA to regulate repression of JA signaling. Based on our RNA-seq data we found that this occurs at least at the transcription level, but likely also at other levels. Indeed, using a transient protoplast expression assay we found that ABA reduces expression of the JA marker *PDF1.2* by reducing ORA59 protein stability. Our study gives unique insights into the effects of ABA on the dynamics of the JA GRN and provides new insights into how the ABA GRN and different sections of the JA GRN are integrated.

INTRODUCTION

Plant hormones are crucial in the interaction between plants and their often-hostile environment. They regulate responses to abiotic stresses, such as heat and drought, as well as biotic stresses, such as pathogen infection and insect infestation. Among the hormones that contribute to plant immunity, jasmonic acid (JA), salicylic acid (SA), abscisic acid (ABA) and ethylene (ET) are the most significant (Pieterse *et al.*, 2012, Aerts *et al.*, 2021). Since different kinds of attackers have different strategies to derive nutrients from the plant, the plant needs to activate a specific immune response that is tailored to the attacker that it encounters. This specificity is achieved in part by producing a specific blend of interacting immunity-related hormones dependent on the type of attacker. These hormones subsequently activate a complex and highly integrated immune network that eventually regulates the tailored immune response (Aerts *et al.*, 2021).

Within the integrated plant immune network, the individual hormone (sub)networks have specific but also overlapping functions (Tsuda *et al.*, 2009, Pieterse *et al.*, 2012). The SA pathway is generally associated with defense against pathogens with a biotrophic lifestyle. The JA pathway works in concerted action with ABA to regulate defense against insects, while coregulation of the JA pathway by ET leads to enhanced defense against pathogens with a necrotrophic lifestyle (Glazebrook, 2005, Pieterse *et al.*, 2012). ABA on the other hand represses defense against necrotrophic pathogens (Audenaert *et al.*, 2002, Anderson *et al.*, 2004, Sánchez-Vallet *et al.*, 2012). The branch of the JA pathway co-regulated by ABA is referred to as the MYC branch, after the central role of MYC transcription factors (TFs), namely MYC2, MYC3 and MYC4. The branch co-regulated by ET is referred to as the ERF branch, after the central role of ERF TFs, namely ERF1 and ORA59 (Pieterse *et al.*, 2012). Integration of these hormone-induced pathways occurs at various levels of molecular regulation, ensuring a robust defense response optimized for the attacker at hand (Aerts *et al.*, 2021). These interactions are referred to as crosstalk between hormone pathways. This study focuses on the modulation of the JA gene regulatory network (GRN) by ABA, which we will refer to as ABA/JA crosstalk.

JA signaling is initiated by a release-from-repression mechanism. Under basal conditions JASMONATE ZIM-domain (JAZ) proteins bind to and repress JA-related TFs such as the MYC branch regulators MYC2, MYC3 and MYC4 (Chini *et al.*, 2007, Fernández-Calvo *et al.*, 2011) and the ERF branch regulators EIN3 and EIL1 (Zhu *et al.*, 2011). However, when JA levels are high, the bioactive form of JA, JA-Ile (JA conjugated to isoleucine), mediates degradation of JAZs by facilitating their interaction with the E3 ubiquitin ligase complex SCF^{CO11}. This interaction targets the JAZs for degradation by the 26S proteasome (Thines *et al.*, 2007, Sheard *et al.*, 2010), leading to the release of TFs previously bound by the JAZs. This initiates a transcriptional cascade that involves thousands of genes (Hickman *et al.*, 2017). Characterization of this transcriptional cascade showed that it consists of multiple

phases of up- and downregulation of genes and includes the coordinated expression of clusters of genes that perform specific functions in the JA response (Hickman *et al.*, 2017).

Many studies have investigated the integration of the MYC and ERF branch in the JA GRN. In these studies, MYC and ERF branch activity is generally quantified based on marker gene expression. *VSP1* and *VSP2* are the most frequently used marker genes of the MYC branch and are activated by MYC2, MYC3 and MYC4, either directly or via ANAC019 and ANAC055 (Bu *et al.*, 2008, Fernández-Calvo *et al.*, 2011, Pieterse *et al.*, 2012). *PDF1.2* is the most frequently used marker gene of the ERF branch (Pieterse *et al.*, 2012). It is induced by both the ERF TFs *ORA59* (Pré *et al.*, 2008, Zarei *et al.*, 2011) and *ERF1* (Solano *et al.*, 1998, Berrocal-Lobo *et al.*, 2002, Lorenzo *et al.*, 2003, Zarei *et al.*, 2011). *ORA59* and *ERF1* are believed to positively affect each other's transcription (Çevik *et al.*, 2012, Van der Does *et al.*, 2013, Zander *et al.*, 2014, Yang *et al.*, 2021), but conflicting results suggesting no effects on each other have also been found (Pré *et al.*, 2008). Together, this suggests that *ERF1* and *ORA59* play a partly interdependent and partly overlapping role within the ERF branch of defense. Transcription of *ORA59* and *ERF1* is regulated by the TFs *EIN3* and *EIL1*, although direct TF-target regulation has only been convincingly shown for *EIN3-ERF1* (Solano *et al.*, 1998, Pré *et al.*, 2008, Zhu *et al.*, 2011, Chang *et al.*, 2013, Zander *et al.*, 2014). *EIN3* and *EIL1* are unique TF proteins because they are not only activated by JA signaling through degradation of JAZ proteins, but also by ET signaling through the activity of the ET signal transducer *EIN2* (An *et al.*, 2010, Li *et al.*, 2015, Merchante *et al.*, 2015). As such, *EIN3* and *EIL1* act as master regulators of both the ERF branch of defense and ET signaling in general (Broekgaarden *et al.*, 2015, Dolgikh *et al.*, 2019).

ABA signaling is highly integrated with JA signaling. It has long been known that ABA generally enhances the MYC branch and suppresses the ERF branch of the JA pathway (Pieterse *et al.*, 2012). In *Arabidopsis thaliana* (hereafter: *Arabidopsis*), some of the details of how this works have been elucidated. For example, ABA causes upregulation of *MYC2*, and in turn *MYC2* can regulate genes relevant for ABA signaling (Abe *et al.*, 1997, Abe *et al.*, 2003). ABA can also promote the biosynthesis of JA (Adie *et al.*, 2007, Fan *et al.*, 2009, Wang *et al.*, 2018), which may at least partly be attributed to ABA's effect on *MYC2* described above, since *MYC2* is known to upregulate genes involved in JA biosynthesis genes either directly or via upregulation of *ORA47*, which in turn induces JA (and ABA) biosynthesis genes (Pauwels *et al.*, 2008, Chen *et al.*, 2016, Hickman *et al.*, 2017, Zander *et al.*, 2020). Next to this, ABA causes upregulation of *PLIP2* and *PLIP3*, two genes that encode lipases that catalyze the release of polyunsaturated fatty acids that form the precursors for JA (Wang *et al.*, 2018). Overexpression lines of these genes display enhanced JA signaling, indicating the functional importance of these genes in ABA/JA crosstalk. ABA/JA crosstalk also occurs at other regulatory levels. For example, the ABA receptor *PYL6* interacts with *MYC2* in an ABA-dependent way, altering the DNA binding specificity of *MYC2* such that its activation of *JAZ6* transcription is enhanced and of *JAZ8* transcription is reduced (Aleman *et al.*, 2016).

However, the genome-wide implications hereof are not yet clear. ABA can also enhance JA signaling by promoting degradation of JAZ12, a protein that inhibits JA signaling. This degradation is achieved by ABA-promoted self-ubiquitination of KEG, a RING E3 ligase that in the absence of ABA decreases COI1-mediated JAZ12 degradation (Pauwels *et al.*, 2015). In summary, ABA enhances JA signaling in general (e.g., by promoting JA biosynthesis) and the MYC branch specifically.

While multiple effects of ABA on the MYC branch have been found, research on the mechanisms by which ABA suppresses the ERF branch has been lagging. Most papers only note that ABA suppresses ERF branch marker gene expression and defense against necrotrophic pathogens (Audenaert *et al.*, 2002, Anderson *et al.*, 2004, Sánchez-Vallet *et al.*, 2012). Some mechanistic insights were given by a preprint by Vos *et al.* (2019), who used a *myc2* mutant and *myc2,3,4* triple mutant to show that ABA-induced suppression of the ERF branch is likely not dependent on these MYC TFs. The researchers also found that ABA can still suppress *PDF1.2* expression in a $35S_{pro}::ORA59$ overexpression line after herbivory by *Pieris rapae* (hereafter: Pieris), suggesting that ABA acts downstream of transcription of *ORA59*. Using a transgenic line ectopically expressing a tandem of four copies of the GCC box, which is the DNA binding site for ERF TFs such as *ORA59* (Zarei *et al.*, 2011), they found that ABA was also able to suppress the GCC box. These results suggest that ABA targets GCC-box-binding ERF TFs, although the level at which this occurs is still to be elucidated.

In addition to direct effects of ABA on the MYC and ERF branch, research has also discovered ABA-independent mechanisms of MYC/ERF branch antagonism. For instance, *MYC2* and *EIN3* were found to interact at the protein level, leading to reciprocal inhibition of each other's transcription activation activity (Song *et al.*, 2014, Zhang *et al.*, 2014). Similarly, *MYC2* and *ORA59* can repress each other's expression (Verhage *et al.*, 2011, Zhai *et al.*, 2013). However, only in the case of *ORA59* suppression it was shown that this is the result of direct binding of *MYC2* to the *ORA59* promoter (Zhai *et al.*, 2013).

Despite all the advances in our understanding of the integrated JA and ABA network, there is still much information missing. In this study we investigated how ABA affects the temporal dynamics and architecture of the JA GRN at the whole genome transcriptome level. This led to the prediction of novel players in the ABA/JA crosstalk and revealed how key JA master regulators are targeted by ABA, leading to rewiring of the JA GRN.

RESULTS

High-density time series of the ABA and JA GRNs and their interaction

To obtain detailed insight into the modulating effect of ABA on the JA GRN, we profiled the transcriptome of a just-matured leaf from 5-week-old *Arabidopsis* rosettes treated with either 50 μM ABA, 100 μM MeJA (a methylated form of JA that is converted to free JA in the plant), a combination of the two, or a mock solution. Plant material was harvested at 14 time points after treatment: 0.25, 0.5, 1, 1.5, 2, 3, 4, 5, 6, 7, 8, 10, 12 and 16 h (Table S1). Data for the MeJA time series were described previously (Hickman *et al.*, 2017). In the present study, we compared the ABA time series to the MeJA time series and assessed the modulation of the JA network by ABA in the combined time series.

We used a generalized linear model (GLM) to identify differentially expressed genes (DEGs) in the three time series: ABA, MeJA and ABA + MeJA. This resulted in 7151, 3529 and 9829 DEGs respectively, with roughly equal numbers of upregulated and downregulated genes (Figure 1A, E). We observed a high overlap between the three time series, with 2194 genes being differentially expressed in all treatments, representing more than 60% of all genes that were differentially expressed after MeJA treatment and more than 30% after ABA treatment (Figure 1C). Additionally, almost 2/3rd of the genes that were differentially expressed after MeJA treatment (2292/3529) were significantly differentially expressed after ABA + MeJA treatment compared to the MeJA treatment alone (Figure 1B). In the majority of the cases (1398/2292 genes) ABA reinforced the effect that MeJA already had (e.g., genes that were upregulated or downregulated after MeJA treatment were even higher upregulated or downregulated, respectively, after ABA + MeJA treatment), but there was also a considerable portion of genes (894/2292 genes) where the effect of MeJA was counteracted by ABA in the double treatment (Figure 1B). Only 73 genes were differentially expressed after both ABA and MeJA single treatments, but not the ABA + MeJA double treatment (Figure 1C). Of these 73 genes, 56 were regulated in the opposite direction by ABA and MeJA, so in the double treatment the two hormones likely canceled each other's effect. In contrast, 2470 genes (around 25%) were uniquely differentially expressed after the double treatment (Figure 1C), although the amplitude of their expression was generally low (Figure S1A). These genes could require input from both hormones for differential expression (e.g., requiring two TFs), or their expression after each single treatment fell below the threshold to be considered differentially expressed, but did make the threshold after the combined treatment.

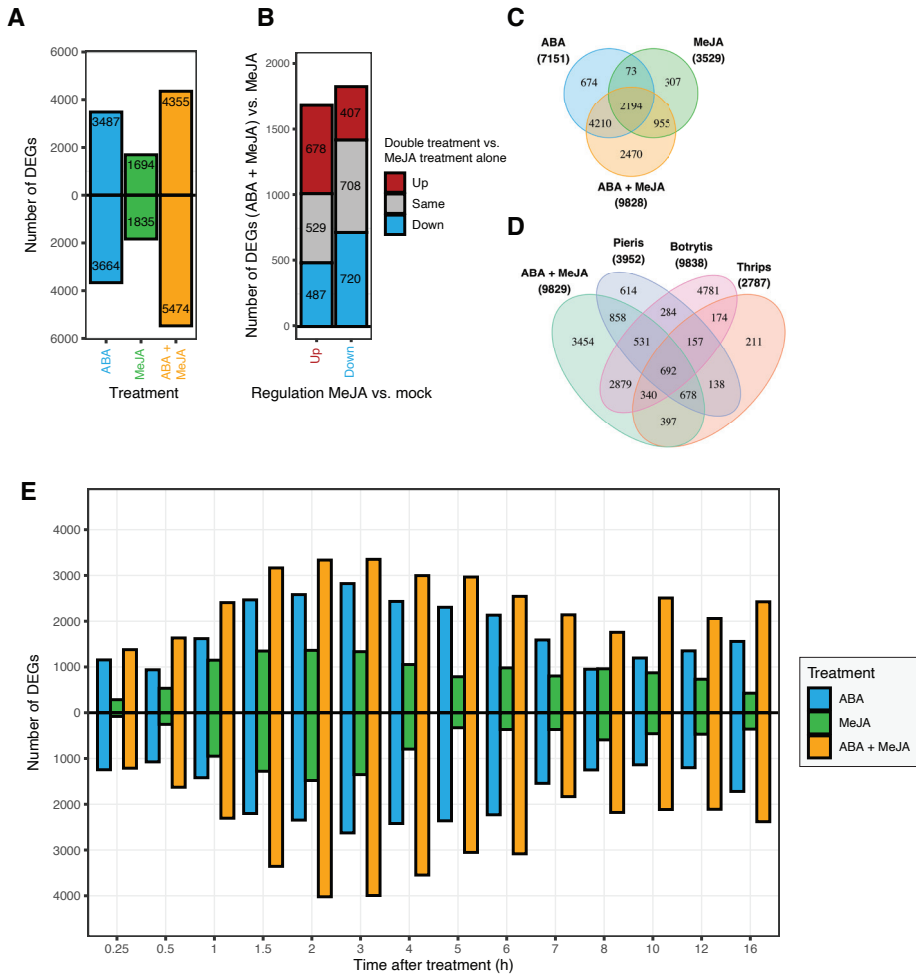


Figure 1: Analysis of DEGs in the ABA, MeJA and ABA + MeJA time series.

Differential expression was determined compared to mock treatment using a GLM approach (Methods).

(A) Overview of DEGs in the entire time series. Genes are categorized as upregulated or downregulated based on the mean \log_2 -fold change compared to mock for significant time points ($|Z\text{-score}| > 2.5758$).

(B) Overview of the number of genes that are up- or downregulated after MeJA treatment and are differentially expressed after ABA + MeJA treatment compared to MeJA treatment alone. The direction of differential expression (up/down) is based on the mean \log_2 -fold change compared to MeJA for significant time points ($|Z\text{-score}| > 2.5758$).

(C) Venn diagram showing overlap in DEGs between the three different time series.

(D) Venn diagram showing overlap between DEGs from the ABA + MeJA time series and time series data of leaves attacked by *Pieris rapae* (Coolen *et al.*, 2016), *Botrytis cinerea* (Windram *et al.*, 2012) or Western flower thrips (Steenbergen, 2022). Number between parentheses indicates total number of DEGs.

(E) Number of DEGs at each time point in the ABA, MeJA and ABA + MeJA time series. A DEG at a time point was defined as a DEG for the overall time series according to the GLM and a $|Z\text{-score}| > 2.5758$ at that time point according to the GLM (Methods).

To investigate to what extent the ABA and MeJA response reflect responses to pests and pathogens we assessed the overlap between the ABA + MeJA time series with time series data of leaves attacked by the chewing caterpillar *Pieris* (Coolen *et al.*, 2016), the necrotrophic pathogen *Botrytis cinerea* (hereafter: Botrytis) (Windram *et al.*, 2012) and the cell-sucking insect Western flower thrips (*Frankliniella occidentalis*; hereafter: thrips) (Steenbergen, 2022). Of the 9829 genes affected by ABA + MeJA treatment, 6375 (64.9%) were affected in at least one of the pest/pathogen time series (Figure 1D), illustrating the important role of JA and ABA in defense against these attackers. Overlapping genes were more often regulated in the same direction between the ABA + MeJA time series and the pest/pathogen time series (e.g., up/up) than in opposite directions (e.g., up/down; Figure S1B-E), suggesting a positive contribution of these hormones to the defense response. The overlap with the *Pieris* dataset was particularly large, indicating the important role of ABA in defense against this chewing insect.

We next investigated the transcriptional dynamics over time after ABA, MeJA and double treatment. First, we plotted the number of DEGs at each time point. Differential expression of genes already occurred at 15 min after treatment, particularly in the ABA and ABA + MeJA time series, with more than 2000 DEGs each (Figure 1E). The total number of DEGs peaked between about 1.5 and 3 h after each hormone treatment and gradually decreased thereafter (Figure 1E), suggesting that this is the period of maximum activation of the networks. Also, the number of DEGs in the ABA and double treatment time series was larger than in the MeJA time series, suggesting that the ABA GRN encompasses more genes than the JA GRN. The general trend in number of DEGs per time point was similar for the different time series, except for the fact that in the MeJA time series downregulation generally occurred later and affected relatively fewer genes than in the other time series. This suggests that the quickest responses in the JA network mostly involve upregulation of target genes.

Next, to better assess similarities and differences in transcriptional dynamics over time we performed a principal component analysis (PCA) on all samples based on the union of all genes that were differentially expressed in at least one time series. The first principal component (PC1) mostly captured the variation caused by the treatment, while PC2 seemed to capture mostly the circadian rhythm (Figure 2). The larger spreading of ABA than MeJA samples on PC1 and moderately also PC2 confirmed that ABA alone had a larger effect on the transcriptome than MeJA alone. Also, the samples from between 1.5 and 3 h after treatment with either hormone deviated mostly from the first and final time points on PC1, confirming that at these time points the JA and ABA networks are the most activated. Based on this plot the ABA + MeJA time series seems to be an exaggerated response of the single ABA and MeJA time series, resulting in larger transcriptional programming than each of the single treatments. This confirms our analysis as presented

in Figure 1B and 1C that the two hormones generally have a similar effect on target gene expression instead of cancelling out each other's effect.

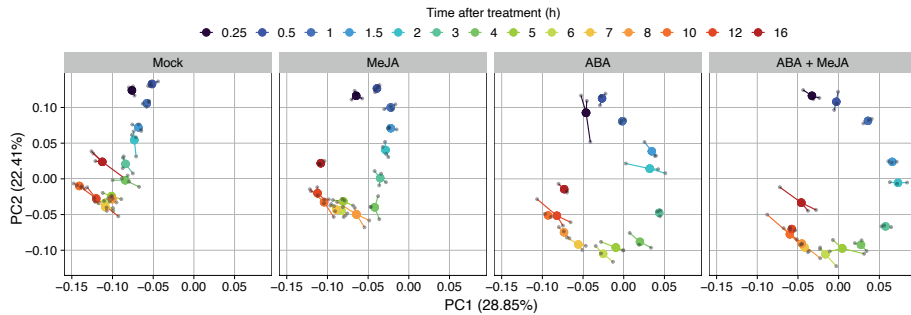


Figure 2: Principal Component Analysis (PCA) of the ABA, MeJA and ABA + MeJA RNA-seq time series.

PCA was conducted on the \log_2 -transformed read counts of the union of genes that were differentially expressed after ABA, MeJA and/or ABA + MeJA treatment compared to mock. For each timepoint the centroid is displayed in color and the corresponding samples in gray ($n=3$ for ABA and ABA + MeJA and $n=4$ for mock and MeJA). For clarity purposes the different treatments are plotted in their own panel, but each panel represents the same space. Colors represent time after treatment (in hours). PC: principal component.

Because we were mostly interested in the effect of ABA on the JA network we also performed a PCA on all samples based on only the genes that were differentially expressed after MeJA treatment. Similarly to the PCA based on DEGs in any treatment (Figure 2), PC1 and PC2 seemed associated with the treatment and circadian effect, respectively (Figure S2). To better visualize how treatment and circadian effects progressed over time, we plotted each of the PCs against the time after treatment (Figure 3). This PCA verified that what we found for the union of DEGs in all of the time series, also held true for just the DEGs after the single MeJA treatment: ABA has a similar effect as MeJA on genes that respond to MeJA and it seems to generally reinforce the effect of MeJA in the combined treatment (Figure 3A). This reinforcing effect was especially clear during the peak of expression (1.5-3 h after treatment), but is evident throughout the entire time series. Figure 3B also shows that in the timing-dominated PC2 the samples of the MeJA treatment are slightly higher than the mock samples at the earliest time points and the ABA samples are slightly lower than the mock samples from 4 h on; the MeJA + ABA samples generally follow the pattern of the most influential single treatment. This analysis suggests that first MeJA and then ABA exaggerates the timing/circadian effect, but PC2 may as well capture treatment effects that are independent of the circadian rhythm.

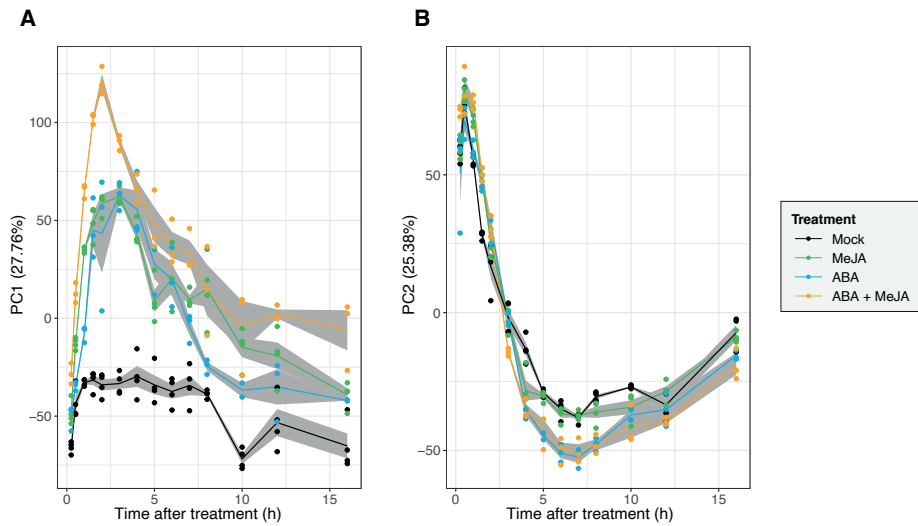


Figure 3: PCA on expression levels of all MeJA-responsive genes in the ABA, MeJA and ABA + MeJA time series, plotted against time after treatment.

Principal component analysis was applied to \log_2 -transformed reads of genes that were differentially expressed upon the single MeJA treatment. X-axis represents time after treatment, Y-axis represents the position on (A) the first or (B) the second principal component (PC) from this MeJA-based PCA. Samples were colored according to their treatment. Dots represent individual samples, the line represents the mean per timepoint, and the ribbon represents the standard error. A plot of the first against the second PC, on which this figure is based, is presented in Figure S2.

To investigate if the observed high overlap between the single ABA and MeJA response held true over all time points we compared the Z-scores that were produced by the GLM between the two time series for each gene that was differentially expressed in the ABA and/or the MeJA time series at each time point (union of DEGs). A Z-score in this context is the estimated effect of the treatment at that time point divided by the standard error. The analysis showed a clear correlation between Z-scores of genes for both time series, especially between 1.5 and 4 h after treatment (Figure 4A), suggesting that the response to ABA and MeJA is – to some extent – qualitatively comparable. We also considered the possibility that the two responses may be even more similar, but with different timing. For example, the ABA response may be similar to a delayed JA response because ABA promotes JA biosynthesis (Adie *et al.*, 2007, Fan *et al.*, 2009, Wang *et al.*, 2018) (Aerts *et al.*, 2021). To analyze this, we calculated the correlation coefficient of the Z-scores of the two time series for every possible combination of time points. However, this analysis showed that the highest correlation was between the 4-h time points of both time series and that generally the highest correlations were between the same time points (although with some exceptions, Figure 4B), suggesting the timing of the responses is in general quite similar.

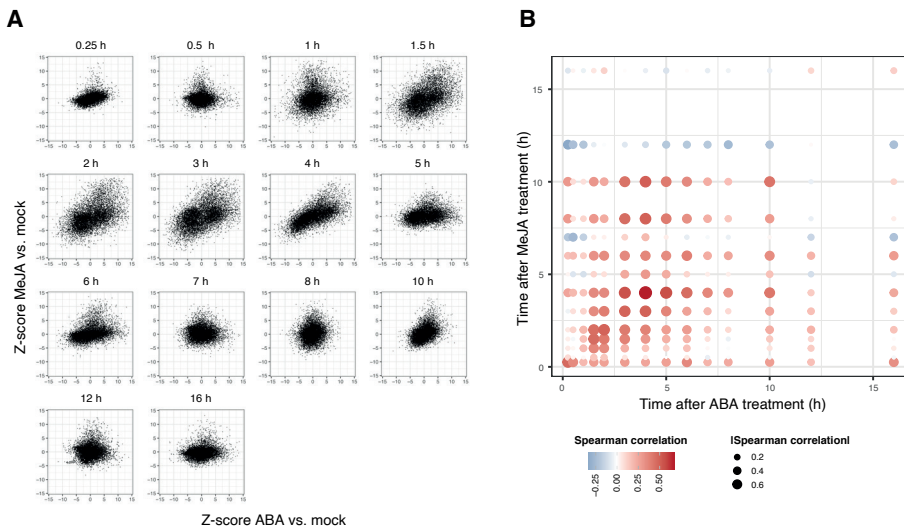


Figure 4: Correlation between ABA- and MeJA-responsive gene expression profiles.

Z-scores per gene per timepoint were calculated for the ABA and the MeJA time series vs. mock using a GLM (Methods). The union of genes that were differentially expressed after single ABA or MeJA treatment were considered for the analysis ($n=8413$).

(A) Scatter plot per time point, where each dot represents one gene. h = hours after treatment.

(B) The Spearman correlation coefficient was calculated for each treatment/time point combination and plotted in a dot plot. Dot color reflects the Spearman correlation coefficient and dot size reflects the absolute Spearman correlation coefficient.

Combined activation of the JA and ABA networks generally has non-additive effects on gene expression

To better understand how the ABA and JA network are integrated we turned our focus to the double treatment time series. We were first interested to see if expression in the double time series differed from a simple addition of the single treatments, since this would point towards extensive crosstalk between the two pathways. We thus plotted the expression of each gene that was differentially expressed in at least one of the treatments and determined how much the double treatment differed from the sum of the single treatments (assuming addition on a \log_2 scale). This showed that the double treatment was generally not a simple addition of the single treatments for the majority of genes at more than one time point (Figure 5), suggesting extensive crosstalk between the two pathways. One of the major patterns was that genes that were strongly upregulated or downregulated by both single treatments were usually lower upregulated or downregulated than expected after the double treatment, respectively. This is well illustrated by the expression profiles of *VSP2* and *ORA59*. *VSP2* was strongly upregulated by both ABA and MeJA, which was slightly enhanced by the double treatment, being less

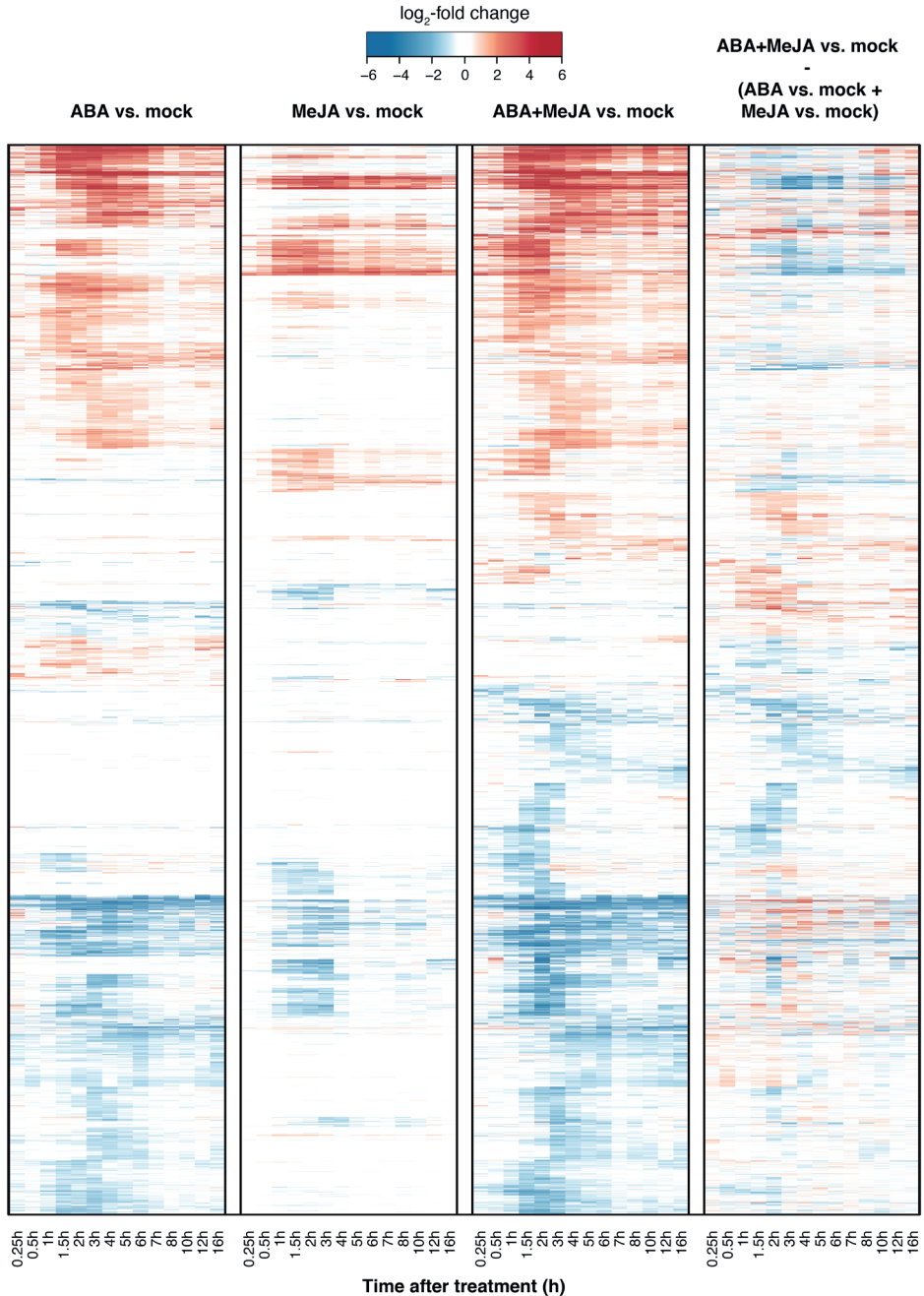


Figure 5: Relative expression of the union of genes that were differentially expressed after ABA, MeJA and/or ABA + MeJA treatment.

\log_2 -fold change is depicted for ABA vs. mock, MeJA vs. mock, and ABA + MeJA vs. mock. For all these comparisons, \log_2 -fold change of genes that were not significantly different at a specific time point according to the GLM described in the 'Methods' section [$|Z\text{-score}| < 2.5758$] was set to 0 at that time point. In the fourth panel, the

difference between the ABA + MeJA vs. mock comparison and the sum of the ABA vs. mock and MeJA vs. mock comparisons was depicted, to assess if the expression after ABA + MeJA treatment was more, less or no different from an additive effect of the two single treatments. Genes were ordered based on their expression patterns in all four panels using the `hcluster` function with the `ward.D` method in R.

than the sum of the single treatments (Figure 6A). Similarly, *ORA59*, which was mostly downregulated by the single treatments, was less downregulated than expected by the double treatment, except for some time points (Figure 6B). The downregulation of *ORA59* after single MeJA treatment is somewhat counterintuitive, since it is known as a positive regulator of JA signaling. It may possibly be explained by relatively high endogenous levels of ABA and low levels of ET in plants used in our experiment, causing mostly activation of the MYC branch by MeJA (with the marker gene *VSP2*) and repression of the ERF branch (which includes *ORA59*). The observed non-additive effects in the double treatment suggest some level of interaction between the two pathways, for example competition for the same TF binding sites in the promoter of target genes.

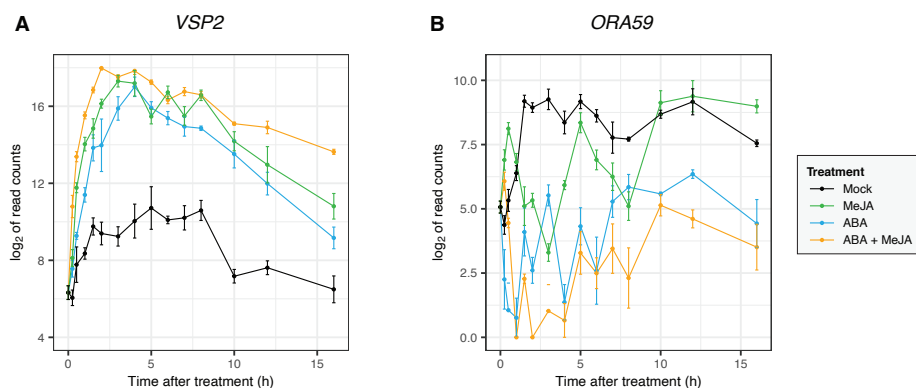


Figure 6: Expression profiles of JA marker genes.

Expression profiles of (A) *VSP2* and (B) *ORA59* in a time course of 14 time points after treatment of 5-week-old rosettes with ABA, MeJA, ABA + MeJA or mock. Expression profiles were plotted based on mean and standard deviation of \log_2 -transformed read counts.

ABA has a large effect on expression of JA metabolism genes

One possible explanation for the overlap between the MeJA and ABA response is that ABA may influence JA biosynthesis. Indeed, previous studies showed that ABA promotes JA biosynthesis (partly) via regulation of the JA master regulator *MYC2* and the TF *ORA47*, which is also a transcriptional target of *MYC2* (Adie *et al.*, 2007, Fan *et al.*, 2009, Chen *et al.*, 2016, Wang *et al.*, 2018). Our data confirmed that ABA upregulates *MYC2* and *ORA47* (Figure S3A, B), especially at earlier time points. To further investigate the effect of ABA on JA

metabolism we plotted the expression of JA biosynthesis genes, ranging from the lipases that start the pathway to JAR1 that converts JA to bioactive JA-Ile (Figure 7A), and of JA catabolism genes (Figure 7B). Most JA biosynthesis genes were upregulated by ABA in at least one time point, and only *OPR1* was downregulated (Figure 7A). This again confirms that ABA can induce JA biosynthesis (Adie *et al.*, 2007, Fan *et al.*, 2009, Wang *et al.*, 2018) and shows that this is likely achieved via upregulation of many different JA biosynthesis genes. Similarly, MeJA treatment also caused upregulation of many JA biosynthesis genes (Figure 7A), as described in e.g., our earlier report on the single MeJA time series (Hickman *et al.*, 2017). Although there was much overlap with ABA with respect to which genes were upregulated, MeJA treatment generally caused a longer lasting change in expression. Genes exclusively upregulated by ABA were the lipases *PLIP2* and *PLIP3* (Wang *et al.*, 2018), and *KAT2*, which is involved in the β -oxidation rounds in the final steps of JA biosynthesis (Cruz Castillo *et al.*, 2004). Interestingly, combined ABA and MeJA treatment seemed to cause a shift in timing of upregulation of JA biosynthesis genes compared to JA treatment alone: genes generally had an earlier peak in expression, but expression also decreased faster. This suggests that ABA may speed up the positive feedback of JA on its own levels, possibly providing a faster and stronger defense response against certain attackers.

Interestingly, JA catabolism genes were also highly induced by both ABA and MeJA treatment (Figure 7B). This suggests that there is also strong negative feedback of JA on its own levels, and of ABA on JA levels. Combined ABA and MeJA treatment caused the highest and longest upregulation of JA catabolism genes. The peak of expression seems to be slightly later than that of JA biosynthesis genes, possibly causing a short peak of enhanced JA levels that declines later in our experiment, which could be a mechanism to quickly return JA to basal levels.

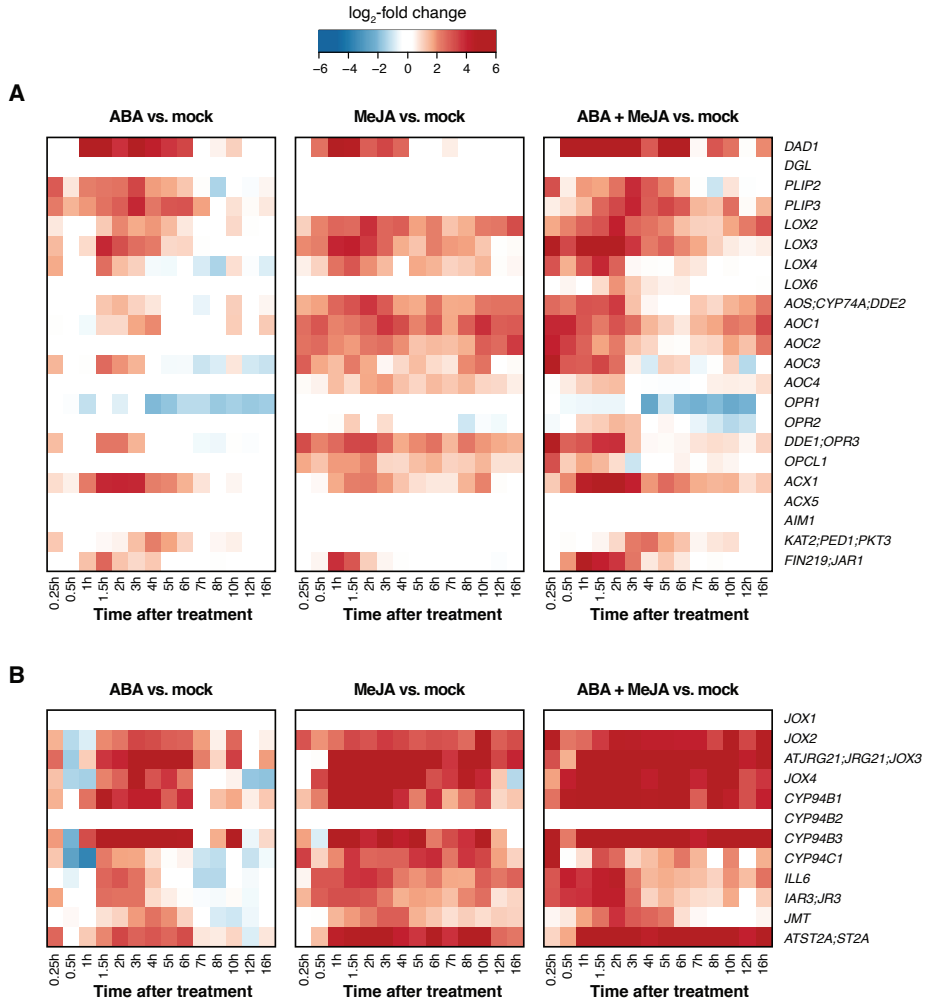


Figure 7: Expression of JA biosynthesis and catabolism genes after ABA, MeJA or combined ABA + MeJA treatment.

Log₂-transformed read counts of treatment vs. mock are displayed. At time points where the change was not significantly different according to a GLM, the log₂-fold change was set to 0. If a gene was not differentially expressed in the time series, all time points were set to 0.

(A) Relative expression of JA biosynthesis genes.

(B) Relative expression of JA catabolism genes.

Transcriptional regulation of ABA/JA crosstalk

The effect of ABA on the JA pathway cannot be explained solely by its effect on JA biosynthesis, since it is known to affect different sectors of the JA GRN differently, and our previous analysis showed that it reinforced the effect of MeJA for some genes, but it also counteracted MeJA action on other genes (Figure 1B). Transcriptional regulation is a major mechanism for hormone crosstalk (Chapter 1), and therefore we first focused on finding TF binding sites (TFBSs) that may explain why different genes respond differently in the combination treatment. As a first step to understand how TFBSs affect hormone responsiveness, we investigated if there was an association between the number of TFs that can potentially regulate transcription of a certain gene and the ability of that gene to respond specifically to ABA or MeJA, or to both. For this analysis, we initially used TFBSs inferred from DAP-seq data filtered for the top 25% strongest peaks (Methods, "Use of other datasets"; O'Malley *et al.*, 2016). Genes that responded to either hormone treatment generally had clearly more TFBSs than genes that did not (Figure S4A). Moreover, genes that responded to both ABA and MeJA generally had more TFBSs than genes that responded to only one of the two hormones (Figure S4A). Unexpectedly, genes that responded to MeJA generally had more TFBSs than genes that responded to ABA (Figure S4A). To verify whether this is a real biological feature or a bias that was introduced by the selection of specific TFs used for the DAP-seq dataset, we performed a similar analysis using another TFBS dataset. This dataset, called iGRN, was created using a machine learning model that combined data on DNA motifs, chromatin accessibility, conservation, co-expression and *in vivo* DNA binding to predict new TFBSs (De Clercq *et al.*, 2021). While the filtered DAP-dataset includes 347 TFs, the iGRN dataset contains 1491 TFs and comprises 1.7 million TFBSs. Comparison of two analyzed datasets shows that the general pattern of TFBS distribution over the different hormone treatments is similar for both datasets (Figure S4B), suggesting that the conclusions we drew from the DAP-seq dataset are robust. In summary, there seems to be an association between the number of TFBSs in the promoter of a gene and its responsiveness to ABA and MeJA, where genes that respond to MeJA usually have more binding sites than genes that respond to ABA, and genes that respond to the combined treatment contain even more binding sites.

Next, we set out to find TFBSs that were associated with the differential expression in the ABA + MeJA combination treatment compared to MeJA single treatment (Figure 1B). We reasoned that the corresponding TFs would be good candidate regulators of ABA/JA crosstalk. We focused on modulation of MeJA-activated rather than MeJA-repressed genes, since GO-terms of upregulated genes are much more related to the JA response than that of downregulated genes (Hickman *et al.*, 2017), suggesting that the core JA response takes place via upregulation of certain genes. Of the 1694 MeJA-upregulated genes, 678 (40%) were even more upregulated by the combined treatment, 487 (28.7%) were relatively lower expressed, and 529 (31.2%) responded the same regardless of ABA

co-application (Figure 1B). We next searched for TFs associated with the different effects of ABA on expression of the MeJA-activated genes using a stepwise regression approach. Briefly, we took the maximum \log_2 -fold difference of ABA + MeJA treatment compared to MeJA treatment alone as a response variable, and presence/absence of either DAP-seq- or iGRN-inferred TFBSs as independent variables. We then carried out bidirectional stepwise regression to come to a final model, where the differential expression of genes after ABA + MeJA treatment compared to MeJA treatment alone is modeled as dependent on the presence/absence of binding sites of certain TFs. The stepwise regression approach using the DAP-seq data yielded four significant TFs in the final model: ANAC055, bZIP68 and BIM2 binding sites were associated with upregulated genes after double treatment compared to MeJA treatment alone, whereas HSF6 binding sites were associated with downregulated genes (Figure 8A). The approach using the iGRN data resulted in the identification of 16 TFs, of which 10 were associated with upregulated genes and 6 with downregulated genes (Figure 8B). The reason for the higher number of significant TFs from the iGRN analysis and for identifying other TFs compared to the DAP-seq analysis could be that the iGRN dataset contains information on TFBSs of more TFs than the DAP-seq dataset (1491 vs. 347). Moreover, the iGRN data were derived from combined information of different experiments, meaning that there are fewer wrongly predicted target genes and the dataset may thus be more accurate than the DAP-seq data (De Clercq *et al.*, 2021). To estimate the importance of the predicted TFs for ABA/JA crosstalk, we looked at their expression profile after ABA, MeJA and the combined treatment. ABA-regulated TFs that modulate the JA pathway would be expected to be differentially expressed after ABA and/or ABA + MeJA treatment, but not necessarily after MeJA treatment alone. This holds true for *ANAC055*, *BIM2*, *HSF6* (from the DAP-seq analysis) and *ATC3H3*, *AT1G17520*, *MYB78*, *DREB2*, *ANAC072*, *ATHB12*, *AT5G08750*, *GBF3*, *BIM3*, *ASG4*, *MYB8* and *HSFA1D* (from the iGRN analysis; Figure 8C). For the other TFs it cannot be excluded that they are activated by ABA at the post-transcriptional level and thus also contribute to ABA/JA crosstalk (see also Chapter 2). *ANAC055* and likely also *ANAC072* have been reported to be ABA-mediated regulators of the MYC branch, and are also known to be regulated by MYC2 itself (Tran *et al.*, 2004, Bu *et al.*, 2008, Zheng *et al.*, 2012, Schweizer *et al.*, 2013).

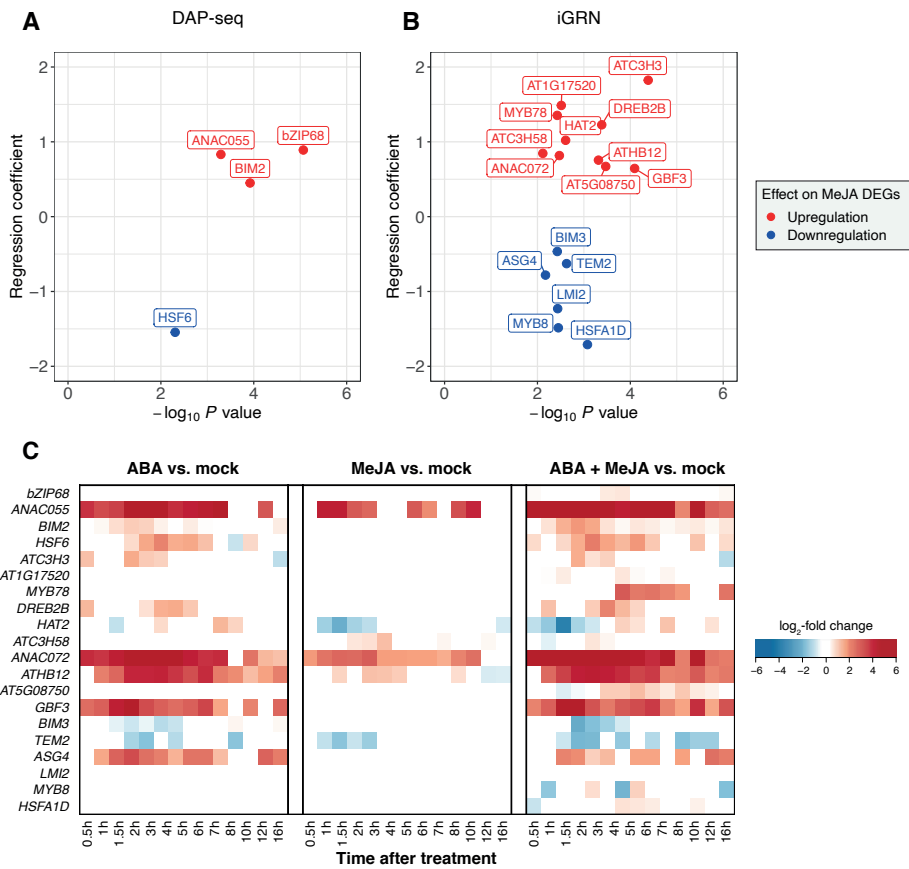


Figure 8: Linear regression model of the contribution of TFBSs to expression amplitude after ABA + MeJA treatment compared to MeJA treatment alone for genes that were upregulated by MeJA.

(A) DAP-seq data from O'Malley *et al.* (2016) were analyzed (Methods).

(B) The iGRN data from De Clercq *et al.* (2021) were analyzed.

For A and B bidirectional stepwise regression was done using only TFs that were expressed after ABA treatment as potential independent variables. The maximum log₂-fold difference after ABA + MeJA treatment compared to MeJA treatment for each gene was taken as dependent variable. Individual TFs are plotted according to their regression coefficient and the log₁₀ of their *P* value. For visualization purposes TFs predicted to positively or negatively contribute to target gene expression are colored red or blue, respectively.

(C) Relative expression levels of significant TFs from both models depicted as log₂-counts of ABA/mock, MeJA/mock, and (ABA + MeJA)/mock.

The ERF branch marker regulator *ORA59* is targeted by ABA at the transcriptional and protein level

In the previous analyses we focused on transcriptional regulation of JA target genes by ABA-regulated TFs and predicted the importance of several TFs, including a known regulator of the MYC branch. We likely did not pick up ERF branch master regulators because the single MeJA treatment mostly activated the MYC branch in our experiment, as shown by, e.g., the lack of upregulation of the ERF branch master regulator *ORA59* by MeJA. We therefore used a slightly different approach to study the effect of ABA on the ERF branch master regulator *ORA59*. We already established that *ORA59* was repressed by ABA at the transcriptional level (Figure 6B) and we observed a similar effect of ABA on *ERF1* expression, except at the earliest time points (Figure S3C). While this is one possible mechanism by which ABA represses the ERF branch, crosstalk can occur at many different levels of regulation (Aerts *et al.*, 2021). *ORA59* is known to be targeted at the protein level by SA, reducing *ORA59* stability and causing repression of the ERF branch (Van der Does *et al.*, 2013, He *et al.*, 2017). Because ABA also suppresses the ERF branch, we were interested to see if this also involves degradation of *ORA59*. We tested this in a transient protoplast expression system using a single plasmid that expressed different gene modules (Figure 9A). Firstly, the plasmid contained the *PDF1.2* promoter fused to the β -glucuronidase (*GUS*) gene to serve as a readout for ERF branch activity. Secondly, it contained *ORA59* expressed from the 35S promoter and fused to the luciferase gene from *Renilla reniformis* (hereafter: *LucR*). With this element we could both measure relative *ORA59* protein levels based on the *LucR* fusion protein and we could assess if ABA-mediated suppression of *PDF1.2* expression is dependent on *ORA59* transcription (since *ORA59* was expressed from the 35S promoter). The construct also contained luciferase from firefly (hereafter: *LucF*), expressed from the 35S promoter, to normalize for the number of transfected protoplasts. Finally, the construct contained *Enhanced Yellow Fluorescent Protein (EYFP)* expressed from the 35S promoter to visualize transfection efficiency under the microscope.

Treatment of protoplasts with ABA significantly decreased constitutive *ORA59*-induced *PDF1.2* expression (Figure 9B), suggesting that the involved mechanism acts downstream of *ORA59* transcription. Indeed, ABA induced a small but significant reduction in relative *ORA59* protein levels (Figure 9C). Because *ORA59* was transcribed from a constitutively activate promoter this suggests that ABA reduces *ORA59* protein stability, which leads to decreased *PDF1.2* expression. Together with the expression profile of *ORA59* in the time series, this suggests that ABA can suppress the ERF branch of the JA pathway by targeting both *ORA59* transcription and *ORA59* protein stability.

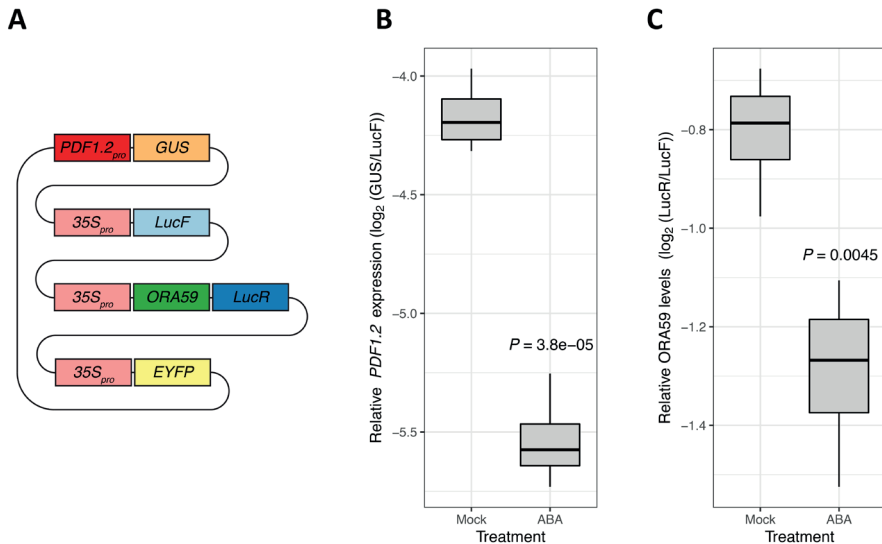


Figure 9: ABA-mediated reduction of ORA59-induced *PDF1.2* expression and ORA59 protein levels in protoplast.

(A) Overview of the plasmid used in the experiment. The single plasmid had four modules: the *PDF1.2_{pro}::GUS* module served as a readout for ERF branch activity, the *35S_{pro}::LucF* module served for signal normalization, the *35S_{pro}::ORA59-LucR* module served both to activate the ERF branch and to read out relative ORA59 protein levels, and the *35S_{pro}::EYFP* module served to visualize transfection efficiency under the microscope.

(B) Relative *PDF1.2* expression in Arabidopsis protoplasts transfected with the plasmid in (A) and treated with ABA or mock for 20 h. *PDF1.2* expression was determined by taking the \log_2 of the GUS signal divided by the LucF signal. The displayed statistics were calculated using Student's *t*-test ($n=4$).

(C) Relative ORA59 protein levels from the same experiment. Relative ORA59 protein levels were determined by taking the \log_2 of LucR divided by LucF. The displayed statistics were calculated using Student's *t*-test ($n=4$). The experiment was repeated an additional four times, all with the same results (not shown).

Both ORA59 and ERF1 are likely targeted by ABA to suppress the ERF branch in planta

After our finding that targeting of ORA59 protein levels is likely important for suppression of the ERF branch of the JA pathway by ABA in protoplasts, we wanted to determine if this also held true *in planta* under biotic stress and if other master regulators of the ERF and/or MYC branch may also be involved. To this end, we pre-treated 5-week-old Arabidopsis plants with a root drench of 10 μ M ABA or a mock solution at 3 and 0 days before inoculation with 5×10^5 spores/ml of *Botrytis* or a mock solution. We sampled one leaf of the rosette (the 8th developmental leaf) and subjected it to qRT-PCR to assess *PDF1.2* expression. We did this for Col-0 and for mutants and overexpressors of the ERF branch of defense (*ein3 eil1*, *ora59*, *erf1*, *35S_{pro}::EIN3*, and *35S_{pro}::ORA59*), and a mutant line of the MYC branch master regulator *myc2*. In Col-0, *Botrytis* inoculation caused strong, highly significant upregulation of *PDF1.2* (Figure 10A). In line with the protoplast assay, treatment

with ABA suppressed *PDF1.2* expression, which occurred in both the Botrytis-challenged plants and in the mock-treated plants (as shown by the non-significant interaction term in the 2-way ANOVA; Figure 10A). In the *ein3 eil1* mutant Botrytis inoculation did not lead to upregulation of *PDF1.2* (Figure 10B). EIN3 and EIL1 form the convergence point for both JA and ET signaling, (Zhu *et al.*, 2011), meaning that *PDF1.2* cannot be induced by either hormone in the double mutant, and our data corroborate that EIN3 and EIL1 are essential for ERF branch induction during Botrytis attack. ABA was still able to suppress *PDF1.2* expression in both the *ein3 eil1* mutant and the *35S_{pro}:EIN3* overexpression line, suggesting that suppression of the ERF branch of defense occurs downstream of EIN3 and EIL1 (Figure 10B, C). In the *erf1* mutant, Botrytis inoculation caused similar upregulation of *PDF1.2* expression as in Col-0, but ABA was unable to suppress it (Figure 10D). This suggests that ERF1 is not essential for *PDF1.2* induction, but that it does play a role in ABA-mediated suppression of *PDF1.2* expression. In accordance, *ERF1* expression was suppressed at most time points by ABA in our time series, although at the earliest time points it was slightly upregulated by ABA (Figure S3C). This suggests that ABA targets the ERF branch partly by targeting *ERF1* transcription, although the somewhat erratic expression pattern of *ERF1* after ABA treatment suggests that this is unlikely the only mechanism. In the *ora59* mutant *PDF1.2* expression was at lower basal levels than in Col-0, but could still be induced after Botrytis inoculation, albeit it to a relatively low level (Figure 10E). This confirms that ORA59 is important but not exclusively needed for basal *PDF1.2* expression and induction after Botrytis infection. ABA could suppress *PDF1.2* expression after Botrytis inoculation, but could not further suppress the already very low *PDF1.2* level after mock inoculation. Conversely, in the *35S_{pro}:ORA59* line ABA was unable to suppress *PDF1.2* expression, although there was a statistical trend (Figure 10G). These results contradict the results in protoplasts, where ABA treatment did suppress ORA59-induced *PDF1.2* expression (Figure 9). Together this suggests that the mechanisms by which ABA suppressed *PDF1.2* expression are context-dependent and may involve suppression of both ERF1 and ORA59 at different levels of regulation (transcription and protein level). Since the ERF branch of defense is suppressed by the MYC branch, we tested also a mutant in *MYC2*, the most prominent master regulator of this branch (Kazan and Manners, 2013). Interestingly, the *myc2* mutant showed more or less the same pattern of Botrytis induction and ABA-mediated suppression as Col-0 (Figure 10G). This suggests that even though ABA upregulates the MYC branch and downregulates the ERF branch, its downregulation of the ERF branch does not require *MYC2*.

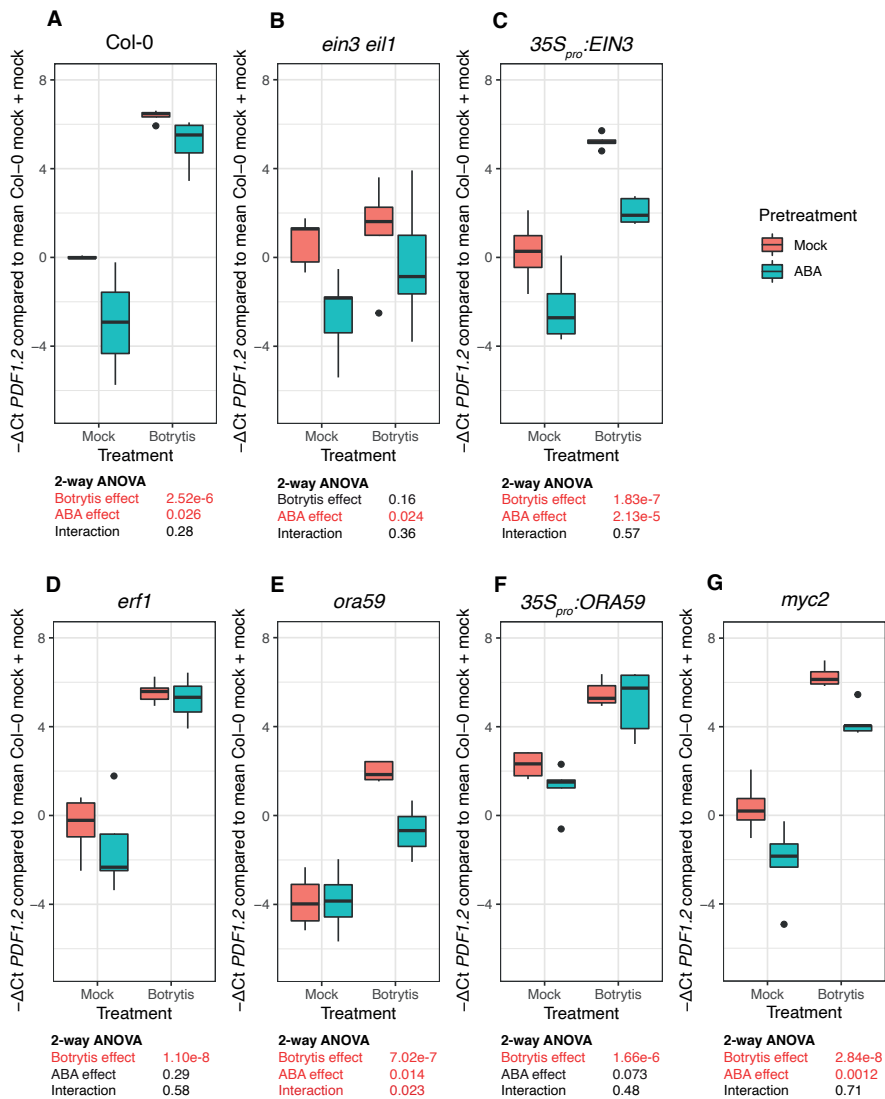


Figure 10: Relative *PDF1.2* expression in different JA-related mutants after Botrytis inoculation and/or ABA treatment.

Five-week-old plants were pre-treated with a 20-ml root drench of 10 μM ABA or a mock solution at 3 and 0 days before Botrytis or mock inoculation. One inoculated leaf (the 8th leaf, which had just matured) was harvested for qRT-PCR analysis. Relative *PDF1.2* expression was determined by subtracting the Ct value of *PDF1.2* from that of the reference gene *AT1G13320*, and then subtracting a fixed number such that the mock-pre-treated, mock-treated Col-0 samples had a mean $-\Delta Ct$ of 0. Panels indicate different mutants. Below the panel the results of a 2-way ANOVA ($n=5$) are indicated, where 'Botrytis effect' refers to the Treatment parameter and 'ABA effect' refers to the Pretreatment parameter. The 'Interaction' term indicates if the Treatment*Pretreatment interaction from the 2-way ANOVA is significant. The tested lines were (A) Col-0, (B) *ein3 eil1*, (C) $35S_{pro}$:*EIN3*-GFP (referred to as $35S_{pro}$:*EIN3*), (D) *erf1*, (E) *ora59*, (F) $35S_{pro}$:*ORA59*, and (G) *myc2*.

DISCUSSION

The ABA and JA GRNs are highly interconnected

JA has an essential role in Arabidopsis as a regulator of defense against necrotrophic pathogens and insects. ABA modulates the JA pathway, reinforcing the MYC branch, which is directed against insects, and repressing the ERF branch, which is directed against necrotrophic pathogens (Pieterse *et al.*, 2012). To study this modulation more in-depth we conducted and analyzed a high-density time series of Arabidopsis rosettes treated with MeJA, ABA, or the combination. ABA was found to induce more than two times the number of DEGs as MeJA (Figure 1). One possible interpretation is that this hormone regulates a broader response in terms of functions, or a response that requires the collaborative action of more genes than JA does. An alternative explanation is that we applied a more effective dose of ABA than of MeJA, leading to the induction of more genes. Furthermore, ABA single treatment modulated expression of about 2/3rd of all MeJA-responsive genes, and also modulated the expression a similar number of genes in the ABA + MeJA double treatment compared to MeJA treatment alone (Figure 1B, C). This shows that the ABA GRN overlaps with a large part of the JA GRN and confirms that ABA is an important modulator of the JA pathway (Pieterse *et al.*, 2012).

We found that the transcriptional responses to ABA and MeJA have many similarities, especially between 1.5 and 4 h after treatment (Figure 4). Not only were many of the same genes regulated by the two hormones, but also the direction of regulation (up/down) and the timing was similar. One possible explanation may be that the hormones stimulate each other's biosynthesis, as we showed for the expression of JA biosynthesis genes, which was induced by both MeJA and ABA (Figure 7). However, compared to exogenous application of MeJA, this transcriptional activation by ABA would likely lead to activation of the JA GRN at a much later time point because it takes time to produce the enzymes and catalyze the production of more hormone. We did not find such a difference in timing, so while effects on biosynthesis, possibly also regulated post-transcriptionally, could still explain some of the overlap between the two GRNs, it is unlikely the only explanation. Alternatively, both hormones may (partly) activate or repress the same master regulator genes, as is known for e.g., *MYC2* (Abe *et al.*, 1997, Abe *et al.*, 2003) and also apparent in our data, which showed that both hormones quickly upregulated *MYC2* expression (Figure S3A).

The large overlap in target genes of ABA and JA is reminiscent of the overlap between plant immunity network sectors regulated by the hormones SA, JA and ET and the crucial immunity gene *PAD4*, which were studied in the context of AvrRpt2-mediated effector-triggered immunity (ETI) against *Pseudomonas syringae* pv. *tomato* DC3000 (Tsuda *et al.*, 2009). All four sectors were found to contribute to ETI against the pathogen, but the combined contribution of the network sectors was lower than the sum of each

sector. This suggested that the different sectors of the immune network negatively affect each other during AvrRpt2-triggered ETI. The advantage of such a network architecture is that the loss of one sector can be compensated by another sector, which is no longer repressed. These compensatory interactions provide robustness to the network when one of the sectors is disrupted by e.g., the actions of a pathogen. Similarly, the large overlap in output of the ABA and JA network and the fact that the combined effect is usually lower than the sum of the single effects (if the single effects are in the same direction; Figure 5) suggests that the two hormones also have compensatory effects and provide the plant with a robust immune network against JA/ABA-related attackers such as chewing insects. Future studies may investigate the biological relevance of these compensatory actions by investigating if they can also be measured after attack by an insect (e.g., by measuring resistance in wild type and single and double ABA and JA biosynthesis knockout lines) and how these compensatory actions are achieved mechanistically. One possible mechanism would be the competition for the same binding sites by JA- and ABA-activated TFs. For example, bHLH TFs acting in the JA pathway and bHLH and bZIP TFs acting in the ABA pathway bind very similar motifs (Hickman *et al.*, 2017; Chapter 2). It is thus well possible that they regulate their overlapping targets by targeting the exact same motifs, hindering binding of the other TF, resulting in less-than-additive regulation of target genes. This can be especially important if it happens at the promoters of master regulators that are targeted by both ABA and JA. These TF genes then act as 'bottleneck genes': they are important regulators for the expression of many overlapping ABA and JA targets, but their own expression after combined activation of the ABA and JA pathway is never the sum of that after ABA and JA treatment because the TFs competing for promoter binding hinder each other. The early expression profile of *MYC2* after ABA, MeJA and the combination treatment fits such a bottleneck effect (Figure S3A).

The different PCA analyses in this chapter (Figure 2 and Figure 3) suggested that time after treatment (PC1) and the treatment itself (PC2) are the largest contributors to global gene expression patterns after the different treatments. The importance of time after treatment is likely mostly related to circadian regulation, since variation on PC1 was also observed in the mock treatment and it is known that about one-third of all genes are circadian regulated (Covington *et al.*, 2008), so these are expected to significantly contribute to the global expression pattern in our different treatments. The fact that the first PC captured variation that was also seen in the mock treatment corroborates the importance of the mock time series to control for, e.g., circadian effects. As expected, treatment was the other major contributor to global expression patterns. We found that the global effect of combined treatment was usually bigger than that of the single treatments (Figure 2) and that when only genes that were affected by MeJA were considered the combination effect on global expression patterns peaked higher and earlier than the effect of the single treatments (Figure 3). This included higher and

faster upregulation of genes involved in JA biosynthesis (Figure 7). The earlier peak of the molecular response could be important to ward off a feeding insect as fast as possible before it can do any damage. In general the expression of many genes in the double treatment also rapidly returned to levels similar to those after single MeJA treatment in our experiment (Figure 3A), which suggests an attenuation of the defense response. Such negative feedback on the JA pathway could partly result from the upregulation of JA catabolism genes that we observed (Figure 7). Since we only did a single (“pulse”) treatment with the hormones at time point zero of the experiment we cannot predict if these negative feedback mechanisms are also dominant during an insect attack when ABA and JA signaling is continuously stimulated.

Regulation of the JA GRN by ABA-induced/suppressed TFs

We used a bidirectional stepwise regression approach to find TFs that are associated with the differential effect of ABA on MeJA-upregulated genes (Figure 8). This resulted in the discovery of 20 such TFs. If these are indeed ABA-activated modulators of the JA pathway it would be expected that they are transcriptionally regulated by ABA or at least differentially regulated in the ABA + MeJA treatment compared to the MeJA treatment alone. Indeed, this was the case for 14/20 TFs (Figure 8), which supports the idea that this analysis can pick up relevant TFs. Alternatively, TFs may be activated post-transcriptionally by ABA (Yang *et al.*, 2017; Chapter 2). The analysis also identified ANAC055 and ANAC072 as putative regulators of ABA/JA crosstalk. Expression of both encoding genes was induced by ABA (Figure 8C) and the presence of ANAC055 and ANAC072 binding sites was associated with genes that were higher expressed after ABA + MeJA treatment compared to MeJA treatment alone (Figure 8A, B). ANAC055 is a known activator of MYC-branch-related transcription and a suppressor of the ERF branch, confirming that the approach is suitable for finding modulators of the JA pathway (Bu *et al.*, 2008, Schweizer *et al.*, 2013). ANAC072 has high sequence similarity to ANAC055 and has a similar function in, e.g., ABA signaling (Tran *et al.*, 2004) and JA-induced repression of SA signaling (Zheng *et al.*, 2012), but has not been well studied regarding its effect on JA-responsive gene expression. Our analysis suggests they both have a role in ABA-mediated MYC branch activation.

It is to be noted that all these predictions rely on information on TFBSs derived from databases that are not perfect: DAP-seq involves *in vitro* experiments with a non-complete set of TFs, and, for example, does not take the chromatin context into account. Similarly, the iGRN network relies on machine-learning-inferred TFBS predictions. It is therefore important in the future to experimentally validate the importance of the identified TFs, for example by doing chemical crosstalk assays or bioassays with insects/necrotrophic pathogens using mutant and/or overexpression lines of the TFs.

ABA suppresses the ERF branch by targeting ORA59 and possibly ERF1

Besides our interest in which TFs actively regulate ABA/JA crosstalk, we also wanted to learn which JA master regulators are themselves targeted by ABA. We investigated this using a different experimental approach, for which we decided to focus on ERF branch master regulators. We chose these because induction of the ERF branch was not so clear in our RNA-seq time series experiment, which was possibly due to a relatively high ratio of endogenous ABA over ET. Therefore, our experiments to study the effects of ERF branch overexpression or mutation nicely complement the other findings in the manuscript. First, we used a protoplast system to assess the negative effect of ABA on the ERF branch, and found that ABA reduced *PDF1.2* expression and ORA59 protein levels (Figure 9). Because we used a constitutively active promoter this likely means that ABA reduces ERF-branch-related transcription by reducing ORA59 protein stability, although effects on any of the steps between transcription and completion of translation cannot be ruled out (see also Aerts *et al.*, 2022). Additionally, in our time series ABA also reduced *ORA59* transcription (Figure 6B). This suggests that ABA targets the ERF branch via ORA59 via at least two levels of regulation. Surprisingly, in whole plants we found that ABA was unable to suppress *PDF1.2* expression in a $35S_{pro}::ORA59$ line, even though such a line is comparable to our protoplast setup where we transiently expressed *ORA59* from the 35S promoter. It could be that in stable lines there is so much ORA59 protein that ABA is unable to break down enough protein to cause any changes in *PDF1.2* expression. In line with our observation, while SA is generally accepted to repress *PDF1.2* expression at least partly by reducing ORA59 protein levels (Van der Does *et al.*, 2013, He *et al.*, 2017), the *PDF1.2* expression level was not reduced by SA in the $35S_{pro}::ORA59-GFP$ line (Van der Does *et al.*, 2013). This indicates that our observed targeting of ORA59 protein levels by ABA in the protoplast system can still point to this being an important mechanism for our observed suppression of the ERF branch marker gene *PDF1.2* in other backgrounds than $35S_{pro}::ORA59-GFP$. Notably, in earlier work we also found that ABA could not suppress *PDF1.2* expression in the $35S_{pro}::ORA59$ line under basal conditions; however, when these plants were fed on by *Pieris*, the resultant high *PDF1.2* induction could be repressed by ABA (Vos *et al.*, 2019). Overall, the role of degradation of ORA59 mediated by hormones such as ABA and SA may thus be context-dependent.

We also determined whether more ERF branch regulators are involved in ABA-mediated suppression of the ERF branch. For example, in the case of SA-mediated suppression of the ERF branch, it was found that EIN3 and EIL1 are involved in degradation of ORA59 (He *et al.*, 2017). We were unfortunately unable to test if this was also the case for ABA-mediated degradation of ORA59 due to inconsistent results of and technical difficulties with the required protoplast assays. The fact that suppression of *PDF1.2* expression by ABA is unaffected in the *ein3 eil1* mutant and the $35S_{pro}::EIN3-GFP$ overexpression line in our *Botrytis* experiment (Figure 10) suggests that the two

proteins are likely not involved in this. We found that ABA was unable to suppress *PDF1.2* expression in an *erf1* mutant (Figure 10). This is unlikely due to an upstream effect of ERF1 on *ORA59* as we observed that *PDF1.2* induction by *Botrytis* was not affected in *erf1*, suggesting *ORA59* functioned normally (Figure 8). Thus, our results suggest that targeting of ERF1 by ABA is also important for suppression of *PDF1.2* and that perhaps intact ERF1 is required for the effect of ABA on *ORA59*. We also tested if the MYC branch master regulator *MYC2* was involved in the suppression of the ERF branch, since *MYC2* is known to suppress the ERF branch and ABA upregulates the MYC branch (Pieterse *et al.*, 2012, Aerts *et al.*, 2021). We found that *MYC2* was not required for suppression of *PDF1.2* by ABA (Figure 10), suggesting this takes place via a *MYC2*-independent pathway. This confirmed our earlier findings in the context of Pieris feeding (Vos *et al.*, 2019).

Concluding remarks

We investigated crosstalk between the ABA and JA pathway by analyzing RNA-seq time series data of ABA-, MeJA- and double-treated *Arabidopsis* leaves. We found that the two pathways alone have a significant level of similarity and when activated together generally reinforce each other, although often less than additive. We also found that ABA modulates the JA pathway by altering transcription of MeJA-responsive genes, among which genes involved in JA biosynthesis and catabolism, through a set of TFs, which we predicted through statistical analyses. Also the JA master regulators *ORA59* and *ERF1* are downregulated by ABA at the transcriptional level and *ORA59* likely also at the protein level, which affects expression of the target marker gene *PDF1.2*. Our work represents a starting point for research into the integration of ABA and JA signaling, which is essential for understanding how defense against insects and necrotrophic pathogens is regulated.

METHODS

Plant material and growth conditions

In all experiments, *Arabidopsis* accession Col-0 was used as wild type. The mutants and overexpression lines used were all in the Col-0 background: *ein3 ein1* (Alonso *et al.*, 2003; both are mutant allele 1 from this paper), *35S_{pro}:EIN3-GFP ein3 ein1* (He *et al.*, 2011), *erf1* (Caarls *et al.*, 2017), *ora59* (Zander *et al.*, 2014), *35S_{pro}:ORA59* (Pré *et al.*, 2008), and *myc2* (Lorenzo *et al.*, 2004; described there as *jin1-7*). For soil-grown plant cultivation, the seeds were stratified in 0.1% plant agar (Duchefa Biochemie, Haarlem, the Netherlands) at 4°C for 48 h and then sown on two-times autoclaved river sand, which filled an open box. The box was placed in a tray, which was closed with a transparent lid and had a layer of

water on the bottom to increase humidity to about 100%. The plants were grown for 2 weeks at 21°C with a light/dark cycle of 10 h light (75 $\mu\text{mol}/\text{m}^2/\text{s}$ for the RNA-seq time series experiment, 200 $\mu\text{mol}/\text{m}^2/\text{s}$ for the Botrytis experiment) and 14 h of darkness. Subsequently, the plants were transferred to 60-ml pots filled with a mixture of river sand and potting soil in a 5:12 ratio, which had been autoclaved twice. The pots were kept in a tray under the same conditions, but after 2 days the lid was first opened slightly and after 2 more days completely removed, decreasing the humidity to 70%. The plants were watered three times per week, with one watering per week being a modified half-strength Hoagland solution containing 10 μM sequestren ((Fe-EDDHA), Royal Brinkman, 's-Gravenzande, the Netherlands), instead of water.

For protoplast experiments, a volume of approximately 50 μl of Arabidopsis Col-0 seeds were surface-sterilized by putting them in an open 1.5-ml tube (Greiner Bio-One, Kremsmünster, Austria), which was placed in a glass desiccator that also contained a beaker with a mixture of 100 ml of commercial bleach (Manutan B.V., Den Dolder, the Netherlands) and 3.2 ml of 37% HCl. The desiccator was immediately closed after preparation of the gaseous sterilization mixture and the seeds were incubated in the desiccator for 4 h. Afterwards, the sterile seeds were sown on a 120x120 square Petri dish containing 70 ml of $\frac{1}{2}$ Murashige and Skoog (MS) medium with 2% sucrose, buffered with MES (pH = 5.7) and solidified with 1% plant agar (Duchefa Biochemie). Seeds were stratified on the plates in the dark at 4°C and then incubated lying down in a growth chamber at 21°C with a 10-h light/14-h dark cycle at a light intensity of 75 $\mu\text{mol}/\text{m}^2/\text{s}$.

RNA-seq time series experimental setup

RNA-seq time series were generated largely as described previously (Hickman *et al.*, 2017, Hickman *et al.*, 2019; Chapter 2). In brief, rosettes of 5-week-old plants were dipped for 3 s in a tap-water-based solution containing either 50 μM ABA (Duchefa Biochemie), 100 μM MeJA (Duchefa Biochemie), 50 μM ABA and 100 μM MeJA, or a mock solution, which contained 0.1% ethanol, the solvent for ABA and MeJA. The solutions also contained 0.015% (v/v) Silwet L77 (Van Meeuwen Chemicals BV, Weesp, the Netherlands; nowadays this compound is known as CoatOSil 77 (Momentive, New York, NY, USA)). The sixth true leaf (counted from the oldest) from each rosette was harvested, representing one replicate, at 15 min, 30 min, and 1, 1.5, 2, 3, 4, 5, 6, 7, 8, 10, 12 and 16 h after treatment. For the mock and MeJA time series four replicates were sequenced, while for the ABA and ABA + MeJA time series three replicates were sequenced, as was explained in Chapter 2.

RNA extraction, sequencing and data processing

RNA extraction, library preparation and data processing was done as described in Chapter 2. Notably, the mock and MeJA time series were processed in a different study than the ABA and ABA + MeJA time series and thus library prep and sequencing was done slightly differently between those groups of samples, as described in Chapter 2 for the mock and ABA time series. The mock and MeJA time series sequencing libraries were prepared using the Illumina TruSeq mRNA Sample Prep Kit and libraries for the ABA and ABA + MeJA time series were prepared using the Illumina TruSeq mRNA Stranded Sample Prep Kit. Sequencing was done on the Illumina HiSeq 2000 platform with read lengths of 50 bases (mock and MeJA; see also Hickman et al., 2017 and Hickman et al., 2019) or the Illumina NextSeq 500 platform with read lengths of 75 bases (ABA and ABA + MeJA). Read alignment, annotation and normalization were done as described in Chapter 2. During data processing all reads were regarded as coming from an unstranded library prep and sequencing platform (see also Chapter 2). Verification that the differences in sample processing did not lead to large biases in the data was described in Chapter 2. Analysis of DEGs was done using a generalized linear model (GLM), as described in Chapter 2.

Data analysis tools

Unless stated otherwise, data analysis was done using R version 4.1.2. Visualization was done using the ggplot2 v3.3.5 and gplots v3.3.1 packages. Colors were picked using the RColorBrewer v1.1-2 package and via <http://www.ColorBrewer.org> (Cynthia A. Brewer, accessed December 2022/January 2023).

Principal component analysis

A PCA was done on the \log_2 of read counts using the prcomp function from the stats package in R with default settings. The exact set of genes and samples used for PCA differed per analysis, as explained in the Results section and figure legends.

Use of publicly available datasets

MeJA-responsive clusters of coexpressed genes were downloaded from Hickman *et al.* (2017). Notice that this clustering comes from the same data as presented in this chapter, but the read counts in that paper were only normalized on mock and MeJA samples, so they differ slightly from the normalized counts presented in the current study. Expression of genes in each of the clusters was based on the data presented in this manuscript.

Time series data of *Arabidopsis* infested by *Pieris* were downloaded from Coolen *et al.* (2016). Genes that were differentially expressed in at least one of the time points

were considered DEGs in that time series and they were divided into upregulated and downregulated genes based on their mean \log_2 -fold change of Pieris/mock over all time points. DEGs and coexpression clusters derived from Botrytis-infected Arabidopsis were downloaded from Windram *et al.* (2012). In accordance with that paper, genes from clusters 1-22 were considered downregulated and genes from clusters 23-44 were considered upregulated. Thrips data were obtained in-house and are not yet publicly available. The data are described in the PhD dissertation of Steenbergen (2022). DEGs were divided into upregulated and downregulated DEGs based on their mean \log_2 -fold difference of thrips/mock over all time points.

DAP-seq data used in this study came from the work of O'Malley *et al.* (2016). DAP-seq peaks were downloaded from Plant Cistrome DB, excluding the ampDAP data. The dataset was reduced to contain only the TFBS based on the 25% most significant peaks in the whole dataset, as described in Chapter 2.

iGRN data, described by De Clercq *et al.* (2021), were obtained from <http://bioinformatics.psb.ugent.be/webtools/iGRN/pages/download>. No further filtering of the dataset was done. Gene codes were converted to common names using a curated version of the file `gene_aliases_20130831.txt`, which was downloaded from <ftp.arabidopsis.org>. To ensure accurate gene names, the file was manually curated for genes incorporated in this manuscript's figures, as the downloaded file is outdated and lacks certain common names. These new common names were retrieved from the gene's page at www.arabidopsis.org. In cases where a gene had multiple common names, the most frequently used common name in publications mentioning the gene was used.

Correlation analysis of ABA with MeJA time series

The union of DEGs from the ABA and MeJA time series was taken for this analysis. For each gene and for each time point combination of the two time series the Z-scores of the time*treatment interaction parameter outputted by the GLM (see "RNA extraction, sequencing and data processing" and Chapter 2") were correlated with Spearman's rank correlation.

Analysis of additive/synergistic expression of time series

The union of DEGs of the MeJA vs. mock, ABA vs. mock and ABA + MeJA vs. mock time series was taken. The \log_2 -fold change was calculated for each comparison, and was set to 0 at timepoints where the difference was not significant according to the GLM (see "RNA extraction, sequencing and data processing" and Chapter 2). For each gene and timepoint the difference was calculated between the expression after ABA + MeJA and the expected expression based on the single time series. This was done by adding

the \log_2 -fold change of ABA vs. mock to the \log_2 -fold change of MeJA vs. mock and subtracting the resulting number from the \log_2 -fold change of ABA + MeJA vs. mock. For heatmap visualization, the four dataframes were concatenated by column and the rows were clustered and ordered based on the first three dataframes using the `hclust` function in R with the `ward.D` agglomeration method.

Predicting TFs associated with ABA/JA crosstalk

A stepwise regression approach was used to predict TFs associated with ABA/JA crosstalk. First, all upregulated DEGs after MeJA treatment were taken ($n=1694$). Next, the maximum absolute \log_2 -fold difference between ABA + MeJA and MeJA treatment for each gene out of the 14 time points was determined. This was used as dependent variable in a linear regression model where each TF from the filtered DAP-seq dataset or (in a different analysis) from the iGRN dataset (see "Use of publicly available datasets") were used as independent variables, using only presence/absence of TFBSs per gene. Only TFs with binding sites in at least 16 MeJA DEGs (about 1% of total number of upregulated MeJA DEGs) were considered for the analysis. Bidirectional stepwise regression was used to come to a final model, using the `stepAIC` function from the MASS package (v7.3-55) in R.

Transient expression assay in protoplasts

Transient expression assays in protoplasts were conducted using a custom protocol based on protocols by Yoo *et al.* (2007) and Mathur and Koncz (1998). Details of our protocol are described in Chapter 4. The protoplasts were isolated from rosettes of 3-to-4-wk-old *Arabidopsis* plants grown on plate (see 'Plant material and growth conditions'). The construction of the level 0 and level 1 plasmids and the procedure for creating the level 2 plasmid are described in Chapter 4. Table S2 lists the level 1 plasmids that were combined into the final level 2 plasmid for the current study. Hormone treatment (1 μM ABA or mock) was done by adding 1.2 μl of 1 mM ABA solution (1000x stock in 96% ethanol) or 0.096% ethanol (for the mock treatment) to 500 μl WI right before adding 700 μl of just-transfected protoplast suspension in 6-well plates used for overnight incubation (see Chapter 4 for details on the procedure). The plates were incubated at 21°C in the dark for approximately 20 h. Measurements of GUS, LucR and LucF were performed as described in Chapter 4. One biological replicate in the experiment originated from a single well of protoplasts transfected in that well.

Botrytis infection assays and qRT-PCR analysis

Plants grown for 33 days under conditions as described in “Plant material and growth conditions” were subjected to Botrytis infection. Three days prior to inoculation, pots were placed on 60-mm petri dishes, which served as saucers, and supplied with 20 ml of 100 μ M ABA (dissolved from a 1000x stock in 96% ethanol) in tap water, or the corresponding amount of ethanol in tap water as a mock pretreatment. This pretreatment was repeated at approximately one hour before Botrytis inoculation. Botrytis inoculation was performed as described previously (Van Wees *et al.*, 2013) using strain B05.10. The eighth developmental leaf of each plant was inoculated with one 5- μ l droplet containing spores at a density of 5×10^5 spores/ml or with 5 μ l of half-strength potato dextrose broth as a mock treatment. Trays were watered well and shut-closed with transparent lids using tape. After 48 h the 8th developmental leaf (which was inoculated) was harvested and snap-frozen in liquid nitrogen in a 2-ml tube containing two 3-mm glass beads.

RNA for qRT-PCR analysis was extracted as described by Oñate-Sánchez and Vicente-Carbajosa (2008). Genomic DNA was removed using DNase I (Fermentas, St. Leon-Rot, Germany). DNA-free total RNA was converted to cDNA using RevertAid H minus Reverse Transcriptase (Fermentas). PCR reactions were performed in optical 384-well plates with a ViiA 7 realtime PCR system (Applied Biosystems, Carlsbad, CA, USA), using SYBR[®] Green to monitor the synthesis of double-stranded DNA. Primers used were TAACGTGGCCAAAATGATGC and GTTCTCCACAACCGCTTGGT for the reference gene *AT1G13320* (Czechowski *et al.*, 2005), and TTTGCTGCTTTTCGACGCAC and CGCAAACCCCTGACCATG for *PDF1.2*. A standard thermal profile was used: 50°C for 2 min, 95°C for 10 min, 40 cycles of 95°C for 15 s and 60°C for 1 min. Amplicon dissociation curves were recorded after cycle 40 by heating from 60 to 95°C with a ramp speed of 1.0°C/min. Expression of *PDF1.2* was calculated as $-\Delta C_t$ relative to the reference gene.

ACKNOWLEDGEMENTS

We thank Richard Hickman and Marcel Van Verk for their contributions in designing and executing the RNA-seq time series experiment (MVV), setting up a basic analysis pipeline for the resulting data (RH and MVV) and providing examples of analyses of the double treatment data (RH). Renée Kapteijn is acknowledged for her help in the development of the multimodular plasmid and the protoplast transient transfection assay, and Folkert Sanders, Ellinor Keepers, Raquel Ledo Doval and Berend Groutars for their help in optimizing our protoplast transfection and GUS and LucF measurement protocols. This work was supported by the Netherlands Organization for Scientific Research, grant no. ALWGS.2016.005

SUPPLEMENTARY MATERIAL

Supplementary figures

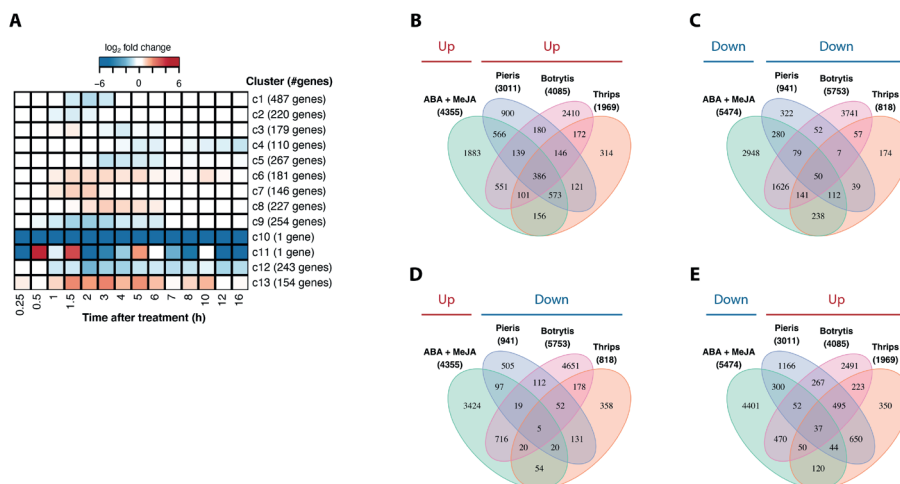


Figure S1: Expression of unique ABA + MeJA DEGs and overlap between all DEGs from the ABA + MeJA time series and public pest/pathogen datasets.

(A) DEGs after ABA + MeJA treatment but not after single ABA and MeJA treatment were clustered based on the log₂-fold change between ABA + MeJA and mock treatment using SplineCluster (Heard *et al.*, 2006), and the mean of each cluster per time point is plotted here.

(B-E) Overlap is shown between ABA + MeJA DEGs and DEGs after inoculation with Pieris (Coolen *et al.*, 2016), Botrytis (Windram *et al.*, 2012) or thrips (Steenbergen, 2022). Numbers between parentheses indicate total number of DEGs. Venn diagrams were made using (B) only upregulated genes from each dataset; (C) only downregulated genes from each dataset; (D) upregulated genes from the ABA + MeJA dataset and downregulated genes from the pest/pathogen datasets; (E) downregulated genes from the ABA + MeJA dataset and upregulated genes from the pest/pathogen datasets. A gene was considered up or downregulated when the mean over the time series was more than 0 or less, respectively.

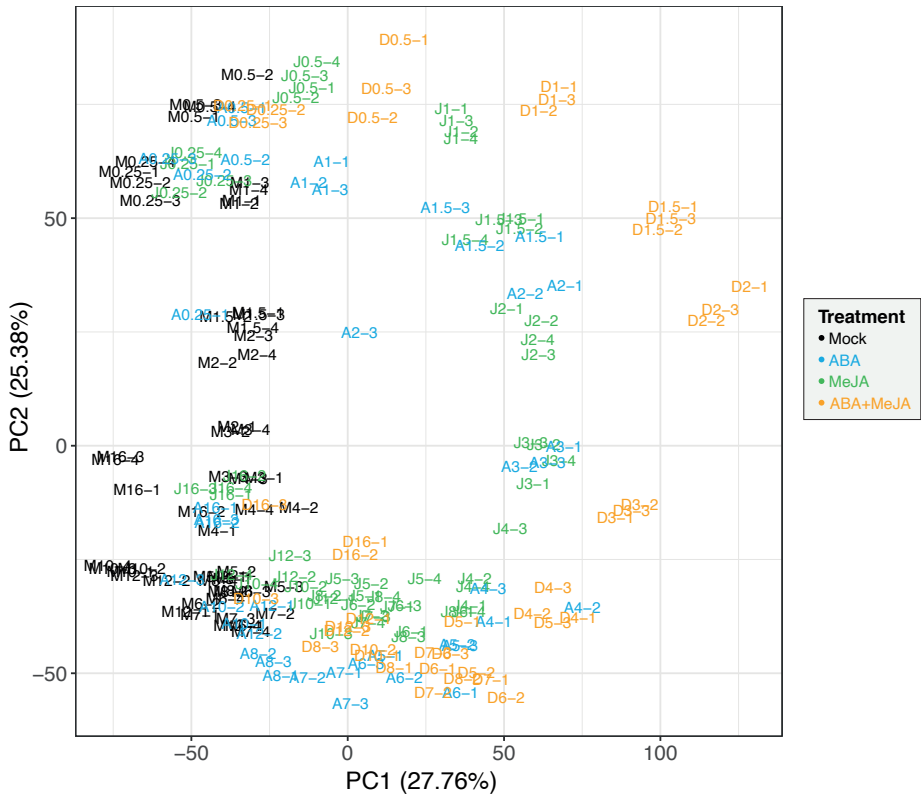


Figure S2: PCA of all samples from the ABA, MeJA and ABA + MeJA time series based on all genes that are differentially expressed after single MeJA treatment.

PCA was performed based on the \log_2 of all genes that are differentially expressed after MeJA treatment. Sample names reflect their treatment (M for mock, A for ABA, J for MeJA and D for double treatment), time (h) after treatment and replicate number (after the dash). Samples are colored according to their treatment. PC: principal component.

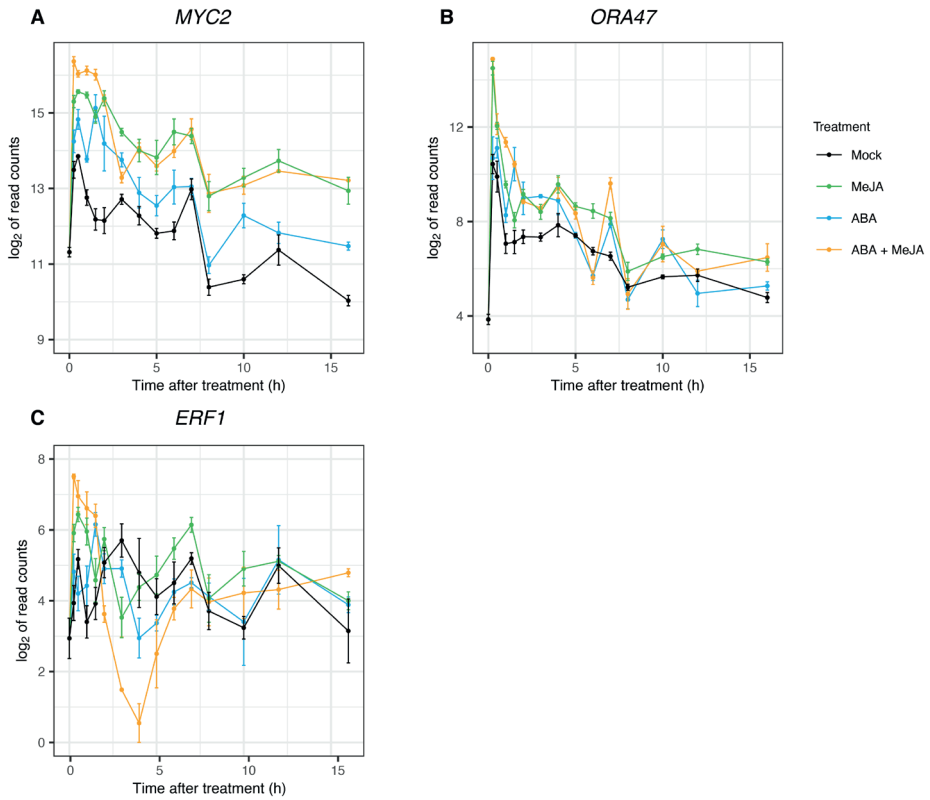


Figure S3: Expression of selected JA-related TF genes.

Expression profiles were plotted based on mean and standard deviation of \log_2 -transformed read counts. Expression profiles were plotted for (A) *MYC2*, (B) *ORA47* (B), (C) and *ERF1*.

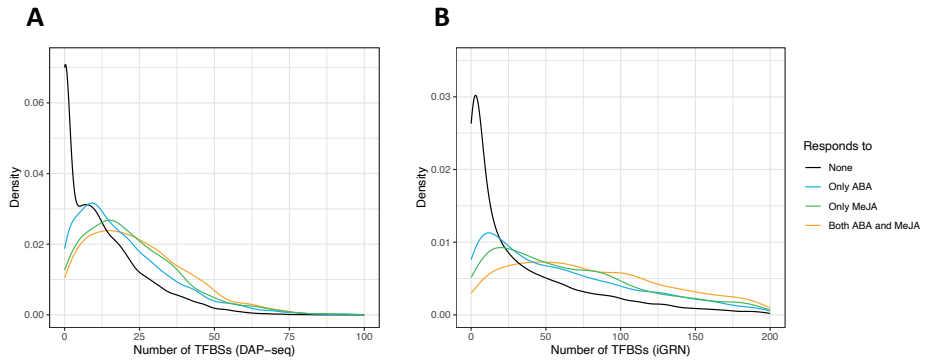


Figure S4: Density of TFBSs for genes that respond to ABA, MeJA, both or neither.

Genes were assigned as responsive to one, both or none of the hormones using the GLM described in the Methods section (“RNA-seq data processing and differential expression analysis”). Mitochondrial or chloroplast genes were not considered for this analysis, as DAP-seq is done with nuclear-extracted DNA. Number of genes was 24974 for ‘None’, 4820 for ‘Only ABA’, 1262 for ‘Only MeJA’ and 2267 for ‘Both ABA and MeJA’. Densities of TF binding sites are plotted for each of these categories. TFBSs sites were taken **(A)** from the filtered DAP-seq data (Methods, “Use of publicly available datasets”) and **(B)** the iGRN network (Methods, “Use of publicly available datasets”).

Supplementary tables

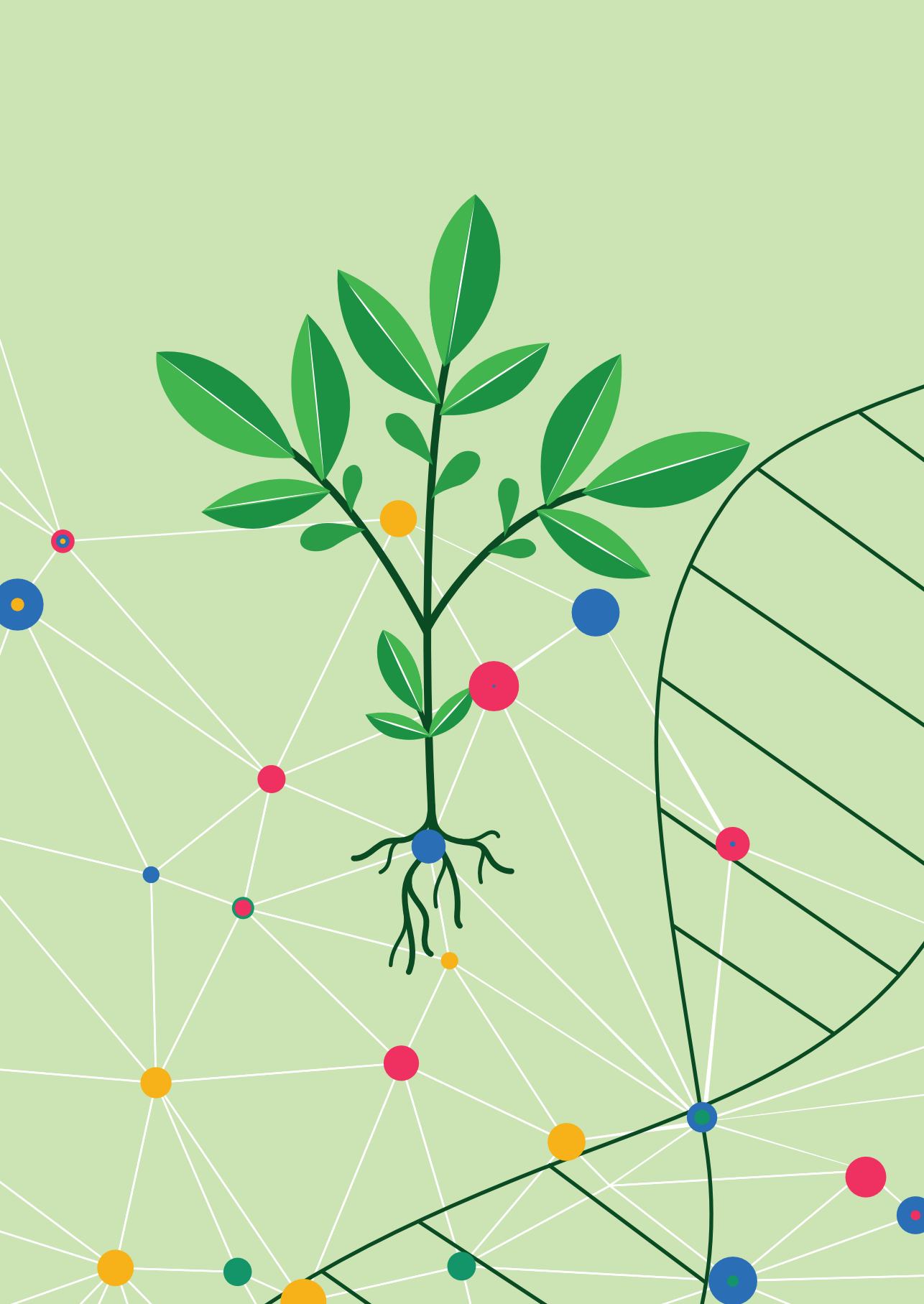
Table S1: Time series experimental set-up and mRNA sequencing details.

Available upon request.

Table S2: DNA components for assembly of a level 2 vector for a transient protoplast expression assay.

Plasmids were derived from the MoClo plant parts toolkit (Weber *et al.*, 2011, Werner *et al.*, 2012) or from level 1 reactions described in Chapter 4, where also the content of each numbered plasmid is described (Table S4 of Chapter 4). NB: a dummy was used at the fourth position because we already cloned *EYFP* into the fifth position for another project (Chapter 4) and without a dummy on position 4, there can be no connection between position 3 and position 5.

Component	Component description	Vector used
Backbone vector	Backbone	pAGM4673
First gene construct	<i>PDF1.2_{pro};GUS</i>	1.1.2
Second gene construct	<i>35S_{pro};LucF</i>	1.2.2
Third gene construct	<i>35S_{pro};ORA59-LucR</i>	1.3.3
Fourth gene construct	Dummy position 4	pICH54044
Fifth gene construct	<i>35S_{pro};EYFP</i>	1.5.1
End-linker 5	End-linker to link position 5 to the backbone vector	pICH41800



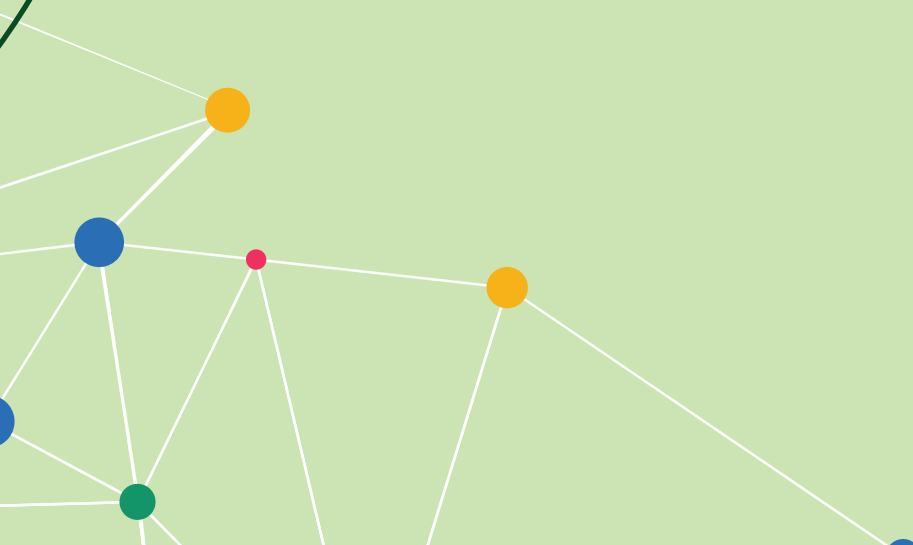


CHAPTER 4

Nuclear NPR1 modulates salicylic acid/jasmonic acid crosstalk via transcriptional control of WRKY transcription factors

Niels Aerts, Lotte Caarls, Tessa Visscher, Berend Groutars, Renée Kapteijn, Corné M.J. Pieterse and Saskia C.M. Van Wees

Plant-Microbe Interactions, Department of Biology, Science4Life, Utrecht University, P.O. Box 800.56, 3408 TB Utrecht, The Netherlands



ABSTRACT

The plant immune signaling network is controlled by different hormone-regulated pathways that exhibit extensive interplay. The key plant defense-related hormones salicylic acid (SA) and jasmonic acid (JA) are known to antagonize each other's activity. NPR1, the master transcriptional regulator of the SA pathway, is also functioning in the antagonistic action of SA on JA signaling (known as SA/JA crosstalk), but the molecular mechanism of NPR1-mediated SA/JA crosstalk is largely unclear. Here, we assayed SA/JA crosstalk in several *Arabidopsis npr1* mutant variants with altered nucleo-cytosolic localization or mutations in specific cysteine residues. Assays with the NPR1-HBD and *npr1-nls* lines revealed a nuclear role of NPR1 in the suppression of JA-responsive gene expression. Interestingly, mutation of two cysteine residues in NPR1 (Cys⁸² or Cys²¹⁶), which changes the conformation of NPR1 and possibly affects multimerization of NPR1 and interactions of NPR1 with other proteins, disrupted the suppression of the JA marker genes *PDF1.2* and *VSP2* by SA, while SA-induced expression of the SA marker gene *PR1* was intact. This allowed us to distinguish the function of NPR1 in activation of the core SA pathway from its function in SA/JA crosstalk. RNA-seq analysis identified 32 SA-responsive genes that were significantly lower expressed in the Cys⁸²-mutated NPR1 line than in Col-0, and thus may be involved in NPR1-mediated SA/JA crosstalk. This included four genes encoding WRKY transcription factors (WRKY18, WRKY38, WRKY53 and WRKY70). Of these, WRKY53, and to a lesser extent WRKY70, were able to suppress *PDF1.2* expression induced by the JA master regulator ORA59 in an *Arabidopsis* protoplast expression system. Other tested SA-inducible WRKYs (WRKY50, WRKY54, WRKY63, and WRKY67) also suppressed ORA59-induced *PDF1.2* expression. Then, the stability of the ORA59 protein was determined in the protoplast system, and WRKY53 and WRKY67 were demonstrated to likely contribute to the SA- or SA/NPR1-mediated suppression of *PDF1.2* by causing degradation of the ORA59 protein.

INTRODUCTION

The plant immune system is activated upon recognition of pathogen- or insect-derived molecules or altered self-molecules of the attacked host (Dodds and Rathjen, 2010). Recognition leads to the activation of defenses that, when successful, stop infection and signal systemic tissue to become primed for enhanced defense against future attacks (Gao *et al.*, 2015). Downstream of recognition, plant hormones play vital roles in triggering the plant immune signaling network (Pieterse *et al.*, 2012, Aerts *et al.*, 2021). Salicylic acid (SA) and jasmonic acid (JA) are major defense hormones important for shaping both the locally induced defense response to the attacker at hand and in the establishment of systemic resistance in distal, still healthy tissues. In general, SA is essential in the defense response against biotrophic pathogens, which feed on living host cells. Conversely, the JA pathway is generally effective against herbivorous insects and necrotrophic pathogens, which kill host tissue and feed on the contents (Glazebrook, 2005).

Activation of the SA or JA pathway triggers massive transcriptional reprogramming, which includes activation of a distinct set of pathogenesis-related (*PR*) genes by both hormones (Van Loon *et al.*, 2006, Hickman *et al.*, 2017, Hickman *et al.*, 2019). Signaling downstream of SA is largely regulated by the transcriptional regulator NPR1, which is required for the activation of many SA-responsive genes, including the SA marker gene *PR1*, and for SA-dependent disease resistance (Cao *et al.*, 1994, Delaney *et al.*, 1995, Vlot *et al.*, 2009). NPR1 interacts with TGA transcription factors (TFs) to activate downstream gene expression, including the marker gene *PR1* and many WRKY TF genes, which fine-tune and amplify downstream responses (Wang *et al.*, 2006, Blanco *et al.*, 2009, Pandey and Somssich, 2009).

Activation of JA-responsive genes relies on JA-induced degradation of JASMONATE ZIM-domain (JAZ) repressor proteins, which under basal conditions suppress the activity of JA-responsive TFs (Chini *et al.*, 2007, Thines *et al.*, 2007). COI1 is the F-box protein in the SCF^{COI1} complex that targets JAZs for degradation when binding JA-Ile, the biologically active form of JA (Pauwels and Goossens, 2011). Two branches are distinguished in JA-dependent defense signaling. The first is co-regulated by ethylene and controlled by ERF TFs, such as ORA59, which activates the expression of many genes, including the marker gene *PDF1.2* (Pré *et al.*, 2008, Zarei *et al.*, 2011). The other branch is co-regulated by ABA and controlled by MYC TFs, which activate another large set of genes, including the JA marker gene *VSP2* (Fernández-Calvo *et al.*, 2011). These branches are referred to as the ERF branch and MYC branch, respectively. In general, the ERF branch is effective against necrotrophic pathogens whereas the MYC branch is mostly directed against herbivorous insects and is also activated upon wounding (Pieterse *et al.*, 2012).

The hormonal signaling pathways involved in plant defense are interconnected in an intricate signaling network, acting at multiple levels of regulation (Aerts *et al.*, 2021). This

complex network involves many antagonistic and synergistic interactions between the pathways, a phenomenon that is referred to as hormonal crosstalk (Robert-Seilaniantz *et al.*, 2011, Pieterse *et al.*, 2012). Well-known examples of hormonal crosstalk in plant defense are antagonism between the SA and JA pathway and between the MYC and ERF branch of the JA pathway (Pieterse *et al.*, 2012). Several studies have contributed to the elucidation of the molecular mechanism underlying SA-mediated suppression of the JA response (from hereon: SA/JA crosstalk). In the model plant *Arabidopsis thaliana* (from hereon: Arabidopsis), SA was shown to significantly affect the expression pattern of 69% of >3500 MeJA-responsive genes (Hickman *et al.*, 2019), highlighting the magnitude of the effect of SA on JA signaling. SA was further shown to target the JA pathway downstream of JA biosynthesis and of COI1 via multiple mechanisms, such as direct repression of JA-induced transcription and degradation of the positive ERF branch regulator ORA59 (Leon-Reyes *et al.*, 2010b, Van der Does *et al.*, 2013, He *et al.*, 2017). Several SA-controlled transcriptional (co)regulators that can suppress JA-dependent gene expression have been identified (Caarls *et al.*, 2015). The TFs TGA2, TGA5 and TGA6 (Leon-Reyes *et al.*, 2010a, Zander *et al.*, 2014) and WRKY41, WRKY46, WRKY50, WRKY51, WRKY53, WRKY62 and WRKY70 have all been shown to be involved in suppression of JA-responsive genes (Li *et al.*, 2004, Mao *et al.*, 2007, Higashi *et al.*, 2008, Gao *et al.*, 2011, Hu *et al.*, 2012, Yan *et al.*, 2018). In contrast, SA-induced EAR-motif containing transcriptional repressors from the ERF family were shown not to play a role in SA/JA crosstalk (Caarls *et al.*, 2017).

NPR1 emerged as an important transcriptional co-regulator of SA/JA crosstalk. It is required for SA-mediated suppression of JA marker genes *VSP2*, *PDF1.2* and *LOX2* (Spoel *et al.*, 2003, Nomoto *et al.*, 2021) and controls the SA-mediated suppression of JA-induced resistance against herbivorous insects and necrotrophic pathogens in Arabidopsis (Spoel *et al.*, 2007, Leon-Reyes *et al.*, 2009). Also in tomato, rice and *Nicotiana attenuata*, NPR1 is important for the interaction between the SA and JA signaling pathways (Rayapuram and Baldwin, 2007, Yuan *et al.*, 2007, El Oirdi *et al.*, 2011), suggesting a conserved role for NPR1 as an SA-activated modulator of the JA pathway. Recently, it was shown that NPR1 can suppress the MYC branch by interacting with MYC2 at the same position as the mediator subunit MED25 (Nomoto *et al.*, 2021). Thereby, NPR1 prevents the MYC2-MED25 interaction, which is otherwise necessary for full MYC branch activation (Çevik *et al.*, 2012, Chen *et al.*, 2012). For the ERF branch of the JA pathway, however, the mechanism by which NPR1 affects ERF branch target genes is not yet known.

SA-mediated regulation of the NPR1 protein and subsequent activation of SA-responsive gene expression have been extensively studied (Chen *et al.*, 2021) and recently the crystal structure of NPR1 was solved (Kumar *et al.*, 2022). The NPR1 protein contains several conserved domains that enable it to act as a transcriptional co-activator. The ankyrin repeat domain mediates the interaction of NPR1 with TGA TFs, which is required for *PR* gene activation (Zhang *et al.*, 1999, Zhou *et al.*, 2000, Després *et al.*, 2003, Kumar *et*

al., 2022). Secondly, NPR1 contains a BTB domain, which mediates NPR1 oligomerization (Kumar *et al.*, 2022) and interacts with TGA2 to counteract the effects of TGA2's N-terminal repression domain, thereby promoting downstream transcription (Boyle *et al.*, 2009). Moreover, under non-inducing conditions the BTB domain acts as an auto-inhibitory domain that masks the C-terminal transactivation domain (Wu *et al.*, 2012). This C-terminal transactivation domain is also where SA binds to NPR1, which disrupts the interaction between the C-terminal domain and the BTB domain and induces docking of the C-terminal domain onto the ankyrin repeats 3 and 4, converting NPR1 into an activated transcriptional co-activator (Rochon *et al.*, 2006, Wu *et al.*, 2012, Manohar *et al.*, 2015, Kumar *et al.*, 2022). While the role of different NPR1 domains in SA-induced *PR* gene expression starts to be resolved, which NPR1 domains are important for SA/JA crosstalk is still largely unknown.

NPR1 can reside in the cytoplasm and in the nucleus. Under non-inducing conditions, intramolecular disulfide bonds are formed between certain cysteine residues of NPR1 monomers, resulting in the formation of oligomers, which are sequestered in the cytosol due to their large size. Meanwhile, any of the few monomers that still enter the nucleus are subjected to proteasomal degradation (Spoel *et al.*, 2009). Changing either Cys⁸² or Cys²¹⁶ to an alanine results in decreased oligomerization and increased nuclear localization of NPR1, showing the importance of the cysteine residues in regulating the oligomer/monomer status of NPR1 (Mou *et al.*, 2003, Kumar *et al.*, 2022). The Cys⁸² residue is also important for the formation of dimeric NPR1 in the nucleus (Kumar *et al.*, 2022). In addition, S-nitrosylation of Cys¹⁵⁶ of NPR1 increases oligomerization (Tada *et al.*, 2008). Accumulation of SA causes a redox change in the cell after which thioredoxins (TRX) TRX-h3 and TRX-h5 reduce the cysteine residues, breaking the intramolecular disulfide bonds, and thus releasing NPR1 monomers that can move to the nucleus via nuclear pore proteins (Mou *et al.*, 2003, Tada *et al.*, 2008, Cheng *et al.*, 2009). Our earlier work showed that single mutants of these thioredoxins are not affected in crosstalk, suggesting that they either play no role or a redundant role in SA/JA crosstalk (Caarls, 2016).

In the nucleus, NPR1 is further modified by sumoylation of serine residues, which enhances the interaction of NPR1 with TGA3 and promotes expression of *PR1* (Saleh *et al.*, 2015). The stability and activity of NPR1 is tightly regulated via various phosphorylation and ubiquitination processes (Spoel *et al.*, 2009, Skelly *et al.*, 2019, Shen *et al.*, 2020, Wang *et al.*, 2022b). Also, the closely related NPR1 proteins NPR3 and NPR4 were proposed to act on the stability of NPR1 by acting as CUL3 ligase adapter proteins in an SA-dependent manner, regulating proteasome-mediated degradation of NPR1 (Fu *et al.*, 2012). This was initially proposed as the main mechanism by which SA activates NPR1, where NPR3 and NPR4, but not NPR1, are SA receptors (Fu *et al.*, 2012). Later research however pointed towards a different mechanism: NPR1, NPR3 and NPR4 can all bind SA and regulate a similar set of SA-responsive genes (Ding *et al.*, 2018, Kumar *et al.*, 2022). NPR1 however acts as a

co-activator, and this is increased by SA, whereas NPR3 and NPR4 act as co-repressors and this is suppressed by SA (Ding *et al.*, 2018). Despite their important role in SA signaling, we found in earlier work that mutants *npr3* and/or *npr4* were not affected in SA/JA crosstalk (Caarls, 2016), suggesting that they mostly contribute to the core SA response.

Redox-based protein modifications regulate NPR1 activity and are likely also important for the establishment of SA/JA crosstalk. SA treatment increases the total glutathione levels and results in a higher ratio of reduced (GSH) to oxidized glutathione (GSSG). Interestingly, JA treatment decreases the total amount of glutathione, and increases the amount of GSSG relative to GSH (Spoel and Loake, 2011). The timeframe in which SA was able to suppress *PDF1.2* coincided with the cellular redox change. In addition, treatment with glutathione biosynthesis inhibitor BSO prevented SA-mediated suppression of *PDF1.2* (Koornneef *et al.*, 2008). These results suggested a role for redox regulation in prioritization of the SA pathway over the JA pathway. Glutaredoxins (GRXs) are small ubiquitous enzymes that use glutathione to reduce disulfides and have also been implicated in suppression of JA-responsive gene expression. Several members of the group III class of GRXs in Arabidopsis interact with TGA TFs and suppress expression of *ORA59* and *PDF1.2* (Ndamukong *et al.*, 2007, Zander *et al.*, 2012). Redox-induced activation of NPR1 might play a role in the suppression of JA responses, but our earlier work with redox-related mutants suggested that it is not a major mechanism, or at least it was not apparent in mature plants under our experimental conditions (Caarls, 2016).

Many questions remain on the mechanism of SA- and SA/NPR1-mediated suppression of JA responses, especially for the ERF branch of the JA pathway. For example, it is not yet clear if NPR1 can regulate SA/JA crosstalk in the nucleus or the cytosol, or both. In Arabidopsis, a fusion protein of NPR1 and the hormone binding domain (HBD), which was retained in the cytosol, was shown to suppress *PDF1.2* expression in seedlings treated with a combination of SA and methyl JA (MeJA). This suggested that a function of NPR1 in suppression of JA-induced gene expression takes place in the cytosol (Spoel *et al.*, 2003). Moreover, in rice, overexpression of *OsNPR1* resulted in suppression of JA-responsive gene expression and reduced defense against an insect herbivore, but overexpression of a form of NPR1 that was constitutively localized in the nucleus due to mutation of two cysteines (Cys⁷⁶ and Cys²¹⁶) impaired suppression of JA-responsive genes under basal conditions and reduced the resistance level against insects (Yuan *et al.*, 2007). These results suggested that the suppression of JA responses by NPR1 can occur via a function of NPR1 in the cytosol, and that cysteine residues in NPR1 that influence multimerization are involved in JA-mediated defense suppression. Moreover, it was discovered that NPR1 can form SA-induced condensates in the cytosol that contain stress- and immunity-related proteins, which are ubiquitinated and degraded (Zavaliev *et al.*, 2020). However, these bodies were not enriched for components related to JA signaling (Zavaliev *et al.*, 2020), so this does not directly provide a lead towards a cytosolic mechanism that governs

SA/JA crosstalk. In line with a role for NPR1 in the nucleus during SA/JA crosstalk, our earlier work with mature plants using the same NPR1-HBD line as Spoel *et al.* (2003) and an *npr1-nls* line, containing NPR1 without its NLS, showed that SA/JA crosstalk was impaired in these *npr1* mutants where NPR1 was located in the cytosol (Caarls, 2016). Together, this suggests that nuclear NPR1 can play an essential role in SA/JA crosstalk, depending on the (experimental) conditions.

In this study, we followed a genetic, transcriptomic, and molecular approach to further investigate the nuclear role of NPR1 in SA-mediated suppression of JA-induced gene expression. In agreement with our earlier findings in mature plants (Caarls, 2016), we found that SA/JA crosstalk is impaired in mutants carrying variants of NPR1 that are retained in the cytosol in our experimental setup in in-vitro-grown seedlings. Furthermore, we found that two lines overexpressing NPR1 protein of which either Cys⁸² or Cys²¹⁶ was mutated were impaired in SA-mediated suppression of JA marker genes *PDF1.2* and *VSP2*, but were not affected in SA-induced *PR1* expression, therewith separating the transcriptional activator role of NPR1 from its transcriptional repressor role. Subsequent analyses uncovered several WRKY TFs as novel players in NPR1-regulated SA/JA crosstalk, acting downstream of the ORA59 TF protein, partly via degradation of the protein, resulting in reduced *PDF1.2* expression.

RESULTS

Nuclear NPR1 functions in the suppression of *PDF1.2*

In a previous study we investigated the effect of mutations that alter localization, redox regulation and stability of NPR1 in mature plants on SA/JA crosstalk (Caarls, 2016). We demonstrated that only variants of NPR1 that affect its nuclear localization were affected in SA/JA crosstalk, acting on both the ERF branch marker gene *PDF1.2* and the MYC branch marker gene *VSP2*. However, these experiments were executed with mature plants, and because these findings contradict seminal work done in seedlings (Spoel *et al.*, 2003) we decided to repeat our experiments in seedlings to assess if the plant development stage influences the effect of intracellular localization of NPR1 on SA/JA crosstalk. We grew plants for 12 days on ½ MS agar plates and transferred them to new ½ MS agar plates containing MeJA or SA + MeJA, and incubated them for 48 h. To assess the importance of nuclear localization of NPR1 we used a fusion protein of NPR1 that was retained in the cytosol (NPR1-HBD). This line was also used by Spoel *et al.* (2003), who showed that in this line SA could still suppress *PDF1.2* expression. In addition, we used the *npr1-nls* mutant, in which five amino acids in the nuclear localization signal are mutated, resulting in exclusive cytosolic localization of NPR1 (Kinkema *et al.*, 2000). As a positive control we used *npr1-1*,

which has a non-functional version of NPR1. As expected, when plants were treated with SA + MeJA the SA marker gene *PR1* was induced in the wild type Col-0, but not in *npr1-1* or the two lines with cytosolic NPR1 (Figure 1A). *PDF1.2* expression was significantly reduced by SA + MeJA compared to MeJA alone in Col-0, but SA in the double treatment did not affect *PDF1.2* expression in *npr1-1* or the two mutants with cytosolic NPR1 (Figure 1B). These results in seedlings confirm our earlier findings with mature plants (Caarls, 2016) and reinforce that under our experimental conditions nuclear localization of NPR1 is required for SA/JA crosstalk, regardless of the plant's developmental stage. Notably, suppression of *VSP2* was relatively less affected by these variants of NPR1 as well as in the positive control *npr1-1* (Figure S1A), suggesting that under our experimental conditions NPR1 was mostly required for SA/JA crosstalk acting on the ERF branch of the JA pathway.

Two different cysteine mutations in NPR1 affect SA/JA crosstalk, but not the core SA pathway

Cysteine-based modifications of the NPR1 protein are important for its functioning (Spoel and Loake, 2011, Kumar *et al.*, 2022). When either one of two specific cysteine residues in NPR1, Cys⁸² or Cys²¹⁶, are mutated to alanine in the transgenic lines *35S:NPR1^{C82A}-GFP npr1-1* (from hereon: C82A) or *35S:NPR1^{C216A}-GFP npr1-1* (from hereon: C216A), the protein displays reduced oligomerization and increased nuclear localization (Mou *et al.*, 2003, Kumar *et al.*, 2022). Based on our results presented above we hypothesized that reduced oligomerization and thus also increased nuclear localization of NPR1 in these lines would result in a greater repression of JA-responsive transcription by NPR1. To address this, we performed several experiments with these lines. Please note that the results of our experiments with C82A and C216A described below (qRT-PCR and RNA-seq) were already described by Caarls (2016), but because they are essential to this work we present them again here. We performed hormone dip experiments in 5-week-old plants and found that *PR1* induction after 24 h of SA + MeJA treatment was not significantly altered in any of the cysteine mutant NPR1 lines (Figure 1C), suggesting that induction of the core SA pathway was not affected by these NPR1 cysteine mutations. Surprisingly, in both mutants, treatment with SA + MeJA did not suppress MeJA-induced expression of *PDF1.2* (Figure 1D) or *VSP2* (Figure S1B). This shows that while expression of *NPR1^{C82A}* or *NPR1^{C216A}* complemented the *PR1* activation of the *npr1-1* mutant background, it did not restore suppression of JA-responsive genes by SA. This suggests that the mutation of Cys⁸² and Cys²¹⁶ disrupts the function of NPR1 in SA/JA crosstalk while leaving the function of NPR1 on SA-responsive gene expression intact.

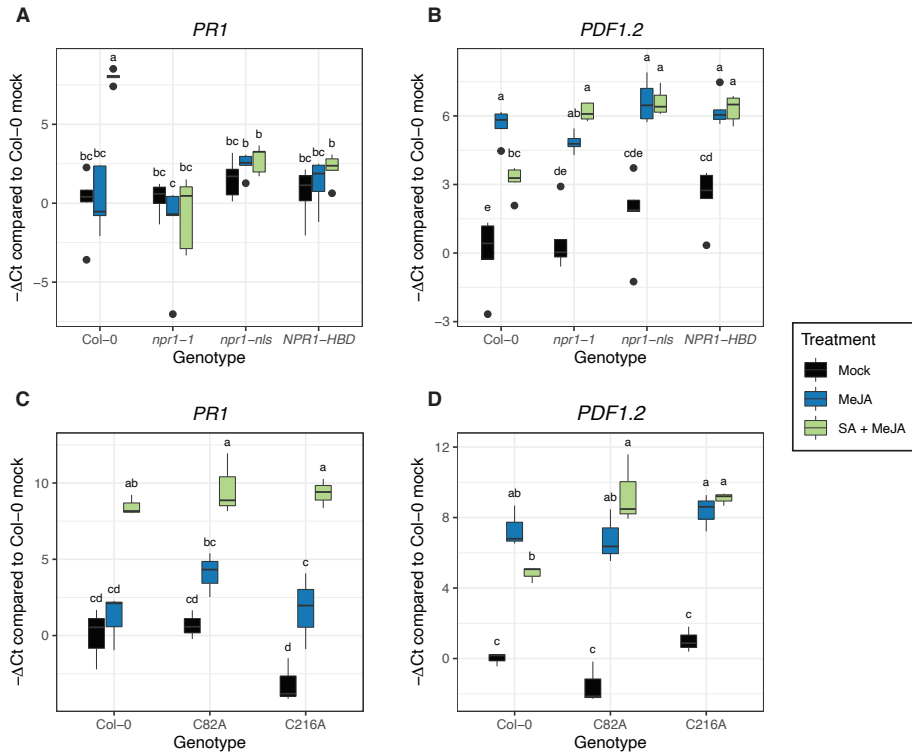


Figure 1: Effects of mutations in NPR1 on SA/JA crosstalk.

qRT-PCR expression analysis of (A, C) SA marker gene *PR1* and (B, D) JA marker gene *PDF1.2* after hormone treatments.

(A, B) Gene expression measured in 12-day-old seedlings on plates. Plants were treated for 48 h with MeJA (0.02 mM) and SA (0.5 mM).

(C, D) Gene expression measured in 5-week-old plants in pots. Plants were dipped in hormone solution (0.1 mM MeJA and/or 1 mM SA or mock) and harvested after 24 h.

For relative expression levels the ΔC_t values per gene/sample were determined relative to *AT1G13320*. The plot shows $-\Delta C_t$ values that are normalized so that the mean $-\Delta C_t$ value of mock-treated Col-0 is 0. Letters indicate significance levels according to a Tukey's HSD test; $n=5$ (for A and B) or $n=3$ (for C and D). Experiments were repeated with similar results (not shown). See Figure S1 for expression of *VSP2*.

RNA-seq of mutants in NPR1 revealed WRKY TFs as potential SA/JA crosstalk regulators

To gain more knowledge on the mechanism of nuclear NPR1-mediated suppression of JA responses, we next investigated which processes are impaired in the C82A and C216A mutants that may cause the detected defect in SA/JA crosstalk. We hypothesized that the cysteine mutations alter the properties of NPR1 such that it can no longer interact with certain TFs that activate regulatory genes that repress JA signaling, while it can still interact with TFs that regulate the core SA response. To investigate the hypothesis that

NPR1 regulates crosstalk as a co-regulator of genes encoding JA signaling suppressors, we performed RNA-seq analysis on the mutants *npr1-1*, C82A, and C216A after the combination treatment of SA + MeJA, mimicking a situation where SA/JA crosstalk is active in Col-0, but not in *npr1-1*, C82A and C216A. For each of the three biological replicates, developmental leaf number 8 of one plant was harvested at 5 h after treatment, because at this time SA-responsive genes such as *PR1* are induced by SA and early JA-responsive genes such as *VSP2* are suppressed by SA (Hickman *et al.*, 2019). First, we analyzed the expression level of the *NPR1* gene itself. As shown in Figure 2A, the expression of wild-type *NPR1* was 2.5 times upregulated in Col-0 after SA + MeJA treatment and, as expected, not detectable in *npr1-1*, C82A, and C216A. In all biological replicates of the C82A and C216A lines, in which C>A mutant versions of *NPR1* are overexpressed in the *npr1-1* background, the C>A variants of *NPR1* were indeed higher expressed compared to the wild-type *NPR1* version in Col-0. In three replicates (i.e., individual plants), namely C82A replicate 2 (C82A-2), C82A replicate 3 (C82A-3) and C216A replicate 3 (C216A-3), the C>A *NPR1* transcript levels were around 15- to 25-fold induced, whereas in the other three replicates the induction was around 5-fold (Figure 2A). The RNA-seq data enabled us to verify the presence of the expected mutations in *NPR1* in all tested lines. In the *npr1-1* mutant, as well as in the C82A and C216A mutants (in the *npr1-1* background), mutant *npr1-1* mRNA levels were detected at low levels (Figure 2A), confirming that the lines behaved as expected.

We then determined if the different expression levels of C>A *NPR1* in the three replicates of C82A and C216A influenced NPR1-mediated transcriptional activity. Two distinct transcriptome patterns after SA + MeJA treatment could be distinguished in the replicates. One was comparable to that of expression in *npr1-1* plants treated with SA + MeJA, and the other to that of Col-0 plants treated with SA + MeJA. For example, the SA marker gene *PR1* was lowly expressed in the three replicates that also expressed relatively low levels of the C>A-mutated *NPR1* allele, but highly expressed in the three replicates that also have relatively high expression of the C>A-mutated *NPR1* allele (Figure 2). We thus speculate that expression of C>A-mutated *NPR1* in C82A-1, C216A-1 and C216-2 was too low to result in complementation of core SA signaling in the *npr1-1* mutant. We thus disregarded the transcript profiles of these replicates in the follow-up analyses.

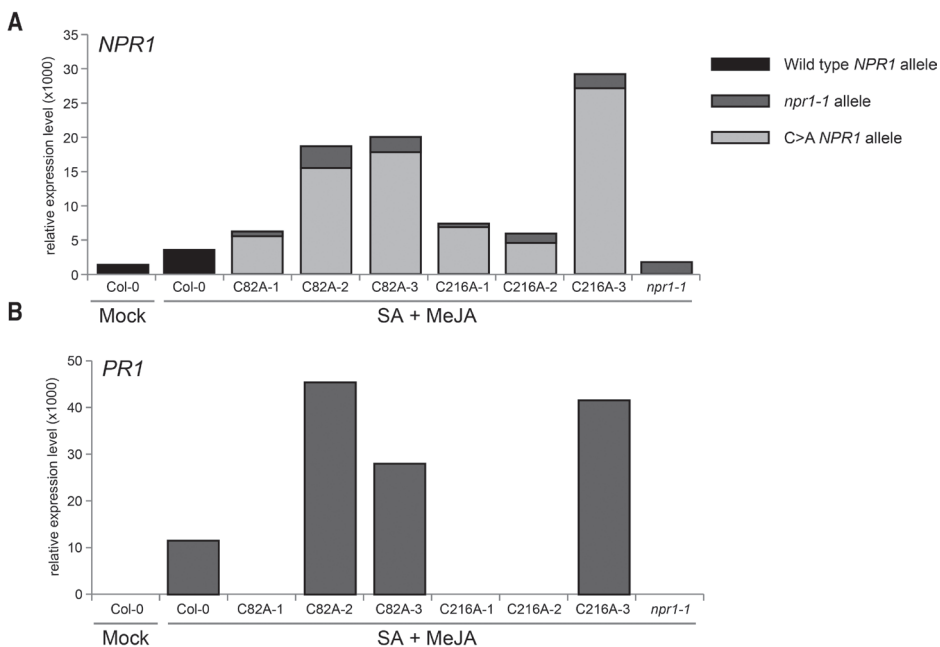


Figure 2: Expression levels of *NPR1* and *PR1* in Col-0, *npr1-1* and two *NPR1* cysteine mutants revealed by RNA-seq.

(A) Expression levels of *NPR1* (normalized RNA-seq read counts). Expression of the *npr1-1* allele was estimated by multiplying the total number of *NPR1* counts with the ratio of counts containing the C1000T point mutation of the *npr1-1* allele. The rest of the counts were assigned to the wild-type *NPR1* allele (for Col-0) or the C>A *NPR1* allele (for C82A and C216A).

(B) Expression levels of *PR1* (normalized RNA-seq read counts).

Expression was measured in mock-treated Col-0 plants or SA + MeJA-treated Col-0, *npr1-1* (average of three replicates), and C82A and C216A mutants (three separate replicates) with RNA-seq.

We analyzed in closer detail the two replicates of the C82A line that showed enhanced *PR1* expression after SA + MeJA treatment. The differentially expressed genes in SA + MeJA-treated Col-0 plants relative to SA + MeJA-treated *npr1-1* or SA + MeJA-treated C82A-2 and C82A-3 mutants (C82A-2/3) were compared. We first investigated which section of the *NPR1*-affected transcriptome was also affected in C82A-2/3. In SA + MeJA-treated *npr1-1*, 5499 genes were significantly differentially expressed compared to SA + MeJA-treated Col-0 ($P \leq 0.05$; Table S1), highlighting the major role of *NPR1* in the SA GRN. Of these genes, 2480 were higher expressed in Col-0 than in *npr1-1*. This group included many known genes that are inducible by SA in an *NPR1*-dependent manner. The other 3019 genes were significantly lower expressed in Col-0 than in *npr1-1*. In contrast, in SA + MeJA-treated C82A-2/3 plants, only 97 genes were significantly differentially expressed compared to SA + MeJA-treated Col-0 ($P \leq 0.05$; Table S1). This shows that only a small part of the transcriptome is affected by the mutation in Cys⁸². Of these genes, 46 were lower

expressed in C82A-2/3 than in Col-0, and 51 were higher expressed in C82A-2/3 compared to Col-0. The majority of the genes that were lower expressed in C82A-2/3, namely 40 of the 46 genes, were also lower expressed in SA + MeJA-treated *npr1-1* compared to SA + MeJA-treated Col-0, suggesting that the C>A mutation in Cys⁸² of NPR1 results in reduced expression of a subset of genes whose expression is dependent on NPR1, while leaving the NPR1 dependency of the majority of the NPR1-dependent genes intact.

Genes that are upregulated by SA + MeJA in Col-0 but significantly less in both C82A-2/3 and *npr1-1* are potential candidates with a role in NPR1-regulated SA/JA crosstalk. In Col-0, SA + MeJA treatment induced the expression of 33 of the 46 genes that were lower expressed in SA + MeJA-treated C82A-2/3 than in SA + MeJA-treated Col-0. The expression of 32 of these genes (all genes except *ARACNIN1*) was also significantly lower in the *npr1-1* mutant compared to Col-0, confirming their NPR1 dependency. Figure 3 shows a heat map of the log₂-fold changes of these 33 genes in Col-0, C82A-2/3 and *npr1-1* treated with SA + MeJA, relative to mock-treated Col-0. For many of these genes the function is still unknown. Interestingly, four genes affected in C82A-2/3 encode TFs that have been described to be direct transcriptional targets of NPR1 (Wang *et al.*, 2006). These are *WRKY18*, *WRKY38*, *WRKY53*, and *WRKY70*, indicated with a red dot in Figure 3. This suggests that the C82A mutation in NPR1 leads to reduced activation of these genes by NPR1.

WRKY53 represses *PDF1.2* expression downstream of *ORA59* transcription

Reduced expression of *WRKY18*, *WRKY38*, *WRKY53* and *WRKY70* is a plausible explanation for the lack of SA/JA crosstalk in the C82A mutant, since *WRKY53* and *WRKY70* were previously implicated in the regulation of SA/JA crosstalk (Caarls *et al.*, 2015). We set up a transient protoplast assay to test whether any of these WRKY TFs can suppress JA signaling. We chose to focus on the effect of these WRKY TFs on the ERF branch (measured by the marker gene *PDF1.2*), since the effect of NPR1 on the MYC branch was already found to be dependent on the NPR1-MYC2 interaction (Nomoto *et al.*, 2021). We made a single plasmid expressing multiple genes (Figure 4A). Firstly, it contained the *PDF1.2* promoter fused to the β -glucuronidase (*GUS*) gene as a readout for JA pathway activity. Additionally, it had the *ORA59* gene expressed from the constitutively active 35S promoter to activate transcriptional activity of the ERF branch. With this setup, crosstalk mechanisms acting downstream of *ORA59* transcription can be investigated, which is the level at which SA can suppress *PDF1.2* induction in whole plants (Van der Does *et al.*, 2013). We also added the luciferase gene from firefly (*LucF*) expressed from the 35S promoter to the construct to normalize the *GUS* signal for the number of transfected protoplasts. Additionally, the construct contained a candidate WRKY TF expressed from the 35S promoter, or an empty module as a control. We also added *Enhanced Yellow*

Fluorescent Protein (EYFP) expressed from the 35S promoter to the construct to verify transfection of the protoplasts during our experimental procedure. As expected, *ORA59* overexpression strongly induced *PDF1.2* expression in comparison to a control where an empty module was put in the place of 35S:*ORA59* (Figure 4B). Interestingly, overexpression of *WRKY53* together with *ORA59* significantly suppressed *PDF1.2* expression compared to *ORA59* overexpression alone. Also, overexpression of *WRKY70* significantly reduced *PDF1.2* expression, albeit to a weaker level than *WRKY53*. In three independent experiments only the strong suppression by *WRKY53* was consistent (Figure S2). In contrast to *WRKY53* and *WRKY70*, overexpression of *WRKY18* or *WRKY38* did not affect *PDF1.2* expression (Figure 4B; Figure S2), except for a small effect of *WRKY18* in one experiment (Figure S2A), which is likely not biologically meaningful. Altogether, this suggests that *WRKY53* and possibly *WRKY70* regulate SA/JA crosstalk downstream of *ORA59* transcription.

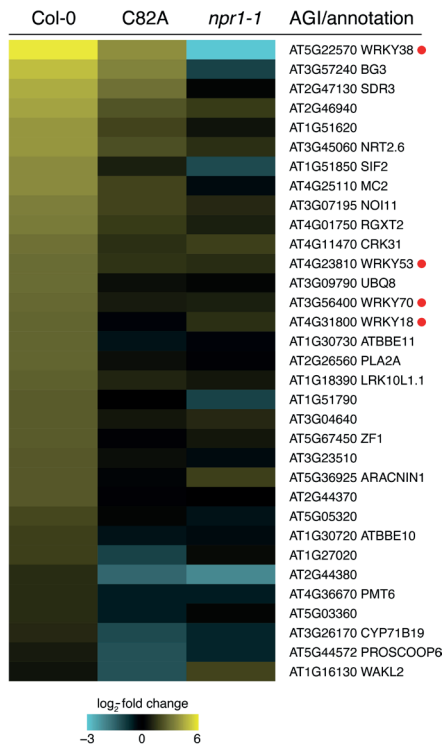


Figure 3: Reduced SA + MeJA-induced expression of WRKY genes in NPR1 cysteine mutant C82A.

Heat map representation of gene expression in Col-0, C82A and *npr1-1* plants measured with RNA-seq. Shown is the log₂-fold change in expression of genes in SA + MeJA-treated plants (Col-0, C82A or *npr1-1*) relative to mock-treated Col-0 plants. The 33 genes depicted here were significantly lower expressed in C82A-2/3 compared to Col-0 (adjusted $P \leq 0.05$) and induced by SA + MeJA in Col-0 (log₂-fold change (SA + MeJA)/mock Col-0 ≥ 0.6). Genes are identified with AGI and (if available) TAIR annotation. A red dot indicates that the gene is a direct NPR1 target (Wang *et al.*, 2006). See Table S1 for all differentially expressed genes between Col-0 and *npr1-1* and between Col-0 and C82A-2/3.

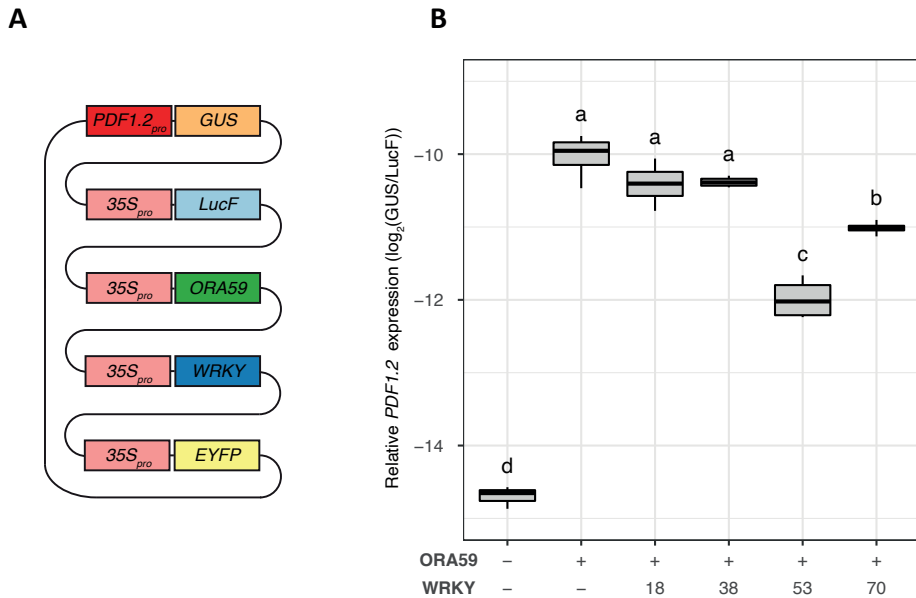


Figure 4: Suppression of ORA59-induced *PDF1.2* expression by WRKY TFs in Arabidopsis protoplasts.

(A) Schematic representation of the plasmid used in the experimental setup. Protoplasts isolated from 3-week-old plants were transfected with a single plasmid containing the *GUS* gene expressed from the *PDF1.2* promoter, the *LucF* gene expressed from the 35S promoter and the *EYFP* gene expressed from the 35S promoter. Additionally, constructs contained either the *ORA59* gene expressed from the 35S promoter ('ORA59 +′ in panel B) or only the 35S promoter and terminator ('ORA59 -′ in panel B), and they contained one of four WRKY TFs ('WRKY 18, 38, 53 or 70′ in panel B) expressed from the 35S promoter, or only the 35S promoter and terminator ('WRKY -′ in panel B). (B) Relative *PDF1.2* expression was determined as the log₂ of relative *GUS* levels divided by relative *LucF* levels, as quantified using the substrates MUG and luciferin, respectively. Letters indicate significant differences according to Tukey's HSD test ($n=4$). See Supplemental Figure S2 for two other repeats of the same experiment.

Four additional WRKY TFs can suppress ORA59-induced *PDF1.2* expression

Regulation of plant processes is often carried out by redundantly functioning proteins. For example, it was already shown that WRKY53 operates redundantly with WRKY46 and WRKY70 in basal resistance against *Pseudomonas syringae* and likely also in suppression of *PDF1.2* (Hu *et al.*, 2012). We therefore considered the possibility that other WRKY TFs related to WRKY53 are also involved in suppression of ORA59-induced *PDF1.2* expression. WRKY53 is part of a clade of WRKY TFs known as group III (Kalde *et al.*, 2003; Figure S3). The majority of TFs in this group are induced by SA (Hickman *et al.*, 2019) and a number of TFs were already implicated in SA/JA crosstalk (Kalde *et al.*, 2003, Caarls *et al.*, 2015). We therefore decided to analyze all TFs in this clade that were induced by SA according to Hickman *et al.* (2019), as well as other WRKY TFs known to suppress JA signaling according to Caarls *et al.* (2015). We tested this in the same protoplast system as before so that we could assess which of these WRKY TFs suppress *PDF1.2* expression downstream of ORA59

transcription, and what the relative suppression strength of each WRKY TF is. We did not include WRKY55 and WRKY64 in this experiment because we were unable to clone it. In this experiment, ORA59 again strongly induced *PDF1.2* expression and WRKY53 suppressed it, as expected (Figure 5). Four other WRKY TFs were also able to suppress ORA59-induced *PDF1.2* expression: WRKY50, WRKY54, WRKY63 and most notably WRKY67. Of these TFs, WRKY50 (Gao *et al.*, 2011) and WRKY54 (Li *et al.*, 2017) were previously associated with suppression of JA signaling, but to the best of our knowledge WRKY63 and WRKY67 were not. In our RNA-seq dataset of SA + MeJA-treated Col-0 and *npr1-1* plants (Table S1) *WRKY50*, *WRKY53* and *WRKY54* were differentially expressed, suggesting they act in NPR1-dependent SA/JA crosstalk. In contrast, *WRKY63* and *WRKY67* were not differentially expressed, suggesting that their role in SA/JA crosstalk may be independent of NPR1. There was no clear phylogenetic relationship between the suppressing WRKY TFs within group III of the WKRY TF family (Figure S3).

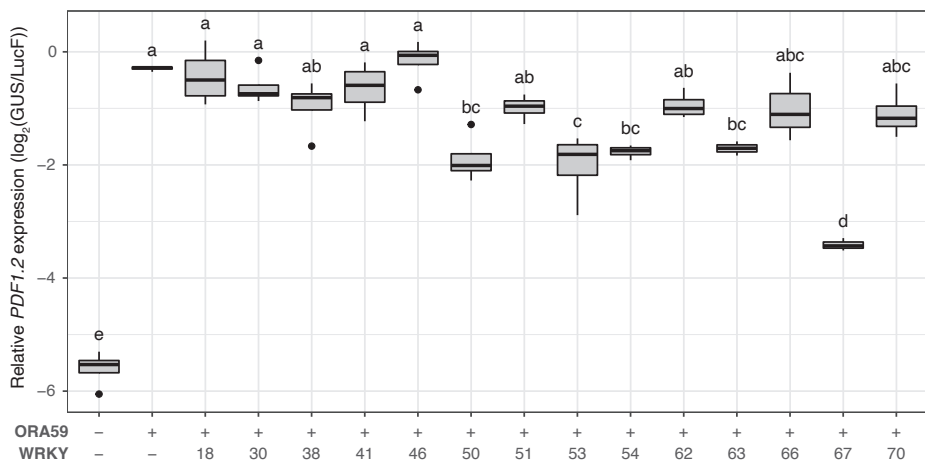


Figure 5: Suppression of ORA59-induced *PDF1.2* expression by selected WRKY TFs in Arabidopsis protoplasts.

Protoplasts isolated from 3-week-old plants were transfected with a single plasmid, depicted and described in (the legend of) Figure 4A. Relative *PDF1.2* expression was determined as the log₂ of relative GUS levels divided by relative LucF levels, as quantified using the substrates MUG and Luciferin, respectively. Letters indicate significant differences according to Tukey's HSD test ($n=4$).

WRKY53 and WRKY67 regulate SA/JA crosstalk by reducing ORA59 protein levels

SA is known to suppress ORA59-induced *PDF1.2* expression by inducing degradation of ORA59 protein (Van der Does *et al.*, 2013, He *et al.*, 2017). We hypothesized that our identified suppressive WRKY TFs may (indirectly) affect ORA59 protein stability. To test

this, we used the same protoplast system as in the previous section. However, we now coupled *ORA59* to the gene for luciferase derived from *Renilla reniformis* (*LucR*; Figure 6A). This allowed us to use the ratio *LucR* to *LucF* as a proxy for *ORA59* protein levels. Because the addition of *LucR* made the already large plasmid that we used even larger, we decided to express the *WRKY* TFs from a separate plasmid and transfect protoplasts with both plasmids at once (Figure 6A). As found previously (Figure 5), overexpression of all five tested *WRKY* TFs (*WRKY50*, *WRKY53*, *WRKY54*, *WRKY63* and *WRKY67*) reduced relative *PDF1.2* expression, showing that transfection of the protoplasts with the two plasmids was similarly effective as with one plasmid (Figure 6B). Notably, overexpression of *WRKY53* and *WRKY67* led to a small but significant reduction of relative *ORA59* protein levels, while *ORA59* was expressed from a constitutively active promoter (Figure 6C). This suggests that these two *WRKY* TFs suppress *PDF1.2* expression - at least partly - by targeting *ORA59* protein levels.

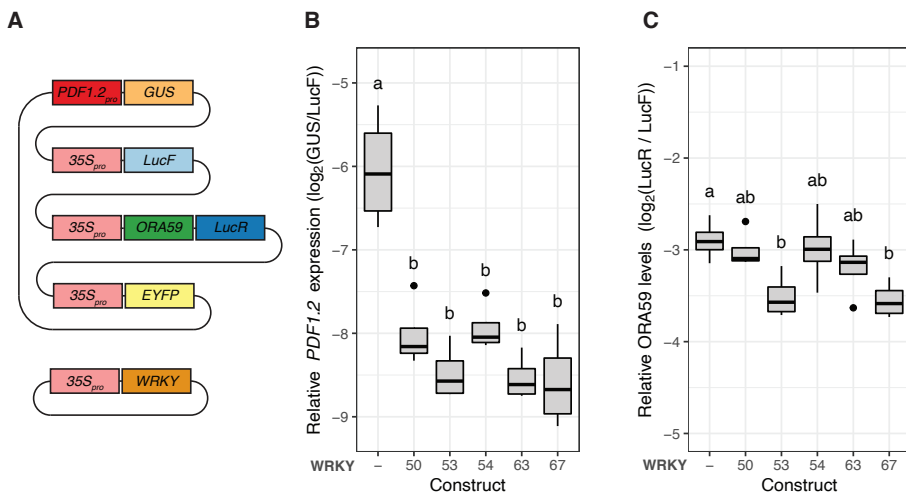


Figure 6: Suppression of *PDF1.2* expression and relative *ORA59* protein levels by selected *WRKY* TFs.

(A) Protoplasts isolated from 3-week-old plants were transfected with two plasmids. The first contained the *GUS* gene expressed from the *PDF1.2* promoter, the *LucF* gene expressed from the 35S promoter, the *ORA59* gene fused to the *LucR* gene expressed from the 35S promoter, and the *EYFP* gene expressed from the 35S promoter. The second plasmid contained a *WRKY* TF (indicated with its number in panels B and C) expressed from the 35S promoter, or only the 35S promoter and terminator ('*WRKY* -' in panels B and C). Protoplasts were harvested approximately 20 h after transfection.

(B) Relative *PDF1.2* expression was determined as the log₂ of relative *GUS* levels divided by relative *LucF* levels, as quantified using the substrates MUG and luciferin, respectively.

(C) Relative *ORA59* levels were determined as the log₂ of relative *LucR* levels divided by relative *LucF* levels, as quantified using the substrates coelenterazine and luciferin, respectively.

Letters in (B) and (C) indicate significant differences according to Tukey's HSD test ($n=4$).

DISCUSSION

NPR1 is an important regulator of SA-induced gene expression and defense, and of SA/JA crosstalk. While regulation of the NPR1 protein in response to SA has been studied extensively, the mechanism of NPR1-mediated SA/JA crosstalk is less clear, especially concerning the ERF branch of the JA pathway. This study investigated the function of NPR1 in SA/JA crosstalk, focusing on the role of its localization and the effect on downstream transcription. In our experimental setup, cytosolic NPR1 did not contribute to the suppression of JA marker genes in both seedlings and mature plants (Caarls, 2016; Figure 1). As this contradicts findings of a seminal study by Spoel *et al.* (2003), the role of nuclear/cytosolic NPR1 in regulating SA/JA crosstalk is likely context-dependent, modulated by factors that are currently unknown. We further tested two lines overexpressing cysteine>alanine-mutated versions of the NPR1 protein, C82A and C216A, which were impaired in SA-mediated suppression of JA marker genes *PDF1.2* and *VSP2*, but displayed normal levels of SA-induced *PR1* expression. This allowed us to distinguish the function of NPR1 in SA-mediated activation of *PR1* from its function in repression of *PDF1.2* and *VSP2*, and to pinpoint five SA- or SA/NPR1-regulated WRKY TFs that suppressed ORA59-induced *PDF1.2* expression in a protoplast expression system. Of these TFs, WRKY53 and WRKY67 reduced the accumulation of ORA59 protein, independent of *ORA59* transcription. Together, this points to a model where SA induces expression of specific crosstalk-regulating WRKY TF genes, for which Cys⁸² and Cys²¹⁶ of NPR1 are important. Other SA-inducible crosstalk-regulating WRKY TFs can be transcriptionally activated in an NPR1-independent pathway, but may still need NPR1 for their crosstalk effect. The encoded WRKY TFs can suppress JA-activated *PDF1.2* expression partly via regulating degradation of ORA59 (Figure 7).

Cytosolic NPR1 did not suppress JA marker genes in this study

In seedlings that express a mutated NPR1 protein that is localized to the cytosol (NPR1-HBD), MeJA-induced *PDF1.2* expression was reported to be suppressed after SA treatment (Spoel *et al.*, 2003). In addition, the *npr1-3* mutant, which lacks the C-terminal part of the NPR1 protein that contains the nuclear localization signal, was demonstrated to still exhibit SA-mediated suppression of *PDF1.2*, albeit to a lower extent as wild-type plants (Leon-Reyes *et al.*, 2009). This suggested that a cytoplasmic function of NPR1 plays a role in SA/JA crosstalk. However, under the experimental conditions of the current study, the MeJA-induced expression of *VSP2* (in adult plants) and *PDF1.2* (in adult plants and seedlings) was not suppressed by SA treatment in two different genotypes that express a cytosolic version of NPR1, i.e., NPR1-HBD and *npr1-nls* (Figure 1; Figure S1; Caarls, 2016). These results point to a nuclear function of NPR1 in SA/JA crosstalk in our study, and

suggest that the cytoplasmic function of NPR1 in SA/JA crosstalk is context dependent. Notwithstanding, the experimental conditions of the present study allowed us to mechanistically investigate the nuclear function of NPR1 in SA/JA crosstalk.

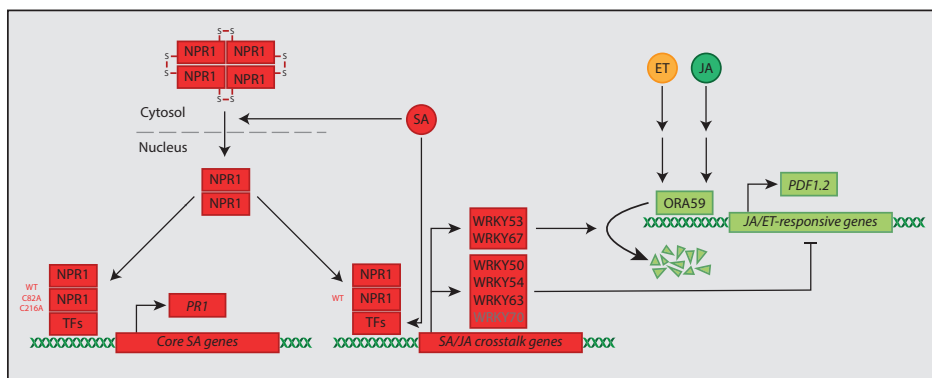


Figure 7: Schematic model of NPR1's and WRKYs' role in repression of the ERF branch of the JA pathway.

NPR1 resides in the cytosol as an oligomer held together by disulfide bridges between cysteine residues such as Cys⁸² and Cys²¹⁶. SA triggers a redox change, which causes reduction of these cysteine residues, leading to reduced oligomerization and increased nuclear localization of NPR1. In the nucleus, NPR1 forms a homodimer and acts as a transcriptional co-factor and, together with specific TFs, activates core SA genes, such as *PR1*, and SA/JA crosstalk regulatory genes, including specific WRKY TF genes. In the C82A and C216A mutants NPR1 is only able to activate core SA genes such as *PR1*, but not crosstalk-specific WRKY TF genes. SA can also induce expression of specific WRKY TF genes independently of NPR1. When ET and JA levels are high, they activate *ORA59* together, which causes upregulation of JA/ET-responsive genes such as *PDF1.2*. WRKY53 and WRKY67 cause degradation of the *ORA59* protein, leading to reduced *PDF1.2* expression. WRKY50, WRKY54, WRKY63 and possibly WRKY70 repress *PDF1.2* through a different, unknown mechanism.

Cysteine>alanine mutations in NPR1 disrupt suppression of JA marker genes by SA

The mutation of one of two cysteines in NPR1 (Cys⁸² and Cys²¹⁶) into alanines caused the transgenic C82A and C216A lines that overexpress these mutated versions of the NPR1 protein in the *npr1-1* background to lose suppression of MeJA-induced *PDF1.2* and *VSP2* by SA (Figure 1D; Figure S1B). Interestingly, similar mutations in rice NPR1 (Cys⁷⁶ and Cys²¹⁶ changed to alanine) were previously tested and also shown to result in a loss of suppression of JA-dependent genes and defense (Yuan *et al.*, 2007). As the Cys-mutated NPR1 in rice was constitutively localized to the nucleus, these results were interpreted as evidence for a cytosolic role of NPR1 in suppression of JA responses. Mutation of Cys⁸² or Cys²¹⁶ in the Arabidopsis C82A and C216A lines caused the Cys-mutated NPR1 protein to localize in both the nucleus and the cytosol (Mou *et al.*, 2003). Therefore, the

impairment in SA/JA crosstalk in both Cys-mutated NPR1-overexpressing Arabidopsis and rice is unlikely due to exclusion of NPR1 from the cytosol but rather caused by other effects of the mutations in the Cys residues. For example, the mutation may lead to loss of interaction with other proteins, such as specific TFs, causing reduced activation of particular NPR1 target genes. Unfortunately, we were unable to execute interaction assays with the different NPR1 variants to test this hypothesis.

While SA/JA crosstalk was impaired in the C82A and C216A mutants, *PR1* expression was the same as in Col-0, under basal and SA-treated conditions (Figure 1C). Another study found that the C82A and C216A mutant lines had higher basal *PR1* expression than their reference, *35S_{pro}:NPR1-GFP* (Mou *et al.*, 2003). A recent study also found that the C82A mutant exhibited higher basal resistance against *Pseudomonas syringae* pv. *maculicola* ES4326 than *35S_{pro}:NPR1-GFP*, which was not further enhanced by SA pretreatment, even though C82A exhibited relatively high SA-induced *PR1* expression (although lower than *35S_{pro}:NPR1-GFP*) (Kumar *et al.*, 2022). While these studies by the Dong lab do not 100% match our findings, it can still be concluded that the C82A and C216A mutants are able to activate core SA responses, albeit not to a completely similar extent as overexpressed wild-type NPR1.

In their study, Kumar *et al.* (2022) found that the C82A mutant was still able to homodimerize, while a fully dimerization-defective mutant was defective in *PR1* induction and resistance. Therefore, they concluded that the NPR1 homodimer is the functional unit in activating core SA-dependent defense gene expression. Our finding that the C82A line was impaired in SA/JA crosstalk suggests that the NPR1 homodimer is not per se functional in regulating suppression of the JA pathway. Whether this is due to its oligomerization status or to other structural changes that, e.g., make it unable to interact with certain crosstalk-regulating TFs is unknown.

Identification of WRKY TF genes that may have a role in SA/JA crosstalk

The fact that *PR1* expression was intact in C82A and C216A whereas suppression of the JA pathway was impaired, gave us a unique opportunity to find potential suppressors of the JA pathway acting downstream of NPR1. To test the hypothesis that the cysteine mutations affected part of the SA-responsive, NPR1-dependent transcriptome involved in suppression of the JA pathway, the C82A mutant was subjected to RNA-seq after SA + MeJA treatment. In the treated C82A mutant, 32 genes that were induced by SA in Col-0 in an NPR1-dependent manner were considered interesting candidates for a role in SA/JA crosstalk. Many of the identified genes have no known function in defense (Figure 3; Table S1) and are interesting candidates for crosstalk regulation that require further investigation. This set of 32 genes also contained four known TF-encoding genes that are direct targets of NPR1, namely *WRKY18*, *WRKY38*, *WRKY53* and *WRKY70* (Wang *et al.*, 2006).

WRKY TFs are suppressors of ORA59-induced *PDF1.2* expression

To expand our knowledge on SA- and SA/NPR1-mediated suppression of JA signaling by WRKY TFs we employed a protoplast system to initially investigate if WRKY18, WRKY38, WRKY53 and WRKY70 suppress *PDF1.2* expression downstream of *ORA59* transcription. We found that this was the case for WRKY53 and possibly WRKY70 (Figure 4; Figure S2), confirming earlier reports (Li *et al.*, 2004, Hu *et al.*, 2012). We next investigated the suppression of ORA59-induced *PDF1.2* expression by other WRKY TFs of group III (where WRKY53 and WRKY70 also belong to) and by other WRKY TFs that have been reported to suppress JA signaling according to Caarls *et al.* (2015). We found that this was the case for WRKY50, WRKY54, WRKY63 and WRKY67 (Figure 5). Of the five WRKY TFs that consistently repressed ORA59-induced *PDF1.2* expression, WRKY50, WRKY53 and WRKY54 had been linked to suppression of JA signaling before, and our RNA-seq data indicated that they likely act in NPR1-dependent crosstalk (Table S1). WRKY50 can suppress *PDF1.2* expression together with WRKY51 (Gao *et al.*, 2011), and WRKY53 suppresses *PDF1.2* expression redundantly with WRKY46 and WRKY70 (Hu *et al.*, 2012). Additionally, a recent report suggested that WRKY53 negatively regulates resistance against insects by directly binding to and repressing the promoters of the JA biosynthesis genes *LOX3* and *LOX4* (Jiao *et al.*, 2022), which corroborates that repression of JA signaling is important for plants and regulated by different mechanisms. Because in our system we overexpressed *ORA59* to activate the JA pathway rather than treating with JA, a possible decrease in JA levels cannot explain our results. Indeed, we found that WRKY53 caused a reduction in *ORA59* levels (Figure 6), providing a possible mechanism. WRKY54 has also been linked to suppression of the JA pathway, as the *wrky54 wrky70* double mutant has increased resistance against necrotrophic pathogens and elevated *PDF1.2* expression, as well as higher SA levels (Li *et al.*, 2017). The mechanism hereof was not elucidated. The finding that WRKY63 and WRKY67 can suppress ORA59-induced *PDF1.2* expression is, to the best of our knowledge, novel, and our RNA-seq data indicated that they likely act in NPR1-independent crosstalk (Table S1). Especially WRKY67 is an interesting new candidate regulator of SA/JA crosstalk, as it was found to cause the strongest reduction in ORA59-induced *PDF1.2* expression in protoplasts (Figure 5) and a reduction in *ORA59* protein levels (Figure 6). We found that the group III WRKY TFs that suppressed ORA59-induced *PDF1.2* expression were not phylogenetically related within group III of the WRKY family (Figure S3). This supports the notion discussed above that the different WRKY TFs likely have various modes of action.

Interestingly, we did not observe suppression of ORA59-induced *PDF1.2* expression by WRKY41, WRKY46, WRKY51 and WRKY62, and inconsistent suppression of ORA59-induced *PDF1.2* expression by WRKY70 between experiments, even though all of these WRKY TFs have been implicated in suppression of JA signaling (Caarls *et al.*, 2015). This

could indicate that these WRKY TFs act upstream of *ORA59* transcription or require certain cofactors that were not present under our experimental conditions.

WRKY53 and WKRY67 affect ORA59 protein accumulation

SA is known to repress the ERF branch by destabilizing ORA59 (Van der Does *et al.*, 2013, He *et al.*, 2017). Using our protoplast system, we found that WRKY53 and WRKY67 reduce ORA59 accumulation and thus may affect ORA59 stability, e.g., by increasing ORA59 protein turnover, or by influencing *ORA59* transcript stability or translation efficiency. Future research may be focused on finding downstream targets of these WRKY TFs to see if this includes, for example, certain ubiquitin ligases that may reduce ORA59 stability. Also, future research can investigate the targets of the other WRKY TFs to elucidate how they regulate suppression of ORA59-induced *PDF1.2* expression.

In conclusion, this study identified a nuclear function of NPR1 in SA/JA crosstalk. SA activates NPR1 and induces its nuclear localization. In the nucleus, NPR1 can promote transcription of specific SA/JA crosstalk-regulating WRKY TF genes, for which it requires Cys⁸² and Cys²¹⁶. Some other WRKY TF genes can also be transcriptionally activated by SA independently of NPR1. The encoded WRKY TFs in turn regulate suppression of JA-responsive gene expression by diverse mechanisms, including decreasing the protein level of the ERF branch TF ORA59 (Figure 7).

METHODS

Plant material and growth conditions

In all experiments, Col-0 was used as wild type and was the background accession for all mutant and transgenic lines studied. The mutants and overexpression lines used were generated by previous studies and are: *35S:NPR1-HBD npr1-1* (NPR1-HBD), *35S:npr1-nls-GFP npr1-1 (npr1-nls)* (Kinkema *et al.*, 2000), *npr1-1* (Cao *et al.*, 1994), *35S:NPR1^{C82A}-GFP npr1-1 (C82A)*, *35S:NPR1^{C216A}-GFP npr1-1 (C216A)* (Mou *et al.*, 2003).

For experiments with mature plants, sowing and plant growth was done as described in Chapters 2 and 3. Briefly, stratified Arabidopsis seeds were sown on river sand. Two weeks after germination, seedlings were transferred to 60-ml pots containing a sand/potting soil mixture (5:12 v/v) that had been autoclaved twice for 45 min with a 24-h interval. Plants were cultivated in a growth chamber with a 10-h day and 14-h night cycle at 70% relative humidity and 21°C. For experiments with seedlings, seeds were first surface sterilized by mixing 100 ml of commercial bleach (Manutan B.V., Den Dolder, the Netherlands) with 3.2 ml 37% HCl in a beaker in a desiccator, after which the

desiccator was closed immediately and seeds were incubated in the desiccator for 4 h. For protoplast experiments, 50 μ l of sterilized seeds were sown directly onto 120x120 mm square Petri dishes that contained 70 ml of $\frac{1}{2}$ Murashige and Skoog (MS) medium with 2% sucrose, buffered with MES (pH=5.7) and solidified with 1% plant agar. For hormone treatment experiments, sterilized seeds were sown in 120x120 mm square Petri dishes on an autoclaved, fluid-permeable nylon membrane that lay on top of 50 ml of solidified $\frac{1}{2}$ MS medium (same as for protoplasts except 0.8% agar). Seeds were sown in two rows on the plates, making sure that all plates had five seeds of each line. For both types of experiments, the seeds were stratified on the plates in the dark at 4°C for three days and then incubated lying down (protoplast experiments) or upright (hormone experiments) in a growth chamber at 21°C with a 10-h light/14-h dark cycle at a light intensity of 75 (protoplast experiments) or 100 (hormone experiments) μ mol/m²/s.

Chemical treatments

For hormone treatment of mature plants, 5-week-old plants were treated with SA and/or MeJA by dipping the leaves into a solution containing 0.015% (v/v) Silwet L77 (Van Meeuwen Chemicals BV, Weesp, the Netherlands; nowadays this compound is known as CoatOSil 77 (Momentive, New York, NY, USA)) and either 0.1 mM MeJA (Serva, Brunschwig Chemie, Amsterdam, the Netherlands), or 1 mM SA (Mallinckrodt Baker, Deventer, the Netherlands) and 0.1 mM MeJA. For mock treatments, plants were dipped into a solution containing 0.015% (v/v) Silwet L77 and 0.1% ethanol, as ethanol was the solvent for the 1000x MeJA stock. Leaves were harvested for RNA isolation 5 and 24 h after treatment.

For hormone treatments of seedlings, nylon membranes with 12-day-old seedlings previously grown on $\frac{1}{2}$ MS agar plates were transferred to new plates containing the same $\frac{1}{2}$ MS agar medium, but with 0.02 mM MeJA, 0.5 mM SA + 0.02 mM MeJA (diluted from a 5000x stock in ethanol) or a mock treatment ($\frac{1}{2}$ MS agar medium with 0.02% ethanol). Plants were incubated upright in the growth chamber for 48 h under the conditions described above. Harvesting was done by putting one seedling of a genotype from each of five plates in a 2-ml tube (Greiner Bio-One, Kremsmünster, Austria) containing two glass beads, and immediately snap-freezing it in liquid nitrogen. As each plate contained five plants, a total of five replicates were harvested.

RNA extraction and qRT-PCR analysis

For qRT-PCR analysis, RNA was extracted as described for vegetative tissues by Oñate-Sánchez and Vicente-Carbajosa (2008). RNA was pretreated with DNase I (Thermo Fischer Scientific, Waltham, MA, USA) to remove genomic DNA. RevertAid H minus Reverse Transcriptase (Thermo Fisher Scientific) was used to convert DNA-free total RNA into

cDNA. PCR reactions were performed in optical 384-well plates with a ViiA 7 realtime PCR system (Applied Biosystems, Carlsbad, CA, USA), using SYBR[®] Green to monitor the synthesis of double-stranded DNA. The primers used to analyze expression by qRT-PCR are described in Table S2. A standard thermal profile was used: 50°C for 2 min, 95°C for 10 min, 40 cycles of 95°C for 15 s and 60°C for 1 min. Amplicon dissociation curves were recorded after cycle 40 by heating from 60 to 95°C with a ramp speed of 1.0°C/min. Expression was calculated as $-\Delta\text{Ct}$ relative to the reference gene *At1g13320* (Czechowski *et al.*, 2005) and normalized to the mean $-\Delta\text{Ct}$ value of mock-treated Col-0.

Analysis of RNA-seq results

For RNA-seq, developmental leaf 8 was harvested from three individual mock-treated wild-type Col-0 plants or SA + MeJA-treated Col-0, *npr1-1*, C82A, and C216A plants, 5 h after treatment. RNA extraction and alignment to the genome was done as described in Chapter 2 for the ABA samples. Aligned reads were summarized over annotated gene models (TAIR version 10) using HTseq-count version 0.5.3p9 (<http://www-huber.embl.de/users/anders/HTSeq/>) with parameters: 'stranded no', '-i gene_id'. Sample counts were depth-adjusted and differential expression was determined using the DESeq package with default settings (Anders and Huber, 2010). Genes with a corrected *P* value (*P* adjusted) of ≤ 0.05 were called as differentially expressed. All statistics associated with testing for differential gene expression were performed with R (www.r-project.org). Expression of the *npr1-1* allele was estimated by multiplying the total number of *NPR1* counts with the ratio of counts containing the C1000T point mutation of the *npr1-1* allele. The rest of the counts were assigned to the wild-type *NPR1* allele (for Col-0) or the C>A *NPR1* allele (for C82A and C216A).

Creating the plasmid for the protoplast expression assays

The plasmid used for transfection into protoplasts for a transient expression assay was assembled with Golden Gate cloning using the Moclo kit (Weber *et al.*, 2011, Werner *et al.*, 2012). For creation of level 0 plasmids, a 1.2 kb fragment of the *PDF1.2* promoter was amplified from gDNA, the CDSs of *ORA59* and of several WRKY TF genes were amplified from cDNA, and the *LucR* CDS was amplified from the pBS-35S-Rluc plasmid. Primers used are listed in Table S3. The primers were designed to add a restriction site for BbsI and a specific sequence of 4 bp that would become the overhang needed to clone the product into the correct vector. For some constructs, an internal restriction site needed to be removed from the CDS. This was done by PCR-amplifying two fragments around the restriction site with primers that introduced a nucleotide change so that the restriction site was removed and that added an external BbsI restriction site to re-

assemble the fragments in the level 0 reaction (Table S3). The PCR product was purified after gel electrophoresis using the Illustra GFX PCR DNA and Gel Band Purification Kit (Merck, Darmstadt, Germany). Some very small DNA fragments for the construct were not created by PCR, but by annealing two custom-designed single stranded oligonucleotides (ordered from Integrated DNA Technologies, Coralville, IA, USA), such that on each side an overhang of 4 bp was created that could be used for ligation in a level-0 reaction (Table S3). The two oligonucleotides were annealed by combining 25 μl of each (100 μM) in a 1.5-ml tube, heating at 95°C and slowly cooling to room temperature in (initially) hot tap water.

The different PCR products and annealed fragments were cloned into the appropriate vector (Table S3) using a standard Golden Gate reaction. For this, 2 μl of 10x buffer G, 0.2 μl of 100 mM ATP, 1 μl of 10U/ μl BbsI (Thermo Fisher Scientific), 0.4 μl of 5U/ μl T4 DNA ligase (Thermo Fisher Scientific), 100 ng of vector DNA, and PCR/annealing product in an approximate molar ratio of 1:2 were mixed in a total of 20 μl . The mix was then incubated for 3 cycles of 10 min at 37°C and 10 min at 22°C, which after the final cycle was followed by 10 min at 37°C and 20 min at 65°C. The product was transformed into *Escherichia coli* DH5 α , after which the amplified plasmid was isolated using the GenElute™ Plasmid Miniprep Kit (Sigma Aldrich, St. Louis, MO, USA) and the correct insertion of the PCR fragment(s) was verified using Sanger sequencing.

The level 1 reactions followed a similar procedure to the level 0 reactions, with the exception of using different vectors (Table S4) and the restriction enzyme BsaI. The correctness of the assembly was evaluated through a restriction reaction. Subsequently, various combinations of level 1 vectors were cloned into distinct level 2 vectors (Table S5) using a Golden Gate reaction, which was similar to the reactions performed for level 0 and level 1, employing the restriction enzyme BbsI. However, in this particular reaction, instead of 3 cycles, 12 cycles were conducted, consisting of 10 minutes at 37°C followed by 10 minutes at 22°C. The final construct was confirmed by a restriction reaction.

Preparation of protoplasts for transient expression assays

Transient expression assays in protoplasts were conducted using a custom protocol based on protocols by Yoo *et al.* (2007) and Mathur and Koncz (1998). Rosettes of 3-to-4-wk-old Arabidopsis plants grown on plate (see 'Plant material and growth conditions') were cut off from their roots using a razor blade and immediately submerged in 12.5 ml of protoplasting enzyme solution consisting of Cellulase R10 (1.5% (w/v); Duchefa Biochemie, Haarlem, the Netherlands), 0.4% (w/v) Macerozyme R10 (Duchefa Biochemie), 0.4 M Mannitol, 20 mM KCl, 20 mM MES (pH=5.7), 10 mM CaCl₂ and 0.1% BSA in a 60-mm Petri dish. The enzyme solution was prepared by heating everything except CaCl₂ and BSA to 55°C for 10 min and adding the last two components after cooling the solution to room

temperature. After the rosettes were submerged, they were cut further into fine strips (± 1 mm) using a razor blade. Next, they were put under vacuum for 2x 5 min using the Savant DNA 110 SpeedVac Concentrator with drying rate set to 'low'. The suspension was briefly swirled in between. From this point onward the protoplast suspension was handled with extreme care, avoiding excessive movement. After the vacuum infiltration, the plate was wrapped in aluminum foil and incubated at 28°C for 3.5 h, with gentle swirling every 30 min. Subsequently, the protoplast suspension was gently pipetted through a 70- μ m filter into a 50-ml tube (Greiner Bio-One). The tube and filter were previously prepared by pipetting 5 ml of W5 solution (0.2 mM MES (pH=5.7), 154 mM NaCl, 125 mM CaCl₂, and 5 mM KCl) through the filter into the tube. After filtering the protoplast suspension, another 5 ml of W5 was added to the plate, the plate was gently swirled and the suspension was pipetted through the filter into the tube. Next, the tube was centrifuged at 200 *g* for 2 min in the swing out Multifuge X3R Refrigerated Centrifuge (Thermo Fischer Scientific). Acceleration was set at 5 (out of 9) and brake at 3 to minimize mechanical stress. The supernatant was removed, and the protoplasts were resuspended in 10 ml of W5 and incubated on ice for 30 min. The suspension was centrifuged at the same settings and in case the supernatant was not clear, the addition of W5, incubation on ice and centrifugation was repeated. After removal of clear supernatant the protoplasts were resuspended in 5 ml of MMG solution (4 mM MES (pH=5.7), 0.4 M Mannitol, 15 mM MgCl₂). The protoplast density was determined in a hemocytometer, and after centrifuging at the same settings and removing the supernatant the protoplasts were resuspended in MMG to a density of 1×10^6 cells/ml, after which they were immediately transfected.

Transfection of protoplasts with a plasmid

Protoplast transfection was done in 12-well cell culture plates with relatively high hydrophobicity (Greiner Bio-One, Item No. 665102). Per transfection a protoplast suspension droplet of 100 μ l was pipetted in the middle of each well and 110 μ l of PEG solution (40% (w/v) PEG4000 (Fluka; Sigma-Aldrich, St. Louis, MO, USA), 100 mM CaCl₂, 200 mM mannitol) was added around the edge of the well, avoiding mixing with the protoplasts. Approximately 20 μ g of plasmid DNA (concentration range 4-12 μ g/ μ l) was added to the protoplast suspension in the well and gently mixed while pipetting. After 5 min of incubation, the plate was swirled, allowing mixing between the PEG solution and the protoplast suspension. After 10 min of incubation in a tilted position, 440 μ l of W5 was added to stop transfection and the content of each well was transferred to a 2-ml tube (Greiner Bio-One). The tubes were centrifuged for 2 min at 1000 *g* at the 'soft' setting in the fixed-rotor 5424 R centrifuge (Eppendorf, Hamburg, Germany). After careful removal of the supernatant, the protoplasts were resuspended in 700 μ l of WI solution (4 mM MES (pH=5.7), 20 mM KCl, 0.5 M Mannitol) and immediately transferred to 6-well

cell culture plates (Greiner Bio-One) that already contained 500 μ l of WI solution. The plates were incubated at 21°C in the dark for approximately 20 h.

Before harvesting, transfection efficiency was estimated under the microscope based on EYFP fluorescence in transfected protoplasts. When the efficiency was at least 20% the protoplasts were harvested. Experiments where multiple samples had less than 20% transfection efficiency were discarded. For harvesting, the protoplast suspension was transferred to 2-ml tubes and centrifuged at maximum speed for approximately 10 s in the 5424 R centrifuge at the 'soft' setting. Supernatant was removed and the tubes with the protoplast pellet were snap-frozen in liquid nitrogen and then stored at -80°C until further processing.

Measuring transient expression in transfected protoplasts

For GUS, LucR and LucF measurements the protoplast pellet was resuspended in 50 μ l of lysis buffer (2.5 mM Tris-phosphate (pH=7.8), 1 mM DTT (1,4-dithiothreitol), 2 mM DACTAA (*trans*-1,2-diaminocyclohexane-N,N,N',N'-tetraacetic acid), 10% (v/v) glycerol, 1% (v/v) Triton X-100). Protoplasts were ruptured by vortexing for 2 s, briefly spinning in a tabletop centrifuge at 2000 *g*, and vortexing again for 1 s, after which the suspension was incubated on ice for 30 min. After warming up to room temperature the suspension was centrifuged at 1000 *g* for 2 min in the 5424 R centrifuge.

For the GUS assay, 10 μ l of supernatant of the centrifuged protoplast lysate (from one well of transfected protoplasts per biological replicate) was mixed with 100 μ l of freshly prepared MUG substrate (10 mM Tris-HCl (pH=8.0), 2 mM MgCl₂, 1 mM 4-MUG (4-Methylumbelliferyl- β -D-glucuronide)) and incubated at room temperature for 90 min. Next, 990 μ l of 0.2 M Na₂CO₃ was added and mixed by pipetting up and down three times to stop the reaction. The solution was then divided into 5x 200 μ l in a clear F-bottom 96-well plate (Greiner Bio-One), serving as five technical replicates. Fluorescence of the solution was then determined on the Synergy™ HTX Multi-Mode Microplate Reader (Agilent, Santa Clara, CA, USA), with excitation at 360 nm and emission at 460 nm. Measurements were done three times to minimize technical variation. Therefore, the GUS measurement for one sample was the mean of three measurements of five wells.

For the LucF and LucR measurements the remaining lysate (from one well of transfected protoplasts per biological replicate, corresponding to the GUS measurements) was divided into 3x 10 μ l in non-transparent, white F-bottom 96-well plates (Greiner Bio-One). Luciferase measurements were done on the Promega™ GloMax® Plate Reader. For experiments where only LucF was measured the Luciferase Assay System kit (Promega, Madison, WI, USA) was used, and for dual luciferase measurements the Dual-Luciferase® Reporter Assay System kit (Promega) was used. First, the luciferin (single luciferase) or the LARII and Stop&Glo solutions (dual luciferase) were prepared from the kits according

to the manufacturer's instructions. Next, one (single luciferase) or two (dual luciferase) injectors of the machine were primed with the appropriate solutions, after which LucF or LucF and LucR measurements were done per well with delay set at 2 s and integration time at 10 s. The measurements consisted of injection of 25 μ l of luciferin followed by measurement of LucF (single luciferase), or sequential injection of 50 μ l of the LARII solution followed by measurement of LucF, and then injection of 50 μ l of the Stop&Glo solution followed by measurement of LucR (dual luciferase). The measurement of one sample for both LucF and LucR was the mean of the measurements of three wells in which the lysate of one sample was divided.

ACKNOWLEDGEMENTS

We thank Vince Deosarran for performing pilot experiments with the nuclear localized *npr1* mutant lines and *npr1* cysteine mutant lines. We thank Marcel Van Verk and Richard Hickman for their help in execution and analysis of the RNA-seq experiment. We are grateful for the work of Folkert Sanders, Ellinor Keepers and Raquel Ledo Doval in optimizing our protoplast transfection and GUS and LucF measurement protocols. We are grateful to Xinnian Dong for sharing the NPR1-HBD, *npr1-nls*, C82A and C216A seeds. This work was supported by ERC Advanced Grant no. 269072 of the European Research Council (to CMJP), the Netherlands Organization for Scientific Research (ALWGS.2016.005 to NA and VID1 11281 to SCMWW).

SUPPLEMENTARY MATERIAL

Supplementary figures

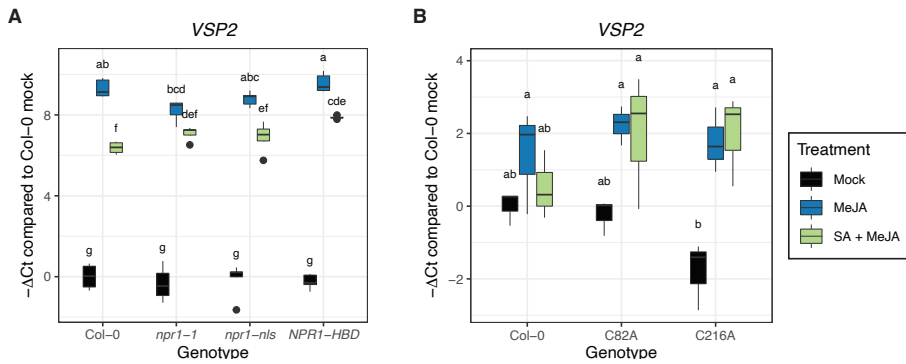


Figure S1: effect of mutations in NPR1 on SA/JA crosstalk.

qRT-PCR analysis of *VSP2* expression in (A) 12-day-old or (B) 5-week-old plants treated with water (Mock), 0.1 mM MeJA or 1 mM SA and 0.1 mM MeJA, and harvested at (A) 48 h or (B) 5 h after treatment. The ΔCt values per gene/sample were determined relative to *AT1G13320*. The plot shows $-\Delta\text{Ct}$ values that are normalized so that the mean $-\Delta\text{Ct}$ value of mock-treated Col-0 is 0. Letters indicate significance levels according to a Tukey HSD test ($n=5$ (A) or $n=3$ (B)). Experiments were repeated with similar results (not shown).

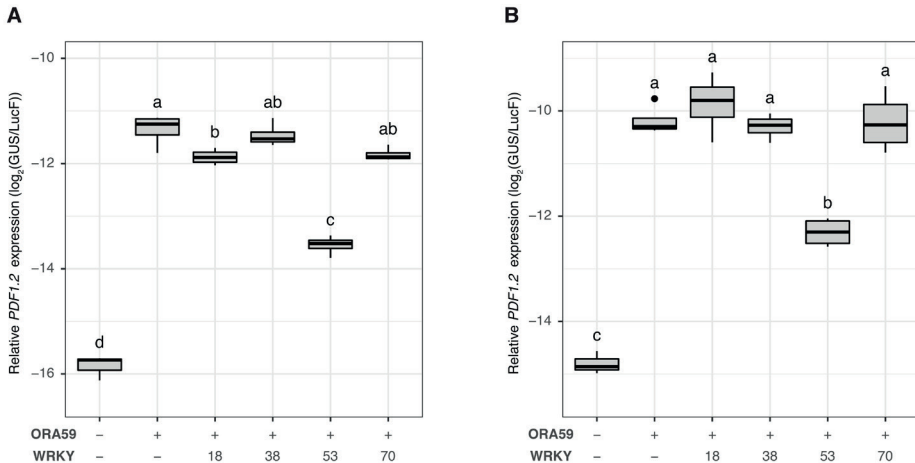


Figure S2: Suppression of ORA59-induced *PDF1.2* expression by four candidate WRKY TFs in Arabidopsis protoplasts.

Panels A and B are two repeats of the same experiment. The third repeat is included as Figure 4. For more information, see the legend of Figure 4.

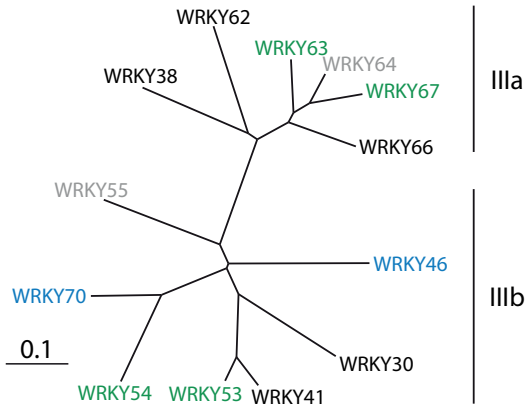


Figure S3: Phylogenetic analysis of the WRKY group III.

Figure was adapted from Kalde *et al.* (2003). Phylogeny is based on the WRKY domain of each TF. The diagram shows an unrooted tree constructed by Kalde *et al.* (2003) using TREEVIEW (Page, 1996). All WRKY TFs shown were tested for suppression of ORA59-induced *PDF1.2* expression in our protoplast expression assays, except WRKY55 and WRKY64 (indicated in gray), which we were unable to clone. WRKY TFs that were consistently found to suppress ORA59-induced *PDF1.2* expression in our experiments are indicated in green (note that for WRKY70 the results were variable between experiments (Figures 4, 5, S2)). WRKY TFs that have been linked to SA/JA crosstalk in other papers, but were not (consistently) found to suppress ORA59-induced *PDF1.2* expression in our setup are indicated in blue. WRKY50, which we found suppressed ORA59-induced *PDF1.2* expression, is not included here because it does not belong to group III.

Supplementary tables

Table S1: Genes differentially expressed between SA + MeJA-treated Col-0 and SA + MeJA-treated *npr1-1* plants (sheet 'Col-0' vs. *npr1-1*), and SA + MeJA-treated Col-0 and SA + MeJA-treated C82A plants (sheet 'Col-0 vs. C82A').

Available upon request.

Table S2: List of all primers used for qRT-PCR in this study.

Name	Sequence (5'→ 3')
AT1G13320_fw	TAACGTGGCCAAAATGATGC
AT1G13320_rv	GTTCTCCACAACCGCTTGGT
PR1_fw	CTCGGAGCTACGCAGAACAAC
PR1_rv	TTCTCGCTAACCCACATGTTCA
PDF1.2_fw	TTTGCTGCTTTTCGACGCAC
PDF1.2_rv	CGCAAACCCCTGACCATG
VSP2_fw	ACGGAACAGAGAAGACCGAC
VSP2_rv	TCTTCCACAACCTCCAACGG

Table S3: primers used for amplification of level 0 plasmids and vector name after level 0 reaction.

The part of the primer designed to overlap with the DNA template is denoted in uppercase and any added nucleotides are denoted in lowercase (except in the EM primer, which does not match any piece of existing DNA). The four base pairs that form the overhang after the BbsI restriction reaction are denoted in blue. In cases where a nucleotide was altered in the overhang to take out an internal restriction site, this nucleotide is denoted in red. The restriction recognition site is denoted in green. The fragments were cloned into the plasmid denoted under 'New plasmid name' before the underscore using a Golden Gate reaction with BbsI. The 'New plasmid name' is the name used for the plasmid after cloning.

Name	Sequence	Fragment size (bp)	New plasmid name
PDF1.2_BbsI_fw	gactgaagacatggaagGCATGCAATCGCATCGCCGCATCGATATCC	1230	pICH41295_PDF1.2
PDF1.2_BbsI_rv	gactgaagacatcattGATGATTACTATTGTTTTCATATGATAGATGATG		
ORA59_BbsI_1_fw	gactgaagacataTGGAAATCAAACAACTTAAGTGAGAGTTTTTC	632	pAGM1287_ORA59 (no stop codon version)
ORA59_BbsI_1_rv	gactgaagacagAgCGAAGAAGATGAATAGGAGGAGGAG		
ORA59_BbsI_2_fw	gactgaagaccgTcCTCTTCTTTGTGTCGAAGAAGTAGAAAACAGAG	159	pICH41308_ORA59 (stop codon version)
ORA59_ns_BbsI_2_rv ¹	gactgaagacatgaaaccAGAAACATGATCTCATAAGCTCTCTAAGTATTC		
ORA59_stop_BbsI_2_rv ²	gactgaagacataaagcTCAAGAACATGATCTCATAAGCTCTCTAAGTATTC	160	
WRKY18_BbsI_1_fw	gactgaagacataTGGACGGTCTTCGTTTCTCGACATC	108	
WRKY18_BbsI_1_rv	gactgaagactaGAACCTCTCTTTCGGAAGTTTTGCGG		
WRKY18_BbsI_2_fw	gactgaagacatTtCAGTTTTGGCTTCTACTCACTTAAAGAGG	882	pICH41308_WRKY18
WRKY18_BbsI_2_rv	gactgaagacataaagcTCATGTTCTAGATTGCTCCATTAACTCCC		
WRKY30_BbsI_fw	gactgaagacataTGGAGAAGAACCATAGTAGTGGGA	941	pICH41308_WRKY30
WRKY30_BbsI_rv	gactgaagacataaagcCTAAGAATAAGAACCCACCAAAATCC		
WRKY38_BbsI_fw	gactgaagactaaATGGAAATGAACTCCCCACACGAAAAGG	870	pICH41308_WRKY38
WRKY38_BbsI_rv	gactgaagacataaagcTCAAAAGTAAACTGATCATAACGATCCACG		
WRKY41_BbsI_1_fw	gactgaagactaaATGAATGGAATGATGAAATGGGAGC	113	
WRKY41_BbsI_1_rv	gactgaagactaAtGACGAACCCCTGAAAGCTGC		
WRKY41_BbsI_2_fw	gactgaagactaTcCTCCATCGTTTTCAGCTTC		
WRKY41_BbsI_2_rv	gactgaagactaaagcTAAATCGAATTGGAAAAAAGTGG	887	pICH41308_WRKY41

Name	Sequence	Fragment size (bp)	New plasmid name
WRKY46_BbsI_1_fw	gactgaagacctaATGATGATGAGGAGAAACTTGTGAATCAACGAA	254	
WRKY46_BbsI_1_rv	gactgaagacctAACCTTTAGAAATCCTTCCATCGATCTCAAGGCT		
WRKY46_BbsI_2_fw	gactgaagaccaaGTTTCAAAAAAGAGGAAAGTATCGGA	310	pICH41308_WRKY46
WRKY46_BbsI_2_rv	gactgaagaccaaTTTCGGGGATGTGATGTTGTT		
WRKY46_BbsI_3_fw	gactgaagaccaaAAACGACGACGAACCTCTCTGTT	110	
WRKY46_BbsI_3_rv	gactgaagaccaaCCTCCGATTGCTCTGTAAACATG		
WRKY46_BbsI_4_fw	gactgaagaccaaGAGACATGAAACCCGACCAAGTC	328	
WRKY46_BbsI_4_rv	gactgaagaccaaagcCTACGACCAACCAACCAATCCTG		
WRKY50_BbsI_fw	gactgaagacataTGAATGATGCAGACACAAACTT	551	pICH41308_WRKY50
WRKY50_BbsI_rv	gactgaagactaaagcCTAGTTCACTAGAGTGATTGTGGAAACCCCTC		
WRKY51_BbsI_fw	gactgaagacataATGAATATCTCTCAAAAACCCCTAGCC	514	pICH41308_WRKY51
WRKY51_BbsI_rv	GactgaagactaaagcTTAAGATCGAAGAAGAGAGTGTGG		
WRKY53_BbsI_fw	gactgaagaccaaATCGAAGGAAAGATATGTTAAGTTGG	1004	pICH41308_WRKY53
WRKY53_BbsI_rv	gactgaagaccaaagcTTAATAATAAATCGACTCTGTAAAAAAC		
WRKY54_BbsI_1_fw	gactgaagacataATGGATTCCGAATAGTAACAACACAGC	161	
WRKY54_BbsI_1_rv	gactgaagacataTTCATCGATGTGTTACTGGTTAGA		
WRKY54_BbsI_2_fw	gactgaagacatGATACCCGCTTGTTCCTCCGG	352	pICH41308_WRKY54
WRKY54_BbsI_2_rv	gactgaagacatCCTCAGAACTTTAGCTTCCACGA		
WRKY54_BbsI_3_fw	gactgaagacatGAGACAGATATGCTTGGAGGAAAT	235	
WRKY54_BbsI_3_rv	gactgaagacatTTTCGCGTGCGTTGGT		
WRKY54_BbsI_4_fw	gactgaagacataAACCCGACCTTTTGTATCAAGA	412	
WRKY54_BbsI_4_rv	gactgaagacataaagcTCACATAGCCTTGTTCCTTCATAA		
WRKY55_BbsI_fw	gactgaagacataATGTACTCGTACAAAAAATAAGTTACCA	911	Unable to obtain a correct plasmid
WRKY55_BbsI_rv	gactgaagacataaagcCTAAGATGGTCTTCTTGGAAATATGAAATCCATGTTGGTTTC		

Name	Sequence	Fragment size (bp)	New plasmid name
WRKY62_Bbsl_1_fw	gactgaagacataATGAACCTCTTGGCCAAACAAAGG	720	pICH41308_WRKY62
WRKY62_Bbsl_1_rv	gactgaagacatGtGACCAATCTTGTCTATCACCG		
WRKY62_Bbsl_2_fw	gactgaagacatTCaCCATCCAGTGGGTGTCG	120	
WRKY62_Bbsl_2_rv	gactgaagacataaagcTCATGATGATAAGTCGTGAGATG		
WRKY63_Bbsl_1_fw	gactgaagacataATGTTTTCAAAACATCGATCACAAGG	225	
WRKY63_Bbsl_1_rv	gactgaagacatAtGACTCATGTTGGTTGACG		
WRKY63_Bbsl_2_fw	gactgaagacatTCaTCTTCGAGACATGGCAGG	553	pICH41308_WRKY63
WRKY63_Bbsl_2_rv	gactgaagacatCGATGAAATAGAGGAAATTCATTCCC		
WRKY63_ann_3_fw ³	ATCG GA ₉ GACCTGATGTTTTTGA	29	
WRKY63_ann_3_rv ³	aagc TCAAAACACATCAGGTcTC		
WRKY64_Bbsl_1_fw	gactgaagacataATGTTCTCCAACATCGATCAAA	200	
WRKY64_Bbsl_1_rv	gactgaagacatTAGGCGGGTCCACAAAAG		
WRKY64_ann_2_fw ³	CCTAGcTTCTACCACACAATGAGTcaTC	33	Unable to obtain a correct plasmid
WRKY64_ann_2_rv ³	AAGAGA ₉ GACTCATTGTGGTAGAAGc		
WRKY64_Bbsl_3_fw	gactgaagacatTCTTCAAAAACATGACAAGTCATGTTCC	536	
WRKY64_Bbsl_3_rv	gactgaagacatCtCCGATGAAAATGGAGAAATTG		
WRKY64_ann_4_fw ³	GA ₉ GACATTATGTTTTTGACAATATTGCTAATCTTGATTAG	46	
WRKY64_ann_4_rv ³	aagcTAATCAAGATTAGCAATATTGTCAAAAACATAATGT		
WRKY66_Bbsl_1_fw	gactgaagacataATGTCCTTTGAGATTGATGCGAAG	195	pICH41308_WRKY66
WRKY66_Bbsl_1_rv	gactgaagacatAtGACAGAGCAAAACGAGAAAGAATC		
WRKY66_Bbsl_2_fw	gactgaagacatTCaTCTCAGAACATACCACGTCATG	540	
WRKY66_Bbsl_2_rv	gactgaagacataaagcTTAAGATTTAATGTTCAATCTGGAAAG		
WRKY67_Bbsl_fw	gactgaagacataATGTTTTCCAACATTTGATCACAAG	794	pICH41308_WRKY67
WRKY67_Bbsl_rv	gactgaagacataaagcCTAATCAAAAAGCAGAAATGTTTTCCAAG		

Name	Sequence	Fragment size (bp)	New plasmid name
WRKY70_BbsI_1_fw	gactgaagacata ATG GATACTAATAAAGCAAAAAAGCTTAAAGTTATGAACC	268	pICH41308_WRKY70
WRKY70_BbsI_1_rv	gactgaagacta C TTCCTTCATTGAGGTAGATAAACTAGGAC		
WRKY70_BbsI_2_fw	gactgaagaccga GAG ACAATCCTCATCGTCATCATGGTTCGTC	732	
WRKY70_BbsI_2_rv	gactgaagacata aaagc TCAAGATAGATTCGAACATGAACCTGAAGATAGAG		
LucR_BbsI_1_fw	gatcgaagacatt tcg ATGGCTTCGAAAAGTTTATGATCC	879	pAGM1301_LucR
LucR_BbsI_1_rv	gatcgaagacat A GACCTTTTACTTTTGACAAATTCAGTATTAGG		
LucR_BbsI_2_fw	gatcgaagacat TCTa CAITTTTGGCAAGAAAGATGC	125	
LucR_BbsI_2_rv	gatcgaagacata aaagc CTAGATAGATCTTTGTTTCATTTTGGAGAA		
EM_ann_fw ³	AATG TGATCGAGAATTCGAGCTCGAGCTCGGTAC	34	pICH41308_EM
EM_ann_rv ³	AAGG TACCGAGCTCGAGCTCGAATTTCTCGATCA		

¹This primer does not include the stop codon.

²This primer includes the stop codon.

³This primer was used for an annealing-based protocol rather than PCR.

Table S4: DNA components for assembly of level 1 plasmids for transient protoplast assays.

Components were assembled using Golden Gate cloning with BsaI. Plasmids were derived from level 0 reactions (Table S3) or the MoClo plant parts toolkit (Weber *et al.*, 2011, Werner *et al.*, 2012). Name codes represent level, intended position in the level 2 vector and a unique number, all separated by dots. NB: the unique number does not always start with 1 because the plasmids were part of a series of experiments with different plasmids.

Description	Backbone vector	Promoter + 5'UTR	CDS	3' tag	3' UTR + terminator	New vector name
<i>PDF1.2_{pro}:GUS</i>	pICH47732	pICH41295_ PDF1.2	pICH75111	-	pICH41414	1.1.2
<i>35S_{pro}:LucF</i>	pICH47742	pICH51277	pICSL80001	-	pICH41414	1.2.2
<i>35S_{pro}:ORA59</i>	pICH47751	pICH51277	pICH41308_ORA59	-	pICH41414	1.3.1
<i>Empty module position 3</i>	pICH47751	pICH51277	pICH41308_EM	-	pICH41414	1.3.2
<i>35S_{pro}:ORA59-LucR</i>	pICH47751	pICH51277	pAGM1287_ORA59	pAGM1301_ LucR	pICH41414	1.3.3
<i>35S_{pro}:WRKY_{xx}¹</i>	pICH47751	pICH51277	pICH41308_WRKY _{xx} ¹	-	pICH41414	1.4.x ¹
<i>Empty module position 4</i>	pICH47751	pICH51277	pICH41308_EM	-	pICH41414	1.4.5
<i>35S_{pro}:EYFP</i>	pICH47772	pICH51277	pICSL80014	-	pICH41414	1.5.1

¹xx refers to a unique WRKY TF number.

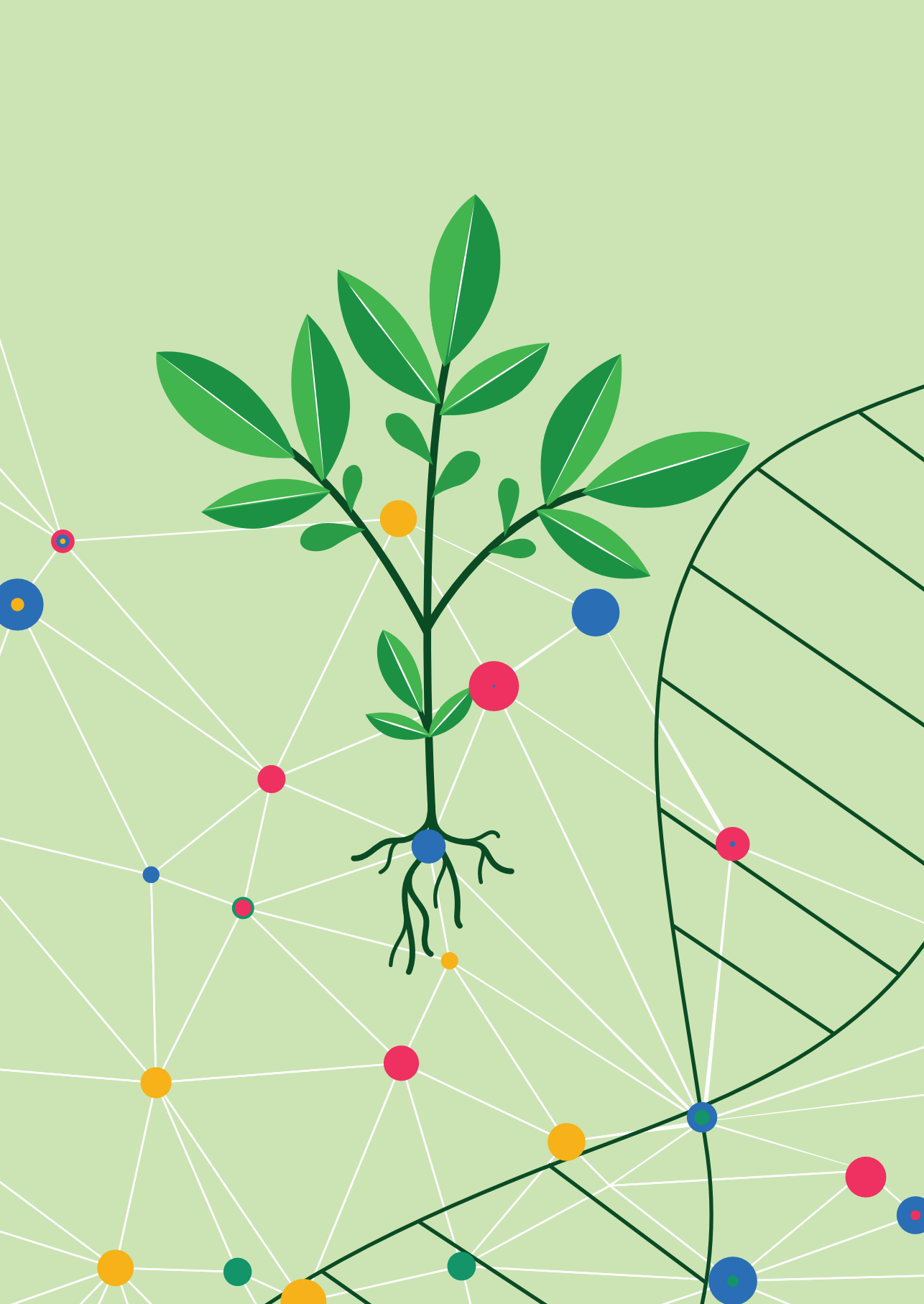
²x refers to a unique number for each WRKY TF level 1 construct (except 5 which refers to the construct with an empty module instead of a WRKY TF).

Table S5: DNA components for assembly of level 2 plasmids for a transient protoplast assay.

Plasmids were derived from level 1 reactions (Table S4) or the MoClo plant parts toolkit (Weber *et al.*, 2011, Werner *et al.*, 2012). All constructs had pAGM4673 as acceptor vector and used end-linker 5 to link the fragment of position 5 to the backbone vector.

Construct description	Position 1	Position 2	Position 3	Position 4	Position 5
Control plasmid for <i>PDF1.2</i> induction	1.1.2	1.2.2	1.3.2	1.4.5	1.5.1
Control plasmid for WRKY repression	1.1.2	1.2.2	1.3.1	1.4.5	1.5.1
Plasmid including WRKY TF	1.1.2	1.2.2	1.3.1	1.4.x ¹	1.5.1
Readout plasmid for ORA59 degradation (transfected together with level 1 WRKY-containing plasmid)	1.1.2	1.2.2	1.3.3	pICH54044	1.5.1
Plasmid for ORA59 degradation including WRKY TF	1.1.2	1.2.2	1.3.3	1.4.x ¹	1.5.1

¹x refers to any number of a construct that contains a WRKY TF.





CHAPTER 5

Transcriptional regulation of plant innate immunity

Niels Aerts^{1*}, Himanshu Chhillar^{2*}, Pingtao Ding², Saskia C.M. Van Wees¹

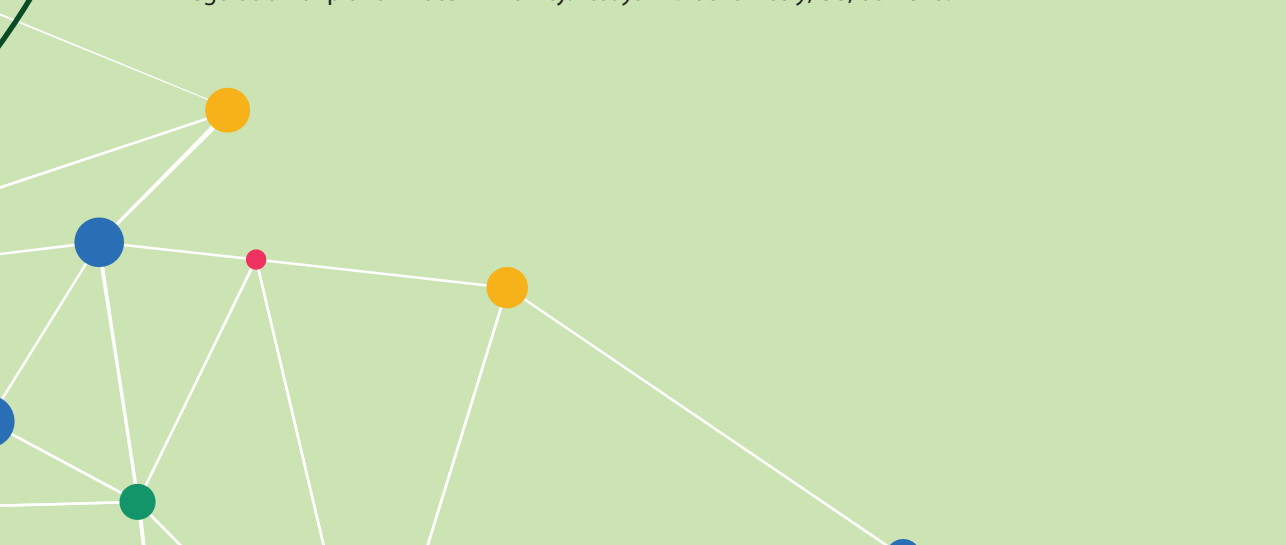
¹Plant-Microbe Interactions, Department of Biology, Utrecht University, P.O. Box 800.56, 3508 TB Utrecht, The Netherlands

²Institute of Biology Leiden, Leiden University, 2333 BE Leiden, The Netherlands

*These authors have equal contributions to this article.

Adapted from:

Aerts, N., Chhillar, H., Ding, P. and Van Wees, Saskia C.M. (2022) Transcriptional regulation of plant innate immunity. *Essays in Biochemistry*, **66**, 607-620.



ABSTRACT

Transcriptional reprogramming is an integral part of plant immunity. Tight regulation of the immune transcriptome is essential for a proper response of plants to different types of pathogens. Consequently, transcriptional regulators are proven targets of pathogens to enhance their virulence. The plant immune transcriptome is regulated by many different, interconnected mechanisms that can determine the rate at which genes are transcribed. These include intracellular calcium signaling, modulation of the redox state, post-translational modifications of transcriptional regulators, histone modifications, DNA methylation, modulation of the Mediator complex and RNA polymerases, and regulation by non-coding RNAs. In addition, on their journey from transcription to translation, mRNAs are further modulated through mechanisms such as RNA retention, storage of mRNA in stress granules and P-bodies, and post-transcriptional gene silencing. In this review, we highlight the latest insights into these mechanisms in the context of plant immunity. Furthermore, we discuss some emerging technologies that promise to greatly enhance our understanding of the regulation of the plant immune transcriptome in the future.

INTRODUCTION

Plant diseases caused by different pathogens pose a major threat to crop productivity. However, plants do respond to pathogens by activating their robust yet specialized innate immune system. General pathogen-associated molecular patterns (PAMPs) and specific apoplastic pathogen effectors are perceived by the plants' surface-localized pattern-recognition receptors (PRRs), leading to activation or prevention of pattern-triggered immunity (PTI), respectively. In addition, specific pathogen effector molecules that are secreted into plant cells are recognized by intracellular nucleotide-binding leucine-rich repeat receptors (NLRs), activating effector-triggered immunity (ETI) (Ngou *et al.*, 2022). Depending on the pathogen, a mix of PTI, ETI and other immune responses are induced, which are largely mediated by differential accumulation of phytohormones like salicylic acid (SA), jasmonic acid (JA), abscisic acid (ABA), and ethylene (ET) (Bürger and Chory, 2019). The different hormones act together in synergistic, antagonistic and additive manners, a phenomenon known as crosstalk (Aerts *et al.*, 2021). Diverse regulators, interacting with each other in gene regulatory networks (GRNs), orchestrate the transcriptional reprogramming that results from pathogen recognition. In this review, we refer to all the different immune-related transcriptional reprogramming as the plant immune transcriptome. Mechanistically, the plant immune transcriptome is determined by the coherent control of multiple transcriptional regulatory machineries including transcription factors (TFs), Mediator, co-regulators, DNA and RNA modifiers, chromatin remodelers, etc. (Garner *et al.*, 2016, Li *et al.*, 2016). These molecular components can be directly or indirectly post-transcriptionally modified by kinases/proteases, SUMO/ubiquitin, and second messengers like reactive oxygen species (ROS) and calcium ions (Ca²⁺) (Tsuda and Somssich, 2015, Andersen *et al.*, 2018). The plant immune network is robust enough to resist a pathogen as long as the recognition and immune activation are timely, despite some of the transcriptional machineries being hijacked by the pathogen (Ngou *et al.*, 2022). Here, we briefly summarize the transcriptional plant targets of pathogen virulence factors, which facilitate our understanding of the plant immune transcriptome. We highlight how multi-scale regulations of transcription and mRNA modulation are accomplished by different proteinaceous components, which determine induction of different sectors in the immune gene regulatory network. Moreover, we highlight the future multi-omics directions to achieve a systems level comprehension of regulation of the plant immune transcriptome.

THE PLANT IMMUNE TRANSCRIPTOME IS TARGETED BY PATHOGENS

The timing and efficiency of elicitation of the immune transcriptome is essential for plants to halt pathogens. Of all the cellular components that are involved in transcriptional reprogramming, the role of transcription factors (TFs) in regulating crucial defense responses is best studied. Mutations in TFs including WRKYs, TGAs, NACs, CBP60s/SARD1, ERFs, bZIPs, bHLHs, MYBs, CAMTAs, and TCPs alter plant disease resistance against different pathogens (Zhang *et al.*, 2010, Fernández-Calvo *et al.*, 2011, Li, 2015, Tsuda and Somssich, 2015, Akio Amorim *et al.*, 2017, Yuan *et al.*, 2019, Kim *et al.*, 2020). Some of these plant TFs are popular targets of pathogens to arrest induced immune responses in plants (reviewed by Ding and Redkar, 2018, Han and Kahmann, 2019, Wang *et al.*, 2022a), underpinning their importance for defense. We refer to Table 1 for a summary of effector molecules of different pathogens that target transcriptional regulators, like TFs, transcriptional (co-)activators or repressors, or Mediator subunits. Many of these effectors modulate SA signaling (Chen *et al.*, 2017, Li *et al.*, 2019a), JA signaling (Plett *et al.*, 2014) or SA-JA crosstalk (Caillaud *et al.*, 2013, Jiang *et al.*, 2013, Gimenez-Ibanez *et al.*, 2014, Raffener *et al.*, 2022), leading to enhanced susceptibility to the biotrophic or necrotrophic pathogen at hand.

Another well studied example of direct interference with plant immune transcription is that of transcription activator-like effectors (TALEs), which are deployed by many plant-pathogenic xanthomonads. TALEs bind to effector binding elements (EBEs) in the promoters of host susceptibility (*S*) genes that contribute to disease (Boch *et al.*, 2014, Wang *et al.*, 2017). Recently, TALEs Tal2b and Tal2c from *Xanthomonas oryzae* pv. *oryzicola* (*Xoc*) were shown to activate expression of *OsF3H03g*, encoding a 2-oxoglutarate-dependent dioxygenase that negatively regulates SA-related defense and promotes susceptibility against *Xoc* in *Oryza sativa* (Wu *et al.*, 2021b). Moreover, several TALEs from *Xanthomonas* spp. induce SWEET sugar transporter genes, resulting in an increased availability of sugar for the pathogen, thereby promoting pathogenesis (Doyle *et al.*, 2013, Cox *et al.*, 2017).

Table 1. Pathogen effectors and their host targets that are involved in transcriptional regulation during plant immunity.

This table summarizes some well-studied effectors secreted by different pathogens that hijack diverse transcriptional regulators of the host plant, including transcription factors, and transcriptional (co-) activators and repressors, to facilitate infection.

Pathogen	Pathogen effector	Function of host target	Name of host target	Host species	References
<i>Ralstonia solanacearum</i>	RipAB	Transcription factor	TGAs	<i>Arabidopsis thaliana</i>	(Qi <i>et al.</i> , 2022)
<i>Xanthomonas campestris</i> pv <i>vesicatoria</i>	XopD	Transcription factor	MYB30	<i>Arabidopsis thaliana</i>	(Canonne <i>et al.</i> , 2011)
<i>Xanthomonas campestris</i> pv <i>vesicatoria</i>	XopS	Transcription factor	WRKY40	<i>Capsicum annuum</i>	(Raffeiner <i>et al.</i> , 2022)
<i>Ralstonia solanacearum</i>	PopP2	Transcription factor	WRKY	<i>Arabidopsis thaliana</i>	(Roux <i>et al.</i> , 2011)
<i>Pseudomonas syringae</i>	AvrRps4	Transcription factor	WRKY	<i>Arabidopsis thaliana</i>	(Sarris <i>et al.</i> , 2015)
<i>Verticillium dahliae</i>	VdSCP41	Transcription factor	CBP60g, SARD1	<i>Arabidopsis thaliana</i>	(Qin <i>et al.</i> , 2018)
<i>Pseudomonas syringae</i>	HopBB1	Transcription factor	TCP14	<i>Arabidopsis thaliana</i>	(Yang <i>et al.</i> , 2017a)
Phytoplasma	Phyllogen	Transcription factor	MADS-box	<i>Arabidopsis thaliana</i> , <i>Oryza sativa</i>	(Kitazawa <i>et al.</i> , 2022)
<i>Hyaloperonospora arabidopsidis</i>	HaRxL44	Mediator complex	MED19a	<i>Arabidopsis thaliana</i>	(Caillaud <i>et al.</i> , 2013)
<i>Hyaloperonospora arabidopsidis</i>	HaRxL21	Transcriptional Co-repressor	TPL	<i>Arabidopsis thaliana</i>	(Harvey <i>et al.</i> , 2020)
<i>Pseudomonas syringae</i>	HopZ1, HopX1	Transcriptional repressor	JAZ	<i>Arabidopsis thaliana</i>	(Jiang <i>et al.</i> , 2013, Gimenez-Ibanez <i>et al.</i> , 2014)
<i>Laccaria bicolor</i>	MiSSP7	Transcriptional repressor	JAZ	<i>Populus trichocarpa</i>	(Plett <i>et al.</i> , 2014)
<i>Pseudomonas syringae</i>	AvrPtoB	Transcriptional Co-activator	NPR1	<i>Arabidopsis thaliana</i>	(Chen <i>et al.</i> , 2017)
<i>Phytophthora capsici</i>	RxLR48	Transcriptional Co-activator	NPR1	<i>Arabidopsis thaliana</i>	(Li <i>et al.</i> , 2019a)

REGULATION OF THE PLANT IMMUNE TRANSCRIPTOME OCCURS AT MULTIPLE SCALES

The plant immune transcriptome encompasses both activation and repression of genes with diverse molecular functions, ranging from the control of general metabolic processes

to highly specific responses that are directed towards a particular organism (Windram *et al.*, 2012, Lewis *et al.*, 2015, Hickman *et al.*, 2017, Hickman *et al.*, 2019, Zander *et al.*, 2020, Bjornson *et al.*, 2021, Maier *et al.*, 2021, Tang *et al.*, 2021, Winkelmüller *et al.*, 2021). The relatively early response to attackers is usually a ‘general stress response’ (GSR) to danger, which is similarly activated after both biotic and abiotic stresses (Walley *et al.*, 2007, Benn *et al.*, 2014, Bjornson *et al.*, 2021, Maier *et al.*, 2021), and was demonstrated to be important for defense against *P. syringae* pv. *tomato* DC3000 (*Pto*) (Bjornson *et al.*, 2021, Maier *et al.*, 2021). Furthermore, for both pathogenic and non-pathogenic bacteria, it was found that the strength of this early response is correlated positively with the number of differentially expressed genes, although it is not clear whether this is based on a causal relationship (Maier *et al.*, 2021). The later responses are more specific, depending on the eliciting organism or its derived molecular patterns, and show a high degree of plasticity, which ensures a tailored response to the perceived signal. The transcriptional changes result from multi-scale regulations, including post-translational modifications of TFs, association of TFs with co-regulators and their target DNA sequences, regulation of stability and turnover of TFs, chromatin remodeling, DNA methylation, association of TFs with the Mediator complex, regulation of the RNA polymerases, and post-transcriptional regulation of mRNAs (Figure 1). Below, we highlight some of these mechanisms. We also recommend the recently published focused reviews on TFs functioning in different molecular contexts (Strader *et al.*, 2022) and epigenetics in plant immunity (Hannan Parker *et al.*, 2022).

Transcription-related physiological homeostasis

A rapid influx of calcium and a change in redox status are vital parts of the plant immune response and they play intertwined roles in PTI and ETI (Xu *et al.*, 2022). Calcium influx is induced immediately upon perception of PAMPs and effectors, which has been coupled to classical calcium channels, but also to recently identified noncanonical calcium channels formed by NLR-based resistosomes (Bi *et al.*, 2021, Jacob *et al.*, 2021) (Figure 1A). Intracellularly, the calcium signal is decoded by calcium binding proteins like calmodulin (CaM) and Ca²⁺-dependent protein kinases (CDPKs). These can directly activate TFs, such as those of the defense-regulating CaM-binding TF family CAMTA, the CaM-binding protein CBP60g, and the WRKY TFs WRKY33, WRKY28 and WRKY48, which are phosphorylated by CPK5 and CPK6 (Figure 1E). This leads to altered defense-related transcription by these TFs, which influences resistance to diverse pathogens (Wang *et al.*, 2011, Gao and He, 2013, Kim *et al.*, 2013, Zhou *et al.*, 2020). Although in general positive effects of calcium signaling on immunity have been reported, this is not always the case. For example, the Ca²⁺-activated CAMTA3 (or AtSR1) TF represses expression of the SA regulator *NPR1* and the SA biosynthesis gene *ICS1* (Yuan *et al.*, 2021b). However, since *NPR1* is a negative regulator of HR (Rate and Greenberg, 2001, Yuan *et al.*, 2022), its repressed

expression by CAMTA3 positively affects ETI-mediated HR (Yuan *et al.*, 2021). Several other CaM-regulated and CaM-like proteins like CBP60a, CML46 and CML47 negatively impact SA-related gene expression and accordingly, mutant lines are enhanced resistant to virulent *P. syringae* (Lu *et al.*, 2018).

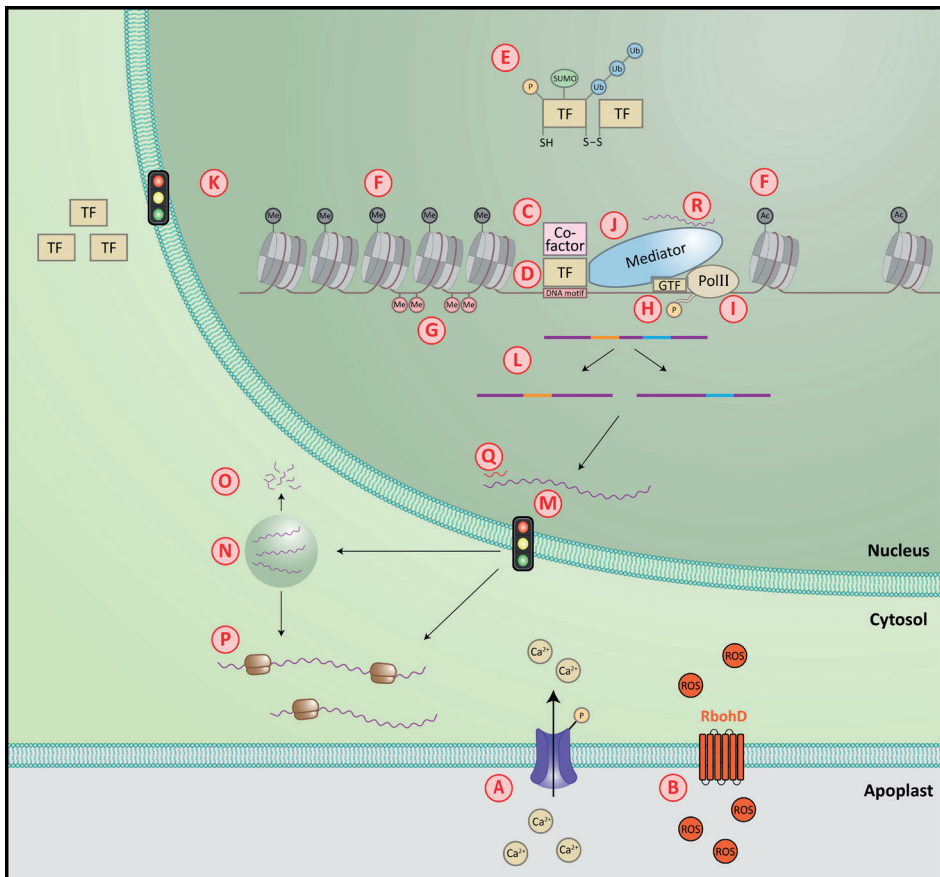


Figure 1: Mechanisms involved in the regulation of immune-related transcription.

(A) Regulation of calcium (Ca^{2+}) influx, which may lead to post-translational modifications of TFs (see also Figure 1E); (B) generation of ROS by RbohD, which may lead to post-translational modifications of TFs (see also Figure 1E); (C) co-factors that may contribute to regulation of transcription; (D) TFs regulate transcription by binding to a motif; (E) post-translational modifications of TFs, such as phosphorylation (P), sumoylation (SUMO), ubiquitination (Ub) and forming of oligomers through S-S bridges depending on the redox state; (F) modifications of histones (methylation (Me) or acetylation (Ac)) to regulate the chromatin state; (G) methylation of DNA; (H) Phosphorylation of the C-terminal domain of RNA-polymerase II (PolII) promotes transcription; (I) PolII may initiate transcription at alternative transcription start sites; (J) the Mediator complex forms the bridge between specific TFs, general TFs (GTF) and PolII; (K) selective import of TFs or other proteins; (L) alternative splicing; (M) selective retention of mRNAs in the nucleus; (N) temporary storage of mRNAs in stress granules or P-bodies; (O) degradation of mRNAs from P-bodies; (P) release of mRNAs from stress granules or P-bodies into the cytosol, followed by translation; (Q) post-transcriptional gene silencing by small RNAs. (R) Long non-coding RNAs can regulate transcription in different ways. Depicted here is modulation of MED19a by *ELENA1*.

The production and signaling of reactive oxygen species (ROS) is tightly connected to that of calcium, as these molecules can (in)directly regulate each other's cellular concentrations (Xu *et al.*, 2022). Both PTI and ETI trigger a burst of ROS, which is mainly caused by activation of the NADPH oxidase RbohD (Torres *et al.*, 2002) (Figure 1B). The changed redox state impacts many aspects of a plant's physiology, including transcription (Mittler, 2017). In plant immunity, NPR1 is the best-known converter of the redox state to transcriptional reprogramming. Under oxidizing conditions, NPR1 resides in the cytosol. According to the classical view it mostly forms oligomers in the cytosol that are held together by disulfide bridges formed between cysteine residues (Mou *et al.*, 2003), which break under more reduced redox conditions, such as occur during a prolonged defense response, resulting in monomeric NPR1 that relocates to the nucleus (Mou *et al.*, 2003) (Figure 1E, K). In the nucleus, NPR1 acts as a transcriptional co-activator together with TGA TFs to activate many genes involved in defense (Zhang *et al.*, 1999, Zhou *et al.*, 2000) (Figure 1C, D). The NPR1-TGA1 interaction itself is also affected by the redox status (Després *et al.*, 2003). Interestingly, recent research has challenged the classical literature on the multimerization of NPR1. The oligomeric form of NPR1 in the cytosol that was observed by Mou *et al.* (2003) was found to be likely formed *in vitro* only (Ishihama *et al.*, 2021). However, recently, the cryo-EM structure of NPR1 showed that its predominant functional form is a dimer, which forms oligomers in the quiescent state, but also can interact with two TGA3 dimers to form a TGA3₂-NPR1₂-TGA3₂ complex, and possibly also form complexes with other transcription regulators, to regulate the immune transcriptome (Kumar *et al.*, 2022).

Post-translational modifications of TFs

Post-translational regulation of TFs can alter their activities (Figure 1E). This is well-studied for the WRKY33 TF that promotes resistance to the necrotrophic pathogen *Botrytis cinerea* by regulating crucial defense-related responses such as camalexin production in *Arabidopsis thaliana* (hereafter: *Arabidopsis*) (Zheng *et al.*, 2006, Mao *et al.*, 2011). The WRKY33 protein is activated by phosphorylation through at least two pathways: one involves the calcium-dependent kinases CPK5 and CPK6 that phosphorylate the Thr-229 residue of WRKY33 (Zhou *et al.*, 2020), and the other one involves a MAPK cascade consisting of YDA (a MAPKKK), MKK4 and MKK5 (MAPKKs), and MPK3 and MPK6 (MPKs) that eventually phosphorylate five Ser residues in the N terminus of WRKY33 (Bergmann *et al.*, 2004, Lukowitz *et al.*, 2004, Meng *et al.*, 2012, Zhou *et al.*, 2020, Cai *et al.*, 2021). Moreover, SUMOylation of WRKY33 increases its interaction with MPK3 and MPK6, thereby further enhancing WRKY33 phosphorylation via this pathway (Verma *et al.*, 2021). The phosphorylation of WRKY33 by the calcium pathway increases its binding to DNA, whereas phosphorylation by the MAPK pathway increases its transactivation

activity (Yang *et al.*, 2020, Zhou *et al.*, 2020). Genetic studies implied that the same two phosphorylation pathways may also activate MYB51 to regulate indole glucosinolate biosynthesis, but it is not known whether these pathways also play distinct roles in MYB51 functioning (Yang *et al.*, 2020).

Phosphorylation has also been shown to be important for the transactivation activity and binding specificity to DNA motifs of the ERF TF ORA59, which is required for defense induction in *Arabidopsis* against *B. cinerea* (Pré *et al.*, 2008). The hormones JA and ET can induce phosphorylation of ORA59, which increases ORA59's binding specificity towards the canonical GCC box or a newly identified motif named ERELEE4, respectively, depending on the corresponding hormone stimulus (Yang *et al.*, 2021). This can explain partly that the ERELEE4 motif is enriched in genes that are induced by ET treatment in an ORA59-dependent manner, while JA treatment is associated with an ORA59-dependent induction of GCC-box containing genes (Yang *et al.*, 2021).

Ubiquitination also regulates TF activities via protein turnover. For instance, SA induces ORA59 ubiquitination and degradation via the 26S proteasome pathway (Van der Does *et al.*, 2013, He *et al.*, 2017). The transcriptional co-regulator NPR1 of SA-induced transcription, and the JAZ repressor proteins and MYC TFs that function in JA-induced transcription, are also regulated by phosphorylation-mediated proteasomal degradation via covalent addition of small ubiquitin proteins (Furniss and Spoel, 2015, Chico *et al.*, 2020, Ban and Estelle, 2021). Their turnover provides a mechanism to control timing of activation and repression of the plant immune transcriptome. Additionally, SA induces cytoplasmic condensates containing NPR1 and many stress proteins, including specific WRKY TFs and proteins involved in programmed cell death (PCD). NPR1 recruits ubiquitin ligases to these condensates, leading to ubiquitination and subsequent degradation of the proteins and enhanced cell survival during ETI (Zavaliev *et al.*, 2020).

Chromatin context

Chromatin context is a major determinant for transcriptional activities in all eukaryotic cells. The accessibility of chromatin can influence when and where TFs, other regulators, and RNA polymerases find their targets to activate transcription. The chromatin state can be altered through modification of histone tails and deposition of histone variants (Figure 1F). Recently, Ding *et al.* (2021) used the method Assay for Transposase-Accessible Chromatin followed by sequencing (ATAC-seq) to profile the genome-wide chromatin landscape of *Arabidopsis* after infection with an engineered non-pathogenic *Pseudomonas fluorescens* strain either expressing the effector AvrRps4 (thus causing both PTI and ETI) or a non-recognized effector mutant (thus causing PTI only), and this was compared with RNA-seq data. Over one third of all upregulated genes in both PTI and PTI+ETI also contained more open chromatin compared to the control. Moreover,

integration of RNA-seq, ATAC-seq and TF-DNA-binding motif information helped to decipher GRNs mediating PTI, ETI and 'PTI+ETI' (Ding *et al.*, 2021). In another study, Pardal *et al.* (2021) used Micrococcal Nuclease digestion followed by sequencing (MNase-seq) to investigate how treatment with the PAMP flg22 affects genome-wide nucleosome occupancy. They found that flg22 causes genome-wide repositioning of nucleosomes, partly coinciding with the promoters of differentially expressed genes. Repositioning of nucleosomes is mediated by chromatin ATPases (Han *et al.*, 2015). Notably, whereas some chromatin remodeling ATPases like PKR2 and RAD54 promote immunity, others, like EDA16 and SWP73A attenuate it (Huang *et al.*, 2021, Pardal *et al.*, 2021), indicating a complex relationship between chromatin remodeling and immunity. These studies suggest that chromatin remodeling is an important mechanism by which gene transcription is regulated during immune responses mediated by both cell-surface and intracellular receptors.

It is still unclear whether the accessibility of the regulatory DNA regions precedes transcription or vice versa. For example, it was found that WRKY33 enhances accessibility of genes to reinforce gene transcription. The chromatin remodeling complex SWR1 and the MAPK-WRKY33 module promote deposition of H2A.Z (Cai *et al.*, 2021), a variant of the canonical H2A histone subunit that can activate or repress transcription depending on the context (Hannan Parker *et al.*, 2022), and increased H3K4me3 (Cai *et al.*, 2021), a histone mark generally associated with active transcription (Zhang *et al.*, 2009). This happens around WRKY33 target genes, leading to more WRKY33-mediated H2A.Z deposition and H3K4me3 modification (Cai *et al.*, 2021).

Chromatin remodeling also plays a role during ETI-triggered PCD. During this process chromocenters (regions with heterochromatin) get less dense and different chromatin marks get redistributed, such as the repressive marks H3K9me2 and H3K27me3, leading to altered transcription (Dvořák Tomašíková *et al.*, 2021). Studies with chromatin remodeling mutants suggest that this remodeling mostly attenuates PCD, possibly to prevent it from happening too rapidly or at the wrong time (Dvořák Tomašíková *et al.*, 2021).

Chromatin remodeling can also lead to altered transcription via a non-canonical function of the gene-silencing-related component ARGONAUTE1 (AGO1). AGO1 binds to chromatin around specific genes, likely dependent on its association with specific small RNAs and through interaction with several subunits of the SWI/SNF chromatin-remodeling complex (Liu *et al.*, 2018). There, it promotes PolII occupancy around these genes. Notably, treatment with immune-related compounds such as JA, BTH (an SA analog) and flg22 caused AGO1 to bind to genes that are enriched in GO-terms related to the response to the corresponding ligand, suggesting that AGO1 contributes to these responses. In accordance, a mutation in *AGO1* results in reduced JA-induced gene expression (Liu *et al.*, 2018).

DNA methylation

DNA methylation is generally associated with suppression of activity of transposable elements and with transcriptional repression (Figure 1G). DNA methylation in plants can be regulated through RNA-directed DNA methylation (RdDM), which involves small RNAs derived from transcripts resulting from RNA polymerases PolII, PolIV and PolV activity (Erdmann and Picard, 2020). For examples of regulatory components in RdDM, which shape the immune transcriptome, see also 'Modulation of RNA polymerase' and 'The Mediator complex'.

Demethylation of DNA occurs either passively during replication or actively by different demethylases under specific conditions. The DNA methylome is altered upon pathogen attack, which modulates the immune response (Dowen *et al.*, 2012, Halter *et al.*, 2021). The demethylase ROS1 was found to reduce methylation of regulatory regions in or close to flg22-induced defense-related genes, facilitating binding of TFs and subsequent activation of plant immunity (Halter *et al.*, 2021).

Another example is the demethylase DEMETER (DME). Loss-of-function mutants of this enzyme are lethal, but recent studies using plant lines with a weak allele generated by CRISPR-CAS9 or silencing of *dme* revealed that DME alters methylation of hundreds of genomic regions and is affected in defense against bacterial and fungal pathogens (Zeng *et al.*, 2021). Moreover, results obtained with the mutant line in which *dme* was silenced in the background of a triple mutant of the DNA methylases *ros1*, *dml2* and *dml3* (*rdm*) suggest that DME acts redundantly with other demethylases to regulate expression of defense genes via demethylation (Schumann *et al.*, 2019).

In addition, the demethylation-deficient mutant *rdm* is impaired in resistance against *Pto* induced by the immune-stimulating molecular patterns flg22, elf18 and Pep2 (Huang *et al.*, 2022). The flg22 treatment induces hypomethylation of specific regions in the wild-type plant but not in the *rdm* mutant, which is associated with a higher number of differentially methylated promoter regions of defense-related genes and their higher expression level in wild type compared to mutant. Altogether, the studies discussed here show that DNA demethylation of specific regions is important for a proper immune transcriptome. It has not been explored how the four demethylases change their activity during an immune response, so the spatiotemporal relevance of each enzyme in the regulation of the immune transcriptome remains to be determined.

Modulation of RNA polymerase

During immune activation PolII is phosphorylated (Figure 1H). For example, flg22 induces phosphorylation of the C-terminal domain (CTD) of PolII by the two cyclin-dependent kinase Cs CDKC;1 and CDKC;2, which in turn are phosphorylated by flg22-triggered MPK3 and MPK6 (Li *et al.*, 2014). The phosphatase CTD PHOSPHATASE-LIKE3 (CPL3) can

dephosphorylate the CTD and thereby act as a negative regulator of plant immune transcription. Mutants in CDKC and CPL3 were found to be more susceptible to *Pto*, demonstrating the essential role of phosphorylation of the CTD of PolII in regulation of immunity against this pathogen (Li *et al.*, 2014). Another CPL, namely CPL1 of tomato, can reduce defenses against various but not all of the tested pathogens and insects (Thatcher *et al.*, 2018). Additionally, CPL1 negatively regulates defense-related transcription (Thatcher *et al.*, 2018). However, the effect of CPL1 on PolIII was not studied, and it even seems likely that other mechanisms are involved, since the Arabidopsis homologue of CPL1 has previously been associated with miRNA processing (Manavella *et al.*, 2012) and RdDM (Jeong *et al.*, 2013).

Alternative transcription initiation

Alternative transcription initiation can expand the regulatory repertoire of the genome, since it may involve alternative promoters that are differentially induced upon different stimuli, or result in different transcripts and proteins (Figure 1I). Recently, more than 15% of the 3374 transcripts that were induced by flg22 treatment after 30 min were found to be derived from alternative transcription events (Thieffry *et al.*, 2022). The alternative transcripts for example lacked upstream open reading frames (uORFs), which may affect translation efficiency of the transcript, or their encoded proteins lacked a predicted domain or signal peptide, which could potentially alter their function. These predictions were validated for a small set of transcripts, but the overall implications of alternative transcription initiation during PTI remain to be elucidated.

The Mediator complex

TFs recruit PolII through interactions with the multi-subunit Mediator complex (Zhai and Li, 2019) (Figure 1J). Recently, substantial molecular evidence has been provided for a role of the Mediator subunit MED25 in hormone crosstalk. The JA specific TF MYC2 was shown to interact at its same position with the SA regulator NPR1 as well as with MED25 (Nomoto *et al.*, 2021). Consequently, NPR1 reduces the recruitment of MED25 by MYC2 to target promoters of MYC2. This dampens the positive effect of MED25 on MYC2-induced transcription. Interestingly, in the absence of JA, JAZ proteins also repress MYC2-induced transcription in part by preventing the MYC2-MED25 interaction (Zhang *et al.*, 2015), but JAZs are degraded at high JA levels (Chini *et al.*, 2007, Thines *et al.*, 2007). NPR1 therefore mechanistically takes over (part of) the function of the degraded JAZ proteins at high JA and SA levels.

Although Mediator usually connects TFs to PolII, it can also recruit other RNA polymerases that are relevant for defense. The Mediator subunit MED18 interacts with

NUCLEAR RNA POLYMERASE D2a (NRPD2a), a subunit of PolIV and PolV (Zhang *et al.*, 2021). *MED18* and *NRPD2a* are highly expressed after *B. cinerea* infection, and mutants and overexpressors of these genes corroborate their importance for a part of *B. cinerea*-induced gene expression and for resistance against *B. cinerea* (Lai *et al.*, 2014, Zhang *et al.*, 2021). PolIV and PolV are involved in RdDM and other non-coding RNA-mediated gene silencing processes (Haag and Pikaard, 2011), suggesting that impairment of one of these processes may underly the altered gene expression and resistance of the *nripd2a* mutant and possibly also of the *med18* mutant. However, this still needs to be investigated.

Selective nuclear transport of transcriptional components

Nuclear im/export of transcriptional components is a selective mechanism to control the plant immune transcriptome (Figure 1K). This was already described for NPR1 in 'Transcription-related physiological homeostasis'. CONSTITUTIVE EXPRESSER OF PATHOGENESIS-RELATED GENES 5 (CPR5) is a component of the nuclear pore complex that regulates PCD during ETI (Wang *et al.*, 2014, Gu *et al.*, 2016). This protein has three modes of action. Firstly, the conformational change that CPR5 undergoes upon ETI alters the permeability of the nuclear pore and thereby allows influx of several stress-related cargos (such as NPR1 and ABI5) to the nucleus, resulting in massive transcriptional reprogramming (Gu *et al.*, 2016). Secondly, CPR5 is a negative regulator of PCD by binding to the cyclin-dependent kinase inhibitors SIAMESE (SIM) and SIAMESE-RELATED1 (SMR1). Upon ETI, CPR5 releases SIM and SMR1, which activate E2F TFs to induce PCD (Wang *et al.*, 2014). Finally, CPR5 regulates alternative splicing (AS; Figure 1L) via its RNA-binding activity (Peng *et al.*, 2022). Interestingly, the mRNA of the gene-silencing-related *AGO1* and several AS regulators are among its targets, suggesting that apart from its own role in AS, it also indirectly affects gene silencing and AS (Peng *et al.*, 2022). In addition, Exportin-4 (XPO4) mediates nuclear export of TOPLESS-RELATED1 (TPR1), counteracting the translocation of TPR1 into the nucleus during ETI in the presence of high SA levels, as was studied in the *cpr5* background (Xu *et al.*, 2021). This way, XPO4 prevents the repression of negative immune regulators by TPR1 in the nucleus, and likely impedes a runaway immune response during ETI.

RNA processing, storage and degradation

Regulation of messenger RNA (mRNA) largely impacts the formation of proteins. For example, AS of NLR genes and JAZ genes generates isoforms with diverse activities or subcellular localizations, by which plants can control immunity activation (Wu *et al.*, 2020) (Figure 1L). Treatment with flg22 induces MPK4-mediated phosphorylation of splicing factors, leading to AS of genes encoding NLRs, TFs, CDPKs and splicing

factors (Wu *et al.*, 2020). MED25 recruits the splicing factors PRE-mRNA-PROCESSING PROTEIN 39a (PRP39a) and PRP40a to promote the full splicing of JAZ genes, in order to prevent excessive desensitization of JA signaling mediated by JAZ alternative splice variants (Chini *et al.*, 2007, Thines *et al.*, 2007, Chung and Howe, 2009, Wu *et al.*, 2020). Moreover, RNA can be (temporarily) stored in the nucleus, or in special aggregations that are involved in temporary storage and/or degradation, which decreases the pool of translating RNAs (Figure 1M-P). For example, core hypoxia genes in *Lupinus luteus* and *Arabidopsis* are retained in the nucleus during hypoxia, and released in the cytosol upon reaeration (Niedojadło *et al.*, 2016). It is uncertain if such nuclear retention regulation applies during immune activation. Non-translating mRNAs can also be stored in stress granules or P-bodies, which are both quickly disassembled and re-assembled after stress. Stress granules contain mRNAs and translation machinery, and contribute to mRNA storage, whereas P-bodies contain mRNAs and mRNA degrading enzymes, and contribute to mRNA degradation (Decker and Parker, 2012, Mitchell and Parker, 2014). The importance of P-bodies and mRNA decay in PTI was recently reported (Yu *et al.*, 2019). It was shown that the P-body component DECAPPING1 (DCP1), a co-activator of the decapping enzyme DCP2, is phosphorylated by MPK3 and MPK6 within minutes of treatment with several PAMPs. This phosphorylation of DCP1 decreases its binding to DCP2, but increases its binding to XRN4, an exoribonuclease that can degrade decapped mRNA (mRNA decay) (Souret *et al.*, 2004). This leads to degradation of a subset of mRNAs that are downregulated during PTI, to prevent their negative impact on the plant immune response (Yu *et al.*, 2019).

Regulation by non-coding RNAs

Different non-coding RNAs, like small RNAs and long non-coding RNAs (lncRNAs) regulate different steps in gene expression. For a comprehensive overview on non-coding RNAs in plant immunity we refer to a recent review (Song *et al.*, 2021). Small RNAs can interfere with mRNA stability or regulate transcription or translation through mechanisms such as RdDM (see also 'DNA methylation'). MicroRNAs (miRNAs) are small RNAs that are involved in post-transcriptional gene silencing (PTGS) and can thus potentially affect the immune transcriptome (Figure 1Q). A recent study explored the role of miRNAs during infection of soybean with the soybean cyst nematode *Heterodera glycines* (Rambani *et al.*, 2020). They found that differential DNA methylation of miRNA genes influences expression of the miRNAs in resistant and susceptible soybean lines. Overexpression studies show that four miRNAs that are regulated during infection and that are expressed at higher basal levels in a resistant soybean line cause degradation of their target mRNA and accomplish increased resistance of the susceptible line to the nematode. This study shows that

different epigenetic mechanisms (methylation and subsequent miRNA-directed PTGS) interact to finetune the immune response.

A recent study reported that the lncRNA *ELENA1* is induced by treatment with the PAMPs flg22 and elf18 (Seo *et al.*, 2017). Overexpression and knockdown studies with *ELENA1* show that it promotes *PR1* and *PR2* expression and resistance to *Pto*. RNA-seq revealed that a subset of elf18-induced defense genes overlaps with *ELENA1*-induced genes. Upon elf18 treatment, *ELENA1* interacts with MED19a *in vivo*, which promotes binding of MED19a to the promoter of *PR1* and possibly other genes (Seo *et al.*, 2017) (Figure 1R). In a follow-up, it was shown that *ELENA1* also mediates the dissociation of immune suppressor FIBRILLARIN2 from MED19a, providing an additional mechanism by which it can promote target gene transcription (Seo *et al.*, 2019).

MULTI-OMICS: CHALLENGES AND OPPORTUNITIES IN STUDYING TRANSCRIPTIONAL REGULATION IN PLANT IMMUNITY

5

A balanced regulation of gene expression is required to maintain robustness and efficiency of the triggered immune responses. As outlined in this review, different regulatory components should act in conjunction to control the plant immune transcriptome. How different sectors within the immune network are integrated via these different regulatory players, and under which circumstances, remains largely unknown. A network level understanding could provide leads to these answers. For this, different immune-stimulatory treatments should be compared and different whole-genome, multi-omics datasets should be combined, followed by advanced integrated data analysis including the use of mathematical modeling tools (Figure 2). Examples of these omics assays are profiling of chromatin accessibility, RNA variants (mRNA, miRNA, lncRNA, etc.), DNA and histone modifications, etc. (Ko and Brandizzi, 2020, Dorrity *et al.*, 2021, Li *et al.*, 2021). Moreover, the declining costs of nucleotide sequencing, increasing data storage capacities and computer processing power sparks advances in bioinformatic analysis methods and mathematical modeling tools. A systems biology approach will aid in elucidating GRNs and may provide predictive capability on how and when different regulatory components are involved in orchestrating the plant immune network.

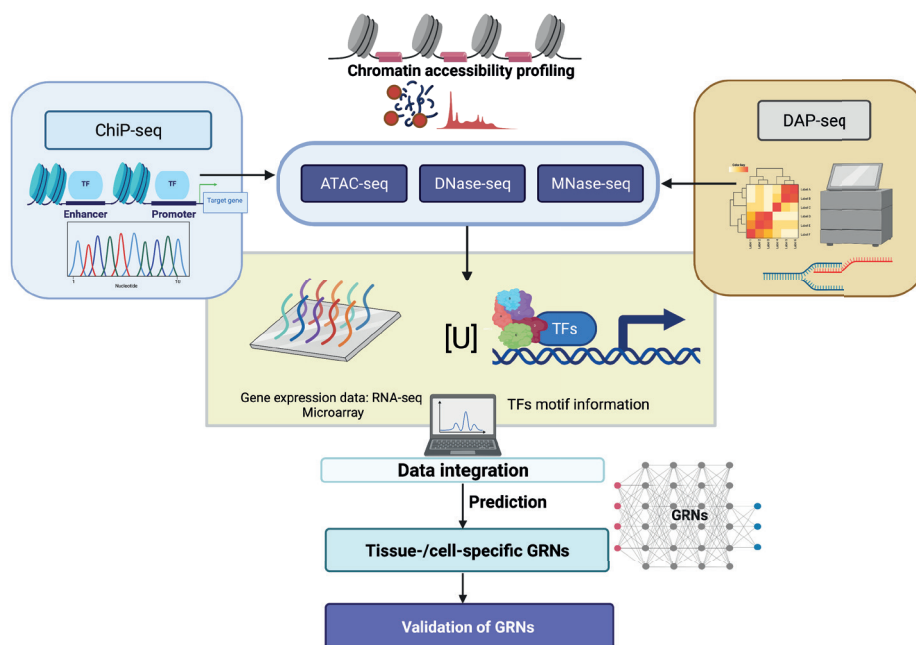


Figure 2: Next-generation toolkit for elucidating immune-responsive GRNs.

Integration of data on TF-DNA binding, chromatin accessibility, and gene expression can be employed as a powerful tool to elucidate the highly interconnected gene GRNs that determine the plant immune transcriptome, even at single cell resolution. For instance, information related to TF binding sites can be obtained from chromatin-immunoprecipitation followed by sequencing (ChIP-seq) and DNA affinity purification sequencing (DAP-seq). Information about chromatin status can be derived from methods such as ATAC-seq, MNase-seq, or DNase-I hypersensitive sites sequencing (DNase-seq). Different variants of RNA (e.g. mRNA, miRNA, lncRNA) can be measured by RNA-seq. These data can be integrated to reveal GRNs that shape the plant immune transcriptome. The functionality of these GRNs can be tested and validated by mutant analysis under different conditions or in different tissues or cell types.

At a finer resolution, namely the cell level, other critical questions need attention. Which of the immune responses are cell-type specific? And does that determine whether the initial infection of a certain cell type propagates further to adjacent cells or is halted? Furthermore, how does cell homeostasis, related to different internal and external conditions, such as plant age, time of day, abiotic stress, and spatiotemporal distance from the infection site, influence the plant immune transcriptome? To answer these questions, single-cell methods instead of bulk analyses using the omics assays and molecular tools mentioned in this review would be extremely meaningful (reviewed by Swift et al., 2022), especially for identifying GRNs in a heterogenous population from infected to non-infected plant cells. Moreover, analogous profiling of cells of the pathogen will provide insight into the intimate communication between the host and the pathogen (Nobori *et al.*, 2020). Approaches such

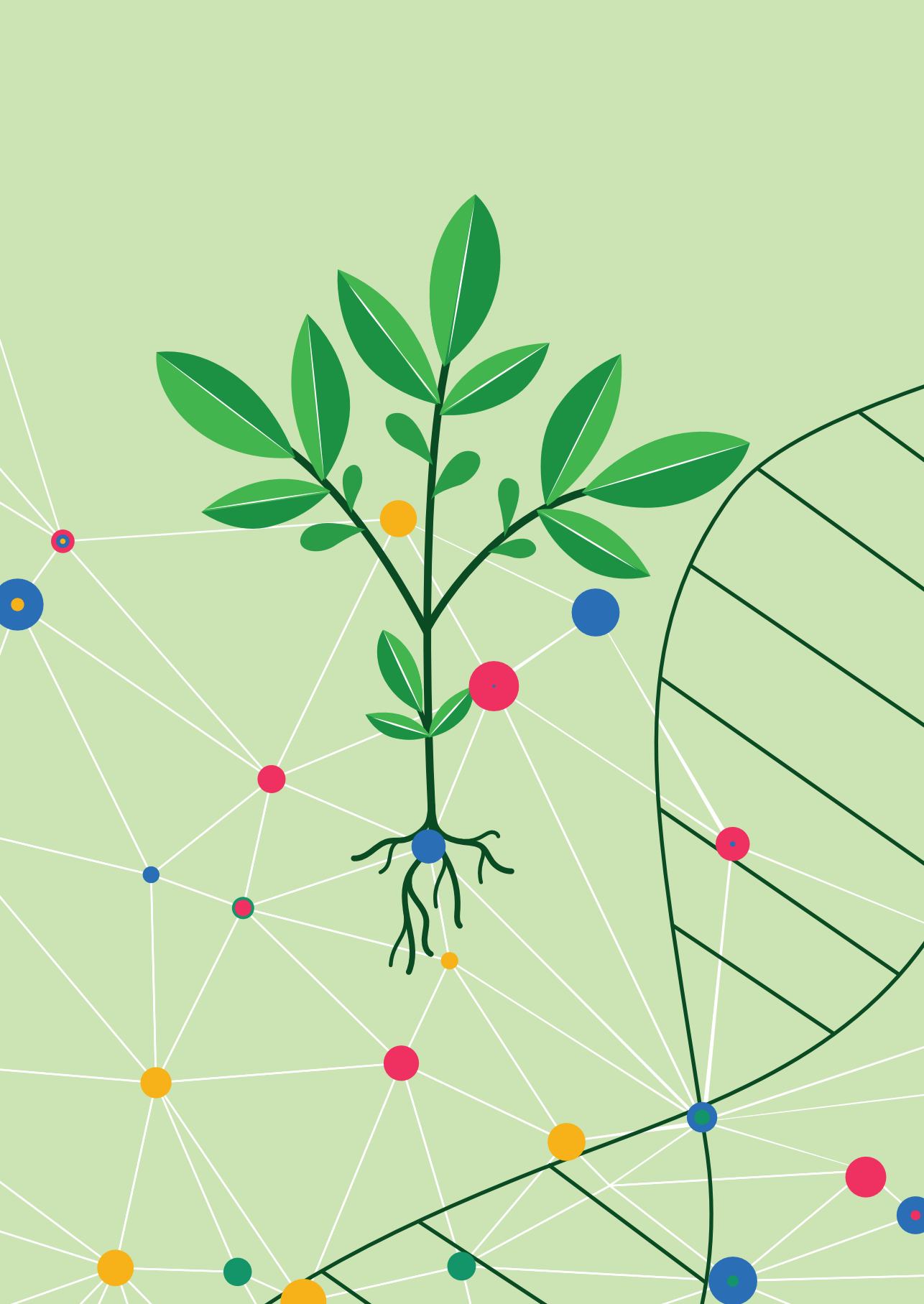
as laser microdissection, which have been used widely in clinical biology for studying cell-specific responses (Bevilacqua and Ducos, 2018), can also be used in plant research for molecular profiling of desired cells. With such knowledge collectively, our chances to succeed in intelligently designing crops with a strengthened immune response under diverse conditions will increase.

Summary points

- The plant immune transcriptome is induced upon pathogen perception and required for disease resistance.
- Many pathogens use effectors to tweak the plant immune transcriptome to their own advantage.
- Plants regulate their immune transcriptome at multiple scales, e.g. post-transcriptional regulation of TFs, modulation of DNA accessibility, and modulation of mRNAs during their journey from transcription to translation.
- A combination of multi-omics datasets can provide new insights into immune-related GRNs.

ACKNOWLEDGEMENTS

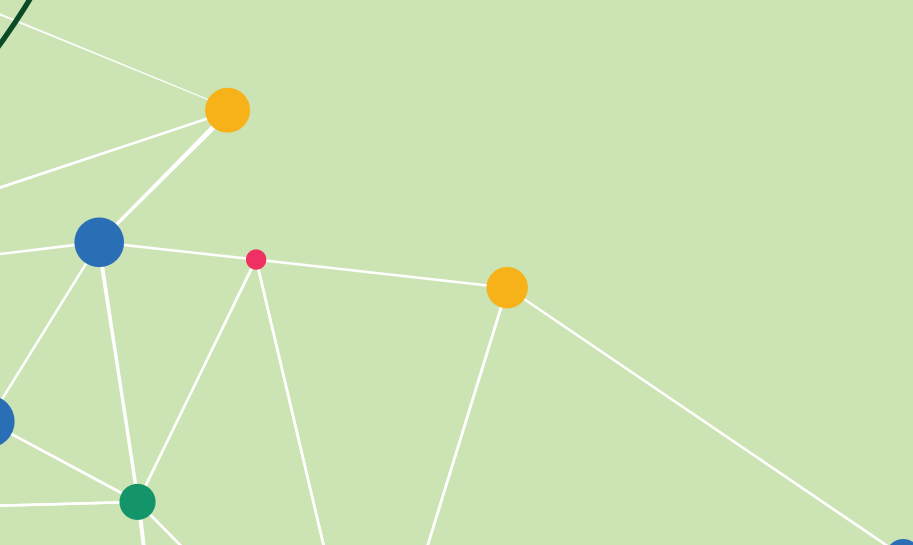
N.A. was supported by the Netherlands Organization for Scientific Research (grant number ALWGS.2016.005). P.D. acknowledges the support from European Union Framework Programme for Research and Innovation, Horizon Europe, European Research Council Starting Grant 'R-ELEVATION' (grant number 101039824).





CHAPTER 6

General discussion



The current state of the plant immunity field

One of the greatest challenges of this era is feeding the growing world population (Misselhorn *et al.*, 2012). Food production is inevitably limited by the amount of arable land, which calls for an increase in yield per unit of surface area. Scientists and especially plant scientists play an essential role in this. In the past, increases in yield were achieved by scientific developments such as the development of synthetic fertilizer and crop varieties that prioritize yield over growth, which led to the so-called 'green revolution' in the second half of the 20th century (Evenson and Gollin, 2003). Other scientific efforts are directed at reducing crop loss caused by pests and pathogens, as these losses are estimated to range between 8% to over 40%, depending on the crop and location (Savary *et al.*, 2019). One strategy to reduce crop loss is to apply chemicals that protect plants against various attackers, but these chemicals have a detrimental effect on the environment (Baweja *et al.*, 2020). Therefore, research on the plant immune system is essential for developing resistant crop varieties that do not require excessive use of chemicals to withstand pests and pathogens.

Contemporary research on the plant immune system can roughly be divided into three partly overlapping fields. The first field primarily focuses on early events in immune signaling. Two important events are: the perception of pathogen/insect- and host-derived molecules by specialized receptors, and the signaling cascade that is triggered by this perception. The molecules that are perceived by the host can be divided into two groups: (i) general molecules known as microbe/pathogen/herbivore/damage-associated molecular patterns (M/P/H/DAMPS), which trigger pattern-triggered immunity (PTI) when they are recognized by so-called pattern recognition receptors, and (ii) specific attacker-produced effectors that are aimed at suppressing PTI, but may lead to effector-triggered immunity (ETI) if recognized by specialized NLR receptors (Jones and Dangl, 2006). Recent developments in this field have provided exciting new insights. For example, recent research on the integration of PTI and ETI signaling (Yuan *et al.*, 2021a) challenged the classic model that postulated PTI and ETI as separate pathways (Jones and Dangl, 2006). Additionally, discoveries of molecular mechanisms that link the reception of pathogen-specific molecules to downstream defense signaling highlighted the importance of non-protein molecules, such as Ca²⁺ signaling and hydrolysis of NAD⁺ (Essuman *et al.*, 2022, Lapin *et al.*, 2022). These discoveries could in the long term help in breeding crops that exhibit a stronger defense response against a larger range of pathogens and pests.

Another research field focuses on the influence of the plant microbiome on plant immunity and growth. In the past decades it has become apparent that plant microbiomes have a large impact on plant health (Pieterse *et al.*, 2014), resulting in great interest for agricultural use of specific microbes. Unfortunately, such initiatives have had limited success, despite successful laboratory trials, emphasizing the need for more research in this field (French *et al.*, 2021). Recent exciting developments in this field include the

discovery that diseased plants can recruit certain beneficial bacteria that can protect a second generation against pathogens (Bakker and Berendsen, 2022), and several studies that map plant genetic traits that select for certain beneficial bacteria and/or their traits (Escudero-Martinez and Bulgarelli, 2023), as well as new insights into bacterial traits that determine how well they can survive and thrive when interacting with a plant (Poppeliers *et al.*, 2023).

The third field focuses on the contribution of plant hormones to plant immunity. Hormones play an important role in the regulation of a large variety of plant immune responses, including those activated in response to beneficial microbes, herbivorous insects, and plant pathogens (Pieterse *et al.*, 2012). Several hormones act downstream of microbe/insect/pathogen recognition and change the expression of thousands of genes to fine-tune plant immunity (Pieterse *et al.*, 2012, Hickman *et al.*, 2017, Hickman *et al.*, 2019). The most important hormones that modulate plant immunity are salicylic acid (SA), jasmonic acid (JA), ethylene (ET) and abscisic acid (ABA) (Aerts *et al.*, 2021). Exciting new developments in this field include a series of studies that show the importance of rapidly induced electric signals after wounding (e.g., by insect herbivory) in triggering biosynthesis of JA (Farmer *et al.*, 2020), the discovery of key steps in SA biosynthesis (Rekhter *et al.*, 2019, Torrens-Spence *et al.*, 2019), the solving of the crystal structure of the SA master regulator NPR1 (Kumar *et al.*, 2022), and the discovery of a mechanism that explains how NPR1 is involved in the SA-mediated suppression of part of the JA pathway (Nomoto *et al.*, 2021). Interactions between different hormone-driven gene regulatory networks (GRNs), such as SA/NPR1-mediated suppression of the JA GRN, are referred to as hormone crosstalk, and are an important topic within the plant hormone field. This is because hormone crosstalk optimizes (defense) responses given the environmental conditions and developmental stage, and is thus vital for plant health under different environmental conditions (Aerts *et al.*, 2021). For plant breeders optimizing hormone crosstalk could mean optimizing resistance without sacrificing growth and yield.

Many questions remain within the field of hormones and hormone crosstalk. For example, while the influence of SA on the JA GRN (SA/JA crosstalk) has been relatively well studied (Caarls *et al.*, 2015), the effect of ABA on the JA GRN (ABA/JA crosstalk) is less well described. Also, while some mechanisms governing crosstalk have been found, many details are unknown and additional mechanisms likely remain to be uncovered.

Highlights of this thesis

In this thesis we carried out various lines of research to further knowledge of immunity-related hormone crosstalk, with a focus on how the JA GRN is modulated by the ABA GRN and by specific components of the SA GRN. Because we already analyzed the JA and SA GRNs in earlier work (Hickman *et al.*, 2017, Hickman *et al.*, 2019), we also analyzed

the ABA GRN by itself. In **Chapter 1** we reviewed that crosstalk can take place at many levels of regulation: the network level, the protein level, the gene expression level and the hormone homeostasis level (see also Figure 1A). In **Chapter 2** and **Chapter 3** we dove deeper into the ABA GRN (**Chapter 2**) and ABA/JA crosstalk (**Chapter 3**) by analyzing high-density time series RNA-seq data of plants treated with ABA, methyl JA (MeJA; a JA variant that is converted to free JA in the plant) and the combination, and integrating it with publicly available transcription factor binding site (TFBS) data and microarray data of ABA-treated plants that were inhibited in translation. We found that the ABA GRN was highly connected through a variety of transcription factors (TFs), of which the bZIP family was the most prominent (**Chapter 2**), and during some stages of its activation had significant similarities to the JA GRN (**Chapter 3**). We also found that ABA modulates the JA GRN at many of the levels described in Chapter 1: it affects the transcription of 2/3rd of all MeJA-responsive genes, including JA biosynthesis and catabolism genes, and affects protein accumulation of the JA master regulator ORA59 in protoplasts (**Chapter 3**). In **Chapter 4** we investigated mechanisms of NPR1-mediated SA/JA crosstalk and found a function for nuclear localized NPR1. We found that two *npr1* mutant lines that expressed *NPR1* with altered cysteine residues (*NPR1^{C82A}* and *NPR1^{C82A}*) were disrupted in SA/JA crosstalk, but not in core SA responses. Further analysis of these lines led to the identification of SA- or SA/NPR1-responsive WRKY TFs that repress expression of the JA marker gene *PDF1.2*. We found that some of these WRKY TFs achieve this by reducing protein accumulation of the JA master regulator ORA59, independent of its transcription.

Overall, I investigated hormone crosstalk at all of the levels described in Chapter 1 (Figure 1B). Nevertheless, the major focus of my research was on transcriptional regulation of GRNs and crosstalk between GRNs, often measured by mRNA levels, as this is the current gold standard for approximation of (changes in) protein levels. However, many steps of regulation determine which gene is described and which mRNAs are translated to protein. These steps are often overlooked in research, including in Chapters 2-4. Therefore, in **Chapter 5** we summarized current knowledge on transcriptional regulation of plant innate immunity and gave an outlook to research in the future, where novel technologies can be used to investigate these overlooked levels in more detail.

In this general discussion, I will discuss the important findings of this thesis and put them into a broader perspective. I will also discuss limitations of our current work and give my view on how research on GRNs governing plant immunity can improve in the future.

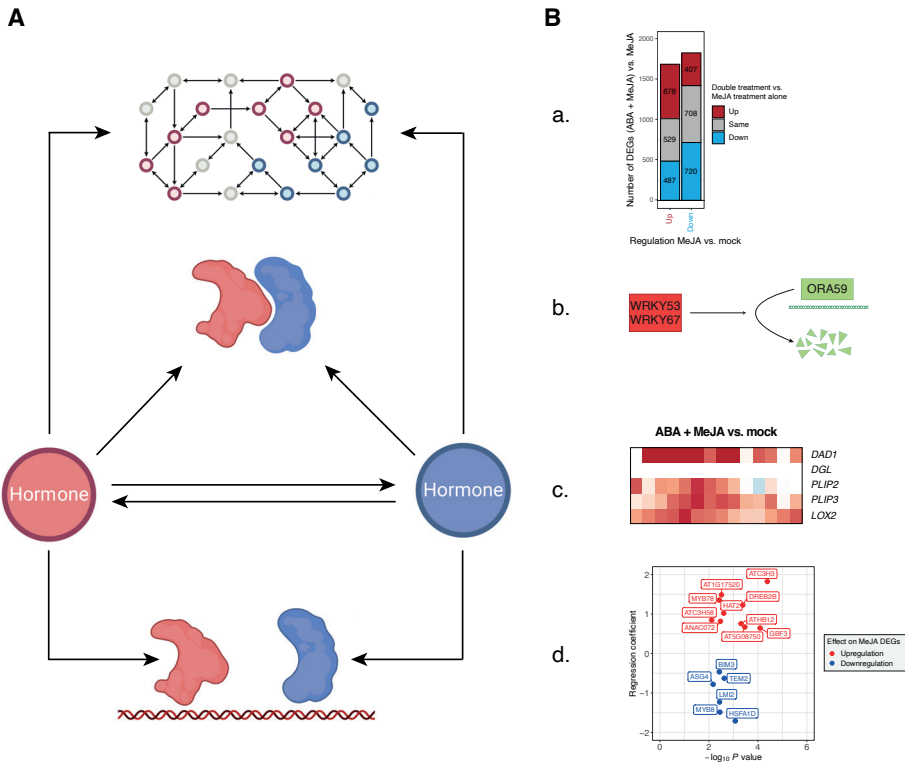


Figure 1: multiple levels of crosstalk in hormone networks regulating defense, with examples from this thesis.

(A) Conceptual framework of the levels at which crosstalk can take place:

- a. the network level;
- b. the protein level;
- c. the hormone homeostasis level.
- d. the gene expression level;

In this figure, genes and proteins are colored according to the hormone (in c) that controls them in these hypothetical examples.

(B) Examples of crosstalk at the indicated levels from this thesis:

- a. ABA affects expression of around 2/3rd of all MeJA-responsive genes (Chapter 3);
- b. WRKY53 and WRKY67 are SA-induced WRKY TFs that reduce accumulation of ORA59 protein (Chapter 4);
- c. ABA affects the expression of many JA biosynthesis and catabolism genes, both in the single treatment and ABA + MeJA double treatment (Chapter 3);
- d. Several TFBSs are associated with differential expression of MeJA responsive genes after ABA + MeJA treatment compared to MeJA treatment alone, suggesting that the corresponding TFs regulate ABA/JA crosstalk at the transcriptional level (Chapter 3).

Panel A was created using Biorender.com with subscription and used as graphical abstract for Aerts *et al.*, 2021 on the website of The Plant Journal. Full legends of the figures shown in (B) can be found in the indicated chapters.

Novel insights into the ABA GRN

ABA is an important regulator of plant responses to many stresses and of several stages of plant development (Chen *et al.*, 2020). Although ABA is mostly known for its role in abiotic stress responses and development, it also plays an important role as a modulator of SA- and JA-regulated defenses, potentiating defense against herbivorous insects and attenuating defense against necrotrophic pathogens (Pieterse *et al.*, 2012). ABA signaling is initiated through a phosphorylation cascade: when PYR/PYL/RCAR receptors bind ABA, they interact with PP2C and likely also PP2A and TOPP phosphatases, preventing them from dephosphorylating SnRK2 kinases (Hou *et al.*, 2016, Yang *et al.*, 2017). Phosphorylated SnRK2 kinases phosphorylate and thereby activate TFs that act as master regulators of the ABA pathway (Umezawa *et al.*, 2010). Several important players in the ABA GRN have been revealed over the years. Most notably, one study combined ChIP-seq and RNA-seq data of mock- or ABA-treated seedlings to reveal the importance of 21 ABA-related TFs in the ABA GRN in seedlings, providing a significant advancement in our understanding of the ABA GRN (Song *et al.*, 2016). However, the study had some limitations. For example, ChIP-seq is inevitably limited in throughput and the researchers used a continuous ABA treatment for their RNA-seq time series (based on seedlings in hydroponics), which only allowed them to look at activation of the network but not the return to basal levels. Therefore, several details of the ABA GRN remained unexplored, especially in mature plants.

In Chapter 2 we analyzed our high-density RNA-seq time series dataset of ABA-treated *Arabidopsis thaliana* (hereafter: *Arabidopsis*) rosettes to get more insight into the architecture and dynamics of the ABA GRN in mature plants. We used a pulse treatment (3 s dipping of rosettes into an ABA solution), which allowed us to look at both activation of the network at early time points and the return to basal levels at later time points. The wide variety in expression patterns that we found likely reflects the various needs of a plant in its response to stress: some processes need to be activated or repressed quickly, whereas other processes may be activated or repressed at later time points. Also, when a stimulus (such as high ABA levels) is gone, some genes need to return to basal level more quickly than others. Genes that return to basal levels quickly would logically be related to processes that cost much energy, however we did not investigate this. The differentially expressed genes we found could be clustered based on their diverse expression patterns into 44 clusters, which were enriched in partly overlapping, partly unique gene ontology terms, suggesting that the modules were indeed biologically functional.

One of our main aims of Chapter 2 was to find important TFs that regulate (part of) the ABA GRN. We predicted these TFs using publicly available DAP-seq data (O'Malley *et al.*, 2016) and data of ABA-treated plants inhibited in translation (Lumba *et al.*, 2014). This allowed us to not only predict these important TFs but also to predict which TFs act at the very earliest stage of activation of the ABA GRN, for example directly downstream of SnRK2 kinases. It is important to note that our predictions were only based on enrichment

analyses: TFs with enriched binding sites in genes that were differentially expressed after ABA treatment when translation was blocked were deemed candidate regulators of the start of the ABA transcriptional cascade. A more thorough study would investigate if these TFs are indeed modulated at the post-translational level after ABA treatment. A logical first step would be to look at phosphorylation, since that is the most well-known way in which the ABA pathway is activated and phosphoproteomics has been used in the past to find regulators of the ABA pathway (Chong *et al.*, 2022). However, other processes that modulate protein functioning and structure should also be investigated, and novel technologies such as limited proteolysis-mass spectrometry (LiP-MS) may allow this in the future (reviewed by Chong *et al.*, 2022).

Strategies to optimize prediction and validation of novel transcriptional regulators of GRNs

The prediction and validation of (transcriptional) regulators of GRNs is an important topic within the field of molecular biology and bioinformatics. The increasing availability of large datasets on e.g., transcription, TFBSs and open chromatin have prompted bioinformaticians to develop numerous tools that use these data to infer GRNs (Mercatelli *et al.*, 2020). Furthermore, the availability of T-DNA insertion lines of almost any gene and (inducible) overexpression lines for many genes in *Arabidopsis* makes biological validations of these predictions in this model species relatively easy. Nevertheless, most studies that predict novel regulators in GRNs – including our own – only manage to validate a handful of these TFs, or do not do any validation at all (Krouk *et al.*, 2010, Windram *et al.*, 2012, Lewis *et al.*, 2015, Song *et al.*, 2016, Hickman *et al.*, 2017, Hickman *et al.*, 2019, Chapters 2 and 3). I will here discuss possible reasons for this, illustrated by our own work, and discuss strategies to efficiently predict and validate important TFs in a GRN of choice.

In Chapter 2 we generated RNA-seq time series data of ABA treated *Arabidopsis* rosettes and used bioinformatics tools and custom scripts to predict transcriptional regulators within the ABA GRN. We then set out to validate these in a biological context, namely by testing mutants or overexpressors of these TFs during drought stress followed by recovery. The results were less than satisfying: out of the eight TFs tested only one, *GT3a*, showed a phenotype. Moreover, this was only in an overexpression line for this gene. Even more TF mutants were tested in a germination assay without success, although technical problems could not be excluded, which is why we did not present these data in this thesis. While this low validation rate seemed to suggest that our bioinformatics prediction were not good, the presence of many known TFs in our predicted network does suggest that the methods we used worked. It could simply be that most of the important regulator TFs of the ABA network are already known. Alternatively, there may

be so much redundancy in the ABA network that higher-order mutants or overexpression lines are needed to get a clear phenotype and thus validate the TFs, as also discussed in Chapter 2. This redundancy was actually predicted by our network models, because they predicted that the same genes were often regulated by multiple, similar TFs. Given that fact, the low success rate of our validations using single mutant lines can be seen as a validation of the complexity and redundancy of the ABA GRN that we predicted. High redundancy of network components may also be the reason why other studies have limited success in large-scale validation of network components.

The success rate of our validations was as low - if not lower - than in our two previous studies on the SA and JA GRNs. In these studies, as candidates for validation, we simply picked TFs from clusters of DEGs that also contained known important TFs in the JA and SA GRN, respectively – a ‘guilt-by-association’ approach (Hickman *et al.*, 2017, Hickman *et al.*, 2019). The success rate of lines with a phenotype compared to TFs tested was 5/13 for the JA study (of which one only in a double mutant) (Hickman *et al.*, 2017) and 2/18 for the SA study (of which one only in a double mutant) (Hickman *et al.*, 2019). This is higher or about as high as the success rate of the current study. The added value of our current network inference methods vs. just doing the quick ‘guilt-by-association’ method for simply detecting novel regulator TFs is thus doubtful, but our current methods do provide more precise predictions of the position of novel TFs in the network. Therefore, if researchers are mostly interested in finding new important TFs in their process of interest without analyzing the position of these TFs in the regulating network, a simple guilt-by-association approach may be more efficient than extensive bioinformatics analyses of the data. For both approaches, a high-density time course is required. Moreover, it is essential that the bioinformatic analyses are combined with efficient phenotyping of higher-order mutants and/or overexpression lines to overcome possible redundancy.

The ‘guilt-by-association’ approach predicts if a TF is involved in a certain process, but not what its position in the regulating GRN is. Uncovering the position of a TF in the network can provide information on the function of the TF and the potential consequences of altering a TFs function, which can be both biologically relevant as well as relevant for breeders who want to optimize defense without affecting other processes. First, large-scale data needs to be analyzed with bioinformatics pipelines that result in a predicted network. For example, in Chapter 2 we used DREM2.0 to predict regulators of certain gene clusters, as well as custom scripts to create a hierarchical ABA network. Many other bioinformatics methods are available and can be chosen depending on the type of data that is analyzed and the desired output (Mercatelli *et al.*, 2020). These data can for example be gene expression data under multiple conditions or at multiple time points after a stimulus (like in Chapter 2 and 3 of this thesis), or genome-wide transcription factor binding site (TFBS) data for a large number of TFs. The generation of these data is usually time-consuming and costly. Therefore, to better predict networks it is important that

these methods are optimized. Validation of the position of a TF in a network is also costly, since specific methods need to be combined to confidently state that a TF regulates certain targets. Such methods include ChIP-seq or DAP-seq combined with RNA-seq, or the protoplast-based method TARGET (Bargmann *et al.*, 2013). To better validate the position of TFs in a network the costs of these methods need to be reduced, or cheaper and more efficient methods need to be developed.

Reliable inference of GRNs currently also has several challenge. For example, since many methods are based on whole-tissue information, regulation at the single-cell level is ‘averaged’, causing loss of information. The advancement of single-cell technologies may solve this in the future. Furthermore, almost all current GRN inference methods suffer from lack of information on levels of regulation that determine where a TF binds and if an mRNA is eventually translated to protein (see also Chapter 5). Many of these levels can currently not be measured on a genomic scale for a large number of samples. This is problematic because, for example, if a gene is subjected to heavy post-transcriptional regulation, it will no longer be coexpressed with genes encoding its regulator(s) and the TF-target relationship will not be predicted by coexpression-based GRN inference algorithms. Also, if binding of a TF to a promoter of a certain target gene is heavily regulated under certain conditions, this is completely missed by DAP-seq experiments, or ChIP-seq experiments if they are done under other conditions. In Chapter 5 we review the many levels of regulation that determine which genes are regulated by a TF and which transcripts eventually get translated. Novel technologies aimed at measuring these types of regulation may in the long run lead to much more accurate predictions of TF-target relations, and therefore the inference of GRNs. Also, integration of different data types by newly developed algorithms, e.g., based on machine learning, can greatly enhance the accuracy of network inference algorithms (see for example De Clercq *et al.*, 2021).

In summary, to quickly find new regulators of a process of interest, a ‘guilt-by-association’ bioinformatics approach followed by phenotypic validation using overexpression lines or double mutants of candidates is recommended. More accurate predictions and validation of GRN components is possible, but to do this on a large scale significant improvements in both *in silico* methods for GRN inference and wet-lab validation pipelines are needed.

The ratio between activating and repressing TFs differs between stress-responsive GRNs

Correct functioning of GRNs requires not only upregulation but also downregulation of genes. For example, during pathogen infection or pest infestation growth is often suppressed, so that resources, which are often limited, can be allocated to defense compounds, and pests find less unprotected nutritious tissue to feed on (He *et al.*, 2022).

It would be expected that downregulation is as tightly regulated as upregulation. However, in Chapter 2 we noticed that TFs in the ABA GRN were more often predicted to contribute to upregulation of target genes than downregulation, even though a similar number of genes was upregulated and downregulated after ABA treatment. Also, in Chapter 3 we used stepwise regression to predict TFs associated with the differential expression of MeJA-upregulated genes after ABA + MeJA treatment compared MeJA treatment alone, and found that the majority of TFs was predicted to further activate MeJA-activated genes. Similarly, in a study of the ABA GRN in seedlings upregulating TFs were also more common than downregulating TFs, based on ChIP-seq of 21 TFs and RNA-seq after ABA treatment (Song *et al.*, 2016). As discussed in Chapter 2, this together suggests that there are more activating than repressing TFs in the ABA GRN. In our previous study on the JA GRN, we also found that enrichment of motifs was more diverse in upregulated compared to downregulated coexpression clusters (Windram *et al.*, 2012). This suggests that the JA GRN also encompasses more upregulating than downregulating TFs, and reinforces our findings from Chapter 3 that the ABA and JA GRNs show significant similarities, in this case qualitatively.

The prediction that there are more activating than repressing TFs in the ABA and JA GRNs is not a general rule for stress-responsive networks. For example, in earlier work we found similar enrichment of motifs in upregulated and downregulated clusters of coexpressed genes after SA treatment (Hickman *et al.*, 2019) and other researchers also found a similar degree of enrichment of motifs in clusters of upregulated vs. downregulated genes after inoculation with *Botrytis cinerea* (Windram *et al.*, 2012) or *Pseudomonas syringae* (Lewis *et al.*, 2015). Together, this suggests that the ratio between activating and repressing TFs differs between specific stress-responsive GRNs. To strengthen above conclusions, data on TFBSs of all Arabidopsis TFs needs to be obtained and compared for different stress- and hormone-related time series experiments.

The reason for the higher number of activating compared to repressing TFs in the ABA and JA GRNs is unclear, especially since in both GRNs there is a similar number of upregulated and downregulated genes. It could be that upregulation is more important for functioning of these GRNs than downregulation, so activation happens via multiple redundantly operating TFs, making the regulation more robust against loss of one of the TFs. It could also point towards higher integration of upregulated genes in the JA and ABA GRNs with other GRNs, as one study found that genes that are targeted by more TFs (which would be the case for upregulated genes in the ABA and JA GRNs) are generally expressed in more conditions (Heyndrickx *et al.*, 2014) and thus likely part of several overlapping GRNs.

New insights into modulation of the JA GRN by ABA

The JA pathway consists of two mutually antagonistic branches. The MYC branch is regulated by MYC TFs such as MYC2, and mostly directed against herbivorous insects, whereas the ERF branch is regulated by ERF TFs such as ORA59 and is mostly directed against necrotrophic pathogens (Pieterse *et al.*, 2012, Aerts *et al.*, 2021). It has long been recognized that ABA modulates the JA GRN. For example, it is known that ABA generally enhances JA biosynthesis (Adie *et al.*, 2007, Fan *et al.*, 2009, Wang *et al.*, 2018), promotes defense against insects and associated marker gene expression (Anderson *et al.*, 2004, Bodenhausen and Reymond, 2007, Dinh *et al.*, 2013, Vos *et al.*, 2013b), and represses defense against necrotrophic pathogens and associated marker gene expression (Audenaert *et al.*, 2002, Anderson *et al.*, 2004, Sánchez-Vallet *et al.*, 2012). Furthermore, it was found that ABA modulates MYC2 transcription (Abe *et al.*, 1997, Abe *et al.*, 2003) and that an ABA-enhanced interaction between the ABA receptor PYL6 and MYC2 changes the transcriptional activity of MYC2 (Aleman *et al.*, 2016). Therefore, ABA is generally seen as a co-activator of the MYC branch and a repressor of the ERF branch. However, the extent to which ABA modulates both branches and the underlying mechanisms were poorly understood.

In Chapter 3 we investigated crosstalk between the ABA and JA GRNs by analyzing the single and combined treatment RNA-seq time series data. We noticed that the two networks already had significant overlap when only the single treatment time series data were considered. This was especially a large portion of MeJA-responsive genes ($\pm 2/3^{\text{rd}}$), since MeJA affects expression of less than half the number of genes compared to ABA. Similarly, in the double treatment around $2/3^{\text{rd}}$ of MeJA responsive genes had a different expression pattern compared to MeJA treatment alone, often reinforcing the effect that MeJA already had. In these cases, the expression levels were often less than the sum of the effects of ABA and MeJA, which could point to redundancy of part of the two GRNs, or saturation of the response (e.g., an upregulated gene already reached its expression ceiling after single treatments).

While we found that ABA both activated and repressed MeJA-responsive genes, closer inspection of the data showed that this did not necessarily reflect MYC/ERF antagonism. ERF branch marker genes such as *ERF1*, *ORA59* and *PDF1.2* were little induced by MeJA in our time series setup, suggesting that MeJA treatment mostly activated the MYC branch, and that the repressed MeJA-responsive genes that we observed may well be enriched for MYC branch genes. The lack of activation of the ERF branch could be due to relatively low levels of ET compared to ABA in our experimental setup, as ET is a co-regulator of the ERF branch and repressor of the MYC branch (Pieterse *et al.*, 2012). The differential effect of ABA on MeJA-responsive genes thus suggests that ABA not only mediates differentiation between the MYC branch and the ERF branch of the JA pathway, but also between other groups of genes that are not yet properly defined as a JA pathway

branch. Future work may look further into these gene sets to investigate to what extent they belong to one of the classic branches of the JA pathway or are distinct groups that should be newly classified as an ABA-modulated sector of the JA GRN.

The MYC and ERF branch are antagonistic, which is mediated, for example, by direct interaction between MYC2 and the ERF branch master regulator EIN3 (Song *et al.*, 2014, Zhang *et al.*, 2014). Because ABA activates the MYC branch it is tempting to speculate that ABA represses the ERF branch simply by activating the MYC branch. However, both in earlier work and in Chapter 3 we found that transcriptional repression of *PDF1.2* by ABA is independent of MYC2 (Vos *et al.*, 2019; Chapter 3). We also found in Chapter 3 that under certain conditions ABA represses the ERF branch by inducing the degradation of ORA59 protein, or possibly post-transcriptionally repressing ORA59 protein accumulation. This is consistent with the finding that suppression of the ERF branch by ABA is independent of MYC2, since MYC2 has not been implicated in degradation of ORA59. In the future, dependency of ABA-mediated ORA59 degradation on MYC2 could be tested by analyzing ABA-mediated ORA59 protein accumulation in *myc2*-derived protoplasts.

In summary, we found that ABA modulates large parts of the JA GRN, that it indeed differentially modulates different parts of the JA GRN, but that this difference is not fully consistent with the model that ABA activates the MYC branch and represses the ERF branch. Also, we found that ABA's repressive effect on the ERF branch is likely partly mediated by ORA59 degradation and independent of ABA's activating effect on the MYC branch.

The WRKY TF family harbors many regulators of SA/JA crosstalk

The WKRY TF family is a relatively large TF family with 74 members in Arabidopsis (Pandey and Somssich, 2009). Many members are important regulators of plant immunity and especially many SA-induced immunity-regulating WRKY TFs are recognized (Wang *et al.*, 2006, Pandey and Somssich, 2009, Hickman *et al.*, 2019). Apart from their role in core SA signaling, many different WRKY TFs have also been implicated in SA/JA crosstalk (Caarls *et al.*, 2015). In Chapter 4 we used a protoplast system to confirm that WRKY50, WRKY53 and WRKY54 are involved in SA/JA crosstalk and also found for the first time that WRKY63 and WRKY67 are likely also involved in SA/JA crosstalk, extending the repertoire of SA/JA crosstalk regulating WRKY TFs.

With our experimental setup we found that the identified WKRY TFs repress *PDF1.2* expression downstream of *ORA59* transcription and that WRKY53 and WKRY67 cause destabilization of the ORA59 protein, although the exact mechanisms are still to be uncovered. Destabilization of ORA59 was already recognized as important for SA/JA crosstalk (Van der Does *et al.*, 2013, He *et al.*, 2017), but it was not yet linked to WRKY-mediated SA signaling. The fact that the other WRKY TFs did not cause reduced ORA59

accumulation suggests that WRKY TFs regulate SA/JA crosstalk via multiple mechanisms. Interestingly, we found that ABA also caused ORA59 degradation, suggesting mechanistical overlap between SA/JA and ABA/JA crosstalk.

In their study on SA-mediated degradation of ORA59, He *et al.* (2017) found that EIN3 and EIL1 contributed to ORA59 degradation. To investigate if EIN3 and EIL1 are also involved in degradation of ORA59 protein mediated by ABA or WRKY TFs we performed protoplast assays in *ein3 eil1*-derived protoplasts. We separately investigated the effect of ABA treatment and of WRKY67 overexpression on both ORA59 protein levels and *PDF1.2* expression in this mutant. Unfortunately, we were unable to obtain consistent results. We also assessed the combined effect of ABA treatment and WRKY67 overexpression on ORA59 protein levels and *PDF1.2* expression to investigate if they act in parallel (likely resulting in additive effects) or via the same mechanism (likely non-additive effects). However, we did not obtain consistent results in these experiments either, and therefore, these results are not included in this thesis. In summary, the question how ABA, WRKY53 and WRKY67 cause degradation of ORA59 remains to be answered.

The fact that so many WRKY TFs have an effect on SA/JA crosstalk could also potentially be related to their regulation. WRKY TFs are known to affect each other's expression by directly binding to promoters of target WRKY TFs. Together, this forms a complex transcriptional network (Birkenbihl *et al.*, 2018). It is well possible that overexpression of a WRKY TF in our protoplast setup activates this WRKY network, which then leads to repression of the JA pathway through effects of (a) member(s) of this network. It is therefore not easy to determine which WRKY TF(s) is/are the WRKY TF(s) with a direct effect on the JA pathway. However, the fact that some WRKY TFs regulate SA/JA crosstalk via degradation of ORA59 and others do not suggests that at least multiple networks are involved or that some WRKY TFs have unique effects.

It is unclear if the different mechanisms for SA/JA crosstalk discovered by us and other researchers always work redundantly at the same time/condition, or are more condition specific. The latter seems likely given the fact that many studies reveal crosstalk mechanisms via mutations of key regulators (Caarls *et al.*, 2015), something that would not be possible if the mechanisms always worked redundantly. Also, it is substantiated by findings such as that NPR1 is not needed for crosstalk under high ethylene levels (Leon-Reyes *et al.*, 2009) and that cytosolic localization of NPR1 was sufficient for SA/JA crosstalk under the conditions of Spoel *et al.* (2003), whereas we found that nuclear localization is required. The many mechanisms for SA/JA crosstalk may thus exist to optimally balance the two pathways under different conditions.

CONCLUDING REMARKS

Crosstalk between hormone GRNs ensures an optimal balance between processes such as plant defense and external and internal conditions (see also Figure 1 of Chapter 1). Understanding the extent to which hormone networks are integrated and the mechanisms by which they are integrated can thus help breeders to develop crops with an optimal defense/growth/yield balance. In this thesis I presented a detailed overview of the extent to which ABA modulates the JA GRN, predicted which TFs are involved in this, and showed that ABA-induced degradation of ORA59 likely is one of the mechanisms. I also provided new insights into the dynamics of the ABA GRN, predicted (part of) its complex architecture and validated the importance of a novel TF in the GRN, namely GT3a. Finally, I showed that NPR1 can have a nuclear-localized role in regulating SA/JA crosstalk, where it activates WRKY TFs that repress the ERF branch, partly by causing degradation of ORA59 protein. Together, this provided novel insights into crosstalk acting at many levels of regulation (Figure 1). Information on the architecture of GRNs and how they are integrated, such as presented in this thesis, is vital for crop breeding. Especially TFs that mostly regulate the desired process and do not affect many other processes are potential prime targets for future breeding of elite crops with optimized defense GRNs that provide immunity against pests and pathogens. However, to find such TFs for improvement of crop health, more detailed information on the GRN architecture is needed. Ideally, breeders would be able to predict how the manipulation of expression of one gene in a network affects global gene expression, so that it can be predicted which manipulation can be done to optimally improve the desired process (e.g., resistance to insects) with minimal impact on other processes (e.g., reduced growth). This will require detailed insights into the architecture and integration of a wide range of GRNs. More importantly, these insights should not only be qualitative (e.g., which TF regulates what target), but also quantitative (e.g., to what extent does a specific TF regulate a specific target), so they can be used in an overarching model that combines all this information. Currently, we are far from these comprehensive insights, but as the technique advances both in the laboratory and in bioinformatics this may well be possible in the future.

References

REFERENCES

- Abe, H., Urao, T., Ito, T., Seki, M., Shinozaki, K. and Yamaguchi-Shinozaki, K.** (2003) Arabidopsis AtMYC2 (bHLH) and AtMYB2 (MYB) function as transcriptional activators in abscisic acid signaling. *Plant Cell*, **15**, 63-78.
- Abe, H., Yamaguchi-Shinozaki, K., Urao, T., Iwasaki, T., Hosokawa, D. and Shinozaki, K.** (1997) Role of Arabidopsis MYC and MYB homologs in drought- and abscisic acid-regulated gene expression. *Plant Cell*, **9**, 1859-1868.
- Adie, B.A.T., Perez-Perez, J., Perez-Perez, M.M., Godoy, M., Sanchez-Serrano, J.J., Schmelz, E.A. and Solano, R.** (2007) ABA is an essential signal for plant resistance to pathogens affecting JA biosynthesis and the activation of defenses in Arabidopsis. *Plant Cell*, **19**, 1665-1681.
- Aerts, N., Chhillar, H., Ding, P. and Van Wees, S.C.M.** (2022) Transcriptional regulation of plant innate immunity. *Essays Biochem.*, **66**, 607-620.
- Aerts, N., Mendes, M.P. and Van Wees, S.C.M.** (2021) Multiple levels of crosstalk in hormone networks regulating plant defense. *Plant J.*, **105**, 489-504.
- Akio Amorim, L.L., da Fonseca dos Santos, R., Pacifico Bezerra Neto, J., Guida-Santos, M., Crovella, S. and Maria Benko-Iseppon, A.** (2017) Transcription factors involved in plant resistance to pathogens. *Curr. Protein Pept. Sci.*, **18**, 335-351.
- Aleman, F., Yazaki, J., Lee, M., Takahashi, Y., Kim, A.Y., Li, Z., Kinoshita, T.i., Ecker, J.R. and Schroeder, J.I.** (2016) An ABA-increased interaction of the PYL6 ABA receptor with MYC2 transcription factor: a putative link of ABA and JA signaling. *Sci. Rep.*, **6**, 28941.
- Alonso, J.M., Stepanova, A.N., Solano, R., Wisman, E., Ferrari, S., Ausubel, F.M. and Ecker, J.R.** (2003) Five components of the ethylene-response pathway identified in a screen for weak ethylene-insensitive mutants in Arabidopsis. *Proc. Natl. Acad. Sci. U.S.A.*, **100**, 2992-2997.
- Altmann, M., Altmann, S., Rodriguez, P.A., Weller, B., Elorduy Vergara, L., Palme, J., Marín-de la Rosa, N., Sauer, M., Wenig, M., Villaécija-Aguilar, J.A., Sales, J., Lin, C.-W., Pandiarajan, R., Young, V., Strobel, A., Gross, L., Carbonnel, S., Kugler, K.G., Garcia-Molina, A., Bassel, G.W., Falter, C., Mayer, K.F.X., Gutjahr, C., Vlot, A.C., Grill, E. and Falter-Braun, P.** (2020) Extensive signal integration by the phytohormone protein network. *Nature*, **583**, 271-276.
- An, C., Li, L., Zhai, Q., You, Y., Deng, L., Wu, F., Chen, R., Jiang, H., Wang, H., Chen, Q. and Li, C.** (2017) Mediator subunit MED25 links the jasmonate receptor to transcriptionally active chromatin. *Proc. Natl. Acad. Sci. U.S.A.*, **114**, E8930-E8939.
- An, F., Zhao, Q., Ji, Y., Li, W., Jiang, Z., Yu, X., Zhang, C., Han, Y., He, W., Liu, Y., Zhang, S., Ecker, J.R. and Guo, H.** (2010) Ethylene-induced stabilization of ETHYLENE INSENSITIVE3 and EIN3-LIKE1 is mediated by proteasomal degradation of EIN3 binding F-box 1 and 2 that requires EIN2 in Arabidopsis. *Plant Cell*, **22**, 2384-2401.
- Anders, S. and Huber, W.** (2010) Differential expression analysis for sequence count data. *Genome Biol.*, **11**, R106.
- Anders, S., Pyl, P.T. and Huber, W.** (2015) HTSeq—a Python framework to work with high-throughput sequencing data. *Bioinformatics*, **31**, 166-169.
- Andersen, E.J., Ali, S., Byamukama, E., Yen, Y. and Nepal, M.P.** (2018) Disease resistance mechanisms in plants. *Genes*, **9**, 339.

- Anderson, J.P., Badruzaufari, E., Schenk, P.M., Manners, J.M., Desmond, O.J., Ehlert, C., Maclean, D.J., Ebert, P.R. and Kazan, K.** (2004) Antagonistic interaction between abscisic acid and jasmonate-ethylene signaling pathways modulates defense gene expression and disease resistance in *Arabidopsis*. *Plant Cell*, **16**, 3460–3479.
- Atkinson, N.J. and Urwin, P.E.** (2012) The interaction of plant biotic and abiotic stresses: from genes to the field. *J. Exp. Bot.*, **63**, 3523–3543.
- Attaran, E., Major, I.T., Cruz, J.A., Rosa, B.A., Koo, A.J.K., Chen, J., Kramer, D.M., He, S.Y. and Howe, G.A.** (2014) Temporal dynamics of growth and photosynthesis suppression in response to jasmonate signaling. *Plant Physiol.*, **165**, 1302–1314.
- Audenaert, K., De Meyer, G.B. and Höfte, M.M.** (2002) Abscisic acid determines basal susceptibility of tomato to *Botrytis cinerea* and suppresses salicylic acid-dependent signaling mechanisms. *Plant Physiol.*, **128**, 491–501.
- Avramova, Z.** (2019) Defence-related priming and responses to recurring drought: Two manifestations of plant transcriptional memory mediated by the ABA and JA signalling pathways. *Plant Cell Environ.*, **42**, 983–997.
- Babitha, K.C., Ramu, S.V., Pruthvi, V., Mahesh, P., Nataraja, K.N. and Udayakumar, M.** (2013) Co-expression of *AtbHLH17* and *AtWRKY28* confers resistance to abiotic stress in *Arabidopsis*. *Transgenic Res.*, **22**, 327–341.
- Bakker, P.A. and Berendsen, R.L.** (2022) The soil-borne ultimatum, microbial biotechnology and sustainable agriculture. *Microb. Biotechnol.*, **15**, 84–87.
- Ban, Z. and Estelle, M.** (2021) CUL3 E3 ligases in plant development and environmental response. *Nat. Plants*, **7**, 6–16.
- Banerjee, A. and Roychoudhury, A.** (2017) Abscisic-acid-dependent basic leucine zipper (bZIP) transcription factors in plant abiotic stress. *Protoplasma*, **254**, 3–16.
- Bargmann, B.O.R., Marshall-Colon, A., Efroni, I., Ruffel, S., Birnbaum, K.D., Coruzzi, G.M. and Krouk, G.** (2013) TARGET: a transient transformation system for genome-wide transcription factor target discovery. *Mol. Plant*, **6**, 978.
- Baweja, P., Kumar, S. and Kumar, G.** (2020) Fertilizers and pesticides: Their impact on soil health and environment. *Soil Health*, 265–285.
- Benn, G., Wang, C.-Q., Hicks, D.R., Stein, J., Guthrie, C. and Dehesh, K.** (2014) A key general stress response motif is regulated non-uniformly by CAMTA transcription factors. *Plant J.*, **80**, 82–92.
- Bensmihen, S., Giraudat, J. and Parcy, F.** (2005) Characterization of three homologous basic leucine zipper transcription factors (bZIP) of the ABI5 family during *Arabidopsis thaliana* embryo maturation. *J. Exp. Bot.*, **56**, 597–603.
- Berens, M.L., Berry, H.M., Mine, A., Argueso, C.T. and Tsuda, K.** (2017) Evolution of hormone signaling networks in plant defense. *Annu. Rev. Phytopathol.*, **55**, 401–425.
- Berens, M.L., Wolinska, K.W., Spaepen, S., Ziegler, J., Nobori, T., Nair, A., Krüler, V., Winkelmüller, T.M., Wang, Y., Mine, A., Becker, D., Garrido-Oter, R., Schulze-Lefert, P. and Tsuda, K.** (2019) Balancing trade-offs between biotic and abiotic stress responses through leaf age-dependent variation in stress hormone cross-talk. *Proc. Natl. Acad. Sci. U.S.A.*, **116**, 2364–2373.
- Bergmann, D.C., Lukowitz, W. and Somerville, C.R.** (2004) Stomatal development and pattern controlled by a MAPKK kinase. *Science*, **304**, 1494–1497.
- Berrocal-Lobo, M., Molina, A. and Solano, R.** (2002) Constitutive expression of *ETHYLENE-RESPONSE-FACTOR1* in *Arabidopsis* confers resistance to several necrotrophic fungi. *Plant J.*, **29**, 23–32.

- Betsuyaku, S., Katou, S., Takebayashi, Y., Sakakibara, H., Nomura, N. and Fukuda, H.** (2018) Salicylic acid and jasmonic acid pathways are activated in spatially different domains around the infection site during effector-triggered immunity in *Arabidopsis thaliana*. *Plant Cell Physiol.*, **59**, 8-16.
- Bevilacqua, C. and Ducos, B.** (2018) Laser microdissection: A powerful tool for genomics at cell level. *Mol. Aspects Med.*, **59**, 5-27.
- Bhandari, D.D., Lapin, D., Kracher, B., von Born, P., Bautor, J., Niefind, K. and Parker, J.E.** (2019) An EDS1 heterodimer signalling surface enforces timely reprogramming of immunity genes in *Arabidopsis*. *Nat. Commun.*, **10**, 772.
- Bi, G., Su, M., Li, N., Liang, Y., Dang, S., Xu, J., Hu, M., Wang, J., Zou, M., Deng, Y., Li, Q., Huang, S., Li, J., Chai, J., He, K., Chen, Y.-h. and Zhou, J.-M.** (2021) The ZAR1 resistosome is a calcium-permeable channel triggering plant immune signaling. *Cell*, **184**, 3528-3541.e3512.
- Binder, B.M.** (2020) Ethylene signaling in plants. *J. Biol. Chem.*, **295**, 7710-7725.
- Birkenbihl, R.P., Kracher, B., Ross, A., Kramer, K., Finkemeier, I. and Somssich, I.E.** (2018) Principles and characteristics of the *Arabidopsis* WRKY regulatory network during early MAMP-triggered immunity. *Plant J.*, **96**, 487-502.
- Bjornson, M., Pimprikar, P., Nürnberger, T. and Zipfel, C.** (2021) The transcriptional landscape of *Arabidopsis thaliana* pattern-triggered immunity. *Nat. Plants*, **7**, 579-586.
- Blanco, F., Salinas, P., Cecchini, N.M., Jordana, X., Van Hummelen, P., Alvarez, M.E. and Holuigue, L.** (2009) Early genomic responses to salicylic acid in *Arabidopsis*. *Plant Mol. Biol.*, **70**, 79-102.
- Boch, J., Bonas, U. and Lahaye, T.** (2014) TAL effectors – pathogen strategies and plant resistance engineering. *New Phytol.*, **204**, 823-832.
- Bodenhausen, N. and Reymond, P.** (2007) Signaling pathways controlling induced resistance to insect herbivores in *Arabidopsis*. *Mol. Plant Microbe Interact.*, **20**, 1406-1420.
- Boter, M., Ruiz-Rivero, O., Abdeen, A. and Pratt, S.** (2004) Conserved MYC transcription factors play a key role in jasmonate signaling both in tomato and *Arabidopsis*. *Genes Dev.*, **18**, 1577-1591.
- Boyle, P., Le Su, E., Rochon, A., Shearer, H.L., Murmu, J., Chu, J.Y., Fobert, P.R. and Després, C.** (2009) The BTB/POZ domain of the *Arabidopsis* disease resistance protein NPR1 interacts with the repression domain of TGA2 to negate its function. *Plant Cell*, **21**, 3700-3713.
- Broekgaarden, C., Caarls, L., Vos, I.A., Pieterse, C.M.J. and Van Wees, S.C.M.** (2015) Ethylene: traffic controller on hormonal crossroads to defense. *Plant Physiol.*, **169**, 2371-2379.
- Bu, Q., Jiang, H., Li, C.-B., Zhai, Q., Zhang, J., Wu, X., Sun, J., Xie, Q. and Li, C.** (2008) Role of the *Arabidopsis thaliana* NAC transcription factors ANAC019 and ANAC055 in regulating jasmonic acid-signaled defense responses. *Cell Res.*, **18**, 756-767.
- Bürger, M. and Chory, J.** (2019) Stressed out about hormones: how plants orchestrate immunity. *Cell Host Microbe*, **26**, 163-172.
- Caarls, L.** (2016) Hormonal signaling in plant immunity. *PhD dissertation, Utrecht University*.
- Caarls, L., Pieterse, C.M.J. and Van Wees, S.C.M.** (2015) How salicylic acid takes transcriptional control over jasmonic acid signaling. *Front. Plant Sci.*, **6**, 170.
- Caarls, L., Van der Does, D., Hickman, R., Jansen, W., Van Verk, M.C., Proietti, S., Lorenzo, O., Solano, R., Pieterse, C.M.J. and Van Wees, S.C.M.** (2017) Assessing the role of ETHYLENE RESPONSE FACTOR transcriptional repressors in salicylic acid-mediated suppression of jasmonic acid-responsive genes. *Plant Cell Physiol.*, **58**, 266-278.

- Cai, H., Huang, Y., Chen, F., Liu, L., Chai, M., Zhang, M., Yan, M., Aslam, M., He, Q. and Qin, Y.** (2021) ERECTA signaling regulates plant immune responses via chromatin-mediated promotion of WRKY33 binding to target genes. *New Phytol.*, **230**, 737-756.
- Caillaud, M.-C., Asai, S., Rallapalli, G., Piquerez, S., Fabro, G. and Jones, J.D.G.** (2013) A downy mildew effector attenuates salicylic acid-triggered immunity in Arabidopsis by interacting with the host Mediator complex. *PLoS Biol.*, **12**, e1001919.
- Canonne, J., Marino, D., Jauneau, A., Pouzet, C., Brière, C., Roby, D. and Rivas, S.** (2011) The *Xanthomonas* type III effector XopD targets the Arabidopsis transcription factor MYB30 to suppress plant defense. *Plant Cell*, **23**, 3498-3511.
- Cao, H., Bowling, S.A., Gordon, A.S. and Dong, X.** (1994) Characterization of an Arabidopsis mutant that is nonresponsive to inducers of systemic acquired resistance. *Plant Cell*, **6**, 1583-1592.
- Çevik, V., Kidd, B.N., Zhang, P., Hill, C., Kiddle, S., Denby, K.J., Holub, E.B., Cahill, D.M., Manners, J.M., Schenk, P.M., Beynon, J. and Kazan, K.** (2012) MEDIATOR25 acts as an integrative hub for the regulation of jasmonate-responsive gene expression in Arabidopsis. *Plant Physiol.*, **160**, 541-555.
- Chakraborty, M., Gangappa, S.N., Maurya, J.P., Sethi, V., Srivastava, A.K., Singh, A., Dutta, S., Ojha, M., Gupta, N., Sengupta, M., Ram, H. and Chattopadhyay, S.** (2019) Functional interrelation of MYC2 and HY5 plays an important role in Arabidopsis seedling development. *Plant J.*, **99**, 1080-1097.
- Chang, K.N., Zhong, S., Weirauch, M.T., Hon, G., Pelizzola, M., Li, H., Huang, S.C., Schmitz, R.J., Urich, M.A. and Kuo, D.** (2013) Temporal transcriptional response to ethylene gas drives growth hormone cross-regulation in Arabidopsis. *Elife*, **2**, e00675.
- Chen, C.Y., Liu, Y.Q., Song, W.M., Chen, D.Y., Chen, F.Y., Chen, X.Y., Chen, Z.W., Ge, S.X., Wang, C.Z., Zhan, S., Chen, X.Y. and Mao, Y.B.** (2019) An effector from cotton bollworm oral secretion impairs host plant defense signaling. *Proc. Natl. Acad. Sci. U.S.A.*, **116**, 14331-14338.
- Chen, H., Chen, J., Li, M., Chang, M., Xu, K., Shang, Z., Zhao, Y., Palmer, I., Zhang, Y., McGill, J., Alfano, J.R., Nishimura, M.T., Liu, F. and Fu, Z.Q.** (2017) A bacterial type III effector targets the master regulator of salicylic acid signaling, NPR1, to subvert plant immunity. *Cell Host Microbe*, **22**, 777-788.e777.
- Chen, H.Y., Hsieh, E.J., Cheng, M.C., Chen, C.Y., Hwang, S.Y. and Lin, T.P.** (2016) ORA47 (octadecanoid-responsive AP2/ERF-domain transcription factor 47) regulates jasmonic acid and abscisic acid biosynthesis and signaling through binding to a novel *cis*-element. *New Phytol.*, **211**, 599-613.
- Chen, J., Zhang, J., Kong, M., Freeman, A., Chen, H. and Liu, F.** (2021) More stories to tell: NONEXPRESSOR OF PATHOGENESIS-RELATED GENES1, a salicylic acid receptor. *Plant Cell Environ.*, **44**, 1716-1727.
- Chen, K., Li, G.-J., Bressan, R.A., Song, C.-P., Zhu, J.-K. and Zhao, Y.** (2020) Abscisic acid dynamics, signaling, and functions in plants. *J. Integr. Plant Biol.*, **62**, 25-54.
- Chen, R., Jiang, H., Li, L., Zhai, Q., Qi, L., Zhou, W., Liu, X., Li, H., Zheng, W., Sun, J. and Li, C.** (2012) The Arabidopsis mediator subunit MED25 differentially regulates jasmonate and abscisic acid signaling through interacting with the MYC2 and ABI5 transcription factors. *Plant Cell*, **24**, 2898-2916.
- Chen, S., Jia, H., Wang, X., Shi, C., Wang, X., Ma, P., Wang, J., Ren, M. and Li, J.** (2020) Hydrogen sulfide positively regulates abscisic acid signaling through persulfidation of SnRK2.6 in guard cells. *Mol. Plant*, **13**, 732-744.

- Cheng, Y.T., Germain, H., Wiermer, M., Bi, D., Xu, F., Garcia, A.V., Wirthmueller, L., Després, C., Parker, J.E., Zhang, Y. and Li, X.** (2009) Nuclear pore complex component MOS7/Nup88 is required for innate immunity and nuclear accumulation of defense regulators in Arabidopsis. *Plant Cell*, **21**, 2503–2516.
- Chico, J.M., Lechner, E., Fernandez-Barbero, G., Canibano, E., García-Casado, G., Franco-Zorrilla, J.M., Hammann, P., Zamarreño, A.M., García-Mina, J.M. and Rubio, V.** (2020) CUL3^{BPM} E3 ubiquitin ligases regulate MYC2, MYC3, and MYC4 stability and JA responses. *Proc. Natl. Acad. Sci. U.S.A.*, **117**, 6205–6215.
- Chini, A., Fonseca, S., Fernandez, G., Adie, B., Chico, J.M., Lorenzo, O., Garcia-Casado, G., Lopez-Vidriero, I., Lozano, F.M., Ponce, M.R., Micol, J.L. and Solano, R.** (2007) The JAZ family of repressors is the missing link in jasmonate signalling. *Nature*, **448**, 666–671.
- Chini, A., Monte, I., Zamarreño, A.M., Hamberg, M., Lassueur, S., Reymond, P., Weiss, S., Stintzi, A., Schaller, A. and Porzel, A.** (2018) An OPR3-independent pathway uses 4,5-didehydrojasmonate for jasmonate synthesis. *Nat. Chem. Biol.*, **14**, 171.
- Choi, H.-I., Hong, J.-H., Ha, J.-O., Kang, J.-Y. and Kim, S.Y.** (2000) ABFs, a family of ABA-responsive element binding factors. *J. Biol. Chem.*, **275**, 1723–1730.
- Chong, L., Hsu, C.-C. and Zhu, Y.** (2022) Advances in mass spectrometry-based phosphoproteomics for elucidating abscisic acid signaling and plant responses to abiotic stress. *J. Exp. Bot.*, **73**, 6547–6557.
- Chung, H.S., Cooke, T.F., Depew, C.L., Patel, L.C., Ogawa, N., Kobayashi, Y. and Howe, G.A.** (2010) Alternative splicing expands the repertoire of dominant JAZ repressors of jasmonate signaling. *Plant J.*, **63**, 613–622.
- Chung, H.S. and Howe, G.A.** (2009) A critical role for the TIFY motif in repression of jasmonate signaling by a stabilized splice variant of the JASMONATE ZIM-domain protein JAZ10 in Arabidopsis. *Plant Cell*, **21**, 131–145.
- Coolen, S., Proietti, S., Hickman, R., Davila Olivas, N.H., Huang, P.P., Van Verk, M.C., Van Pelt, J.A., Wittenberg, A.H., De Vos, M., Prins, M., Van Loon, J.J.A., Aarts, M.G.M., Dicke, M., Pieterse, C.M.J. and Van Wees, S.C.M.** (2016) Transcriptome dynamics of Arabidopsis during sequential biotic and abiotic stresses. *Plant J.*, **86**, 249–267.
- Covington, M.F., Maloof, J.N., Straume, M., Kay, S.A. and Harmer, S.L.** (2008) Global transcriptome analysis reveals circadian regulation of key pathways in plant growth and development. *Genome Biol.*, **9**, R130.
- Cox, K.L., Meng, F., Wilkins, K.E., Li, F., Wang, P., Booher, N.J., Carpenter, S.C.D., Chen, L.-Q., Zheng, H., Gao, X., Zheng, Y., Fei, Z., Yu, J.Z., Isakeit, T., Wheeler, T., Frommer, W.B., He, P., Bogdanove, A.J. and Shan, L.** (2017) TAL effector driven induction of a SWEET gene confers susceptibility to bacterial blight of cotton. *Nat. Commun.*, **8**, 15588.
- Crooks, G.E., Hon, G., Chandonia, J.M. and Brenner, S.E.** (2004) WebLogo: A sequence logo generator. *Genome Res.*, **14**, 1188–1190.
- Cruz Castillo, M., Martínez, C., Buchala, A., Métraux, J.P. and León, J.** (2004) Gene-specific involvement of beta-oxidation in wound-activated responses in Arabidopsis. *Plant Physiol.*, **135**, 85–94.
- Cui, H., Qiu, J., Zhou, Y., Bhandari, D.D., Zhao, C., Bautor, J. and Parker, J.E.** (2018) Antagonism of transcription factor MYC2 by EDS1/PAD4 complexes bolsters salicylic acid defense in Arabidopsis effector-triggered immunity. *Mol. Plant*, **11**, 1053–1066.
- Cui, H., Tsuda, K. and Parker, J.E.** (2015) Effector-triggered immunity: from pathogen perception to robust defense. *Annu. Rev. Plant Biol.*, **66**, 487–511.

- Czechowski, T., Stitt, M., Altmann, T., Udvardi, M.K. and Scheible, W.** (2005) Genome-wide identification and testing of superior reference genes for transcript normalization in Arabidopsis. *Plant Physiol.*, **139**, 5–17.
- Dangl, J.L., Horvath, D.M. and Staskawicz, B.J.** (2013) Pivoting the plant immune system from dissection to deployment. *Science*, **341**, 746–751.
- De Clercq, I., Van de Velde, J., Luo, X., Liu, L., Storme, V., Van Bel, M., Pottie, R., Vanechoutte, D., Van Breusegem, F. and Vandepoele, K.** (2021) Integrative inference of transcriptional networks in Arabidopsis yields novel ROS signalling regulators. *Nat. Plants*, **7**, 500–513.
- Decker, C.J. and Parker, R.** (2012) P-bodies and stress granules: possible roles in the control of translation and mRNA degradation. *Cold Spring Harb. Perspect. Biol.*, **4**, a012286.
- Delaney, T.P., Friedrich, L. and Ryals, J.A.** (1995) Arabidopsis signal transduction mutant defective in chemically and biologically induced disease resistance. *Proc. Natl. Acad. Sci. U.S.A.*, **92**, 6602–6606.
- Després, C., Chubak, C., Rochon, A., Clark, R., Bethune, T., Desveaux, D. and Fobert, P.R.** (2003) The Arabidopsis NPR1 disease resistance protein is a novel cofactor that confers redox regulation of DNA binding activity to the basic domain/leucine zipper transcription factor TGA1. *Plant Cell*, **15**, 2181–2191.
- Ding, P. and Redkar, A.** (2018) Pathogens suppress host transcription factors for rampant proliferation. *Trends Plant Sci.*, **23**, 950–953.
- Ding, P., Sakai, T., Krishna Shrestha, R., Manosalva Perez, N., Guo, W., Ngou, B.P.M., He, S., Liu, C., Feng, X., Zhang, R., Vandepoele, K., MacLean, D. and Jones, J.D.G.** (2021) Chromatin accessibility landscapes activated by cell-surface and intracellular immune receptors. *J. Exp. Bot.*, **72**, 7927–7941.
- Ding, Y., Liu, N., Virilouvet, L., Riethoven, J.-J., Fromm, M. and Avramova, Z.** (2013) Four distinct types of dehydration stress memory genes in *Arabidopsis thaliana*. *BMC Plant Biol.*, **13**, 229.
- Ding, Y., Sun, T., Ao, K., Peng, Y., Zhang, Y., Li, X. and Zhang, Y.** (2018) Opposite roles of salicylic acid receptors NPR1 and NPR3/NPR4 in transcriptional regulation of plant immunity. *Cell*, **173**, 1454–1467.
- Dinh, S.T., Baldwin, I.T. and Galis, I.** (2013) The HERBIVORE ELICITOR-REGULATED1 gene enhances abscisic acid levels and defenses against herbivores in *Nicotiana attenuata* plants. *Plant Physiol.*, **162**, 2106–2124.
- Dodds, P.N. and Rathjen, J.P.** (2010) Plant immunity: towards an integrated view of plant-pathogen interactions. *Nat. Rev. Genet.*, **11**, 539–548.
- Dolgikh, V.A., Pukhovaya, E.M. and Zemlyanskaya, E.V.** (2019) Shaping ethylene response: the role of EIN3/EIL1 transcription factors. *Front. Plant Sci.*, **10**.
- Dombrecht, B., Xue, G.P., Sprague, S.J., Kirkegaard, J.A., Ross, J.J., Reid, J.B., Fitt, G.P., Sewelam, N., Schenk, P.M., Manners, J.M. and Kazan, K.** (2007) MYC2 differentially modulates diverse jasmonate-dependent functions in Arabidopsis. *Plant Cell*, **19**, 2225–2245.
- Dorrity, M.W., Alexandre, C.M., Hamm, M.O., Vigil, A.-L., Fields, S., Queitsch, C. and Cuperus, J.T.** (2021) The regulatory landscape of *Arabidopsis thaliana* roots at single-cell resolution. *Nat. Commun.*, **12**, 3334.
- Downen, R.H., Pelizzola, M., Schmitz, R.J., Lister, R., Downen, J.M., Nery, J.R., Dixon, J.E. and Ecker, J.R.** (2012) Widespread dynamic DNA methylation in response to biotic stress. *Proc. Natl. Acad. Sci. U.S.A.*, **109**, E2183–E2191.

- Doyle, E.L., Stoddard, B.L., Voytas, D.F. and Bogdanove, A.J.** (2013) TAL effectors: highly adaptable phyto-bacterial virulence factors and readily engineered DNA-targeting proteins. *Trends Cell Biol.*, **23**, 390-398.
- Dröge-Laser, W., Snoek, B.L., Snel, B. and Weiste, C.** (2018) The Arabidopsis bZIP transcription factor family—an update. *Curr. Opin. Plant Biol.*, **45**, 36-49.
- Dubos, C., Stracke, R., Grotewold, E., Weisshaar, B., Martin, C. and Lepiniec, L.** (2010) MYB transcription factors in Arabidopsis. *Trends Plant Sci.*, **15**, 573-581.
- Dvořák Tomašítková, E., Hafrén, A., Trejo-Arellano, M.S., Rasmussen, S.R., Sato, H., Santos-González, J., Köhler, C., Hennig, L. and Hofius, D.** (2021) Polycomb Repressive Complex 2 and KRYPTONITE regulate pathogen-induced programmed cell death in Arabidopsis. *Plant Physiol.*, **185**, 2003-2021.
- El Oirdi, M., El Rahman, T.A., Rigano, L., El Hadrami, A., Rodriguez, M.C., Daayf, F., Vojnov, A. and Bouarab, K.** (2011) *Botrytis cinerea* manipulates the antagonistic effects between immune pathways to promote disease development in tomato. *Plant Cell*, **23**, 2405-2421.
- Erb, M. and Reymond, P.** (2019) Molecular interactions between plants and insect herbivores. *Annu. Rev. Plant Biol.*, **70**, 527-557.
- Erdmann, R.M. and Picard, C.L.** (2020) RNA-directed DNA methylation. *PLoS Genet.*, **16**, e1009034.
- Escudero-Martinez, C. and Bulgarelli, D.** (2023) Engineering the crop microbiota through host genetics. *Annu. Rev. Phytopathol.*, **61**, TBD.
- Essuman, K., Milbrandt, J., Dangl, J.L. and Nishimura, M.T.** (2022) Shared TIR enzymatic functions regulate cell death and immunity across the tree of life. *Science*, **377**, eabo0001.
- Evenson, R.E. and Gollin, D.** (2003) Assessing the impact of the green revolution, 1960 to 2000. *Science*, **300**, 758-762.
- Fallath, T., Kidd, B.N., Stiller, J., Davoine, C., Björklund, S., Manners, J.M., Kazan, K. and Schenk, P.M.** (2017) MEDIATOR18 and MEDIATOR20 confer susceptibility to *Fusarium oxysporum* in *Arabidopsis thaliana*. *PLoS One*, **12**, e0176022.
- Fan, J., Hill, L., Crooks, C., Doerner, P. and Lamb, C.** (2009) Abscisic acid has a key role in modulating diverse plant-pathogen interactions. *Plant Physiol.*, **150**, 1750-1761.
- Farmer, E.E., Gao, Y.-Q., Lenzoni, G., Wolfender, J.-L. and Wu, Q.** (2020) Wound- and mechanostimulated electrical signals control hormone responses. *New Phytol.*, **227**, 1037-1050.
- Fernández-Calvo, P., Chini, A., Fernández-Barbero, G., Chico, J.M., Gimenez-Ibanez, S., Geerinck, J., Eeckhout, D., Schweizer, F., Godoy, M., Franco-Zorrilla, J.M., Pauwels, L., Witters, E., Puga, M.I., Paz-Ares, J., Goossens, A., Reymond, P., De Jaeger, G. and Solano, R.** (2011) The Arabidopsis bHLH transcription factors MYC3 and MYC4 are targets of JAZ repressors and act additively with MYC2 in the activation of jasmonate responses. *Plant Cell*, **23**, 701-715.
- Finkelstein, R.R. and Lynch, T.J.** (2000) The Arabidopsis abscisic acid response gene *ABI5* encodes a basic leucine zipper transcription factor. *Plant Cell*, **12**, 599-609.
- Fonseca, S., Chini, A., Hamberg, M., Adie, B., Porzel, A., Kramell, R., Miersch, O., Wasternack, C. and Solano, R.** (2009) (+)-7-*iso*-Jasmonoyl-L-isoleucine is the endogenous bioactive jasmonate. *Nat. Chem. Biol.*, **5**, 344-350.
- Franco-Zorrilla, J.M., López-Vidriero, I., Carrasco, J.L., Godoy, M., Vera, P. and Solano, R.** (2014) DNA-binding specificities of plant transcription factors and their potential to define target genes. *Proc. Natl. Acad. Sci. U.S.A.*, **111**, 2367-2372.
- Franklin, K.A.** (2008) Shade avoidance. *New Phytol.*, **179**, 930-944.

- French, E., Kaplan, I., Iyer-Pascuzzi, A., Nakatsu, C.H. and Enders, L.** (2021) Emerging strategies for precision microbiome management in diverse agroecosystems. *Nat. Plants*, **7**, 256-267.
- Fu, Z.Q., Yan, S., Saleh, A., Wang, W., Ruble, J., Oka, N., Mohan, R., Spoel, S.H., Tada, Y., Zheng, N. and Dong, X.** (2012) NPR3 and NPR4 are receptors for the immune signal salicylic acid in plants. *Nature*, **486**, 228–232.
- Fujii, H., Chinnusamy, V., Rodrigues, A., Rubio, S., Antoni, R., Park, S.-Y., Cutler, S.R., Sheen, J., Rodriguez, P.L. and Zhu, J.-K.** (2009) In vitro reconstitution of an abscisic acid signalling pathway. *Nature*, **462**, 660-664.
- Furniss, J.J. and Spoel, S.H.** (2015) Cullin-RING ubiquitin ligases in salicylic acid-mediated plant immune signaling. *Front. Plant Sci.*, **6**, 154.
- Gao, Q.-M., Zhu, S., Kachroo, P. and Kachroo, A.** (2015) Signal regulators of systemic acquired resistance. *Front. Plant Sci.*, **6**, 228.
- Gao, Q.M., Venugopal, S., Navarre, D. and Kachroo, A.** (2011) Low oleic acid-derived repression of jasmonic acid-inducible defense responses requires the WRKY50 and WRKY51 proteins. *Plant Physiol.*, **155**, 464–476.
- Gao, X. and He, P.** (2013) Nuclear dynamics of Arabidopsis calcium-dependent protein kinases in effector-triggered immunity. *Plant Signal. Behav.*, **8**, e23868.
- Garner, C.M., Kim, S.H., Spears, B.J. and Gassmann, W.** (2016) Express yourself: Transcriptional regulation of plant innate immunity. *Semin. Cell Dev. Biol.*, **56**, 150-162.
- Gimenez-Ibanez, S., Boter, M., Fernandez-Barbero, G., Chini, A., Rathjen, J.P. and Solano, R.** (2014) The bacterial effector HopX1 targets JAZ transcriptional repressors to activate jasmonate signaling and promote infection in Arabidopsis. *PLoS Biol.*, **12**, e1001792.
- Gimenez-Ibanez, S., Boter, M., Ortigosa, A., García-Casado, G., Chini, A., Lewsey, M.G., Ecker, J.R., Ntoukakis, V. and Solano, R.** (2017) JAZ2 controls stomata dynamics during bacterial invasion. *New Phytol.*, **213**, 1378-1392.
- Gimenez-Ibanez, S. and Solano, R.** (2013) Nuclear jasmonate and salicylate signaling and crosstalk in defense against pathogens. *Front. Plant Sci.*, **4**, 72.
- Glazebrook, J.** (2005) Contrasting mechanisms of defense against biotrophic and necrotrophic pathogens. *Annu. Rev. Phytopathol.*, **43**, 205–227.
- Glazebrook, J., Chen, W., Estes, B., Chang, H., Nawrath, C., Métraux, J., Zhu, T. and Katagiri, F.** (2003) Topology of the network integrating salicylate and jasmonate signal transduction derived from global expression phenotyping. *Plant J.*, **34**, 217–228.
- González-Guzmán, M., Apostolova, N., Bellés, J.M., Barrero, J.M., Piqueras, P., Ponce, M.a.R., Micol, J.L., Serrano, R.n. and Rodríguez, P.L.** (2002) The short-chain alcohol dehydrogenase ABA2 catalyzes the conversion of xanthoxin to abscisic aldehyde. *Plant Cell*, **14**, 1833-1846.
- Gordán, R., Shen, N., Dror, I., Zhou, T., Horton, J., Rohs, R. and Bulyk, M.L.** (2013) Genomic regions flanking E-box binding sites influence DNA binding specificity of bHLH transcription factors through DNA shape. *Cell Rep.*, **3**, 1093-1104.
- Grant, C.E., Bailey, T.L. and Noble, W.S.** (2011) FIMO: scanning for occurrences of a given motif. *Bioinformatics*, **27**, 1017–1018.
- Gu, Y., Zebell, S.G., Liang, Z., Wang, S., Kang, B.-H. and Dong, X.** (2016) Nuclear pore permeabilization is a convergent signaling event in Effector-Triggered Immunity. *Cell*, **166**, 1526-1538.
- Haag, J.R. and Pikaard, C.S.** (2011) Multisubunit RNA polymerases IV and V: purveyors of non-coding RNA for plant gene silencing. *Nat. Rev. Mol. Cell Biol.*, **12**, 483-492.

- Halter, T., Wang, J., Ameseffe, D., Lastrucci, E., Charvin, M., Singla Rastogi, M. and Navarro, L.** (2021) The *Arabidopsis* active demethylase ROS1 *cis*-regulates defence genes by erasing DNA methylation at promoter-regulatory regions. *Elife*, **10**, e62994.
- Han, S.-K., Wu, M.-F., Cui, S. and Wagner, D.** (2015) Roles and activities of chromatin remodeling ATPases in plants. *Plant J.*, **83**, 62-77.
- Han, X. and Kahmann, R.** (2019) Manipulation of phytohormone pathways by effectors of filamentous plant pathogens. *Front. Plant Sci.*, **10**, 822.
- Hannan Parker, A., Wilkinson, S.W. and Ton, J.** (2022) Epigenetics: a catalyst of plant immunity against pathogens. *New Phytol.*, **233**, 66-83.
- Harrison, S.J., Mott, E.K., Parsley, K., Aspinall, S., Gray, J.C. and Cottage, A.** (2006) A rapid and robust method of identifying transformed *Arabidopsis thaliana* seedlings following floral dip transformation. *Plant Methods*, **2**, 19.
- Harvey, S., Kumari, P., Lapin, D., Griebel, T., Hickman, R., Guo, W., Zhang, R., Parker, J.E., Beynon, J. and Denby, K.** (2020) Downy mildew effector HaRxL21 interacts with the transcriptional repressor TOPLESS to promote pathogen susceptibility. *PLoS Pathog.*, **16**, e1008835.
- He, W., Brumos, J., Li, H., Ji, Y., Ke, M., Gong, X., Zeng, Q., Li, W., Zhang, X., An, F., Wen, X., Li, P., Chu, J., Sun, X., Yan, C., Yan, N., Xie, D.-Y., Raikhel, N., Yang, Z., Stepanova, A.N., Alonso, J.M. and Guo, H.** (2011) A small-molecule screen identifies L-kynurenine as a competitive inhibitor of TAA1/TAR activity in ethylene-directed auxin biosynthesis and root growth in *Arabidopsis*. *Plant Cell*, **23**, 3944-3960.
- He, X., Jiang, J., Wang, C.Q. and Dehesh, K.** (2017) ORA59 and EIN3 interaction couples jasmonate-ethylene synergistic action to antagonistic salicylic acid regulation of *PDF* expression. *J. Integr. Plant Biol.*, **59**, 275-287.
- He, Y., Hong, G., Zhang, H., Tan, X., Li, L., Kong, Y., Sang, T., Xie, K., Wei, J., Li, J., Yan, F., Wang, P., Tong, H., Chu, C., Chen, J. and Sun, Z.** (2020) The OsGSK2 kinase integrates brassinosteroid and jasmonic acid signaling by interacting with OsJAZ4. *Plant Cell*, **32**, 2806-2822.
- He, Y., Zhang, H., Sun, Z., Li, J., Hong, G., Zhu, Q., Zhou, X., MacFarlane, S., Yan, F. and Chen, J.** (2017) Jasmonic acid-mediated defense suppresses brassinosteroid-mediated susceptibility to Rice black streaked dwarf virus infection in rice. *New Phytol.*, **214**, 388-399.
- He, Z., Webster, S. and He, S.Y.** (2022) Growth–defense trade-offs in plants. *Curr. Biol.*, **32**, R634-R639.
- Heard, N.A.** (2011) Iterative reclassification in agglomerative clustering. *J. Comput. Graph. Stat.*, **20**, 920-936.
- Heard, N.A., Holmes, C.C. and Stephens, D.A.** (2006) A quantitative study of gene regulation involved in the immune response of anopheline mosquitoes: An application of Bayesian hierarchical clustering of curves. *J. Am. Stat. Assoc.*, **101**, 18-29.
- Heyndrickx, K.S., Van de Velde, J., Wang, C., Weigel, D. and Vandepoele, K.** (2014) A functional and evolutionary perspective on transcription factor binding in *Arabidopsis thaliana*. *Plant Cell*, **26**, 3894-3910.
- Hickman, R., Mendes, M.P., Van Verk, M.C., Van Dijken, A.J.H., Di Sora, J., Denby, K., Pieterse, C.M.J. and Van Wees, S.C.M.** (2019) Transcriptional dynamics of the salicylic acid response and its interplay with the jasmonic acid pathway. *bioRxiv*, 742742.

- Hickman, R., Van Verk, M.C., Van Dijken, A.J.H., Mendes, M.P., Vroegop-Vos, I.A., Caarls, L., Steenbergen, M., Van der Nagel, I., Wesselink, G.J., Jironkin, A., Talbot, A., Rhodes, J., De Vries, M., Schuurink, R.C., Denby, K., Pieterse, C.M.J. and Wees, S.C.M.** (2017) Architecture and dynamics of the jasmonic acid gene regulatory network. *Plant Cell*, **29**, 2086-2105.
- Higashi, K., Ishiga, Y., Inagaki, Y., Toyoda, K., Shiraishi, T. and Ichinose, Y.** (2008) Modulation of defense signal transduction by flagellin-induced WRKY41 transcription factor in *Arabidopsis thaliana*. *Mol. Genet. Genom.*, **279**, 303-312.
- Hillmer, R.A., Tsuda, K., Rallapalli, G., Asai, S., Truman, W., Papke, M.D., Sakakibara, H., Jones, J.D., Myers, C.L. and Katagiri, F.** (2017) The highly buffered Arabidopsis immune signaling network conceals the functions of its components. *PLoS Genet.*, **13**, e1006639.
- Hoth, S., Niedermeier, M., Feuerstein, A., Hornig, J. and Sauer, N.** (2010) An ABA-responsive element in the *AtSUC1* promoter is involved in the regulation of *AtSUC1* expression. *Planta*, **232**, 911-923.
- Hou, X., Ding, L. and Yu, H.** (2013) Crosstalk between GA and JA signaling mediates plant growth and defense. *Plant Cell Rep.*, **32**, 1067-1074.
- Hou, X., Lee, L.Y.C., Xia, K., Yen, Y. and Yu, H.** (2010) DELLAs modulate jasmonate signaling via competitive binding to JAZs. *Dev. Cell*, **19**, 884-894.
- Hou, Y.-J., Zhu, Y., Wang, P., Zhao, Y., Xie, S., Batelli, G., Wang, B., Duan, C.-G., Wang, X. and Xing, L.** (2016) Type One Protein Phosphatase 1 and its regulatory protein Inhibitor 2 negatively regulate ABA signaling. *PLoS Genet.*, **12**, e1005835.
- Howe, G.A., Major, I.T. and Koo, A.J.** (2018) Modularity in jasmonate signaling for multistress resilience. *Annu. Rev. Plant Biol.*, **69**, 387-415.
- Hu, Y., Dong, Q. and Yu, D.** (2012) Arabidopsis WRKY46 coordinates with WRKY70 and WRKY53 in basal resistance against pathogen *Pseudomonas syringae*. *Plant Sci.*, **185-186**, 288-297.
- Huang, C.-Y., Rangel, D.S., Qin, X., Bui, C., Li, R., Jia, Z., Cui, X. and Jin, H.** (2021) The chromatin-remodeling protein BAF60/SWP73A regulates the plant immune receptor NLRs. *Cell Host Microbe*, **29**, 425-434.e424.
- Huang, M., Zhang, Y., Wang, Y., Xie, J., Cheng, J., Fu, Y., Jiang, D., Yu, X. and Li, B.** (2022) Active DNA demethylation regulates MAMP-triggered immune priming in Arabidopsis. *J. Genet. Genomics*.
- Huang, P., Dong, Z., Guo, P., Zhang, X.C., Qiu, Y., Li, B., Wang, Y. and Guo, H.J.** (2020) Salicylic acid suppresses apical hook formation via NPR1-mediated repression of EIN3 and EIL1 in Arabidopsis. *Plant Cell*, **32**, 612-629.
- Ishihama, N., Choi, S.-w., Noutoshi, Y., Saska, I., Asai, S., Takizawa, K., He, S.Y., Osada, H. and Shirasu, K.** (2021) Oxycam-type non-steroidal anti-inflammatory drugs inhibit NPR1-mediated salicylic acid pathway. *Nat. Commun.*, **12**, 7303.
- Jacob, P., Kim, N.H., Wu, F., El-Kasmi, F., Chi, Y., Walton, W.G., Furzer, O.J., Lietzan, A.D., Sunil, S., Kempthorn, K., Redinbo, M.R., Pei, Z.-M., Wan, L. and Dangl, J.L.** (2021) Plant helper immune receptors are Ca²⁺-permeable nonselective cation channels. *Science*, **373**, 420-425.
- Jakoby, M., Weissshaar, B., Dröge-Laser, W., Vicente-Carbajosa, J., Tiedemann, J., Kroj, T. and Parcy, F.** (2002) bZIP transcription factors in Arabidopsis. *Trends Plant Sci.*, **7**, 106-111.
- Jeong, I.S., Aksoy, E., Fukudome, A., Akhter, S., Hiraguri, A., Fukuhara, T., Bahk, J.D. and Koiwa, H.** (2013) Arabidopsis C-Terminal Domain Phosphatase-Like 1 functions in miRNA accumulation and DNA methylation. *PLoS One*, **8**, e74739.
- Jiang, S., Yao, J., Ma, K.-W., Zhou, H., Song, J., He, S.Y. and Ma, W.** (2013) Bacterial effector activates jasmonate signaling by directly targeting JAZ transcriptional repressors. *PLoS Pathog.*, **9**, e1003715.

- Jiao, C., Li, K., Zuo, Y., Gong, J., Guo, Z. and Shen, Y.** (2022) CALMODULIN1 and WRKY53 function in plant defense by negatively regulating the jasmonic acid biosynthesis pathway in Arabidopsis. *Int. J. Mol. Sci.*, **23**, 7718.
- Jirage, D., Tootle, T.L., Reuber, T.L., Frost, L.N., Feys, B.J., Parker, J.E., Ausubel, F.M. and Glazebrook, J.** (1999) *Arabidopsis thaliana* PAD4 encodes a lipase-like gene that is important for salicylic acid signaling. *Proc. Natl. Acad. Sci. U.S.A.*, **96**, 13583-13588.
- Jolma, A., Yin, Y., Nitta, K.R., Dave, K., Popov, A., Taipale, M., Enge, M., Kivioja, T., Morgunova, E. and Taipale, J.** (2015) DNA-dependent formation of transcription factor pairs alters their binding specificity. *Nature*, **527**, 384-388.
- Jones, J.D.G. and Dangl, J.L.** (2006) The plant immune system. *Nature*, **444**, 323-329.
- Kadota, Y., Shirasu, K. and Zipfel, C.** (2015) Regulation of the NADPH oxidase RBOHD during plant immunity. *Plant Cell Physiol.*, **56**, 1472-1480.
- Kalde, M., Barth, M., Somssich, I.E. and Lippok, B.** (2003) Members of the Arabidopsis WRKY Group III transcription factors are part of different plant defense signaling pathways. *Mol. Plant Microbe Interact.*, **16**, 295-305.
- Kazan, K. and Manners, J.M.** (2013) MYC2: the master in action. *Mol. Plant*, **6**, 686-703.
- Khanna, R., Shen, Y., Toledo-Ortiz, G., Kikis, E.A., Johannesson, H., Hwang, Y.-S. and Quail, P.H.** (2006) Functional profiling reveals that only a small number of phytochrome-regulated early-response genes in Arabidopsis are necessary for optimal deetiolation. *Plant Cell*, **18**, 2157-2171.
- Kim, T.-W., Guan, S., Sun, Y., Deng, Z., Tang, W., Shang, J.-X., Sun, Y., Burlingame, A.L. and Wang, Z.-Y.** (2009) Brassinosteroid signal transduction from cell-surface receptor kinases to nuclear transcription factors. *Nat. Cell Biol.*, **11**, 1254-1260.
- Kim, Y., Gilmour, S.J., Chao, L., Park, S. and Thomashow, M.F.** (2020) Arabidopsis CAMTA transcription factors regulate pipecolic acid biosynthesis and priming of immunity genes. *Mol. Plant*, **13**, 157-168.
- Kim, Y., Park, S., Gilmour, S.J. and Thomashow, M.F.** (2013) Roles of CAMTA transcription factors and salicylic acid in configuring the low-temperature transcriptome and freezing tolerance of Arabidopsis. *Plant J.*, **75**, 364-376.
- Kim, Y., Tsuda, K., Igarashi, D., Hillmer, R.A., Sakakibara, H., Myers, C.L. and Katagiri, F.** (2014) Mechanisms underlying robustness and tunability in a plant immune signaling network. *Cell Host Microbe*, **15**, 84-94.
- Kinkema, M., Fan, W. and Dong, X.** (2000) Nuclear localization of NPR1 is required for activation of PR gene expression. *Plant Cell*, **12**, 2339-2350.
- Kitazawa, Y., Iwabuchi, N., Maejima, K., Sasano, M., Matsumoto, O., Koinuma, H., Tokuda, R., Suzuki, M., Oshima, K., Namba, S. and Yamaji, Y.** (2022) A phytoplasma effector acts as a ubiquitin-like mediator between floral MADS-box proteins and proteasome shuttle proteins. *Plant Cell*, **34**, 1709-1723.
- Ko, D.K. and Brandizzi, F.** (2020) Network-based approaches for understanding gene regulation and function in plants. *Plant J.*, **104**, 302-317.
- Koornneef, A., Leon-Reyes, A., Ritsema, T., Verhage, A., Den Otter, F.C., Van Loon, L.C. and Pieterse, C.M.J.** (2008) Kinetics of salicylate-mediated suppression of jasmonate signaling reveal a role for redox modulation. *Plant Physiol.*, **147**, 1358-1368.
- Krawczyk, S., Thurrow, C., Niggeweg, R. and Gatz, C.** (2002) Analysis of the spacing between the two palindromes of *activation sequence-1* with respect to binding to different TGA factors and transcriptional activation potential. *Nucleic Acids Res.*, **30**, 775-781.

- Krouk, G., Mirowski, P., LeCun, Y., Shasha, D.E. and Coruzzi, G.M.** (2010) Predictive network modeling of the high-resolution dynamic plant transcriptome in response to nitrate. *Genome Biol.*, **11**, R123.
- Kumar, S., Zavaliev, R., Wu, Q., Zhou, Y., Cheng, J., Dillard, L., Powers, J., Withers, J., Zhao, J., Guan, Z., Borgnia, M.J., Bartsaghi, A., Dong, X. and Zhou, P.** (2022) Structural basis of NPR1 in activating plant immunity. *Nature*, **605**, 561-566.
- Lachowiec, J., Mason, G.A., Schultz, K. and Queitsch, C.** (2018) Redundancy, feedback, and robustness in the *Arabidopsis thaliana* BZR/BEH gene family. *Front. Genet.*, **9**.
- Lai, Z., Schluttenhofer, C.M., Bhide, K., Shreve, J., Thimmapuram, J., Lee, S.Y., Yun, D.-J. and Mengiste, T.** (2014) MED18 interaction with distinct transcription factors regulates multiple plant functions. *Nat. Commun.*, **5**, 3064.
- Lapin, D., Johannrees, O., Wu, Z., Li, X. and Parker, J.E.** (2022) Molecular innovations in plant TIR-based immunity signaling. *Plant Cell*, **34**, 1479-1496.
- Lata, C. and Prasad, M.** (2011) Role of DREBs in regulation of abiotic stress responses in plants. *J. Exp. Bot.*, **62**, 4731-4748.
- Lee, T.A. and Bailey-Serres, J.** (2019) Integrative analysis from the epigenome to translome uncovers patterns of dominant nuclear regulation during transient stress. *Plant Cell*, **31**, 2573-2595.
- Leon-Reyes, A., Du, Y., Koornneef, A., Proietti, S., Körbes, A.P., Memelink, J., Pieterse, C.M.J. and Ritsema, T.** (2010a) Ethylene signaling renders the jasmonate response of *Arabidopsis* insensitive to future suppression by salicylic acid. *Mol. Plant Microbe Interact.*, **23**, 187-197.
- Leon-Reyes, A., Spoel, S.H., De Lange, E.S., Abe, H., Kobayashi, M., Tsuda, S., Millenaar, F.F., Welschen, R.A.M., Ritsema, T. and Pieterse, C.M.J.** (2009) Ethylene modulates the role of NONEXPRESSOR OF PATHOGENESIS-RELATED GENES1 in cross talk between salicylate and jasmonate signaling. *Plant Physiol.*, **149**, 1797-1809.
- Leon-Reyes, A., Van der Does, D., De Lange, E.S., Delker, C., Wasternack, C., Van Wees, S.C.M., Ritsema, T. and Pieterse, C.M.J.** (2010b) Salicylate-mediated suppression of jasmonate-responsive gene expression in *Arabidopsis* is targeted downstream of the jasmonate biosynthesis pathway. *Planta*, **232**, 1423-1432.
- Lewis, L.A., Polanski, K., de Torres-Zabala, M., Jayaraman, S., Bowden, L., Moore, J., Penfold, C.A., Jenkins, D.J., Hill, C., Baxter, L., Kulasekaran, S., Truman, W., Littlejohn, G., Prusinska, J., Mead, A., Steinbrenner, J., Hickman, R., Rand, D., Wild, D.L., Ott, S., Buchanan-Wollaston, V., Smirnov, N., Beynon, J., Denby, K. and Grant, M.** (2015) Transcriptional dynamics driving MAMP-triggered immunity and pathogen effector-mediated immunosuppression in *Arabidopsis* leaves following infection with *Pseudomonas syringae* pv *tomato* DC3000. *Plant Cell*, **27**, 3038-3064.
- Li, B., Meng, X., Shan, L. and He, P.** (2016) Transcriptional regulation of pattern-triggered immunity in plants. *Cell Host Microbe*, **19**, 641-650.
- Li, F., Cheng, C., Cui, F., de Oliveira, M.V.V., Yu, X., Meng, X., Intorne, A.C., Babilonia, K., Li, M., Li, B., Chen, S., Ma, X., Xiao, S., Zheng, Y., Fei, Z., Metz, R.P., Johnson, C.D., Koiwa, H., Sun, W., Li, Z., de Souza Filho, G.A., Shan, L. and He, P.** (2014) Modulation of RNA polymerase II phosphorylation downstream of pathogen perception orchestrates plant immunity. *Cell Host Microbe*, **16**, 748-758.
- Li, J., Brader, G. and Palva, E.T.** (2004) The WRKY70 transcription factor: a node of convergence for jasmonate-mediated and salicylate-mediated signals in plant defense. *Plant Cell*, **16**, 319-331.
- Li, J., Zhong, R. and Palva, E.T.** (2017) WRKY70 and its homolog WRKY54 negatively modulate the cell wall-associated defenses to necrotrophic pathogens in *Arabidopsis*. *PLoS One*, **12**, e0183731.

- Li, M., Yao, T., Lin, W., Hinckley, W.E., Galli, M., Muchero, W., Gallavotti, A., Chen, J.-G. and Huang, S.-s.C.** (2023) Double DAP-seq uncovered synergistic DNA binding of interacting bZIP transcription factors. *Nat. Commun.*, **14**, 2600.
- Li, Q., Chen, Y., Wang, J., Zou, F., Jia, Y., Shen, D., Zhang, Q., Jing, M., Dou, D. and Zhang, M.** (2019a) A *Phytophthora capsici* virulence effector associates with NPR1 and suppresses plant immune responses. *Phytopathol. Res.*, **1**, 6.
- Li, S.** (2015) The *Arabidopsis thaliana* TCP transcription factors: A broadening horizon beyond development. *Plant Signal. Behav.*, **10**, e1044192.
- Li, S., Yan, H. and Lee, J.** (2021) Identification of gene regulatory networks from single-cell expression data. In *Modeling Transcriptional Regulation: Methods and Protocols* (Mukhtar, S. ed). New York, NY: Springer US, pp. 153-170.
- Li, W., Ma, M., Feng, Y., Li, H., Wang, Y., Ma, Y., Li, M., An, F. and Guo, H.** (2015) EIN2-directed translational regulation of ethylene signaling in Arabidopsis. *Cell*, **163**, 670-683.
- Li, Y., Liu, W., Zhong, H., Zhang, H.-L. and Xia, Y.** (2019) Redox-sensitive bZIP68 plays a role in balancing stress tolerance with growth in Arabidopsis. *Plant J.*, **100**, 768-783.
- Liu, C., Xin, Y., Xu, L., Cai, Z., Xue, Y., Liu, Y., Xie, D., Liu, Y. and Qi, Y.** (2018) Arabidopsis ARGONAUTE 1 binds chromatin to promote gene transcription in response to hormones and stresses. *Dev. Cell*, **44**, 348-361.e347.
- Liu, L., Sonbol, F.-M., Huot, B., Gu, Y., Withers, J., Mwimba, M., Yao, J., He, S.Y. and Dong, X.** (2016) Salicylic acid receptors activate jasmonic acid signalling through a non-canonical pathway to promote effector-triggered immunity. *Nat. Commun.*, **7**, 13099.
- Liu, N., Staswick, P.E. and Avramova, Z.** (2016) Memory responses of jasmonic acid-associated Arabidopsis genes to a repeated dehydration stress. *Plant Cell Environ.*, **39**, 2515-2529.
- Liu, W., Tai, H., Li, S., Gao, W., Zhao, M., Xie, C. and Li, W.X.** (2014) bHLH122 is important for drought and osmotic stress resistance in Arabidopsis and in the repression of ABA catabolism. *New Phytol.*, **201**, 1192-1204.
- Liu, Y., Wei, H., Ma, M., Li, Q., Kong, D., Sun, J., Ma, X., Wang, B., Chen, C., Xie, Y. and Wang, H.** (2019) Arabidopsis FHY3 and FAR1 regulate the balance between growth and defense responses under shade conditions. *Plant Cell*, **31**, 2089-2106.
- Lopez-Molina, L., Mongrand, S. and Chua, N.-H.** (2001) A postgermination developmental arrest checkpoint is mediated by abscisic acid and requires the ABI5 transcription factor in Arabidopsis. *Proc. Natl. Acad. Sci. U.S.A.*, **98**, 4782-4787.
- Lorenzo, O., Chico, J.M., Sanchez-Serrano, J.J. and Solano, R.** (2004) *JASMONATE-INSENSITIVE1* encodes a MYC transcription factor essential to discriminate between different jasmonate-regulated defense responses in Arabidopsis. *Plant Cell*, **16**, 1938-1950.
- Lorenzo, O., Piqueras, R., Sánchez-Serrano, J.J. and Solano, R.** (2003) ETHYLENE RESPONSE FACTOR1 integrates signals from ethylene and jasmonate pathways in plant defense. *Plant Cell*, **15**, 165-178.
- Lu, H., McClung, C.R. and Zhang, C.** (2017) Tick tock: circadian regulation of plant innate immunity. *Annu. Rev. Phytopathol.*, **55**, 287-311.
- Lu, Y., Truman, W., Liu, X., Bethke, G., Zhou, M., Myers, C.L., Katagiri, F. and Glazebrook, J.** (2018) Different modes of negative regulation of plant immunity by calmodulin-related genes. *Plant Physiol.*, **176**, 3046-3061.
- Lukowitz, W., Roeder, A., Parmenter, D. and Somerville, C.** (2004) A MAPKK kinase gene regulates extra-embryonic cell fate in Arabidopsis. *Cell*, **116**, 109-119.

- Lumba, S., Toh, S., Handfield, L.F., Swan, M., Liu, R.Y., Youn, J.Y., Cutler, S.R., Subramaniam, R., Provart, N. and Moses, A.** (2014) A mesoscale abscisic acid hormone interactome reveals a dynamic signaling landscape in Arabidopsis. *Dev. Cell*, **29**, 360-372.
- Luo, X., Wu, W., Liang, Y., Xu, N., Wang, Z., Zou, H. and Liu, J.** (2020) Tyrosine phosphorylation of the lectin receptor-like kinase LORE regulates plant immunity. *EMBO J.*, **39**, e102856.
- Ma, Y., Szostkiewicz, I., Korte, A., Moes, D., Yang, Y., Christmann, A. and Grill, E.** (2009) Regulators of PP2C phosphatase activity function as abscisic acid sensors. *Science*, **324**, 1064-1068.
- Maier, B.A., Kiefer, P., Field, C.M., Hemmerle, L., Bortfeld-Miller, M., Emmenegger, B., Schäfer, M., Pfeilmeier, S., Sunagawa, S., Vogel, C.M. and Vorholt, J.A.** (2021) A general non-self response as part of plant immunity. *Nat. Plants*, **7**, 696-705.
- Major, I.T., Guo, Q., Zhai, J., Kapali, G., Kramer, D.M. and Howe, G.A.** (2020) A phytochrome B-independent pathway restricts growth at high levels of jasmonate defense. *Plant Physiol.*, **183**, 733-749.
- Manavella, Pablo A., Hagmann, J., Ott, F., Laubinger, S., Franz, M., Macek, B. and Weigel, D.** (2012) Fast-forward genetics identifies plant CPL phosphatases as regulators of miRNA processing factor HYL1. *Cell*, **151**, 859-870.
- Mangan, S. and Alon, U.** (2003) Structure and function of the feed-forward loop network motif. *Proc. Natl. Acad. Sci. U.S.A.*, **100**, 11980-11985.
- Manohar, M., Tian, M., Moreau, M., Park, S.-W., Choi, H.W., Fei, Z., Friso, G., Asif, M., Manosalva, P., von Dahl, C.C., Shi, K., Ma, S., Dinesh-Kumar, S.P., O'Doherty, I., Schroeder, F.C., van Wijk, K.J. and Klessig, D.F.** (2015) Identification of multiple salicylic acid-binding proteins using two high throughput screens. *Front. Plant Sci.*, **5**, 777.
- Mao, G., Meng, X., Liu, Y., Zheng, Z., Chen, Z. and Zhang, S.** (2011) Phosphorylation of a WRKY transcription factor by two pathogen-responsive MAPKs drives phytoalexin biosynthesis in Arabidopsis. *Plant Cell*, **23**, 1639-1653.
- Mao, P., Duan, M., Wei, C. and Li, Y.** (2007) WRKY62 transcription factor acts downstream of cytosolic NPR1 and negatively regulates jasmonate-responsive gene expression. *Plant Cell Physiol.*, **48**, 833-842.
- Mathelier, A., Xin, B., Chiu, T.-P., Yang, L., Rohs, R. and Wasserman, W.W.** (2016) DNA shape features improve transcription factor binding site predictions in vivo. *Cell Syst.*, **3**, 278-286.
- Mathur, J. and Koncz, C.** (1998) PEG-mediated protoplast transformation with naked DNA. In *Arabidopsis Protocols* (Martinez-Zapater, J.M. and Salinas, J. eds). Totowa, NJ: Humana Press, pp. 267-276.
- Meng, X., Wang, H., He, Y., Liu, Y., Walker, J.C., Torii, K.U. and Zhang, S.** (2012) A MAPK cascade downstream of ERECTA receptor-like protein kinase regulates Arabidopsis inflorescence architecture by promoting localized cell proliferation. *Plant Cell*, **24**, 4948-4960.
- Mercatelli, D., Scalambra, L., Triboli, L., Ray, F. and Giorgi, F.M.** (2020) Gene regulatory network inference resources: A practical overview. *Biochim. Biophys. Acta - Gene Regul. Mech.*, **1863**, 194430.
- Merchante, C., Brumos, J., Yun, J., Hu, Q., Spencer, K.R., Enríquez, P., Binder, B.M., Heber, S., Stepanova, A.N. and Alonso, J.M.** (2015) Gene-specific translation regulation mediated by the hormone-signaling molecule EIN2. *Cell*, **163**, 684-697.
- Merchante, C., Stepanova, A.N. and Alonso, J.M.** (2017) Translation regulation in plants: an interesting past, an exciting present and a promising future. *Plant J.*, **90**, 628-653.

- Meteignier, L.-V., El Oirdi, M., Cohen, M., Barff, T., Matteau, D., Lucier, J.-F., Rodrigue, S., Jacques, P.-E., Yoshioka, K. and Moffett, P.** (2017) Translatome analysis of an NB-LRR immune response identifies important contributors to plant immunity in Arabidopsis. *J. Exp. Bot.*, **68**, 2333-2344.
- Mine, A., Nobori, T., Salazar-Rondon, M.C., Winkelmüller, T.M., Anver, S., Becker, D. and Tsuda, K.** (2017) An incoherent feed-forward loop mediates robustness and tunability in a plant immune network. *EMBO Rep.*, **18**, 464-476.
- Misselhorn, A., Aggarwal, P., Ericksen, P., Gregory, P., Horn-Phathanothai, L., Ingram, J. and Wiebe, K.** (2012) A vision for attaining food security. *Curr. Opin. Environ. Sustain.*, **4**, 7-17.
- Mitchell, S.F. and Parker, R.** (2014) Principles and properties of eukaryotic mRNPs. *Mol. Cell*, **54**, 547-558.
- Mittler, R.** (2017) ROS are good. *Trends Plant Sci.*, **22**, 11-19.
- Monte, I., Kneeshaw, S., Franco-Zorrilla, J.M., Chini, A., Zamarreño, A.M., García-Mina, J.M. and Solano, R.** (2020) An ancient COI1-independent function for reactive electrophilic oxylipins in thermotolerance. *Curr. Biol.*, **30**, 962-971.e963.
- Mou, Z., Fan, W. and Dong, X.** (2003) Inducers of plant systemic acquired resistance regulate NPR1 function through redox changes. *Cell*, **113**, 935-944.
- Muiño, J.M., Smaczniak, C., Angenent, G.C., Kaufmann, K. and Van Dijk, A.D.** (2014) Structural determinants of DNA recognition by plant MADS-domain transcription factors. *Nucleic Acids Res.*, **42**, 2138-2146.
- Nakashima, K., Takasaki, H., Mizoi, J., Shinozaki, K. and Yamaguchi-Shinozaki, K.** (2012) NAC transcription factors in plant abiotic stress responses. *Biochim. Biophys. Acta - Gene Regul. Mech.*, **1819**, 97-103.
- Narsai, R., Gouil, Q., Secco, D., Srivastava, A., Karpievitch, Y.V., Liew, L.C., Lister, R., Lewsey, M.G. and Whelan, J.** (2017) Extensive transcriptomic and epigenomic remodelling occurs during *Arabidopsis thaliana* germination. *Genome Biol.*, **18**, 172.
- Narsai, R., Howell, K.A., Millar, A.H., O'Toole, N., Small, I. and Whelan, J.** (2007) Genome-wide analysis of mRNA decay rates and their determinants in *Arabidopsis thaliana*. *Plant Cell*, **19**, 3418-3436.
- Ndamukong, I., Abdallat, A.A., Thurow, C., Fode, B., Zander, M., Weigel, R. and Gatz, C.** (2007) SA-inducible Arabidopsis glutaredoxin interacts with TGA factors and suppresses JA-responsive PDF1.2 transcription. *Plant J.*, **50**, 128-139.
- Ngou, B.P.M., Jones, J.D.G. and Ding, P.** (2022) Plant immune networks. *Trends Plant Sci.*, **27**, 255-273.
- Niedojadło, J., Deleńko, K. and Niedojadło, K.** (2016) Regulation of poly(A) RNA retention in the nucleus as a survival strategy of plants during hypoxia. *RNA Biol.*, **13**, 531-543.
- Nobori, T. and Tsuda, K.** (2019) The plant immune system in heterogeneous environments. *Curr. Opin. Plant Biol.*, **50**, 58-66.
- Nobori, T., Wang, Y., Wu, J., Stolze, S.C., Tsuda, Y., Finkemeier, I., Nakagami, H. and Tsuda, K.** (2020) Multidimensional gene regulatory landscape of a bacterial pathogen in plants. *Nat. Plants*, **6**, 883-896.
- Nomoto, M., Skelly, M.J., Itaya, T., Mori, T., Suzuki, T., Matsushita, T., Tokizawa, M., Kuwata, K., Mori, H., Yamamoto, Y.Y., Higashiyama, T., Tsukagoshi, H., Spoel, S.H. and Tada, Y.** (2021) Suppression of MYC transcription activators by the immune cofactor NPR1 fine-tunes plant immune responses. *Cell Rep.*, **37**.

- O'Malley, R.C., Huang, S.S.C., Song, L., Lewsey, M.G., Bartlett, A., Nery, J.R., Galli, M., Gallavotti, A. and Ecker, J.R.** (2016) Cistrome and epicistrome features shape the regulatory DNA landscape. *Cell*, **165**, 1280-1292.
- Oñate-Sánchez, L. and Vicente-Carbajosa, J.** (2008) DNA-free RNA isolation protocols for *Arabidopsis thaliana*, including seeds and siliques. *BMC Res. Notes*, **1**, 93.
- Ortigosa, A., Fonseca, S., Franco-Zorrilla, J.M., Fernández-Calvo, P., Zander, M., Lewsey, M.G., García-Casado, G., Fernández-Barbero, G., Ecker, J.R. and Solano, R.** (2020) The JA-pathway MYC transcription factors regulate photomorphogenic responses by targeting HY5 gene expression. *Plant J.*, **102**, 138-152.
- Page, R.D.M.** (1996) Tree View: An application to display phylogenetic trees on personal computers. *Bioinformatics*, **12**, 357-358.
- Pajerowska-Mukhtar, K.M., Wang, W., Tada, Y., Oka, N., Tucker, C.L., Fonseca, J.P. and Dong, X.** (2012) The HSF-like transcription factor TBF1 is a major molecular switch for plant growth-to-defense transition. *Curr. Biol.*, **22**, 103-112.
- Pandey, N., Ranjan, A., Pant, P., Tripathi, R.K., Ateek, F., Pandey, H.P., Patre, U.V. and Sawant, S.V.** (2013) CAMTA1 regulates drought responses in *Arabidopsis thaliana*. *BMC Genom.*, **14**, 216.
- Pandey, S.P. and Somssich, I.E.** (2009) The role of WRKY transcription factors in plant immunity. *Plant Physiol.*, **150**, 1648-1655.
- Pardal, A.J., Piquerez, S.J.M., Dominguez-Ferreras, A., Frungillo, L., Mastorakis, E., Reilly, E., Latrasse, D., Concia, L., Gimenez-Ibanez, S., Spoel, S.H., Benhamed, M. and Ntoukakis, V.** (2021) Immunity onset alters plant chromatin and utilizes EDA16 to regulate oxidative homeostasis. *PLoS Pathog.*, **17**, e1009572.
- Park, S.Y., Fung, P., Nishimura, N., Jensen, D.R., Fujii, H., Zhao, Y., Lumba, S., Santiago, J., Rodrigues, A., Chow, T.F.F., Alfred, S.E., Bonetta, D., Finkelstein, R., Provart, N.J., Desveaux, D., Rodriguez, P.L., McCourt, P., Zhu, J.K., Schroeder, J.I., Volkman, B.F. and Cutler, S.R.** (2009) Abscisic acid inhibits type 2C protein phosphatases via the PYR/PYL family of START proteins. *Science*, **324**, 1068-1071.
- Pauwels, L. and Goossens, A.** (2011) The JAZ proteins: a crucial interface in the jasmonate signaling cascade. *Plant Cell*, **23**, 3089-3100.
- Pauwels, L., Morreel, K., De Witte, E., Lammertyn, F., Van Montagu, M., Boerjan, W., Inzé, D. and Goossens, A.** (2008) Mapping methyl jasmonate-mediated transcriptional reprogramming of metabolism and cell cycle progression in cultured *Arabidopsis* cells. *Proc. Natl. Acad. Sci. U.S.A.*, **105**, 1380-1385.
- Pauwels, L., Ritter, A., Goossens, J., Durand, A.N., Liu, H.X., Gu, Y.N., Geerinck, J., Boter, M., Vanden Bossche, R., De Clercq, R., Van Leene, J., Gevaert, K., De Jaeger, G., Solano, R., Stone, S., Innes, R.W., Callis, J. and Goossens, A.** (2015) The RING E3 ligase KEEP ON GOING modulates JASMONATE ZIM-DOMAIN12 stability. *Plant Physiol.*, **169**, 1405-1417.
- Peng, P., Yan, Z., Zhu, Y. and Li, J.** (2008) Regulation of the *Arabidopsis* GSK3-like kinase BRASSINOSTEROID-INSENSITIVE 2 through proteasome-mediated protein degradation. *Mol. Plant*, **1**, 338-346.
- Peng, S., Guo, D., Guo, Y., Zhao, H., Mei, J., Han, Y., Guan, R., Wang, T., Song, T., Sun, K., Liu, Y., Mao, T., Chang, H., Xue, J., Cai, Y., Chen, D. and Wang, S.** (2022) CONSTITUTIVE EXPRESSER OF PATHOGENESIS-RELATED GENES 5 is an RNA-binding protein controlling plant immunity via an RNA processing complex. *Plant Cell*, **34**, 1724-1744.

- Peng, Y., Yang, J., Li, X. and Zhang, Y.** (2021) Salicylic acid: biosynthesis and signaling. *Annu. Rev. Plant Biol.*, **72**, 761-791.
- Pieterse, C.M.J., Van der Does, D., Zamioudis, C., Leon-Reyes, A. and Van Wees, S.C.M.** (2012) Hormonal modulation of plant immunity. *Annu. Rev. Cell Dev. Biol.*, **28**, 489-521.
- Pieterse, C.M.J., Zamioudis, C., Berendsen, R.L., Weller, D.M., Van Wees, S.C.M. and Bakker, P.A.H.M.** (2014) Induced systemic resistance by beneficial microbes. *Annu. Rev. Phytopathol.*, **52**, 347-375.
- Plett, J.M., Daguerre, Y., Wittulsky, S., Vayssières, A., Deveau, A., Melton, S.J., Kohler, A., Morrell-Falvey, J.L., Brun, A., Veneault-Fourrey, C. and Martin, F.** (2014) Effector MiSSP7 of the mutualistic fungus *Laccaria bicolor* stabilizes the *Populus* JAZ6 protein and represses jasmonic acid (JA) responsive genes. *Proc. Natl. Acad. Sci. U.S.A.*, **111**, 8299-8304.
- Poppeliers, S.W.M., Sánchez-Gil, J.J. and de Jonge, R.** (2023) Microbes to support plant health: understanding bioinoculant success in complex conditions. *Curr. Opin. Microbiol.*, **73**, 102286.
- Postiglione, A.E. and Muday, G.K.** (2020) The role of ROS homeostasis in ABA-induced guard cell signaling. *Front. Plant Sci.*, **11**, 968.
- Pré, M., Atallah, M., Champion, A., De Vos, M., Pieterse, C.M.J. and Memelink, J.** (2008) The AP2/ERF domain transcription factor ORA59 integrates jasmonic acid and ethylene signals in plant defense. *Plant Physiol.*, **147**, 1347-1357.
- Qi, J., Wang, J., Gong, Z. and Zhou, J.-M.** (2017) Apoplastic ROS signaling in plant immunity. *Curr. Opin. Plant Biol.*, **38**, 92-100.
- Qi, P., Huang, M., Hu, X., Zhang, Y., Wang, Y., Li, P., Chen, S., Zhang, D., Cao, S., Zhu, W., Xie, J., Cheng, J., Fu, Y., Jiang, D., Yu, X. and Li, B.** (2022) A *Ralstonia solanacearum* effector targets TGA transcription factors to subvert salicylic acid signaling. *Plant Cell*, **34**, 1666-1683.
- Qian, D., Zhang, Z., He, J., Zhang, P., Ou, X., Li, T., Niu, L., Nan, Q., Niu, Y. and He, W.** (2019) Arabidopsis ADF5 promotes stomatal closure by regulating actin cytoskeleton remodeling in response to ABA and drought stress. *J. Exp. Bot.*, **70**, 435-446.
- Qin, J., Wang, K., Sun, L., Xing, H., Wang, S., Li, L., Chen, S., Guo, H.-S. and Zhang, J.** (2018) The plant-specific transcription factors CBP60g and SARD1 are targeted by a *Verticillium* secretory protein VdSCP41 to modulate immunity. *Elife*, **7**, e34902.
- Raffeiner, M., Üstün, S., Guerra, T., Spinti, D., Fitzner, M., Sonnewald, S., Baldermann, S. and Börnke, F.** (2022) The *Xanthomonas* type-III effector XopS stabilizes CaWRKY40a to regulate defense responses and stomatal immunity in pepper (*Capsicum annuum*). *Plant Cell*, **34**, 1684-1708.
- Rambani, A., Hu, Y., Piya, S., Long, M., Rice, J.H., Pantalone, V. and Hewezi, T.** (2020) Identification of differentially methylated miRNA genes during compatible and incompatible interactions between soybean and soybean cyst nematode. *Mol. Plant Microbe Interact.*, **33**, 1340-1352.
- Ramegowda, V., Gill, U.S., Sivalingam, P.N., Gupta, A., Gupta, C., Govind, G., Nataraja, K.N., Pereira, A., Udayakumar, M., Mysore, K.S. and Senthil-Kumar, M.** (2017) GBF3 transcription factor imparts drought tolerance in *Arabidopsis thaliana*. *Sci. Rep.*, **7**, 9148.
- Rate, D.N. and Greenberg, J.T.** (2001) The Arabidopsis *aberrant growth and death2* mutant shows resistance to *Pseudomonas syringae* and reveals a role for NPR1 in suppressing hypersensitive cell death. *Plant J.*, **27**, 203-211.
- Rawat, R., Schwartz, J., Jones, M.A., Sairanen, I., Cheng, Y., Andersson, C.R., Zhao, Y., Ljung, K. and Harmer, S.L.** (2009) REVELLE1, a Myb-like transcription factor, integrates the circadian clock and auxin pathways. *Proc. Natl. Acad. Sci. U.S.A.*, **106**, 16883-16888.

- Rayapuram, C. and Baldwin, I.T.** (2007) Increased SA in *NPR1*-silenced plants antagonizes JA and JA-dependent direct and indirect defenses in herbivore-attacked *Nicotiana attenuata* in nature. *Plant J.*, **52**, 700–715.
- Rekhter, D., Lüdke, D., Ding, Y., Feussner, K., Zienkiewicz, K., Lipka, V., Wiermer, M., Zhang, Y. and Feussner, I.** (2019) Isochorismate-derived biosynthesis of the plant stress hormone salicylic acid. *Science*, **365**, 498–502.
- Robert-Seilaniantz, A., Grant, M. and Jones, J.D.G.** (2011) Hormone crosstalk in plant disease and defense: more than just jasmonate-salicylate antagonism. *Annu. Rev. Phytopathol.*, **49**, 317–343.
- Rochon, A., Boyle, P., Wignes, T., Fobert, P.R. and Després, C.** (2006) The coactivator function of Arabidopsis NPR1 requires the core of its BTB/POZ domain and the oxidation of C-terminal cysteines. *Plant Cell*, **18**, 3670–3685.
- Roux, M., Schwessinger, B., Albrecht, C., Chinchilla, D., Jones, A., Holton, N., Malinovsky, F.G., Tör, M., de Vries, S. and Zipfel, C.** (2011) The Arabidopsis leucine-rich repeat receptor-like kinases BAK1/SERK3 and BKK1/SERK4 are required for innate immunity to hemibiotrophic and biotrophic pathogens. *Plant Cell*, **23**, 2440–2455.
- Rushton, D.L., Tripathi, P., Rabara, R.C., Lin, J., Ringler, P., Boken, A.K., Langum, T.J., Smidt, L., Boomsma, D.D., Emme, N.J., Chen, X., Finer, J.J., Shen, Q.J. and Rushton, P.J.** (2012) WRKY transcription factors: key components in abscisic acid signalling. *Plant Biotechnol. J.*, **10**, 2–11.
- Sah, S.K., Reddy, K.R. and Li, J.** (2016) Abscisic acid and abiotic stress tolerance in crop plants. *Front. Plant Sci.*, **7**, 571.
- Saleh, A., Withers, J., Mohan, R., Marqués, J., Gu, Y., Yan, S., Zavaliev, R., Nomoto, M., Tada, Y. and Dong, X.** (2015) Posttranslational modifications of the master transcriptional regulator NPR1 enable dynamic but tight control of plant immune responses. *Cell Host Microbe*, **18**, 169–182.
- Sanagi, M., Lu, Y., Aoyama, S., Morita, Y., Mitsuda, N., Ikeda, M., Ohme-Takagi, M., Sato, T. and Yamaguchi, J.** (2018) Sugar-responsive transcription factor bZIP3 affects leaf shape in Arabidopsis plants. *Plant Biotechnol.*, **35**, 167–170.
- Sánchez-Vallet, A., López, G., Ramos, B., Delgado-Cerezo, M., Riviere, M.P., Llorente, F., Fernández, P.V., Miedes, E., Estevez, J.M., Grant, M. and Molina, A.** (2012) Disruption of abscisic acid signaling constitutively activates Arabidopsis resistance to the necrotrophic fungus *Plectosphaerella cucumerina*. *Plant Physiol.*, **160**, 2109–2124.
- Santiago, J., Rodrigues, A., Saez, A., Rubio, S., Antoni, R., Dupeux, F., Park, S.Y., Marquez, J.A., Cutler, S.R. and Rodriguez, P.L.** (2009) Modulation of drought resistance by the abscisic acid receptor PYL5 through inhibition of clade A PP2Cs. *Plant J.*, **60**, 575–588.
- Sarris, Panagiotis F., Duxbury, Z., Huh, Sung U., Ma, Y., Segonzac, C., Sklenar, J., Derbyshire, P., Cevik, V., Rallapalli, G., Saucet, Simon B., Wirthmueller, L., Menke, Frank L.H., Sohn, Kee H. and Jones, Jonathan D.G.** (2015) A plant immune receptor detects pathogen effectors that target WRKY transcription factors. *Cell*, **161**, 1089–1100.
- Sasaki-Sekimoto, Y., Jikumaru, Y., Obayashi, T., Saito, H., Masuda, S., Kamiya, Y., Ohta, H. and Shirasu, K.** (2013) Basic Helix-Loop-Helix transcription factors JA-ASSOCIATED MYC2-LIKE 1 (JAM1), JAM2 and JAM3 are negative regulators of jasmonate responses in Arabidopsis. *Plant Physiol.*, **163**, 291–234.
- Savary, S., Willocquet, L., Pethybridge, S.J., Esker, P., McRoberts, N. and Nelson, A.** (2019) The global burden of pathogens and pests on major food crops. *Nat. Ecol. Evol.*, **3**, 430–439.

- Schulz, M.H., Devanny, W.E., Gitter, A., Zhong, S., Ernst, J. and Bar-Joseph, Z.** (2012) DREM 2.0: Improved reconstruction of dynamic regulatory networks from time-series expression data. *BMC Syst. Biol.*, **6**, 104.
- Schumann, U., Lee, J.M., Smith, N.A., Zhong, C., Zhu, J.-K., Dennis, E.S., Millar, A.A. and Wang, M.-B.** (2019) DEMETER plays a role in DNA demethylation and disease response in somatic tissues of *Arabidopsis*. *Epigenetics*, **14**, 1074-1087.
- Schweizer, F., Bodenhausen, N., Lassueur, S., Masclaux, F.G. and Reymond, P.** (2013) Differential contribution of transcription factors to *Arabidopsis thaliana* defense against *Spodoptera littoralis*. *Front. Plant Sci.*, **4**, 13.
- Seo, J.S., Diloknawarit, P., Park, B.S. and Chua, N.-H.** (2019) ELF18-INDUCED LONG NONCODING RNA 1 evicts fibrillarin from mediator subunit to enhance PATHOGENESIS-RELATED GENE 1 (PR1) expression. *New Phytol.*, **221**, 2067-2079.
- Seo, J.S., Sun, H.-X., Park, B.S., Huang, C.-H., Yeh, S.-D., Jung, C. and Chua, N.-H.** (2017) ELF18-INDUCED LONG-NONCODING RNA associates with Mediator to enhance expression of innate immune response genes in *Arabidopsis*. *Plant Cell*, **29**, 1024-1038.
- Sheard, L.B., Tan, X., Mao, H.B., Withers, J., Ben-Nissan, G., Hinds, T.R., Kobayashi, Y., Hsu, F.-F., Sharon, M., Browse, J., He, S.Y., Rizo, J., Howe, G.A. and Zheng, N.** (2010) Jasmonate perception by inositol-phosphate-potentiated COI1-JAZ co-receptor. *Nature*, **468**, 400-405.
- Shen, M., Lim, C.J., Park, J., Kim, J.E., Baek, D., Nam, J., Lee, S.Y., Pardo, J.M., Kim, W.-Y. and Mackey, D.** (2020) HOS15 is a transcriptional corepressor of NPR1-mediated gene activation of plant immunity. *Proc. Natl. Acad. Sci. U.S.A.*, **117**, 30805-30815.
- Skelly, M.J., Furniss, J.J., Grey, H., Wong, K.-W. and Spoel, S.H.** (2019) Dynamic ubiquitination determines transcriptional activity of the plant immune coactivator NPR1. *Elife*, **8**, e47005.
- Skubacz, A., Daszkowska-Golec, A. and Szarejko, I.** (2016) The role and regulation of ABI5 (ABA-Insensitive 5) in plant development, abiotic stress responses and phytohormone crosstalk. *Front. Plant Sci.*, **c7**, 1884-1884.
- Solano, R., Stepanova, A., Chao, Q.M. and Ecker, J.R.** (1998) Nuclear events in ethylene signaling: A transcriptional cascade mediated by ETHYLENE-INSENSITIVE3 and ETHYLENE-RESPONSE-FACTOR1. *Genes Dev.*, **12**, 3703-3714.
- Song, L., Fang, Y., Chen, L., Wang, J. and Chen, X.** (2021) Role of non-coding RNAs in plant immunity. *Plant Commun.*, **2**, 100180.
- Song, L., Huang, S.C., Wise, A., Castanon, R., Nery, J.R., Chen, H., Watanabe, M., Thomas, J., Bar-Joseph and Ecker, J.R.** (2016) A transcription factor hierarchy defines an environmental stress response network. *Science*, **354**, aag1550.
- Song, S., Huang, H., Gao, H., Wang, J., Wu, D., Liu, X., Yang, S., Zhai, Q., Li, C., Qi, T. and Xie, D.** (2014) Interaction between MYC2 and ETHYLENE INSENSITIVE3 modulates antagonism between jasmonate and ethylene signaling in *Arabidopsis*. *Plant Cell*, **26**, 263-279.
- Souret, F.F., Kastenmayer, J.P. and Green, P.J.** (2004) AtXRN4 degrades mRNA in *Arabidopsis* and its substrates include selected miRNA targets. *Mol. Cell*, **15**, 173-183.
- Spoel, S.H., Johnson, J.S. and Dong, X.** (2007) Regulation of tradeoffs between plant defenses against pathogens with different lifestyles. *Proc. Natl. Acad. Sci. U.S.A.*, **104**, 18842-18847.

- Spoel, S.H., Koornneef, A., Claessens, S.M.C., Korzelius, J.P., Van Pelt, J.A., Mueller, M.J., Buchala, A.J., Métraux, J.-P., Brown, R., Kazan, K., Van Loon, L.C., Dong, X. and Pieterse, C.M.J.** (2003) NPR1 modulates cross-talk between salicylate- and jasmonate-dependent defense pathways through a novel function in the cytosol. *Plant Cell*, **15**, 760–770.
- Spoel, S.H. and Loake, G.J.** (2011) Redox-based protein modifications: the missing link in plant immune signalling. *Curr. Opin. Plant Biol.*, **14**, 358–364.
- Spoel, S.H., Mou, Z.L., Tada, Y., Spivey, N.W., Genschik, P. and Dong, X.** (2009) Proteasome-mediated turnover of the transcription coactivator NPR1 plays dual roles in regulating plant immunity. *Cell*, **137**, 860–872.
- Staiger, D., Korneli, C., Lummer, M. and Navarro, L.** (2013) Emerging role for RNA-based regulation in plant immunity. *New Phytol.*, **197**, 394–404.
- Steenbergen, M.** (2022) Gene regulatory network induced by Western flower thrips in Arabidopsis: Effect of hormone signaling, thrips development and spatial context. *PhD dissertation, Utrecht University*.
- Strader, L., Weijers, D. and Wagner, D.** (2022) Plant transcription factors — being in the right place with the right company. *Curr. Opin. Plant Biol.*, **65**, 102136.
- Ströher, E. and Millar, A.H.** (2012) The biological roles of glutaredoxins. *Biochem. J.*, **446**, 333–348.
- Sun, Y., Oh, D.-H., Duan, L., Ramachandran, P., Ramirez, A., Bartlett, A., Tran, K.-N., Wang, G., Dassanayake, M. and Dinneny, J.R.** (2022) Divergence in the ABA gene regulatory network underlies differential growth control. *Nat. Plants*, **8**, 549–560.
- Swift, J., Greenham, K., Ecker, J.R., Coruzzi, G.M. and Robertson McClung, C.** (2022) The biology of time: dynamic responses of cell types to developmental, circadian and environmental cues. *Plant J.*, **109**, 764–778.
- Tada, Y., Spoel, S.H., Pajerowska-Mukhtar, K., Mou, Z., Song, J., Wang, C., Zuo, J. and Dong, X.** (2008) Plant immunity requires conformational changes of NPR1 via S-nitrosylation and thioredoxins. *Science*, **321**, 952–956.
- Takasaki, H., Maruyama, K., Takahashi, F., Fujita, M., Yoshida, T., Nakashima, K., Myouga, F., Toyooka, K., Yamaguchi-Shinozaki, K. and Shinozaki, K.** (2015) SNAC-As, stress-responsive NAC transcription factors, mediate ABA-inducible leaf senescence. *Plant J.*, **84**, 1114–1123.
- Tang, B., Liu, C., Li, Z., Zhang, X., Zhou, S., Wang, G.-L., Chen, X.-L. and Liu, W.** (2021) Multilayer regulatory landscape during pattern-triggered immunity in rice. *Plant Biotechnol. J.*, **19**, 2629–2645.
- Thatcher, L.F., Foley, R., Casarotto, H.J., Gao, L.-L., Kamphuis, L.G., Melser, S. and Singh, K.B.** (2018) The Arabidopsis RNA Polymerase II Carboxyl Terminal Domain (CTD) Phosphatase-Like1 (CPL1) is a biotic stress susceptibility gene. *Sci. Rep.*, **8**, 13454.
- Thieffry, A., López-Márquez, D., Bornholdt, J., Malekroudi, M.G., Bressendorff, S., Barghetti, A., Sandelin, A. and Brodersen, P.** (2022) PAMP-triggered genetic reprogramming involves widespread alternative transcription initiation and an immediate transcription factor wave. *Plant Cell*.
- Thines, B., Katsir, L., Melotto, M., Niu, Y., Mandaokar, A., Liu, G.H., Nomura, K., He, S.Y., Howe, G.A. and Browse, J.** (2007) JAZ repressor proteins are targets of the SCF^{COI1} complex during jasmonate signalling. *Nature*, **448**, 661–665.

- Torrens-Spence, M.P., Bobokalonova, A., Carballo, V., Glinkerman, C.M., Pluskal, T., Shen, A. and Weng, J.-K.** (2019) PBS3 and EPS1 complete salicylic acid biosynthesis from isochorismate in *Arabidopsis*. *Mol. Plant*, **12**, 1577-1586.
- Torres, M.A., Dangl, J.L. and Jones, J.D.G.** (2002) *Arabidopsis* gp91phox homologues *AtrbohD* and *AtrbohF* are required for accumulation of reactive oxygen intermediates in the plant defense response. *Proc. Natl. Acad. Sci. U.S.A.*, **99**, 517-522.
- Tran, L.-S.P., Nakashima, K., Sakuma, Y., Simpson, S.D., Fujita, Y., Maruyama, K., Fujita, M., Seki, M., Shinozaki, K. and Yamaguchi-Shinozaki, K.** (2004) Isolation and functional analysis of *Arabidopsis* stress-inducible NAC transcription factors that bind to a drought-responsive *cis*-element in the *early responsive to dehydration stress 1* promoter. *Plant Cell*, **16**, 2481-2498.
- Trapnell, C., Pachter, L. and Salzberg, S.L.** (2009) TopHat: discovering splice junctions with RNA-seq. *Bioinformatics*, **25**, 1105-1111.
- Tsuda, K., Sato, M., Stoddard, T., Glazebrook, J. and Katagiri, F.** (2009) Network properties of robust immunity in plants. *PLoS Genet.*, **5**, e1000772.
- Tsuda, K. and Somssich, I.E.** (2015) Transcriptional networks in plant immunity. *New Phytol.*, **206**, 932-947.
- Uhrig, J.F., Huang, L.-J., Barghahn, S., Willmer, M., Thurow, C. and Gatz, C.** (2017) CC-type glutaredoxins recruit the transcriptional co-repressor TOPLESS to TGA-dependent target promoters in *Arabidopsis thaliana*. *Biochim. Biophys. Acta, Gene Regul. Mech.*, **1860**, 218-226.
- Umezawa, T., Nakashima, K., Miyakawa, T., Kuromori, T., Tanokura, M., Shinozaki, K. and Yamaguchi-Shinozaki, K.** (2010) Molecular basis of the core regulatory network in ABA responses: sensing, signaling and transport. *Plant Cell Physiol.*, **51**, 1821-1839.
- Umezawa, T., Sugiyama, N., Mizoguchi, M., Hayashi, S., Myouga, F., Yamaguchi-Shinozaki, K., Ishihama, Y., Hirayama, T. and Shinozaki, K.** (2009) Type 2C protein phosphatases directly regulate abscisic acid-activated protein kinases in *Arabidopsis*. *Proc. Natl. Acad. Sci. U.S.A.*, **106**, 17588-17593.
- Uno, Y., Furihata, T., Abe, H., Yoshida, R., Shinozaki, K. and Yamaguchi-Shinozaki, K.** (2000) *Arabidopsis* basic leucine zipper transcription factors involved in an abscisic acid-dependent signal transduction pathway under drought and high-salinity conditions. *Proc. Natl. Acad. Sci. U.S.A.*, **97**, 11632-11637.
- Van Butselaar, T. and Van den Ackerveken, G.** (2020) Salicylic acid steers the growth-immunity tradeoff. *Trends Plant Sci.*, **25**, 566-576.
- Van der Does, D., Leon-Reyes, A., Koornneef, A., Van Verk, M.C., Rodenburg, N., Pauwels, L., Goossens, A., Körbes, A.P., Memelink, J., Ritsema, T., Van Wees, S.C.M. and Pieterse, C.M.J.** (2013) Salicylic acid suppresses jasmonic acid signaling downstream of SCF^{COI1}-JAZ by targeting GCC promoter motifs via transcription factor ORA59. *Plant Cell*, **25**, 744-761.
- Van Loon, L.C., Rep, M. and Pieterse, C.M.J.** (2006) Significance of inducible defense-related proteins in infected plants. *Annu. Rev. Phytopathol.*, **44**, 135-162.
- Van Wees, S.C.M., Van Pelt, J.A., Bakker, P.A.H.M. and Pieterse, C.M.J.** (2013) Bioassays for assessing jasmonate-dependent defenses triggered by pathogens, herbivorous insects, or beneficial rhizobacteria. *Methods Mol. Biol.*, **1011**, 35-49.
- Verhage, A., Vlaardingbroek, I., Raaymakers, C., Van Dam, N., Dicke, M., Van Wees, S.C.M. and Pieterse, C.M.J.** (2011) Rewiring of the jasmonate signaling pathway in *Arabidopsis* during insect herbivory. *Front. Plant Sci.*, **2**, 47.

- Verma, V., Srivastava, A.K., Gough, C., Campanaro, A., Srivastava, M., Morrell, R., Joyce, J., Bailey, M., Zhang, C., Krysan, P.J. and Sadanandom, A.** (2021) SUMO enables substrate selectivity by mitogen-activated protein kinases to regulate immunity in plants. *Proc. Natl. Acad. Sci. U.S.A.*, **118**, e2021351118.
- Vlad, F., Rubio, S., Rodrigues, A., Sirichandra, C., Belin, C., Robert, N., Leung, J., Rodriguez, P.L., Laurière, C. and Merlot, S.** (2009) Protein Phosphatases 2C regulate the activation of the Snf1-Related Kinase OST1 by abscisic acid in Arabidopsis. *Plant Cell*, **21**, 3170-3184.
- Vlot, A.C., Dempsey, D.A. and Klessig, D.F.** (2009) Salicylic acid, a multifaceted hormone to combat disease. *Annu. Rev. Phytopathol.*, **47**, 177–206.
- Vos, I.A., Moritz, L., Pieterse, C.M.J. and Van Wees, S.C.M.** (2015) Impact of hormonal crosstalk on plant resistance and fitness under multi-attacker conditions. *Front. Plant Sci.*, **6**, 13.
- Vos, I.A., Pieterse, C.M.J. and Van Wees, S.C.M.** (2013a) Costs and benefits of hormone-regulated plant defences. *Plant Pathol.*, **62**, 43–55.
- Vos, I.A., Verhage, A., Schuurink, R.C., Watt, L.G., Pieterse, C.M.J. and Van Wees, S.C.M.** (2013b) Onset of herbivore-induced resistance in systemic tissue primed for jasmonate-dependent defenses is activated by abscisic acid. *Front. Plant Sci.*, **4**, 539.
- Vos, I.A., Verhage, A., Watt, L.G., Vlaardingerbroek, I., Schuurink, R.C., Pieterse, C.M. and Van Wees, S.C.** (2019) Abscisic acid is essential for rewiring of jasmonic acid-dependent defenses during herbivory. *bioRxiv*, 747345.
- Waadt, R., Manalansan, B., Rauniyar, N., Munemasa, S., Booker, M.A., Brandt, B., Waadt, C., Nusinow, D.A., Kay, S.A., Kunz, H.-H., Schumacher, K., DeLong, A., Yates, J.R., III and Schroeder, J.I.** (2015) Identification of Open Stomata1-interacting proteins reveals interactions with sucrose non-fermenting1-related protein kinases2 and with type 2A protein phosphatases that function in abscisic acid responses. *Plant Physiol.*, **169**, 760-779.
- Walley, J.W., Coughlan, S., Hudson, M.E., Covington, M.F., Kaspi, R., Banu, G., Harmer, S.L. and Dehesh, K.** (2007) Mechanical stress induces biotic and abiotic stress responses via a novel cis-element. *PLoS Genet.*, **3**, e172.
- Wang, C., Du, X. and Mou, Z.** (2016) The mediator complex subunits MED14, MED15, and MED16 are involved in defense signaling crosstalk in Arabidopsis. *Front. Plant Sci.*, **7**.
- Wang, C., Yao, J., Du, X., Zhang, Y., Sun, Y., Rollins, J.A. and Mou, Z.** (2015) The Arabidopsis Mediator complex subunit16 is a key component of basal resistance against the necrotrophic fungal pathogen *Sclerotinia sclerotiorum*. *Plant Physiol.*, **169**, 856-872.
- Wang, D., Amornsiripanitch, N. and Dong, X.** (2006) A genomic approach to identify regulatory nodes in the transcriptional network of systemic acquired resistance in plants. *PLoS Pathog.*, **2**, 1042–1050.
- Wang, H., Li, S., Li, Y.a., Xu, Y., Wang, Y., Zhang, R., Sun, W., Chen, Q., Wang, X.-J., Li, C. and Zhao, J.** (2019) MED25 connects enhancer–promoter looping and MYC2-dependent activation of jasmonate signalling. *Nat. Plants*, **5**, 616-625.
- Wang, K., Guo, Q., Froehlich, J.E., Hersh, H.L., Zienkiewicz, A., Howe, G.A. and Benning, C.** (2018) Two abscisic acid-responsive plastid lipase genes involved in jasmonic acid biosynthesis in *Arabidopsis thaliana*. *Plant Cell*, **30**, 1006-1022.
- Wang, L., Rinaldi, F.C., Singh, P., Doyle, E.L., Dubrow, Z.E., Tran, T.T., Pérez-Quintero, A.L., Szurek, B. and Bogdanove, A.J.** (2017) TAL effectors drive transcription bidirectionally in plants. *Mol. Plant*, **10**, 285-296.

- Wang, L., Tsuda, K., Truman, W., Sato, M., Nguyen, L.V., Katagiri, F. and Glazebrook, J.** (2011) CBP60g and SARD1 play partially redundant critical roles in salicylic acid signaling. *Plant J.*, **67**, 1029-1041.
- Wang, S., Gu, Y., Zebell, Sophia G., Anderson, Lisa K., Wang, W., Mohan, R. and Dong, X.** (2014) A noncanonical role for the CKI-RB-E2F cell-cycle signaling pathway in plant effector-triggered immunity. *Cell Host Microbe*, **16**, 787-794.
- Wang, Y., Pruitt, R.N., Nürnberger, T. and Wang, Y.** (2022a) Evasion of plant immunity by microbial pathogens. *Nat. Rev. Microbiol.*, **20**, 449-464.
- Wang, Z., Orosa-Puente, B., Nomoto, M., Grey, H., Potuschak, T., Matsuura, T., Mori, I.C., Tada, Y., Genschik, P. and Spoel, S.H.** (2022b) Proteasome-associated ubiquitin ligase relays target plant hormone-specific transcriptional activators. *Sci. Adv.*, **8**, eabn4466.
- Wasternack, C. and Hause, B.** (2013) Jasmonates: biosynthesis, perception, signal transduction and action in plant stress response, growth and development. An update to the 2007 review in Annals of Botany. *Ann. Bot.*, **111**, 1021-1058.
- Wasternack, C. and Song, S.** (2017) Jasmonates: biosynthesis, metabolism, and signaling by proteins activating and repressing transcription. *J. Exp. Bot.*, **68**, 1303-1321.
- Weber, B., Zicola, J., Oka, R. and Stam, M.** (2016) Plant enhancers: a call for discovery. *Trends Plant Sci.*, **21**, 974-987.
- Weber, E., Engler, C., Gruetzner, R., Werner, S. and Marillonnet, S.** (2011) A modular cloning system for standardized assembly of multigene constructs. *PLoS One*, **6**, e16765.
- Weirauch, M.T., Yang, A., Albu, M., Cote, A.G., Montenegro-Montero, A., Drewe, P., Najafabadi, H.S., Lambert, S.A., Mann, I., Cook, K., Zheng, H., Goity, A., van Bakel, H., Lozano, J.C., Galli, M., Lewsey, M.G., Huang, E., Mukherjee, T., Chen, X., Reece-Hoyes, J.S., Govindarajan, S., Shaulsky, G., Walhout, A.J.M., Bouget, F.Y., Ratsch, G., Larrondo, L.F., Ecker, J.R. and Hughes, T.R.** (2014) Determination and inference of eukaryotic transcription factor sequence specificity. *Cell*, **158**, 1431-1443.
- Weltmeier, F., Ehlert, A., Mayer, C.S., Dietrich, K., Wang, X., Schütze, K., Alonso, R., Harter, K., Vicente-Carbajosa, J. and Dröge-Laser, W.** (2006) Combinatorial control of Arabidopsis proline dehydrogenase transcription by specific heterodimerisation of bZIP transcription factors. *EMBO J.*, **25**, 3133-3143.
- Werner, S., Engler, C., Weber, E., Gruetzner, R. and Marillonnet, S.** (2012) Fast track assembly of multigene constructs using Golden Gate cloning and the MoClo system. *Bioeng. Bugs*, **3**, 38-43.
- Windram, O., Madhou, P., McHattie, S., Hill, C., Hickman, R., Cooke, E., Jenkins, D.J., Penfold, C.A., Baxter, L., Breeze, E., Kiddle, S.J., Rhodes, J., Atwell, S., Kliebenstein, D.J., Kim, Y.S., Stegle, O., Borgwardt, K., Zhang, C.J., Tabrett, A., Legaie, R., Moore, J., Finkenshtadt, B., Wild, D.L., Mead, A., Rand, D., Beynon, J., Ott, S., Buchanan-Wollaston, V. and Denby, K.J.** (2012) Arabidopsis defense against *Botrytis cinerea*: Chronology and regulation deciphered by high-resolution temporal transcriptomic analysis. *Plant Cell*, **24**, 3530-3557.
- Winkelmüller, T.M., Entila, F., Anver, S., Piasecka, A., Song, B., Dahms, E., Sakakibara, H., Gan, X., Kułak, K., Sawikowska, A., Krajewski, P., Tsiantis, M., Garrido-Oter, R., Fukushima, K., Schulze-Lefert, P., Laurent, S., Bednarek, P. and Tsuda, K.** (2021) Gene expression evolution in pattern-triggered immunity within *Arabidopsis thaliana* and across Brassicaceae species. *Plant Cell*, **33**, 1863-1887.
- Wu, F., Deng, L., Zhai, Q., Zhao, J., Chen, Q. and Li, C.** (2020) Mediator subunit MED25 couples alternative splicing of JAZ genes with fine-tuning of jasmonate signaling. *Plant Cell*, **32**, 429-448.

- Wu, T., Hu, E., Xu, S., Chen, M., Guo, P., Dai, Z., Feng, T., Zhou, L., Tang, W. and Zhan, L.** (2021a) clusterProfiler 4.0: A universal enrichment tool for interpreting omics data. *Innovation*, **2**, 100141.
- Wu, T., Zhang, H., Bi, Y., Yu, Y., Liu, H., Yang, H., Yuan, B., Ding, X. and Chu, Z.** (2021b) Tal2c activates the expression of *OsF3H04g* to promote infection as a redundant TALE of Tal2b in *Xanthomonas oryzae* pv. *oryzicola*. *Int. J. Mol. Sci.*, **22**, 13628.
- Wu, Y., Deng, Z., Lai, J., Zhang, Y., Yang, C., Yin, B., Zhao, Q., Zhang, L., Li, Y., Yang, C. and Xie, Q.** (2009) Dual function of Arabidopsis ATAF1 in abiotic and biotic stress responses. *Cell Res.*, **19**, 1279-1290.
- Wu, Y., Zhang, D., Chu, J.Y., Boyle, P., Wang, Y., Brindle, I.D., De Luca, V. and Després, C.** (2012) The Arabidopsis NPR1 protein is a receptor for the plant defense hormone salicylic acid. *Cell Rep.*, **1**, 639-647.
- Xu, F., Jia, M., Li, X., Tang, Y., Jiang, K., Bao, J. and Gu, Y.** (2021) Exportin-4 coordinates nuclear shuttling of TOPLESS family transcription corepressors to regulate plant immunity. *Plant Cell*, **33**, 697-713.
- Xu, G., Greene, G.H., Yoo, H., Liu, L., Marqués, J., Motley, J. and Dong, X.** (2017) Global translational reprogramming is a fundamental layer of immune regulation in plants. *Nature*, **545**, 487-490.
- Xu, G., Moeder, W., Yoshioka, K. and Shan, L.** (2022) A tale of many families: calcium channels in plant immunity. *Plant Cell*.
- Yan, C., Fan, M., Yang, M., Zhao, J., Zhang, W., Su, Y., Xiao, L., Deng, H. and Xie, D.** (2018) Injury activates Ca²⁺/calmodulin-dependent phosphorylation of JAV1-JAZ8-WRKY51 complex for jasmonate biosynthesis. *Mol. Cell*, **70**, 136-149.
- Yang, L., Teixeira, P.J.P.L., Biswas, S., Finkel, O.M., He, Y., Salas-Gonzalez, I., English, M.E., Epple, P., Mieczkowski, P. and Dangl, J.L.** (2017) *Pseudomonas syringae* type III effector HopBB1 promotes host transcriptional repressor degradation to regulate phytohormone responses and virulence. *Cell Host Microbe*, **21**, 156-168.
- Yang, L., Zhang, Y., Guan, R., Li, S., Xu, X., Zhang, S. and Xu, J.** (2020) Co-regulation of indole glucosinolates and camalexin biosynthesis by CPK5/CPK6 and MPK3/MPK6 signaling pathways. *J. Integr. Plant Biol.*, **62**, 1780-1796.
- Yang, W., Zhang, W. and Wang, X.** (2017) Post-translational control of ABA signalling: the roles of protein phosphorylation and ubiquitination. *Plant Biotechnol. J.*, **15**, 4-14.
- Yang, Y.N., Kim, Y., Kim, H., Kim, S.J., Cho, K.-M., Kim, Y., Lee, D.S., Lee, M.-H., Kim, S.Y., Hong, J.C., Kwon, S.J., Choi, J. and Park, O.K.** (2021) The transcription factor ORA59 exhibits dual DNA binding specificity that differentially regulates ethylene- and jasmonic acid-induced genes in plant immunity. *Plant Physiol.*, **187**, 2763-2784.
- Yin, Y., Vafeados, D., Tao, Y., Yoshida, S., Asami, T. and Chory, J.** (2005) A new class of transcription factors mediates brassinosteroid-regulated gene expression in Arabidopsis. *Cell*, **120**, 249-259.
- Yoo, S.-D., Cho, Y.-H. and Sheen, J.** (2007) Arabidopsis mesophyll protoplasts: a versatile cell system for transient gene expression analysis. *Nat. Protoc.*, **2**, 1565-1572.
- Yoshida, T., Fujita, Y., Maruyama, K., Mogami, J., Todaka, D., Shinozaki, K. and Yamaguchi-Shinozaki, K.** (2015) Four Arabidopsis AREB/ABF transcription factors function predominantly in gene expression downstream of SnRK2 kinases in abscisic acid signalling in response to osmotic stress. *Plant Cell Environ.*, **38**, 35-49.

- Yoshida, T., Fujita, Y., Sayama, H., Kidokoro, S., Maruyama, K., Mizoi, J., Shinozaki, K. and Yamaguchi-Shinozaki, K.** (2010) AREB1, AREB2, and ABF3 are master transcription factors that cooperatively regulate ABRE-dependent ABA signaling involved in drought stress tolerance and require ABA for full activation. *Plant J.*, **61**, 672-685.
- You, Y., Zhai, Q., An, C. and Li, C.** (2019) LEUNIG_HOMOLOG mediates MYC2-dependent transcriptional activation in cooperation with the coactivators HAC1 and MED25. *Plant Cell*, **31**, 2187-2205.
- Yu, G., Wang, L.-G., Han, Y. and He, Q.-Y.** (2012) clusterProfiler: an R package for comparing biological themes among gene clusters. *OMICS*, **16**, 284-287.
- Yu, X., Li, B., Jang, G.-J., Jiang, S., Jiang, D., Jang, J.-C., Wu, S.-H., Shan, L. and He, P.** (2019) Orchestration of processing body dynamics and mRNA decay in Arabidopsis immunity. *Cell Rep.*, **28**, 2194-2205.e2196.
- Yuan, H.M., Liu, W.C. and Lu, Y.T.** (2017) CATALASE2 coordinates SA-mediated repression of both auxin accumulation and JA biosynthesis in plant defenses. *Cell Host Microbe*, **21**, 143-155.
- Yuan, M., Ngou, B.P.M., Ding, P. and Xin, X.-F.** (2021a) PTI-ETI crosstalk: an integrative view of plant immunity. *Curr. Opin. Plant Biol.*, **62**, 102030.
- Yuan, P., Tanaka, K. and Poovaiah, B.** (2022) Calcium/calmodulin-mediated defense signaling: What is looming on the horizon for AtSR1/CAMTA3-mediated signaling in plant immunity. *Front. Plant Sci.*, **12**, 3244.
- Yuan, P., Tanaka, K. and Poovaiah, B.W.** (2021b) Calmodulin-binding transcription activator AtSR1/CAMTA3 fine-tunes plant immune response by transcriptional regulation of the salicylate receptor NPR1. *Plant Cell Environ.*, **44**, 3140-3154.
- Yuan, X., Wang, H., Cai, J., Li, D. and Song, F.** (2019) NAC transcription factors in plant immunity. *Phytopathol. Res.*, **1**, 3.
- Yuan, Y., Zhong, S., Li, Q., Zhu, Z., Lou, Y., Wang, L., Wang, J., Wang, M., Li, Q., Yang, D. and He, Z.** (2007) Functional analysis of rice *NPR1*-like genes reveals that *OsNPR1/NH1* is the rice orthologue conferring disease resistance with enhanced herbivore susceptibility. *Plant Biotechnol. J.*, **5**, 313-324.
- Zander, M., Chen, S., Imkamp, J., Thurow, C. and Gatz, C.** (2012) Repression of the *Arabidopsis thaliana* jasmonic acid/ethylene-induced defense pathway by TGA-interacting glutaredoxins depends on their C-terminal ALWL motif. *Mol. Plant*, **5**, 831-840.
- Zander, M., La Camera, S., Lamotte, O., Métraux, J.-P. and Gatz, C.** (2010) *Arabidopsis thaliana* class-II TGA transcription factors are essential activators of jasmonic acid/ethylene-induced defense responses. *Plant J.*, **61**, 200-210.
- Zander, M., Lewsey, M.G., Clark, N.M., Yin, L., Bartlett, A., Saldierna Guzmán, J.P., Hann, E., Langford, A.E., Jow, B., Wise, A., Nery, J.R., Chen, H., Bar-Joseph, Z., Walley, J.W., Solano, R. and Ecker, J.R.** (2020) Integrated multi-omics framework of the plant response to jasmonic acid. *Nat. Plants*, **6**, 290-302.
- Zander, M., Thurow, C. and Gatz, C.** (2014) TGA transcription factors activate the salicylic acid-suppressible branch of the ethylene-induced defense program by regulating *ORA59* expression. *Plant Physiol.*, **165**, 1671-1683.
- Zanetti, M.E., Blanco, F., Reynoso, M. and Crespi, M.** (2020) To keep or not to keep: mRNA stability and translatability in root nodule symbiosis. *Curr. Opin. Plant Biol.*, **56**, 109-117.

- Zarei, A., Korbess, A.P., Younessi, P., Montiel, G., Champion, A. and Memelink, J.** (2011) Two GCC boxes and AP2/ERF-domain transcription factor ORA59 in jasmonate/ethylene-mediated activation of the *PDF1.2* promoter in Arabidopsis. *Plant Mol. Biol.*, **75**, 321–331.
- Zavaliev, R., Mohan, R., Chen, T. and Dong, X.** (2020) Formation of NPR1 condensates promotes cell survival during the plant immune response. *Cell*, **182**, 1093–1108.
- Zeng, W., Huang, H., Lin, X., Zhu, C., Kosami, K.-i., Huang, C., Zhang, H., Duan, C.-G., Zhu, J.-K. and Miki, D.** (2021) Roles of DEMETER in regulating DNA methylation in vegetative tissues and pathogen resistance. *J. Integr. Plant Biol.*, **63**, 691–706.
- Zhai, Q. and Li, C.** (2019) The plant Mediator complex and its role in jasmonate signaling. *J. Exp. Bot.*, **70**, 3415–3424.
- Zhai, Q., Yan, L., Tan, D., Chen, R., Sun, J., Gao, L., Dong, M.-Q., Wang, Y. and Li, C.** (2013) Phosphorylation-coupled proteolysis of the transcription factor MYC2 is important for jasmonate-signaled plant immunity. *PLoS Genet.*, **9**, e1003422.
- Zhang, F., Yao, J., Ke, J., Zhang, L., Lam, V.Q., Xin, X.-F., Zhou, X.E., Chen, J., Brunzelle, J., Griffin, P.R., Zhou, M., Xu, H.E., Melcher, K. and He, S.Y.** (2015) Structural basis of JAZ repression of MYC transcription factors in jasmonate signalling. *Nature*, **525**, 269–273.
- Zhang, X., Bernatavichute, Y.V., Cokus, S., Pellegrini, M. and Jacobsen, S.E.** (2009) Genome-wide analysis of mono-, di- and trimethylation of histone H3 lysine 4 in *Arabidopsis thaliana*. *Genome Biol.*, **10**, R62.
- Zhang, X., Zhu, Z., An, F., Hao, D., Li, P., Song, J., Yi, C. and Guo, H.** (2014) Jasmonate-activated MYC2 represses ETHYLENE INSENSITIVE3 activity to antagonize ethylene-promoted apical hook formation in Arabidopsis. *Plant Cell*, **26**, 1105–1117.
- Zhang, Y., Fan, W., Kinkema, M., Li, X. and Dong, X.** (1999) Interaction of NPR1 with basic leucine zipper protein transcription factors that bind sequences required for salicylic acid induction of the *PR-1* gene. *Proc. Natl. Acad. Sci. U.S.A.*, **96**, 6523–6528.
- Zhang, Y. and Li, X.** (2019) Salicylic acid: biosynthesis, perception, and contributions to plant immunity. *Curr. Opin. Plant Biol.*, **50**, 29–36.
- Zhang, Y., Shi, C., Fu, W., Gu, X., Qi, Z., Xu, W. and Xia, G.** (2021) Arabidopsis MED18 interaction with RNA Pol IV and V subunit NRPD2a in transcriptional regulation of plant immune responses. *Front. Plant Sci.*, **12**.
- Zhang, Y., Xu, S., Ding, P., Wang, D., Cheng, Y.T., He, J., Gao, M., Xu, F., Li, Y., Zhu, Z., Li, X. and Zhang, Y.** (2010) Control of salicylic acid synthesis and systemic acquired resistance by two members of a plant-specific family of transcription factors. *Proc. Natl. Acad. Sci. U.S.A.*, **107**, 18220–18225.
- Zheng, X., Spivey, N.W., Zeng, W., Liu, P.-P., Fu, Z.Q., Klessig, D.F., He, S.Y. and Dong, X.** (2012) Coronatine promotes *Pseudomonas syringae* virulence in plants by activating a signaling cascade that inhibits salicylic acid accumulation. *Cell Host Microbe*, **11**, 587–596.
- Zheng, Z., Qamar, S.A., Chen, Z. and Mengiste, T.** (2006) Arabidopsis WRKY33 transcription factor is required for resistance to necrotrophic fungal pathogens. *Plant J.*, **48**, 592–605.
- Zhou, J., Wang, X., He, Y., Sang, T., Wang, P., Dai, S., Zhang, S. and Meng, X.** (2020) Differential phosphorylation of the transcription factor WRKY33 by the protein kinases CPK5/CPK6 and MPK3/MPK6 cooperatively regulates camalexin biosynthesis in Arabidopsis. *Plant Cell*, **32**, 2621–2638.

- Zhou, J.M., Trifa, Y., Silva, H., Pontier, D., Lam, E., Shah, J. and Klessig, D.F.** (2000) NPR1 differentially interacts with members of the TGA/OBF family of transcription factors that bind an element of the *PR-1* gene required for induction by salicylic acid. *Mol. Plant Microbe Interact.*, **13**, 191–202.
- Zhu, L.J., Gazin, C., Lawson, N.D., Pagès, H., Lin, S.M., Lapointe, D.S. and Green, M.R.** (2010) ChIPpeakAnno: a Bioconductor package to annotate ChIP-seq and ChIP-chip data. *BMC Bioinformatics*, **11**, 237.
- Zhu, Z., An, F., Feng, Y., Li, P., Xue, L., Mu, A., Jiang, Z., Kim, J.-M., To, T.K., Li, W., Zhang, X., Yu, Q., Dong, Z., Chen, W.-Q., Seki, M., Zhou, J.-M. and Guo, H.** (2011) Derepression of ethylene-stabilized transcription factors (EIN3/EIL1) mediates jasmonate and ethylene signaling synergy in Arabidopsis. *Proc. Natl. Acad. Sci. U.S.A.*, **108**, 12539–12544.

SAMENVATTING

Een van de grootste uitdagingen van deze tijd is het voeden van de groeiende wereldbevolking. Omdat er maar een beperkte hoeveelheid vruchtbaar land beschikbaar is voor landbouw, is het noodzakelijk de opbrengst per hectare te verhogen. Een belangrijke methode is het verminderen van oogstverlies veroorzaakt door ziekteverwekkers en insecten. Wereldwijd gaat hier namelijk tussen de 8% en 40% van de oogst aan verloren. Alhoewel sommige chemische bestrijdingsmiddelen een goed wapen zijn tegen dit verlies, hebben deze middelen vaak negatieve effecten op het milieu. Het is daarom essentieel om gewassen te creëren die zich beter kunnen verdedigen tegen ziekteverwekkers en insecten. Om deze ontwikkeling te versnellen is vergroting van de kennis van het immuunsysteem van planten essentieel.

In het verleden is er al veel kennis vergaard over het plantenimmuunsysteem. De plant herkent ziekteverwekkers en insecten doordat speciale plantreceptoren in staat zijn specifieke moleculen van de aanvaller te binden. Bovendien kan de plant plantmoleculen die vrijkomen wanneer bijvoorbeeld een insect schade berokkend herkennen via andere gespecialiseerde receptoren. Deze herkenning van ziekteverwekkers, insecten en/of schade zorgt voor een hele cascade aan reacties, die uiteindelijk leiden tot het doden of verjagen van de aanvaller, mits de plant in staat is een voldoende sterke reactie in gang te zetten. Planthormonen vormen een belangrijk onderdeel van deze cascade. Afhankelijk van de aanvaller wordt een specifieke combinatie van hormonen aangemaakt. Deze hormonen activeren op hun beurt weer een specifiek netwerk van genen. Elk hormoongestuurd netwerk activeert en onderdrukt processen die belangrijk zijn voor verweer tegen de ziekteverwekker die de aanmaak van de hormonen heeft veroorzaakt. Bovendien beïnvloeden de verschillende netwerken elkaar, zodat de respons optimaal kan worden afgestemd op de specifieke ziekteverwekker en de specifieke omstandigheden waarin de plant leeft. In dit proefschrift hebben we een aantal van deze netwerken en de interacties tussen deze netwerken onderzocht. Dit onderzoek vond plaats in de modelplant *Arabidopsis thaliana* (zandraket), een plantensoort die veel wordt gebruikt bij fundamenteel onderzoek vanwege zijn relatief korte levenscyclus, eenvoudige genetica, en kleine formaat.

In Hoofdstuk 1 hebben we de huidige kennis op het gebied van interacties tussen hormoonnetwerken samengevat. We hebben hierbij vooral gefocust op het feit dat deze interacties op meerdere regulatieniveaus kunnen plaatsvinden, bijvoorbeeld door beïnvloeding van genexpressie of door interacties tussen eiwitten die onderdeel uitmaken van verschillende hormoonnetwerken. Voor afweer zijn vier specifieke hormonen het belangrijkste. Twee hormonen, jasmonzuur (JA) en salicylzuur (SA) worden beschouwd als centrale regulatoren van afweer, terwijl twee andere hormonen, abscisinezuur (ABA) en ethyleen (ET) meer worden gezien als modulators van het JA- en

SA-netwerk, en bovendien nog functies in andere processen hebben. In het algemeen heeft SA vooral een rol in afweer tegen ziekteverwekkers die voedsel onttrekken aan levende plantencellen (biotrofe pathogenen), terwijl JA vooral een rol heeft in afweer tegen ziekteverwekkers die plantencellen doden en uit het dode weefsel nutriënten halen (necrotrofe pathogenen), en tegen kauwende insecten. Over het algemeen remmen het SA- en JA-netwerk elkaar. ABA versterkt het gedeelte van het JA-signaleringsnetwerk dat specifiek gericht is tegen insecten (de zogenaamde MYC-tak), terwijl ABA het gedeelte van het JA-signaleringsnetwerk dat gericht is tegen necrotrofe pathogenen (de zogenaamde ERF-tak) onderdrukt. Voor ET geldt dit andersom. In dit proefschrift hebben we onderzocht hoe het ABA-netwerk is opgebouwd, hoe het ABA-netwerk het JA-netwerk beïnvloedt, en hoe SA via specifieke eiwitten het JA-netwerk beïnvloedt.

In Hoofdstuk 2 hebben we het ABA-netwerk onderzocht. Naast de rol van ABA in afweer speelt het ook een belangrijke rol in het remmen van (ongewenste) zaadkieming en in het weerstaan van droogte. Om beter te begrijpen hoe het ABA-netwerk is opgebouwd hebben we gekeken naar de veranderingen in expressie van alle genen van *Arabidopsis thaliana* op 14 verschillende tijdstippen in de 16 uur volgend na toediening van ABA. We zagen dat meer dan zeventuizend genen hun expressie veranderden, waarbij er ongeveer evenveel genen hoger en lager tot expressie kwamen vergeleken met onbehandelde planten. De meeste veranderingen vonden plaats binnen vier uur. Wij konden de genen op basis van de gelijkenissen in expressiepatroon in de tijd indelen in verschillende clusters. Zulke clusters bevatten vaak genen met een gelijke functie, die we met behulp van publiek toegankelijke data over genfuncties in kaart hebben gebracht. De mate van genexpressie wordt voor een groot gedeelte gereguleerd door een specifieke klasse eiwitten die transcriptiefactoren worden genoemd. Deze reguleren namelijk de mate van transcriptie, oftewel de mate waarin DNA wordt overgeschreven naar RNA. Wanneer een groep genen een vergelijkbaar expressiepatroon heeft, is het waarschijnlijk dat ze door een grotendeels gelijke groep van transcriptiefactoren worden gereguleerd. Door onze expressedata te combineren met publiek toegankelijke DNA-bindingsdata van transcriptiefactoren, hebben wij voorspellingen gedaan over welke transcriptiefactoren waarschijnlijk specifieke genclusters reguleren. Verder hebben we nog een aantal andere bioinformatische analyses gedaan om te voorspellen op welk tijdstip welke transcriptiefactoren het belangrijkste zijn, en hoe ze elkaar reguleren in een hiërarchisch genregulatiernetwerk. Bij de groep van voorspelde belangrijke transcriptiefactoren zat een aantal transcriptiefactoren waarvan al bekend was dat ze een functie hebben in het ABA-netwerk, wat bevestigde dat ons experiment en onze gebruikte methodes relevante transcriptiefactoren in het ABA-netwerk konden identificeren. Verder hebben we de vatbaarheid voor droogte onderzocht van planten die gemuteerd zijn in een transcriptiefactor die volgens onze voorspellingen een (tot dan toe)

onbekende functie heeft in het ABA-netwerk. Eén van de geteste transcriptiefactoren, GT3a, leek de weerstand tegen droogte positief te beïnvloeden.

Het is al langer bekend dat ABA het JA-netwerk beïnvloedt, maar de schaal, timing en exacte mechanismes van deze invloed zijn in grote mate onbekend. Ons onderzoek hiernaar is beschreven in Hoofdstuk 3. In dit hoofdstuk analyseerden wij dezelfde ABA-tijdseriesdata als in Hoofdstuk 2, en vergeleken we dat met eenzelfde soort tijdserie-experiment dat wij hadden uitgevoerd na behandeling met MeJA (een variant van JA) en de combinatie van ABA en MeJA. Wij ontdekten dat er veel overeenkomsten waren in de genen die door ABA en MeJA werden beïnvloed. Ongeveer 2/3^e van alle genen die op MeJA reageerden had bovendien een andere mate van expressie in de combinatiebehandeling van ABA en MeJA vergeleken met alleen MeJA-behandeling. Dit laat zien dat de twee netwerken nauw verbonden zijn met elkaar. Verder zagen wij dat ABA veel invloed had op de expressie van JA-biosynthese- en JA-catabolismegenen, wat suggereert dat ABA ook effect heeft op de hoeveelheid geproduceerde JA. Ook voorspelden wij het belang van een aantal ABA-geactiveerde transcriptiefactoren in het moduleren van de transcriptie van JA-gevoelige genen. Tot slot vonden wij dat de JA-masterregulatoren ORA59 en ERF1 de belangrijkste eiwitten zijn binnen de ERF-tak van het JA-netwerk die worden beïnvloed door ABA. Wij vonden bovendien dat ABA waarschijnlijk zorgt voor afbraak van ORA59, waardoor de ERF-tak kan worden geremd.

In Hoofdstuk 4 onderzochten wij een aantal details van hoe SA het JA-netwerk beïnvloedt. Wij ontdekten dat de SA-masterregulator NPR1 functioneert in de celkern bij het remmen van het JA-netwerk. Verder onderzoek suggereerde dat SA, deels via NPR1, de expressie activeert van specifieke genen die coderen voor transcriptiefactoren van de WRKY-familie. Deze transcriptiefactoren zijn op hun beurt in staat de transcriptie te remmen van *PDF1.2*, een merker van de ERF-tak. Verder onderzoek wees uit dat twee van deze transcriptiefactoren, WRKY53 en WRKY67, dit waarschijnlijk doen door afbraak van ORA59 te bevorderen – een effect dat we ook vonden voor ABA in Hoofdstuk 3.

In de drie experimentele hoofdstukken heb ik vooral gekeken naar hoe transcriptie van genen binnen de verschillende hormoonnetwerken wordt beïnvloed, waarbij ik heb gefocust op de rol van transcriptiefactoren. Alhoewel transcriptiefactoren veel invloed hebben op de mate van transcriptie en de uiteindelijke hoeveelheid van het eiwit waar het gen voor codeert, zijn er nog veel andere stappen in genexpressieregulatie die dit bepalen. Deze stappen zijn echter lastiger te onderzoeken en daarom loopt de kennis hierover achter. Wij denken dat het belangrijk is om hier in de toekomst meer op te focussen. Als een soort voorschot hierop hebben we daarom de huidige kennis over alle stappen die belangrijk zijn in de transcriptionele regulatie van plantenimmunitet samengevat in Hoofdstuk 5.

Dit proefschrift biedt verschillende nieuwe inzichten in hormoongestuurde genregulatie-netwerken in de modelplant *Arabidopsis thaliana*. Het geeft bovendien

meerdere aanknopingspunten voor vervolgonderzoek. Het belang van verschillende transcriptiefactoren kan bijvoorbeeld in meer detail worden geanalyseerd, en er kan worden onderzocht hoe de verschillende niveaus van regulatie die beschreven worden in Hoofdstuk 5 aan hormoongestuurde genregulatiernetwerken bijdragen. Bovendien kan worden uitgezocht hoe de verschillende netwerken worden geactiveerd en interacteren wanneer een plant door een insect of pathogeen wordt aangevallen. Dit levert kennis op rondom afweermechanismen van de plant, maar ook over onderdrukking van afweermechanismen door een insect of pathogeen. Dit soort kennis is essentieel om gewassen te kunnen kweken die resistenter zijn tegen ziekteverwekkers en plagen. Hiervoor is het nog wel noodzakelijk om de vertaalslag te maken van de kennis in deze modelplant naar kennis over afweer van verschillende gewassen, omdat verschillende plantensoorten moleculair gezien niet precies hetzelfde in elkaar zitten. De in deze modelplant verkregen kennis en ontwikkelde analytische methoden vormen een belangrijke basis van waaruit verder kan worden gegaan met onderzoek in gewassen. Uiteindelijk kan dit leiden tot de ontwikkeling van gewassen die minder vatbaar zijn voor ziekteverwekkers en plagen, en dus een hogere, betrouwbaardere opbrengst leveren dan de huidige gewassen.

DANKWOORD

Het is eindelijk zover: mijn proefschrift is af! Ik begon er vol goede moed aan in februari 2017 en heb het (pas) op 22 augustus 2023 voltooid, heel wat illusies armer, maar wonder boven wonder met nog veel enthousiasme voor wetenschap, plantenbiologie en het onderzoek in de groep Plant-Microbe Interacties. Dat ik dit enthousiasme heb kunnen behouden heeft veel te maken met de mensen om mij heen, en die wil ik hier dan ook graag bedanken.

Als allereerste wil ik mijn promotor Saskia bedanken. Je zit altijd vol ideeën en het is inspirerend om met jou over wetenschap te praten. Daarnaast geef jij duidelijk ook persoonlijk om mensen en sta jij bovendien open voor feedback wanneer iets in de samenwerking verbeterd kan worden. Ik denk dat we tijdens al deze jaren steeds beter hebben ontdekt hoe we het beste uit elkaar kunnen halen, en ik zie uit in de toekomst nog veel meer op wetenschappelijk gebied te ontdekken! Ook heel veel dank aan mijn andere promotor, Corné. Net als Saskia heb jij een enorme passie voor wetenschap en ik zit na overleg met jou vaak vol nieuwe inspiratie. Je hebt net weer een andere kijk op het werk dan Saskia en zo vullen jullie elkaar aan. Ik voel me vereerd om op basis van jouw Spinoza verder te mogen werken in dit lab, en ik zie uit naar vele mooie ontdekkingen! Ook veel dank aan de andere PI's die ik heb meegemaakt in dit lab: Guido, Peter, Ronnie en Roeland. Ik heb misschien minder vaak direct met jullie te maken gehad, maar heb alsnog bij gelegenheden als half-year reports nuttige ideeën van jullie gekregen. Bovendien waren en zijn jullie erg prettige collega's!

De afgelopen jaren heb ik ook met veel andere ontzettend fijne collega's samengewerkt, die ik hier ook graag voor wil bedanken. De eerste van die lijst moet toch wel Tessa zijn. Heeeeeeeeyyyyyy Teeessssaaaa! Je bent hier gekomen als 'mijn' masterstudent, en daarna 'gepromoveerd' tot collega. Het is bepaald niet overdreven als ik zou zeggen dat zonder jou met name hoofdstuk 4 van dit proefschrift een stuk minder kwaliteit zou hebben; ik ben blij dat jij (in tegenstelling tot ikzelf) protoplasten wel in significante aantallen kan laten overleven! Maar het belangrijkste is natuurlijk dat jij een ontzettend gezellige collega en kantoorgenoot bent, waar ik altijd lol mee kan maken!

Then to my other long-term office mate: Dharani. It was really nice getting to know you better and having fun about all kinds of things. I'm always very much in awe about all your large-scale experiments with ten million different treatments, pretreatments, and what not. Also, it was a lot of fun exploring the (cultural) differences between India and The Netherlands with you. For example, I've found out that what I consider pretty spicy food is not even worth a rating on the spiciness-scale for you, and together we discovered that you are surprisingly good at guessing someone's nationality from their driving style. I wish you good luck with finishing your thesis and working at your new job!

Then there is my final current long-term office mate: Run. You are an interesting combination of being very serious at work, and a lot of fun outside of it. Probably the best way to work actually, but sometimes the contrast still surprises me! I really admire your quick, creative mind, and I'm looking forward to working more with you in the future!

Apart from my current office mates, I also have multiple great ex-office mates. Marrit, je bent helaas met TPB naar een andere gang verhuisd. Ik vond het erg leuk om jou als kantoorgenoot te hebben. Je bent een vrolijke, positieve persoon en het is altijd leuk om met je te kletsen, wat we dan ook vaak hebben gedaan. Gelukkig is de TPB-gang (mag zowel Nederlands als Engels worden gelezen) niet zo ver weg, dus dat gezellig kletsen komt vast nog goed! Ook bedankt aan Kim voor de gezelligheid als kantoorgenoot. Het was leuk om jou naast mij te hebben in het kantoor en we hebben volgens mij veel gelachen over van alles. Also thanks to Richard for being a nice office mate, and of course helping me with many of the RNA-seq analyses!

Of course, outside of the office I have/had many other nice colleagues as well. I should probably write something for all of you individually, but given the limited space I suggest you can come and collect kind words about yourself with me in person, haha! So thank you for all the good times we had together, in no particular order, Sietske, Sanne, Sophie, Robin, Pim, Melissa, Marciel, Vinicius, JJ, Hangyu, Brandon, Shu-Hua, Valerian, Alberto, Dario, Yang, Kumar, Manon, Marjolein, Joel, Claudia, Ke, Pauline, Tom, Alexandra, Colette, Marco, Eline, Jelle, Max, Gijs, Hao, Merel, Tijmen, Dima, Melanie, Iñigo, Joyce, Miek, Ray, Sebastian, Savani, Nicole, Giannis, Changfeng, Sarah, Xintong, Lotje, Erqin, Gilles, Hans, Anja, Jolanda, and Aster.

And then my former students – no less than 15 of them! Similarly to above, I would have loved to write something personal for all of you, but there is so much to say to each of you that I cannot fit it in this book. Above all, I want to give a big thank you to all of you: Renée, Folkert, Ellinor, Raquel, Berend, Tessa, Gian, Aurelio, Priya, Jannes, Eva, Hannah, Leroy, Maroje and Michael. You did great work and I admire the persistence you showed while working on often difficult projects. I thoroughly enjoyed seeing how you progressed and became more comfortable working as a scientist. I wish you all the best in the future!

Buiten mijn werk om heb ik natuurlijk ook veel steun gehad. Ten eerste van mijn ouders, die mij altijd steunen en een ander perspectief kunnen geven, waardoor ik denk ik een gezonde kijk op mijn werk en het leven in het algemeen houd. Natuurlijk ook van mijn broer David, die mij al voor ging als PhD en daarmee een voorbeeld voor mij was. Ook heel erg bedankt aan mijn vrienden van het enige echte A.M. voor een hele hoop gezelligheid, muziek (van metal tot 'Italia') en gesprekken die uiteenlopen van serieus tot absurdistisch ("Loopt een man het ziekenhuis in..."). Ten slotte ook veel dank aan iedereen met wie ik de eer heb om muziek te maken. Muziek is enorm belangrijk in mijn

leven en een goede afleiding van mijn werk, dus het is heel fijn en bijzonder om dit samen met zoveel getalenteerde mensen te mogen doen!

En tot slot de belangrijkste persoon van iedereen. Lieve Bregje, vier dagen na het afronden van dit proefschrift zijn wij getrouwd. Ik denk dat ik op die dag veel beter heb verwoord wat jij voor mij betekent dan dat ik hier kan doen. Ik zal het hier houden bij zeggen dat je een enorme bron van steun en fijnheid bent, en ervoor zorgt dat ik mijn werk makkelijker in perspectief kan plaatsen. Heel van dank daarvoor, en veel liefs van mezelf ;).

CURRICULUM VITAE

Niels Aerts was born on the 13th of September 1991 in Utrecht, the Netherlands. In 2010, he finished his secondary education at KSG De Breul in Zeist. In the same year, he started his Biology study at Utrecht University, where he obtained his Bachelor of Science degree in 2014. He then did the Master's program Environmental Biology and obtained his degree in 2016. During his Master's studies he did a nine-month internship at the Plant-Microbe Interactions group at Utrecht University under the supervision of Dr. Marcel van Verk and Prof. Saskia van Wees, where he characterized a transcription factor with a putative role in the jasmonic acid gene regulatory network. After this, he did a seven-month internship at Wageningen University & Research, supervised by Dr. Aalt-Jan van Dijk from the Bioinformatics group and Prof. Gerco Angenent from the Plant Developmental Systems group. In this internship, he studied binding motifs of MADS-box transcription factors. This work was later published in *BMC Plant Biology*. After this internship, Niels enrolled in the 'Experimental Plant Sciences Graduate Programme', during which he wrote a PhD proposal together with Dr. Marcel van Verk and Prof. Saskia van Wees. Subsequently, he worked for three months as a research assistant in the lab of Prof. Saskia van Wees. In February 2017, after the PhD proposal was granted, he started his PhD project under the supervision of Prof. Saskia van Wees and Prof. Corné Pieterse. In this project, Niels studied the gene regulatory networks induced by the plant hormones abscisic acid and jasmonic acid, and their interplay. Additionally, he worked on a project aimed at uncovering the role of NPR1 and WRKY transcription factors in SA/JA crosstalk, to which he had also contributed as a research assistant. This thesis describes the work done in both projects. Currently, Niels works as a postdoctoral researcher at the Plant-Microbe Interactions group at Utrecht University under the supervision of Prof. Saskia van Wees and Prof. Corné Pieterse.

LIST OF PUBLICATIONS

Aerts, N., De Bruijn, S., Van Mourik, H., Angenent, G.C. and Van Dijk, A.D. (2018) Comparative analysis of binding patterns of MADS-domain proteins in *Arabidopsis thaliana*. *BMC Plant Biol.*, **18**, 131.

Aerts, N., Mendes, M.P. and Van Wees, S.C.M. (2021) Multiple levels of crosstalk in hormone networks regulating plant defense. *Plant J.*, **105**, 489-504

Aerts, N., Chhillar, H., Ding, P. and Van Wees, S.C.M. (2022) Transcriptional regulation of plant innate immunity. *Essays Biochem.*, **66**, 607-620.



